University of Dhaka, Bangladesh.

Development of Electrical Impedance Technique for Assessment of Lung Function.

A dissertation submitted by Md. Shariful Alam
in partial fulfilment of the requirements for the Degree of
Doctor of Philosophy in Electrical and Electronic Engineering.

Registration no. &Session: 147/2020-2021 (New)
23/2014-2015 (Old)

Department of Electrical and Electronic Engineering
University of Dhaka, Dhaka-1000, Bangladesh.

19 October, 2023.

Declaration

I hereby declare that the thesis entitled **"Development of Electrical Impedance Technique for Assessment of Lung Function"** and this is a record of original work was carried out by me for the degree of Doctor of Philosophy in Electrical and Electronic Engineering under the supervisions of Professor Dr. Md. Adnan Kiber and Professor Dr. S. M. Mostafa Al Mamun. This thesis or any part of it has not been submitted elsewhere for the award of any degree or diploma.

Md. Shariful Alam

Registration no. & Session:147/2020-2021 (New)& 23/2014-2015 (Old)

Department of Electrical and Electronic Engineering

University of Dhaka, Dhaka-1000, Bangladesh.

Certificate

This is to certify that the thesis entitled **"Development of Electrical Impedance Technique for Assessment of Lung Function"** submitted by Md. Shariful Alam was carried out this original research work under our supervisions. It meets acceptable standards and can be submitted for evaluation in partial fulfillment of the requirements for the degree of Doctor of Philosophy in Electrical and Electronic Engineering. To the best of my knowledge, this dissertation has not been submitted elsewhere for any other degree or diploma.

Prof. Dr. Md. Adnan Kiber
Department of Electrical and Electronic Engineering
University of Dhaka, Dhaka-1000
Bangladesh.

Prof. Dr. S M Mostafa Al Mamun
Department of Electrical and Electronic Engineering
University of Dhaka, Dhaka-1000
Bangladesh.

Acknowledgements

I would like to express my sincere gratitude to the Almighty Allah for successful completion of this research work. I am greatly indebted to my respected supervisors- Prof. Dr. Md. Adnan Kiber and Prof. Dr. S. M. Mostafa Al Mamun for their proper guidance, supervision and encouragement to complete this research work. I also thank to the Biomedical Physics and Technology department, DU and also Prof. Dr. K.S. Rabbani of the same department for essential help of my research work. I wish to thanks all of my respected colleagues, friends and well-wishers who have inspired and help me to complete this research work.

I am especially grateful to all of my family members who gave me support, help and inspiration to complete this research work.

I appreciate the great support and opportunity of the Directorate of Secondary and Higher Education, Ministry of Education and the University Grants Commission (UGC), Bangladesh for completion my PhD research work.

List of Publications

Journal Paper

1. Alam, M.S., S M Mostafa Al Mamun and Md. Adnan Kiber (2021). Simulation Study of Noninvasive Electrical Impedance Technique for Continuous Monitoring of Acute Respiratory Distress Syndrome. Dhaka University Journal of Applied Science & Engineering, Volume-**6**(1) 1-5, January, 2021 (January).

Conference Paper

1. Alam, M.S., S M Mostafa Al Mamun and Md. Adnan Kiber (2022). Assessment of the Condition of Pneumothorax Lungs using Anterior-Posterior Electrical Impedance Technique. International Conference on Physics in Medicine (ICPM), 58.

2.Alam, M.S., S M Mostafa Al Mamun and Md. Adnan Kiber (2020). Improved Electrical Impedance Measurement (EIM) Method for Lung Disease Detection. International Conference on Physics in Medicine (ICPM), 64

3.Alam, M.S., Md. Adnan Kiber, and S M Mostafa Al Mamun (2017). Simulation study of electrical impedance changes of normal lung compared to diseased lung of pulmonary edema using comsol multiphysics software. International Conference on Physics in Medicine & Clinical Neuroelectrophysiology, 53

Abstract

The Pneumothorax, Pulmonary Edema, Asthma, Acute Respiratory Distress Syndrome (ARDS), Chronic Obstructive Pulmonary Disease (COPD), Pneumonia, Influenza, Lung Cancer are the most common lung diseases. Lung diseases are the major public health burden all over the World including Bangladesh. According to the World Health Organization (WHO, 2020) lung diseases are the third leading causes of death in Bangladesh. People with Lung diseases become economic burden because they cannot perform their work properly and diagnostic and treatments cost a huge amount of money. X-rays, CT scan, Magnetic Resonance Imaging (MRI) are the existing techniques for the diagnosis of lung diseases. X-ray and CT scan are very harmful due to radiation. MRI has high resolution but it is very expensive and non-portable diagnostic system. As Lungs contain large volume of airs, so Ultrasound (US) imaging cannot be used for diagnosis of lung diseases. Due to Anatomical and Physiological changes the Electrical Conductivity, Relative Permittivity and Capacitance of cell membrane do change due to lung diseases. In case of Pulmonary Edema (water in the lung) and the Pneumothorax the electrical conductivity and relative permittivity values do change by large amount than that of a healthy lung. As Electrical current at 1mAat 50 KHz to 200 KHz has no known harmful effects on tissues. Therefore, Electrical Impedance Technique (EIT) method can be used for the assessment of various lung functions and lung diseases as a good complementary to other imaging techniques, though its resolution is low. The most used Electrical Impedance Technique (EIT) uses two surface electrodes for injecting a small amount of current 1 mA at 50 kHz and other surface electrodes are used for voltage sensing. There are four existing EIT Protocols for current injection and voltage measurements are namely-**(P1)** adjacent current drive, **(P2)** opposite current drive at the vertices of the semi-major axis of the chest cross section**, (P3)** opposite current drive at the vertices of the semi-minor axis of the chest cross section**, (P4)** opposite current drive along the right lung. In these existing EIT protocols electrodes are placed on the chest cross section at horizontal plane, the current drive electrodes and voltage sensing electrodes are at the same plane. The Proposed electrical impedance measurement protocol for lung function is Anterior-Posterior Electrical Impedance Technique (APEIT), where two current drive electrodes are placed at the anterior and posterior side of lungs and other eight voltage sensing electrodes at equal spacing in ellipsoid shape at vertical plane at the posterior side following the lung shape and size of lung.

To see the sensitivity of the above five (5) electrical impedance imaging protocols (P1, P2, P3, P4, and APEIT) of computer simulation is conducted by COMSOL Multiphysics software for small current of 1 mA at 50 kHz for assessing the lung functions at two different conditions like, lung at inspiration and at expiration for healthy lungs. In the computer simulation studies the Relative Electric Potential Change (REPC) values were computed for eight voltage sensing electrodes to see the sensitivity at **inspiration and expiration of healthy lungs** for all (5) protocols. The average REPC values were 1.41%, 1.84%, 1.34%, 2.29%, and **3.24%** for P1, P2, P3, P4, and APEIT EIT protocols respectively. The highest average REPC value for the APEIT protocol clearly indicates that this protocol is the most sensitive among all existing protocols for electrical impedance measurement of lung functions. It was found the sensitivity of eight voltage sensing electrodes are more smoothly distributed than all other EIT protocols. In both counts the proposed APEIT protocol is the best amongst all the protocols for electrical impedance measurement and imaging for lung functions.

The average REPC values were also computed for all above five (5) EIT protocols for the following lung conditions:**(a)** lung at inspiration and pneumothorax, **(b)**lung at expiration and pneumothorax**(c)** lung at inspiration and pulmonary edema, and **(d)** lung at expiration and pulmonary edema.

The average REPC values for **lung at inspiration and pneumothorax** of the mentioned five (5) protocols were: 2.97%, 3.89%, 2.41% **,**4.26% and **5.97%** respectively. For **lung at expiration and pneumothorax** the average REPC values were: 1.59 %, 2.10 %, 1.09 %**,** 2.02% and **2.82 % respectively**. The average REPC values for lung at **inspiration and pulmonary edema** were: 4.50 %, 5.99 %, 3.21 %**,** 5.80 % and **8.07 % respectively.** For **lung at expiration and pulmonary edema** the average REPC values were: 3.15 %, 4.24 %, 1.90 %**,** 3.59 % and **4.99 % respectively**. Above results clearly indicates that the above average REPC values in all cases the proposed APEIT protocol is the most sensitive than all other existing protocols for electrical impedance measurement and imaging for lung functions and lung diseases.

Computer simulation was also conducted for calculating the distinguishing factor for the proposed APEIT protocol for different sizes of tumor like,5%, 10%, and 20% of lung volume at the center of the right lung at inspiration and at expiration. Distinguishing factors indicates whether a disease lung condition like a tumor can be detected. The

distinguishing factors were 4.18%, 8.57% and 20.79 % for lung at inspiration, and 4.17%, 8.46% and 16.90 % for lung at expiration for 5%, 10%, and 20% of tumor sizes respectively. In both cases even a small size of the tumors less than 5% of lung volume can be detect by using the proposed APEIT protocol.

Computer simulation also been conducted for **Electrical impedance imaging spectroscopy** i.e. imaging at multiple frequencies namely: 20 kHz, 50 kHz, 100 kHz, 150 kHz, 200 kHz for lung at inspiration for fixed electrical conductivity values of : 0.0824 Sm^{-1} ,0.0927 Sm^{-1} ,**0.103 Sm^{-1}** , 0.1133 Sm^{-1} , and 0.1236 Sm^{-1} (i.e. **0.103 Sm^{-1} ± at steps 10%**) and at expiration for fixed electrical conductivity value of : 0.2096 Sm^{-1} , 0.2358 Sm^{-1} , **0.2620 Sm^{-1}**, 0.2882 Sm^{-1} and 0.3144 Sm^{-1} (i.e. **0.2620 Sm^{-1} ± steps of 10%**) to see the sensitivity to the proposed APEIT protocol to be used as EIT Spectroscopy. The sum of the eight surface electrodes potential for lung at inspiration decreased almost linearly from 591.98 mV to 562.82 mV for electrical conductivity of 0.0824 Sm^{-1},589.90 mV to 561.20 mV for electrical conductivity of 0.0927 Sm^{-1}, 587.97 mV to 559.63 mV for electrical conductivity of 0.103 $Sm^{-1,}$ 586.17 mV to 558.17 mV for electrical conductivity of 0.1133 Sm^{-1} and 584.50 mV to 556.75 mV for electrical conductivity of 0.1236 Sm^{-1} for the range of frequency: 20KHz to 200KHz. In case of lung at expiration the electric potential decreased almost linearly from 573.60 mV to 545.84 mV for electrical conductivity of 0.2096 Sm^{-1}; 571.11 mV to 543.81 mV for electrical conductivity of 0.2358 Sm^{-1}, 568.87 mV to 541.97 mV for electrical conductivity of 0.2620 Sm^{-1}, 566.87 mV to 540.27 mV for electrical conductivity of 0.2882 Sm^{-1}, 565.07 mV to 538.71 mV for electrical conductivity of 0.3144 Sm^{-1} for the same range of frequency. The simulation results show that the proposed APEIT protocol can also be used in **EIT spectroscopy** to identify the different lung diseases. The sum of eight surface electrodes potential values of lung at inspiration condition have higher value than at expiration condition,

For phantom study the Maltron Bio-Scan 920-11 system is used for electrical impedance measurements and for that a human thorax phantom was designed and made, following the dimensions of multipurpose digital chest phantom (Ref. https://www.ncbi.nlm.nih.gov/pmc/articles/PMC4169876). The proposed Anterior-Posterior Electrical Impedance Technique (APEIT) protocol was used for a single channel with four electrodes of Maltron Bio-Scan 920-11 system, where two driving electrodes are used for injecting 1 mA alternating current at 50 kHz and another two electrodes are used for electrical potential measurement. The different conductive material and having

ellipsoidal shape with porous foam representing lung (2.5cm × 9cm× 22 cm) was inserted at 8cm (fixed) away from the frontal of the chest surface in the phantom. Saline water having concentration of 0.54%, 0.72%, 0.90%, 1.08 %, 1.26% of NaCl, the corresponding electrical conductivities are: 0.952 Sm^{-1}, 1.210Sm^{-1},1.520Sm^{-1}, 1.858Sm^{-1}, 2.162 Sm^{-1} were used in phantom study to simulate the different conductive tissues of lungs. Eight voltage sensing electrodes potentials were computed and found that they have distinct electric potentials and the sum of the eight voltage sensing electric potential were 120.40 mV to 54.96 mV at 50 kHz frequency. Electrical conductivity (Sm^{-1}) for different concentrations of NaCl (%) in Phantom solutions have linear relationship and gave a straight line through origin. The sum of eight voltage sensing electrodes electrical potentials (mV) against the above mentioned concentrations of NaCl (%) in Phantom solutions or its corresponding electrical conductivity (Sm^{-1}) is negatively correlated, which is similar to computer simulation studies of the proposed Anterior- Posterior Electrical Impedance Technique (APEIT) protocol.

The proposed Anterior- Posterior Electrical Impedance Technique (APEIT) protocol found the most sensitive method for measurements of Electrical Impedances for the assessment of the lungs functions and diseases. However, it needs preclinical and clinical trials before practical use, in clinics and hospitals.

CONTENTS

CHAPTER -1. INTRODUCTION

CHAPTER-2: LITERATURE REVIEW

CHAPTER-3: THE HUMAN BODY AND RESPIRATORY SYSTEM

CHAPTER-4: ELECTRICAL IMPEDANCE IMAGING METHODS

CHAPTER-5: COMPUTER SIMULATIONS FOR DIFFERENT LUNG CONDITIONSAND PHANTOM STUDY

PhD Thesis Title: Development of Electrical Impedance Technique for Assessment of Lung Function.

CHAPTER -1. INTRODUCTION

Chapter-1. Introduction

1.1 Introduction:

All biological organism including human consists of billions of cells. Different cells are combined themselves to form important organs, like lungs, brain, hearts etc. In a broad sense, cells of organs consist of extracellular & intracellular fluids and bi-lipid cell membrane separating them. Different materials and ions are suspended in the cell fluids, hence, biological tissues and organs have different electrical conductivities, relative permittivity and capacitive properties. These values do change due to structural and physiological changes of tissues and organs. Therefore, electrical impedance measurement may represent the status of tissues and organs, and are used for diagnostic and monitoring purposes. The Pneumothorax (Collapsed Lung), Pulmonary Edema, Asthma, Acute Respiratory Distress Syndrome (ARDS), Chronic Obstructive Pulmonary Disease (COPD), Pneumonia, Influenza, Lung Cancer are the most common lung diseases. Lung diseases are the major public health burden all over the World including Bangladesh. According to the World Health Organization (WHO) published data in 2020 lung diseases are the third leading causes of death in Bangladesh [5]. People with Lung diseases become economic burden because they cannot perform their work properly and diagnostic and treatments cost a huge amount of money. X-rays, CT scan, Magnetic Resonance Imaging (MRI) are the existing techniques for the diagnosis of lung diseases. X-ray and CT scan are very harmful due to radiation. MRI has high resolution but it is very expensive and non-portable diagnostic technique. Lungs contain large amount of gases, so Ultrasound (US) imaging cannot be used for diagnosis of lung diseases. Due to Anatomical and Physiological changes the Electrical Conductivity, Relative Permittivity and Capacitance of cell membrane do change due to lung diseases. As the Electrical measurements at a low current (1mA), at 50 KHz frequency has no known harmful effects on tissues. Therefore, Electrical Impedance Technique (EIT) method can be used for the assessment of various lung functions and lung diseases as a good complementary to other imaging techniques, though its resolution is low.

1.2 Bioimpedance

Animals and plants are living object made up of biological cells which contains intracellular fluids (ICF) and extracellular fluids (ECF) and show a frequency dependent behavior to an alternating electrical signal. Bioelectrical impedance analysis (BIA), electrical impedance spectroscopy (EIS), electrical impedance plethysmography (IPG), impedance cardiography (ICG) and electrical impedance tomography (EIT) are electrical impedance based noninvasive tissue characterizing techniques. These are being used to study the frequency response of the electrical impedance of biological tissues [3,51]. Bioimpedance deals with some passive electrical properties of tissue: the ability to oppose (impede) electric current flow. On the other hand, Bioelectricity deals with the ability of tissue to generate electricity, as for instance done by the heart. The electricity used for measuring bioimpedance is exogenic i.e., with externally applied electric current or voltage. There is a duality in the electrical properties of tissue: tissue may be regarded as a volume conductor or a dielectric. In the frequency range less than 100 kHz, most tissues are predominantly electrolytic conductors. At higher frequencies, the dielectric properties of tissue may have some impact. At the highest frequencies tissue properties become more and more like to that of water, pure water has a characteristic relaxation frequency of approximately 18 GHz [1, 3].

1.3 Mathematical Explanation of Bioimpedance

Bioimpedance is an important electrical property of tissues that is characterized by resistance and capacitance. The resistance is the measure of the level to which a tissue opposes the flow of ions among its cells (obey Ohm's Law (Equation 1.2.1) to current, and capacitance is the property of an electric conductor which is measured by the amount of electric charge separation that can be stored and released in the form of electrical potential.

$$Z = \frac{V}{I} = \frac{|V|e^{j\theta_v}}{|I|e^{j\theta_i}} \text{----------(1.3.1)}$$

Cells may be modeled as simple group of electronic components, Figure 1.1, where the extracellular space is represented by a resistor (R_{ext}), and the intracellular space and the membrane being modeled by a resistor (R_{in}) and a capacitor (C_m).

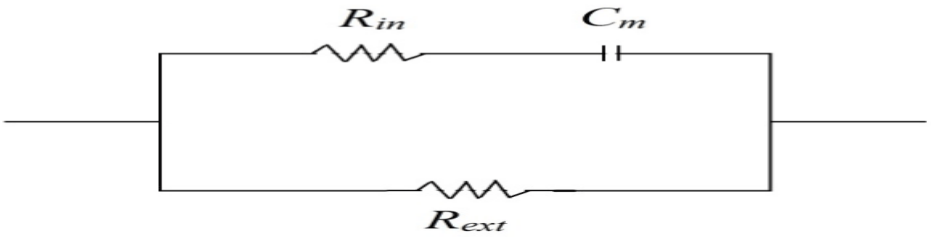

Figure 1.1: Cell Electronic Model.

Because of this model rough prediction of biological tissue behavior, the complex admittance, to model the behavior of a material under the influence of external electromagnetic radiation,

$$Y = \frac{1}{Z} = G + j\,B = \frac{A}{d}\gamma = \frac{A}{d}(\sigma + j\,\omega\epsilon) \text{----------(1.3.2)}$$

Where Y is the complex admittance, G is the conductance, B the susceptance. The complex admittivity, electric conductivity and dielectric permittivity are represented by γ, σ and $\in$ respectively. Finally, A/d is a scaling factor to separate geometrical properties from the constitutive ones and ω the angular frequency.

Whenever A/d is kept constant and the electrodes position remains unaltered, the only changes between impedance measurements are due to changes of target tissue position(r) and angular frequency (ω) in complex admittivity:

$$\gamma(r,\omega) = \sigma(r,\omega) + j\omega\epsilon(r,\omega) \text{----------(1.3.3)}$$

If the tissue under analysis is considered to be isotropic, a simplification commonly found in bioimpedance studies, the dependence on r falls and so $\gamma(r,\omega) = \gamma(\omega)$.

The admittivity dependence on frequency was subject of extensive study over the years, in which is highlighted the work done by Schwan [1988] on the relative permittivity decrease at high frequencies variations in three main steps. These non-linear variations of admittivity with frequency, called dispersions, are found:

-At 10^9Hz the γ dispersion is due to the polarization of water molecules.

- The β dispersion, in the 10^4 Hz region, is due mainly to the polarization of cellular membranes (like barriers to the flow of ions).
- The low frequency α dispersion is associated with ionic diffusion processes in cellular membrane.

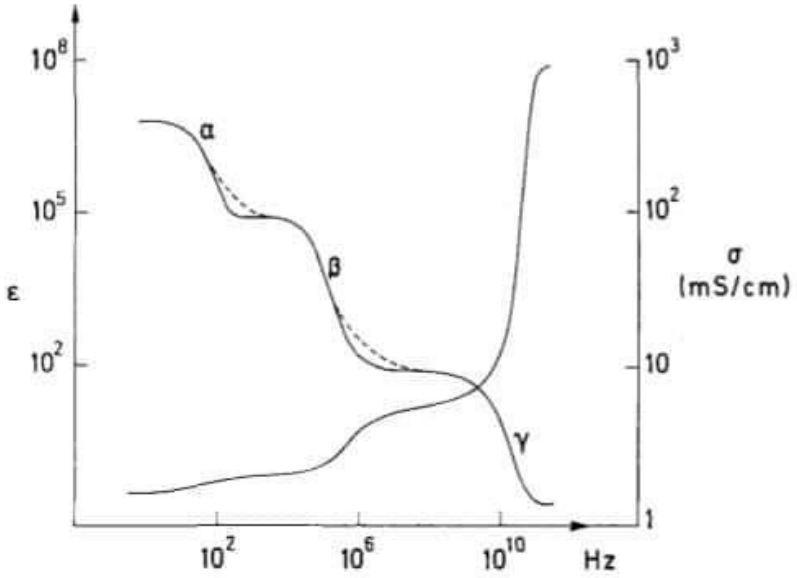

Figure 1.2: Admittivity dependence on frequency, α, β and γ dispersion. Dashed curves indicate additional, and smaller, relaxation effects (Schwan [1988]).

With this diverse information about the internal constituents of the body (cell size and orientation or membrane thickness or water content) there is a great deal of information contained in a bioimpedance map of the body. As such, changes in this map imply a physiological or pathological change that can be monitored and measured [12,13].

Table 1.1: Mean Conductivity and Relative Permittivity values for tissues of interest at 1MHz (required for better tissue characterization-β dispersion). Taken from Hasgall et al. [2014].

Tissue	Electrical Conductivity (σ) Sm^{-1}	Relative Permittivity (ϵ_r)
Heart	3.28×10^{-1}	1.97×10^{3}
Blood	8.22×10^{-1}	3.03×10^{3}
Lung	1.36×10^{-1}	7.33×10^{3}
Liver	1.87×10^{-1}	1.54×10^{3}
Subcutaneous Fat	4.41×10^{-2}	5.08×10^{1}
Bone	2.44×10^{-2}	1.45×10^{2}
Muscle	5.03×10^{-1}	1.84×10^{3}

In the biological tissue, the membrane behaves as a dielectric or an insulator separating two conducting media (Grimnes and Martinsen, 2008); the extra-cellular fluid and the intra-cellular fluid. These fluids act the role of armatures of the biological capacitor. Since the membranes are not good insulators, they act like leakage capacitors. Current at low frequencies does not penetrate cell membranes because of the high reactance of the membrane capacitance, but will pass through cell membrane at higher frequencies because the reactance will be relatively lower (Figure 1.3) [1,2].

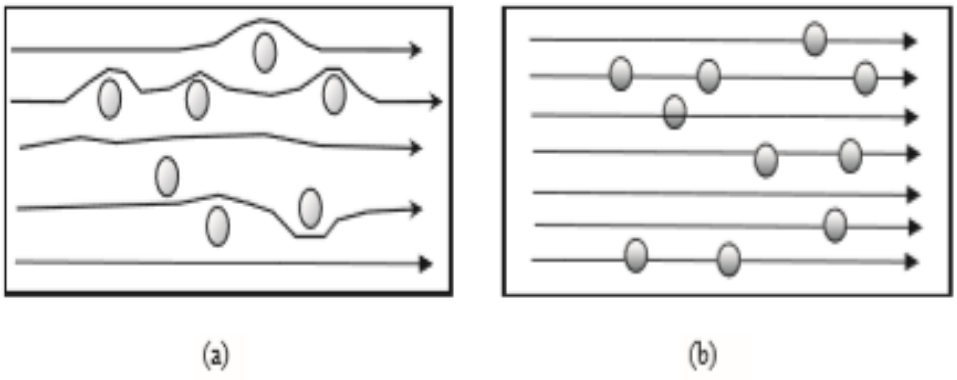

Figure-1.3: Current flow through the cell at (a) low frequency (b) high frequency.

1.4 Introduction to the Respiratory System

The respiratory system is one of the important organs in human body. Lungs are the most important organ of the respiratory system and its main function is gas exchange, it delivers oxygen (O_2) to the blood and remove carbon dioxide (CO_2) from it [6]. Respiratory organ provides maximum surface area (alveolar spaces) for diffusion of O_2 and CO_2.Respiratory function is covered by clinical area where the Scientist with required knowledge of many aspects of physics and engineering can help the clinician in the diagnosis of disease. The lung tissue has higher impedance than the muscle. The lung impedance is higher during inspiration than during expiration due to inhalation of insulating air. Inhalation and Exhalation is the integral to the management of lung function testing hence diseases. Some functions and diseases of lung(s) changes the electrical conductivities of lung tissue and fluids [4, 7]. Resistivity of the lung at 50 kHz during expiration is 12.5 Ω-m and inspiration is 25Ω-m (RieraJ, et al.-Medicina Intensiva-2011). Air enters at breathe-in, thereby increases the impedance of lung and reduces at breathe out. Accumulation and distribution of different body fluids take place within the lungs due to different lung diseases like-pulmonary edema, acute respiratory distress syndrome. These fluids have different electrical conductivity (σ) and relative permittivity (ϵ) than that of normal healthy lung tissues. Diseased lung is expected to have different electrical conductivities and relative permittivities from normal & healthy lungs. In case of fluid accumulation pulmonary edema, acute respiratory distress syndrome in the lungs, due to the downward pull of gravitation, it is expected that larger amount of fluid (volume) will be accumulated in the lower part of lung compared to that of upper part. Since different lungs conditions produce different electrical conductivities. It is hope that distributed measured lung electrical impedance would reflect the lung condition (normal/diseased). Cells in the body have both resistive and capacitive properties and these are typically embedded in a fluid medium with resistive properties. These electrical conduction properties vary from organ to organ, with tissue morphology, physiological dynamic phase, health and disorder. Electrical conductivity and relative permittivity of healthy lung at inspiration is 0.103 (S/m) and 4272.50, and expiration is 0.262(S/m) and 8531.40 [24]. By displaying the distribution of air in the lungs conditions such as Pulmonary Edema, Pneumothorax, Emphysema, and Pneumonia may be investigated. Because peoples are frequently affected of these lung diseases

[4, 51]. Like Pulmonary Edema (i.e. water in the lung) and Pneumothorax (i.e. Collapsed Lung) have the significant change of electrical conductivity values than a healthy lung [24, 33].

1.5 Motivation of this Research

In Bangladesh, over the past decade there has been a significant decline in infant and child mortality, control and prevention of diseases, such as measles, poliomyelitis, and diphtheria along with widespread use of oral saline for diarrheal diseases have great reduced childhood mortality and morbidity. WHO (World Health Organization) is specialized agency of the United Nations. WHO has been working in Bangladesh since 1972.The objective of WHO is the attainment of highest possible level of health by all people. According to the WHO report published in 2018 life expectancy in Bangladesh, for Male 71.1 years, and for female 74.4 years and the average life expectancy is 72.7 years which gives Bangladesh a World Life Expectancy ranking of 97. Peoples are suffering from different lung diseases which causes to death. WHO report in 2018 death due to Lung Disease in Bangladesh reached 64,762 or 8.34 % of total deaths. The age adjusted Death Rate of Lung Disease is 61.82 per 100,000 of population ranks of Bangladesh is 3 and among the world is 7. So, lung diseases and its functions assessment are very important for human life. In this context our attempt to develop methods to easily assess the lung diseases to help the people Live Longer Live Better, & also reducing the excess mortality, morbidity and promoting healthy lifestyles [4,5].

1.6 Introduction to Electrical Impedance Tomography (EIT)

Electrical Impedance Tomography (EIT) is an imaging technique in which an image of the conductivity of a part of a body is inferred from the surface electrical measurements. Most Researchers around the world uses 1 mA alternating current at 50 kHz for EIT technique for human subjects which is assumed to be safe and non-health hazard for biological tissues. In its simplest form, EIT is accomplished by placing electrodes on the surface of the body and passing a current between two of them while measuring the voltages induced on the other electrodes. From these measurements an inverse calculation is performed to find changes in electrical conductivity across the section of the body defined by the surface electrodes. EIT is used on the thorax to measure impedance changes due to investigate the presence of air and blood in the lung. EIT is a relatively new technique being used to study the frequency response of the electrical impedance of biological tissue. EIT has become increasingly important for bedside continuous monitoring of ventilation distribution [3,9]. EIT has several advantages over other computed tomographic imaging techniques used for medical imaging applications. It is noninvasive, radiation free, on-ionizing, low cost, portable, user-friendly and non-health hazardous method [19,75].

1.7 Aims and Objectives of this Study

According to the World Health Organization (WHO) report in 2018 death due to lung diseases rank three in Bangladesh, and seven in the World [5]. Peoples are suffering from various lung diseases like- Pulmonary Edema, Pneumothorax, Pneumonia, Asthma, COPD (Chronic Obstructive Pulmonary Disease), Coronavirus (COVID-19) (Latest WHO report, April,2020) etc. which are serious issue to public health and causes to death. The existing techniques for diagnosis of lung diseases are X-ray, CT scan, MRI (Magnetic Resonance Imaging), EIT (Electrical Impedance Tomography). X-rays and CT scan are very harmful due to radiation. Though MRI has high resolution but it is very expensive and it is non-portable diagnosis technique. It is a relatively new diagnostic technique in healthcare [12,13].

Now talk of the World is Corona Virus which directly affects on the respiratory system. So, existing diagnostic methods like- X-ray, CT scan, MRI are not suitable for continuous lung condition monitoring. Patients with serious or critical conditions

the continuous monitoring of lung conditions are very important. So, that corresponding therapeutic actions can be applied continuously or immediately. This is a lifesaving procedure or protocol for patients. Electrical Impedance Technique is a non-invasive, non-radiative, non-health hazard imaging technique, therefore can be applied to monitor the lung conditions continuously. Till to date there is no other diagnostic technique that can be continuously monitor the lung condition.

Objectives of this study are-

i)To study the sensitivity and accuracy of data for the four existing EIT protocols (like-adjacent current drive, opposite current drive at the vertices of the semi-major axis of the chest cross section, opposite current drive at the vertices of the semi-minor axis of the chest cross section, opposite current drive along the right lung) by computer simulation for assessing lung functions of healthy lung at inspiration and expiration.

ii) To study the sensitivity and accuracy of data for the proposed Anterior-Posterior Electrical Impedance Technique (APEIT) protocol by computer simulation for assessing lung function of healthy lung at inspiration and expiration.

iii) To study the sensitivity and accuracy of data using four EIT protocols by computer simulation for assessing lung functions of healthy lung at inspiration and collapsed lung (pneumothorax)

iv) To study the sensitivity and accuracy of data for the proposed APEIT protocol by computer simulation for assessing lung function of healthy lung at inspiration and collapsed lung (pneumothorax).

v)To study the sensitivity and accuracy of data using existing EIT protocols by computer simulation for assessing lung functions of healthy lung at expiration and collapsed lung (pneumothorax)

vi) To study the sensitivity and accuracy of data for the proposed APEIT protocol by computer simulation for assessing lung function of healthy lung at expiration and collapsed lung (pneumothorax).

vii) To study the sensitivity and accuracy of data using four EIT protocols by computer simulation for assessing lung functions of healthy lung at inspiration and pulmonary edema.

viii) To study the sensitivity and accuracy of data for the proposed APEIT protocol by computer simulation for assessing lung function of healthy lung at inspiration and pulmonary edema.

ix) To study the sensitivity and accuracy of data using four EIT protocols by computer simulation for assessing lung functions of healthy lung at expiration and pulmonary edema.

x)To study the sensitivity and accuracy of data for the proposed APEIT protocol by computer simulation for assessing lung function of healthy lung at expiration and pulmonary edema.

xi) To study proposed APEIT protocol for a single frequency by computer simulation for different electrical conductivities referring healthy lung at inspiration.

xii) To study proposed APEIT protocol for multi frequency by computer simulation for different electrical conductivities referring healthy lung at inspiration.

xiii) To study proposed APEIT protocol for a single frequency by computer simulation for different electrical conductivities referring healthy lung at expiration.

xiv) To study proposed APEIT protocol for multi frequency by computer simulation for different electrical conductivities referring healthy lung at expiration.

xv) To study proposed APEIT protocol for a single frequency by computer simulation for tumor at lung in inspiration condition.

xvi) To study proposed APEIT protocol for a single frequency by computer simulation for tumor at lung in expiration condition.

xvii) To design and construct a human thorax for phantom study to see the sensitivity of the proposed APEIT protocol, using Maltron Bio-Scan 920-11 system.

1.8 Layout of this Dissertation

Theoretical and mathematical aspects of bioimpedance have been discussed with the introduction to respiratory system and electrical impedance tomography in **chapter one**. **Chapter two** contains some relevant scientific reviewed papers on electrical impedance imaging and its application in the healthcare. Like it is widely used in lung functions assessment and also continuous monitoring, breast imaging, brain imaging and sports medicine. In **chapter three** described the human body, the respiratory system and also the mechanics of breathing. Biomedical engineering point of view to apply physics in the respiratory system and particularly diagnosis in the lung diseases. Some common pulmonary function testing methods and lung diseases are discussed here. Some existing electrical impedance imaging methods have discussed in the **chapter four.** COMSOL Multiphysics simulation software version 4.3 has been described briefly in **chapter five** on the basis of AC/DC Module and also this chapter contain computer simulation studies on Existing Electrical Impedance Tomography (EIT) protocols and our proposed Anterior-Posterior Electrical Impedance Technique (APEIT) protocol applied on computer generated human chest phantom for single frequency at different electrical conductivities and also multi frequency (frequency spectrum) at constant electrical conductivities. Single frequency simulation study has been done on Tumor added lung. Maltron BioScan 920-11Analyzeralso used on different concentration of NaCl (%) solutions in Phantom. **Chapter six** contain the computer simulation results for different lung conditions on the basis of chapter five and made detail conclusion & discussion on those results. References (Bibliography) is in **chapter seven.**

CHAPTER-2: LITERATURE REVIEW

Chapter-2: Literature Review

2.1 Introduction

A relatively new impedance imaging technique is known as Electrical Impedance Tomography (EIT) has been developed during the last few decades. It uses a small amount of alternating electric current /voltage and computes or measure the voltage /current developed due to the impedance distribution within the subject. The important features of this technique are, it is non-invasive, non-ionizing, portable, and comparatively inexpensive system that allows real-time imaging of electrical impedance of a subject under test. The EIT method is now widely used in many areas of research and applications such as in clinical environment, including healthcare ecosystems for diagnostics and monitoring purposes, biotechnology, chemical engineering, material engineering, nondestructive testing (NDT), civil engineering, geoscience, environmental engineering etc. [3,9,12]. For lung functions monitoring usually X-rays, CT scan, MRI imaging methods are used. However, X-rays imaging technique and CT scan are uses X-rays as a interacting energy which is harmful for human tissues and organs, therefore can't be used for continuous imaging. On the other hand, though MRI is relatively safe but very expensive and non-portable, therefore, it can't be used for bedside continuous monitoring. In 1983 EIT was first used to monitor respiratory function and remains the only bedside method that allows repeated, non- invasive measurements of lung volume changes [9]. Although EIT has some constraints like low resolution, may play the lead as a diagnostic and guiding tool for an effective of mechanical ventilation in critically ill patients with severe respiratory diseases. EIT contributes to the management of life – threatening lung diseases such as pneumothorax, pulmonary edema, pneumonia, ARDS including patients with covid-19, and also aids in guiding fluid management & ventilation in the critical care setting [9, 12, 19].

2.2 Electrical Impedance Tomography on Lung Functions

The aim of this PhD research work is to develop new protocols for current injection and voltage measurements to improve the sensitivity due to impedance distribution for the detection of pneumothorax and pulmonary edema as well as other lung diseases.

A review of short summaries of many published research work on electrical impedance tomography (EIT) for the detection and monitoring of different lung diseases are described in this section in chronological order.

1. Alien Fein et al. [1979] studied on normal and pulmonary edema diseased patients for the measurement of transthoracic electrical impedance which may be used in clinic. They made their opinion that the clinical state of patients either at risk of developing or with pulmonary edema can be measured by the changes in transthoracic electrical impedance. If the patient's lung with pulmonary edema, the lungs volume will decrease for the presence of fluid in the lungs [21].

2. J. H. Campbell et al. [1994] used electrical impedance tomography system in Sheffield UK for the detection of the changes in intrathoracic fluid. They assessed the changes in lung resistivity for a normal subject and the relationship between the increasing lung resistivity and the lung inflate is approximately in linear character**.** They concluded that the measured electrical potentials using electrical impedance tomography (EIT) method is non-invasive and sensitive for small changes in intrathoracic fluid in disease conditions [22].

3. S. Nebuya et al. [2007] studied on seven normal male subjects of aged between 20.80 yrs to 23.40 yrs by using a Sheffield MK 3.5 EIT system for the accuracy of pulmonary function test and conducted indirect measurement. They compared the EIT data with Spirometry data. They calculated the errors in tidal volumes during tidal and deep breathing, vital capacity, residual volume and functional residual capacity were 20±7.4%, 18±8.4%, 64±49%, 32±15% and 35±17% respectively. They commented that the EIT method can be used for the assessment of tidal volumes during tidal and deep breathing with good accuracy and is possible without aspiration of helium gas [23].

4. Eduardo L.V. Costa et al. [2009] reviewed many research papers on the use of electrical impedance tomography for the critical care patients of lung diseases. They found that EIT has high sensitivity for detection of lung diseases like- pulmonary thromboembolism, advanced chronic obstructive pulmonary disease and acute respiratory distress syndrome (ARDS). The lung recruitment is one of the important steps for mechanical ventilation for critical patients with severe lung diseases They said electrical impedance technique (EIT) can be potential solutions for optimize mechanical ventilation [26].

5. Satoru Nebuya et al. [2010] studied on the mechanical ventilator supported patients for the measurement of lung function by using electrical impedance tomography (EIT)technique. They found that the regional lung densities between the normal lung and diseased lungs associated with pneumonia, atelectasis and plural effusion have significantly different. They observed the changes in lung density using EIT was in good agreement with the results of clinical diagnosis based on X-ray and CT images. These results based on EIT system also gave the feasibility to obtain a quantitative value for regional lung density with no risk of exposure to harmful radiation like-X-ray and CT images [27].

6. Inez Frerichs et al. [2010] studied on the experimental and clinical by using the electrical impedance tomography (EIT) technique and found its potential technique in monitoring regional lung ventilation and aeration at the bedside. They said that this technique can be employed in ARDS (Acute Respiratory Distress Syndrome) patients monitoring. They also found that the electrical impedance will be lower for the accumulation of fluid in the interstitial and alveoli. By performing EIT examination the very good time resolution and dynamic changes in regional lung volumes can easily be assessed. The regional response of the lung tissue gradually change in airway pressure can be studied by EIT and determined the regional respiratory time constants. EIT technique can be potentially found for regional over distension, collapse and recruitment, and it can be used to optimize the ventilator settings and minimize the incidence of ventilator- induced lung injury [28].

7. Denai,M.A.et.al [2010] studied on EIT technique on mechanical ventilation, lung recruitment and on a comprehensive physiological model of lungs. They found that the satisfactory outcome of respiratory physiology and EIT monitoring techniques in

mechanically ventilated patients. They developed computer simulation based model on respiratory physiology and demonstrated that EIT technique can be effectively used in monitoring for mechanical ventilation of ARDS (Acute Respiratory Distress Syndrome). Electrical Impedance Tomography system MK 3.5 is used at the Northern General Hospital (Sheffield, UK) for mechanically ventilated ICU patients and found the good agreement with the said model [29].

8.Pikkemaat R.et al.[2012] studied on the pulmonary function test for the assessment of the severity of obstructive and restrictive lung diseases considering the physical properties of flow resistance and compliance. They obtained positive correlation (r=0.88) between the flow resistance and global time constant, $\tau_{\text{global.}}$ Finally, they commented that their newly introduced regional time constant (RTC) would be enable to visualize the local effects of therapy for obstructive lung disease patients using EIT [30].

9.Wojciech Durlak et al. [2013] reviewed some research papers on electrical impedance tomography (EIT)and found its possible applications in clinical practice in pediatric respiratory medicine. EIT can be used to monitor regional ventilation for children, neonates, and infants distribution over extended periods of time. It can also be used in critically ill newborns and infants and it also be used lung perfusion monitoring. However, in case of lung perfusion sensitivity is relatively low [31].

10. Tushar Kanti Bera [2014] reviewed on the non-invasive health monitoring methods like- bioelectrical impedance and tissue characterization. Some tissue parameters do vary with the applied electrical signal frequency over a wide range. He concluded that Electrical Impedance Spectroscopy (EIS) can be used to find tissue parameters, i.e., tissue characterization can be performed using EIS [32].

11. Deborshi Chakraborty et al. [2014] conducted of 3D simulation study using Finite Element Method (FEM) for monitoring the condition of lungs and heart of Acute Respiratory Distress Syndrome (ARDS) patients. They concluded that the structural changes in the lung due to the gravitationally dependent downward pull like in the case of pulmonary edema. They found satisfactory result for the detection pulmonary edema disease [33].

12. Brain K Walsh et al. [2016] studied on the electrical impedance tomography technology for its clinical application to the monitoring mechanical ventilation of the respiratory patients. They showed that EIT technique to be useful for the detection of pneumothoraxes, quantification of pulmonary edema and also it can compare to the distribution of ventilation between different modes of ventilation [34].

13.Gong B. et al. [2016] studied on the Electrical Impedance Tomography (EIT) in lung horizontally 16 electrodes were placed on the thorax. A small amount of alternating currents were injected through electrodes attached to the skin and a set of induced voltage collected due to impedance distribution. The adjacent current injection pattern is sub-optimal and it is commonly used in EIT devices. They modified the boundary conditions according to the superposition principle of the electrical field [35].

14. Inez Frerichs et al. [2017] suggested that the functional chest examinations with Electrical Impedance Tomography (EIT) are clinically applicable for observing regional lung ventilation in mechanically ventilated patients and for local pulmonary function testing in patients with chronic lung diseases. EIT is also sensitive to periodic and non-periodic changes in electrical tissue conductivity. An increase in intrapulmonary gas volume then decrease conductivity and it may be happened while increased blood or fluid volume. These images may clinically relevant measures to assess the present state of ventilation distribution and its trends [36].

15. Szymon Bialka et al. [2017] studied on the case report and reviewed literature on the electrical impedance tomography (EIT) for diagnosis and monitoring of pulmonary function disorders in the intensive care unit. They observed an improvement of regional ventilation of the upper and middle segments of the left lung and it has similar with laboratory test results, especially arterial blood gas analysis. EIT technique can be used in both mechanically ventilated and spontaneously breathing patients and it is relatively suitable than all other methods [37].

16. Beatriz Lobo et al. [2017] reviewed many research papers on the Electrical Impedance Tomography (EIT) and its applications on many diagnostic purposes. They found that the EIT technique can be used as the continuous assessment of respiratory status of modern intensive care unit (ICU), the monitoring systems of

mechanical ventilation in critical ill patients, to the management of life- threatening lung diseases such as pneumothorax, and aids in guiding fluid management in the critical care setting. EIT for lung can be a diagnostic and a guiding tool for an adequate optimization of mechanical ventilation in critically ill patients, especially on acute respiratory distress syndrome (ARDS) [38].

17. Schullcke B, et al. [2017] conducted the simulation study on the ventilation inhomogeneity measured with electrical impedance tomography. They simulated the mechanically ventilated patients to monitor the regional distribution of ventilation. They studied on the three dimensional (3D) simulation models with different severities of obstruction to realize the impact of ventilation inhomogeneity and lung obstruction on the reconstructed of EIT images. They found EIT images gave the obstructions affecting less than 25% of lung tissue with ventilation inhomogeneity [39].

18. Bachmann MC et al. [2018] reviewed many research papers on electrical impedance tomography (EIT) in acute respiratory distress syndrome (ARDS). They expressed their opinion about EIT and it could be used as a monitoring tool to evaluate the distribution of pulmonary ventilation continuously and optimizing mechanical ventilation parameters in critically ill patients at the bedside. They found different indices like-center of ventilation (Cov), global inhomogeneity index (GI), regional ventilation delay (RVD) index is found from EIT technique and these indices may be used for acute respiratory distress syndrome (ARDS) patients [40].

19. Alessandro et al. [2018] reviewed on many thoracic electrical impedance tomography research papers to demonstrate the present clinical applications on electrical impedance tomography (EIT). They gave emphasis on the setting of pediatric patients and the perioperative (adult and pediatric). They suggested that the non-radiative and non-health hazardous electrical impedance tomography (EIT) technique could be particularly interesting and useful in the pediatric population. Finally, they suggested the clinical management based EIT parameters are alveolar recruitment and lung heterogeneity, which can reduce mortality of Acquired Respiratory Distress Syndrome (ARDS) patients [41].

20.Yan Shi et al. [2021] reviewed on the research progress on image reconstruction, hardware, and clinical applications in lung diseases using the electrical impedance tomography (EIT). They found that EIT is suitable technique for lungs diseases detection, monitoring and treatment for its non-invasive and non-radiative properties. Thus, EIT technique may be used for the early detection of lung diseases and continuous monitoring. They recommended for further development of EIT technique for clinical uses [122].

21.Fedi Zouari et al. [2022] designed on respiratory disease devices which may be applied for lung function screening and monitoring both at homes and clinics. They designed and developed an affordable, and portable, electrical impedance tomography (EIT) system for home- based lung function assessment and telemedicine. With the target of regional mapping of lungs for spirometry indicators MVE, EV1, MEF etc. by producing its images. However, they used electrodes belt at horizontal plane at the chest for measurement and did not describe about the electrical impedance device [123].

CHAPTER-3: THE HUMAN BODY AND RESPIRATORY SYSTEM

Chapter-3: The Human Body and the Respiratory System

3.1 Introduction to the Human Body

Human body is made of basic building blocks called cells that work together to accomplish the specific functions necessary for sustaining life. The human body works properly with eleven organ systems. The systems are- Integumentary System, Skeletal System, Muscular System, Nervous System, Endocrine System, Cardiovascular System, Lymphatics and Immune System, Respiratory System, Digestive System, Urinary System and Reproductive System. Figure 3.1 shows human boy that include the brain, heart, lungs, spleen, muscles, stomach, kidneys and more [7].

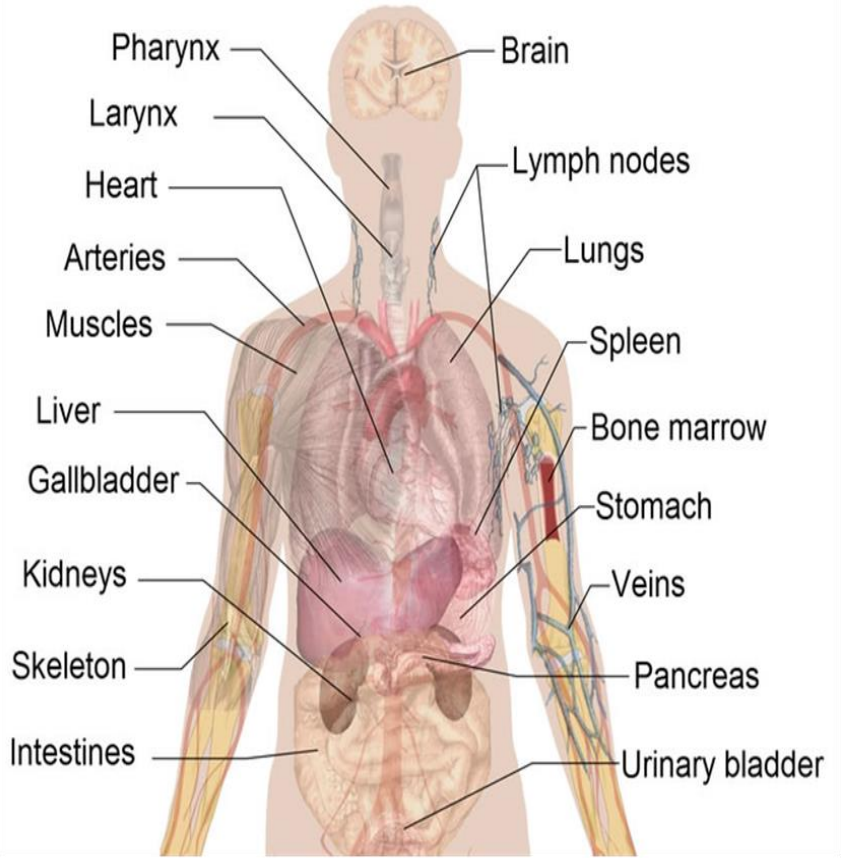

Figure 3.1: Human Organs and Anatomy

3.2 Human Respiratory Organ System

The respiratory organ is one of the most important systems of the above mention eleven system of the human body. A pair of lungs is important organ of the respiratory system. It takes air and supplies oxygen(O_2) to the blood circulatory system and gives off carbon dioxide (CO_2) into the air [Figure-3.2] [51]. The main job of the respiratory system is to move fresh air into our body while removing waste gases and to maintain acid-base balance [5]. Right lung and left lung are not same in size. The right lung is a little wider than the left lung [50]. Human respiratory system with its different parts are shown in the figure 3.2.

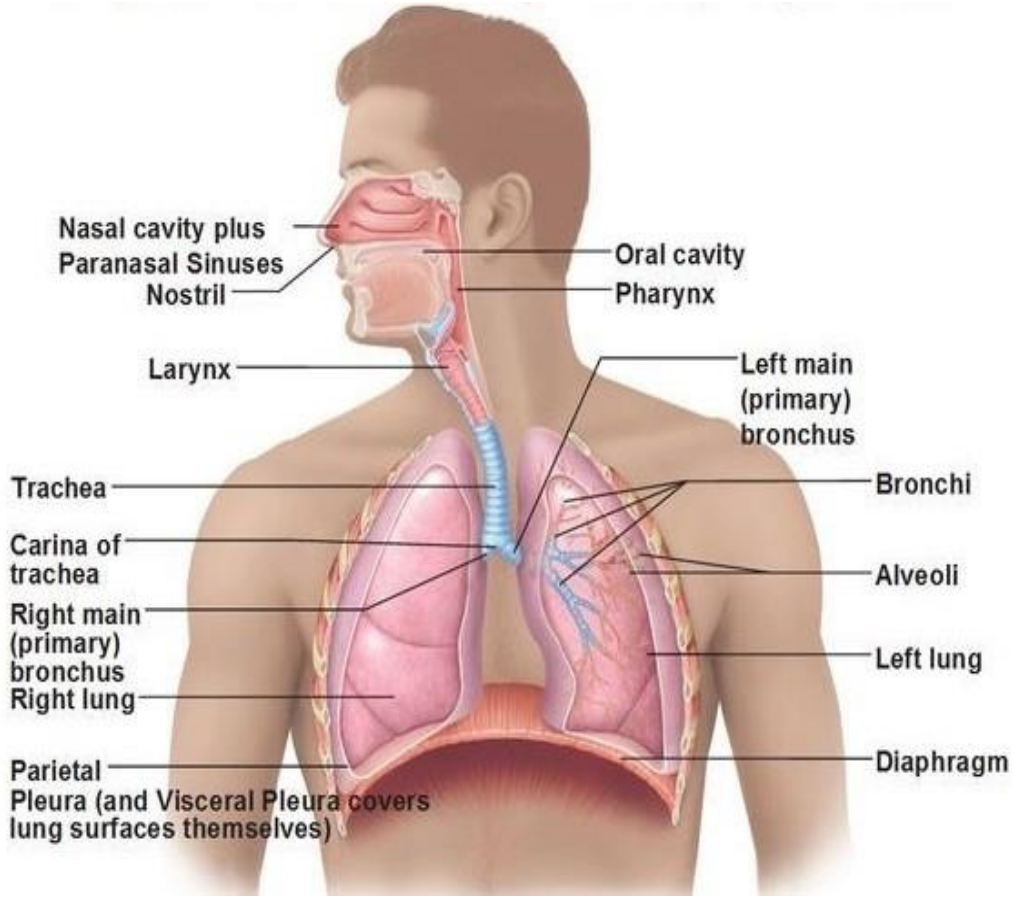

Figure 3.2: Human Respiratory System.

Males lungs capacity is more than female, and normal a male's lungs can hold around 750 cc of air, while a female's can hold around 285 cc to 393 cc of air [50].

3.3 The Mechanics of Breathing

The mechanics of breathing (respiration) involve muscles that change the volume of the thoracic cavity to generate inspiration (intake) and expiration (exhaust). Inspiration and expiration are two main steps in breathing [4]. Normally we breathe in 6L air per minute. We inhale (inspire) 1.2 L oxygen/min which is 20% of air. Normally breathing rate is 12/min for men, 20/min for women, and up to 60/min for infants. The air we inhale has 80% N_2, 20% O_2 (or more precisely 78.084% N_2, 20.947% O_2, 0.934% Air, 0.035% CO_2), and the air we exhale (expire) has 80% N_2, 16% O_2, 4% CO_2 [51].

Inspiration: The process of breathing in is called inspiration or inhalation, by which air is brought into the lungs following some steps [49]. The sequence in inspiration (inhaling) are shown in figure 3.3. The diaphragm and external intercostal or inspiratory muscles increase the dimensions of the rib cage (the thoracic cavity). This causes the visceral and parietal pleurae to separate. The lung volume then increases because

(i) the attraction of the visceral and parietal increases as they are separated further and

(ii) this separation causes P_{lung} - P_{pleura} to decrease even more, from ~ -4 to ~ -6 mmHg (i.e., from ~756 mmHg to 754 mmHg absolute pressure). Because both of these forces in the direction of lung expansion increase, they now overcome the springiness of the lungs that favors lung contraction – and the lung expands. The pressure in the lungs and alveoli decreases from ~ 0 to ~ - 1 mmHg (i.e., from ~ 760 mmHg to 759 mmHg absolute pressure), and then air flows from the mouth and nose into the lungs [51].

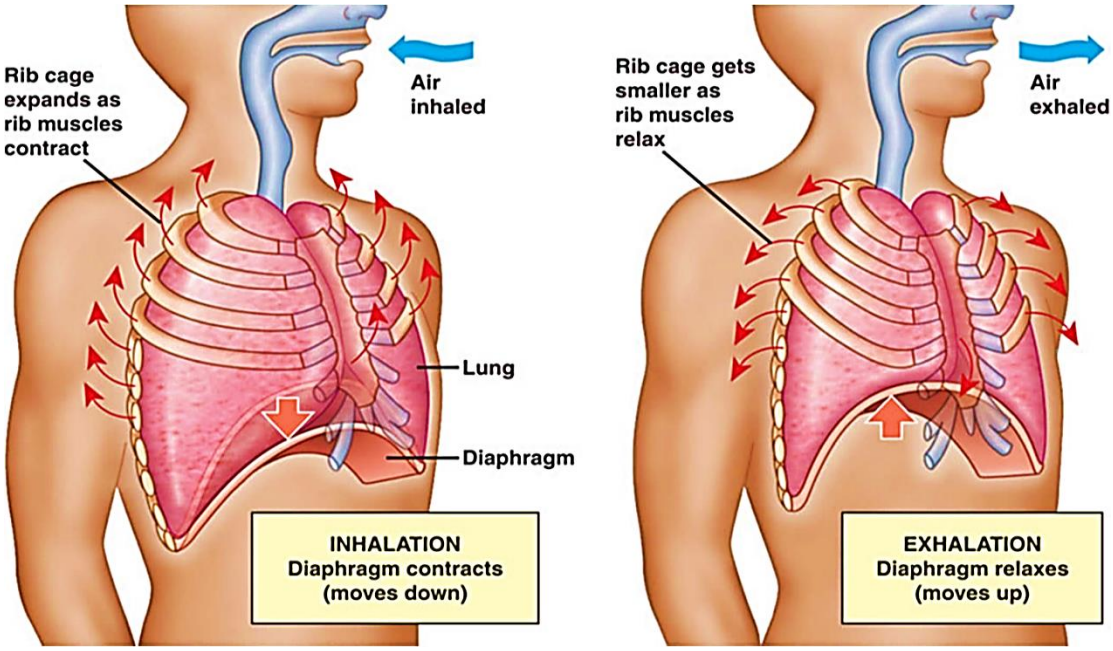

Figure 3.3: Inspiration and Expiration.

Expiration: The process of expiration of the air from the lungs is called expiration. During expiration, muscles attached to the ribs on their inner side contract, and the diaphragm and the abdominal muscles relax. This leads to decrease in the volume of the chest cavity, which increases the pressure on the lungs. The air in the lungs is pushed out and it passes out through the nose. At the time of breathe out, not all of the air in the lungs gets expelled. Some of its remains in the lungs for keeping the lungs from collapsing.

3.4 Pulmonary Function Testing Methods

The flow rate of air into and out of the lungs is the measurement of respiratory performance. The upper airways and the lungs are both of themselves exhibit resistance to airflow and this airways' resistance is changed for many respiratory diseases. By analogy to an electrical circuit, airways' resistance is calculated by dividing pressure (equivalent to voltage) by flow (equivalent to current). Typically, respiration rate for a baby is about 60 min^{-1} but, by the age of one year, this has fallen to 30- 40 min^{-1} and, in an adult, 12- 15 $min^{-1}$is a normal respiration rate [80].

Terminology of Lung Functions Testing: The number of measurements can be made directly from a recording of the lung volume changes which occur when the patient is asked to carry out set procedures [80]. Some of these measurements are illustrated in figure 3.4.The common terminology of lung functions testing are -Vital Capacity (VC)(i.e. the maximum amount of air that can be expelled from the lungs by forceful effort from maximum inspiration) which have standard values for young men about 5L and women about 3.5L and it decreases with age, Residual Volume (RV) (i.e. the amount of air remaining in the lungs at the end of maximum expiration) typically for young men about 1.2 L and slightly lower in women, Forced Vital Capacity (FVC) (i.e. the maximum amount of air that can forcibly exhale from lungs after fully inhaling) Forced Expiratory Volume in one Second (FEV_1) (i.e. the amount of air expired in one second following full inspiration) typical value for young men about 4L and lower for women ,Total Lung Capacity(TLC) (i.e. the amount of air in the lungs upon the maximum effort of inspiration.

Pulmonary Function Tests (PFT's) are an important tool in the investigation and monitoring of patients with respiratory pathology. The most common PFT's are– Spirometry, Pneumotachograph, Peak Flowmetry etc. Spirometry is commonly used Pulmonary Function Testing Method. Briefly this method is being described here.

Spirometer is an instrument which measures the amount (volume) and speed (flow) of air that can be inhaled or exhaled, is the most basic of the pulmonary function tests

[78,80]. Spirometers are noninvasive diagnostic instruments for screening and basic testing of pulmonary function.

The volume of the lungs during different stages of normal and deep breathing is a good diagnostic of lung functionality. It is easily measured using a Spirometer (Figure 3.5). Figure 3.5 shows one such measurement during different types of breathing [51].

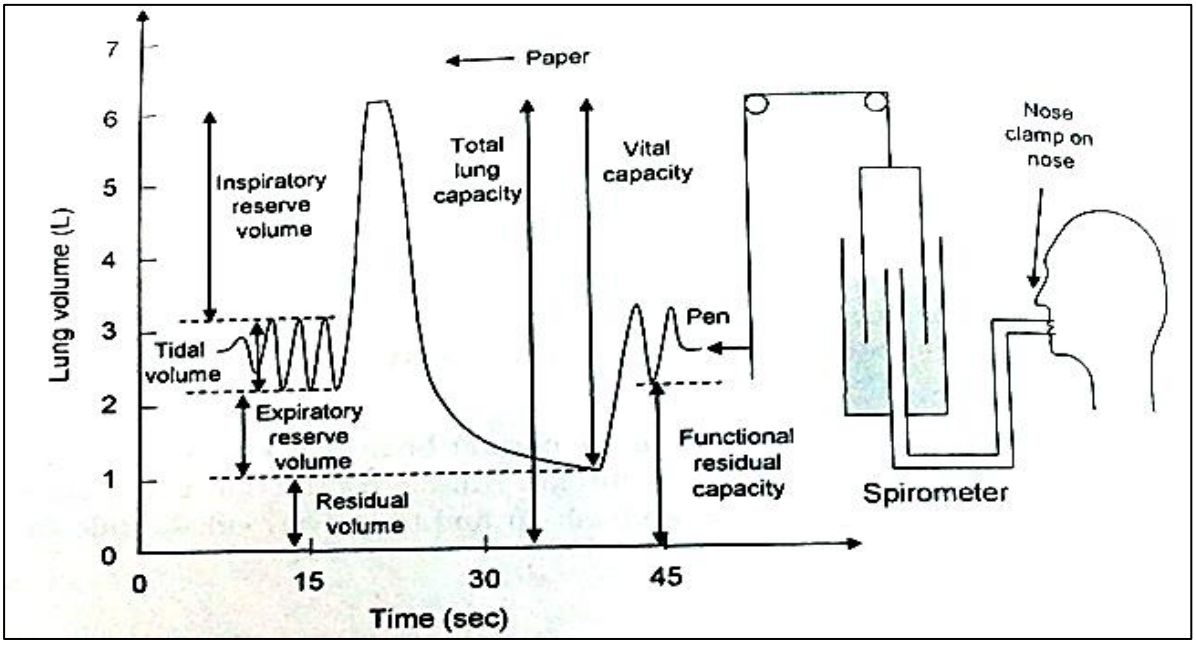

Figure 3.4: Lung volume is changing during breathing cycles.

Hence, Total Lung Capacity (TLC) = Inspiratory Reserve Volume (IRV) +Tidal Volume (TV) + Expiratory Reserve Volume (ERV) + Residual Volume (RV) =Vital Capacity (VC) + Residual Volume (RV)

The vital capacity is an important measure of how well the lungs are functioning. The functional reserve capacity is the volume of stale air that normally mixes with new air (the tidal volume). There is also dead space. Some is anatomic (0.15L), due to the trachea and bronchi, and some is physiological alveoli dead space, where the alveoli have no access to blood.

3.5 Common Lung Diseases

Normally Doctors may classify lung conditions as obstructive lung disease or restrictive lung disease. Obstructive and restrictive lung diseases have the same main symptom. It may shortness of breath with any sort of physical effort [57]. Different types of lungs disorders graph shown in the figure-3.6. Important parameter Compliance $=\frac{\Delta V}{\Delta P}$; is a measure of the effort needed to expand the lungs. Here where ΔV is the change in volume and ΔP is the change in pleural pressure. Lung hysteresis demonstrates the compliance of the lungs [68].

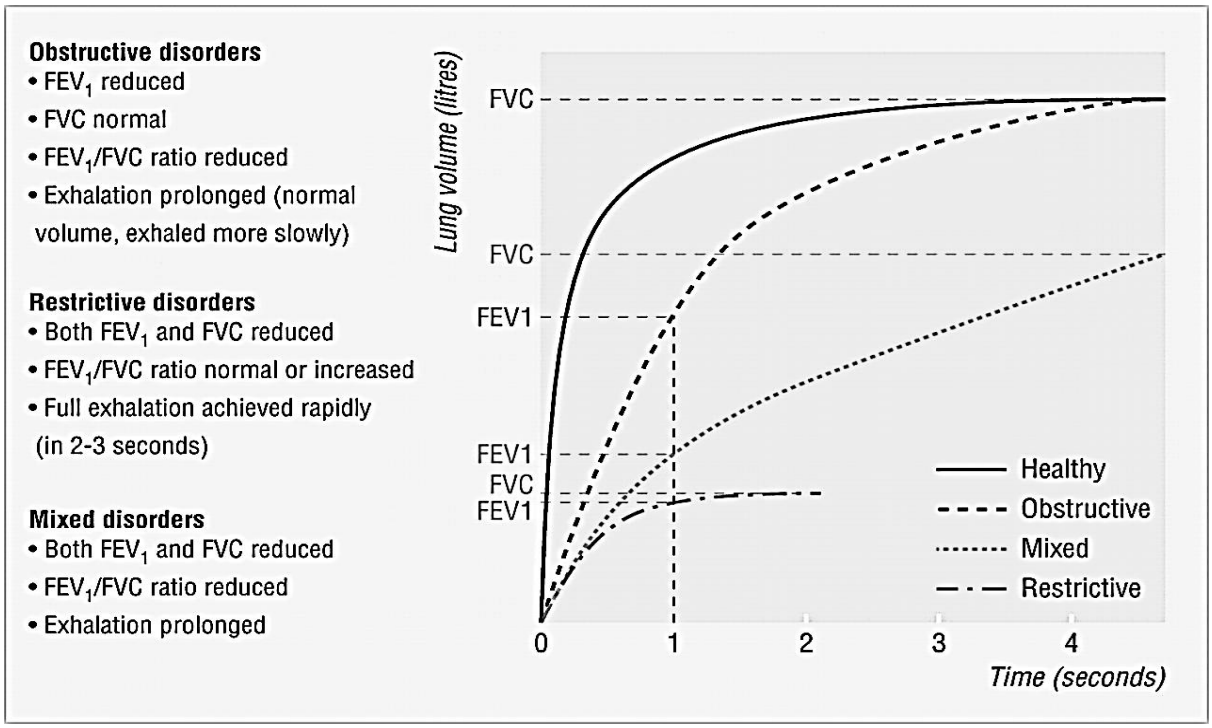

Figure 3.5: Obstructive, Restrictive and Mixed disorders graph of lung.

Restrictive Lung Diseases:

If the people with restrictive lung disease cannot fully fill their lungs with air and restricted lungs from fully expanding [57]. In this case, a greater pressure (ΔP) than normal is required to give the same increase in volume (ΔV). Common causes of decreased lung compliance are Pulmonary Edema, Pneumothorax, Pulmonary fibrosis, and Pneumonia [67].

Pulmonary Edema: Pulmonary edema occurs due to accumulation of excess fluid in the lungs.Very small elastic air sacs(alveoli) collect this fluid.For these reason these alveoli fill with fluid instead of air, preventing oxygen from being absorbed into blood stream. It makes difficult to breathe. A number of things can cause fluid to accumulate in lungs, but most have to do with heart (cardiogenic pulmonary edema) [71]. The electrical conductivity value of this accumulated fluid is 1.5 Sm^{-1}, which is higher than the healthy(normal) lungs [24, 33].

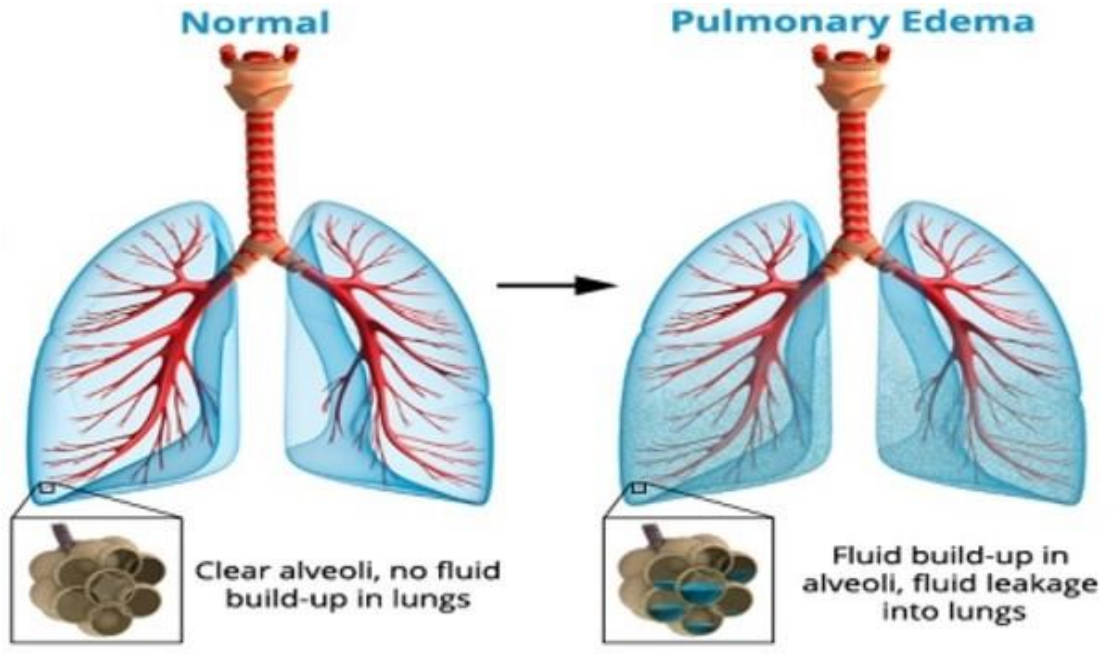

Figure 3.6 : Healthy Lung and Pulmonary Edema Lung.

Pneumothorax (Collapsed Lung): A collapsed lung is also known as pneumothorax and it is a condition that occurs when air enters the space between the chest wall and the lung (pleural space). Symptoms for pneumothorax are chest pain and shortness of breath [59]. The electrical conductivity value for pneumothorax lungs is 0.60 Sm^{-1}, which is higher than the healthy (normal) lungs [24,33].

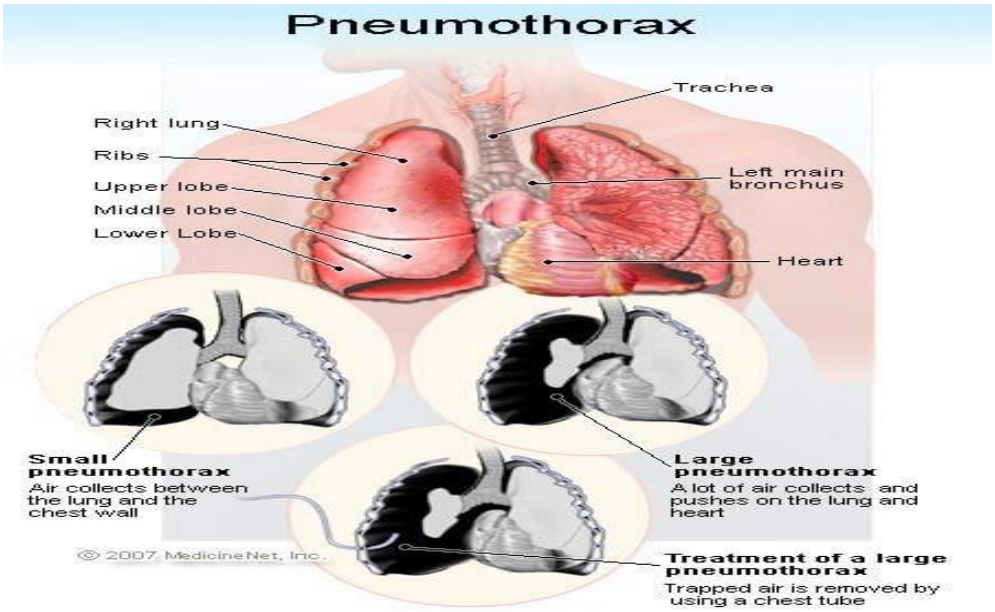

Figure 3.7. Lungs with Pneumothorax.

Obstructive Lung Diseases:

Respiratory diseases are characterized by airway obstruction is known as obstructive lung diseases [60]. It makes the shortness of breath due to difficulty exhaling all the air from the lung. Because of damage to the lungs or narrowing of the airways inside the lungs, exhaled air comes out more slowly than normal. At the end of a full exhalation, an abnormally high amount of air may still linger in the lungs [57]. In an obstructive lung disease, airway obstruction causes an increase in resistance. In case of obstructive lung, the greater pressure is needed to overcome the resistance to flow, and the volume of each breath gets smaller. In the obstructed lung, respiration ends prematurely, thus increasing RV (Residual Volume) and FRC (Functional Residual Capacity) [67].

CHAPTER-4: ELECTRICAL IMPEDANCE IMAGING METHODS

Chapter-4: Electrical Impedance Imaging Methods

4.1 Introduction

Electrical Impedance Tomography (EIT) is a non-invasive, nonionizing, real time, low cost, portable medical imaging technique, where an image of impedance or simply conductivity part of the body constructed from the data collected through the surface electrodes. Relative or functional EIT imaging more frequently done than absolute EIT imaging for medical purposes. A small (in order of milliamp ere) amount of alternating current at a single frequency (KHz range) is used in the case of healthcare imaging. In some cases, EIT system use multiple frequencies, known as electrical impedance spectroscopy to better distinguish between normal and suspected abnormal tissue within the same organ [10]. Referring to figure 4.1 Showing the current stream lines and equipotential from to current drive electrodes in cross of human thorax containing to lungs. It is clearly seen that current lines are bent due to different impedances distribution in the cross section It is also noted that equipotential lines are drown perpendicular to current stream lines.

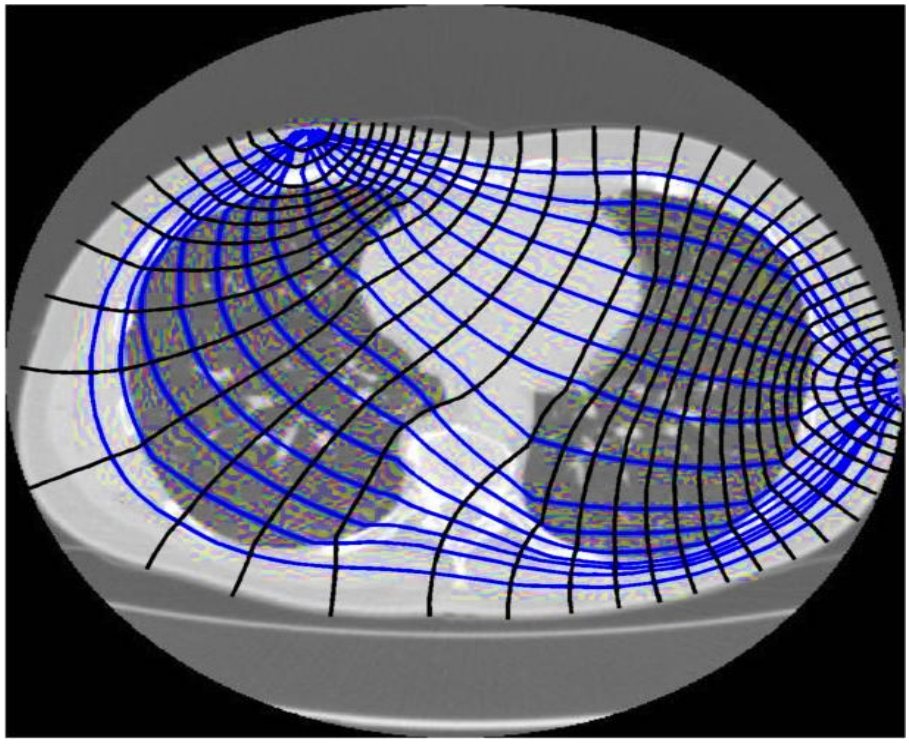

Figure 4.1. Distribution of current stream lines and equipotential voltages due to a pair of current drive electrodes at human thorax cross section containing two lungs.

Electrical impedance imaging system uses a set of surface electrodes, typically 8,16,32 electrodes are used for current injections and measurement of voltages due to impedance distribution. Generally, a pair of electrodes are used through which currents are injected into the subjects and rest of the electrodes are used to measured voltages developed due to currents and impedance distribution. Generally adjacent pair of electrodes, also known as neighboring protocols and opposite pair of electrodes are used for current injection. Figure 4.2 shows a pair adjacent of red color electrodes are used current injection and green color of electrodes are used for voltage measurement.

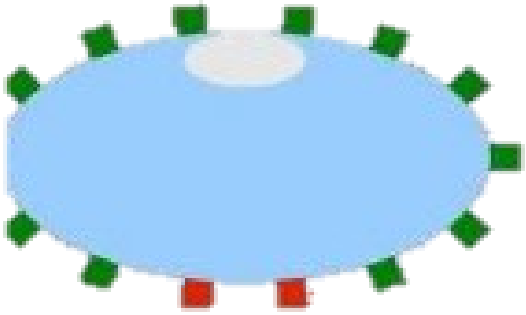

Figure 4.2: Electrodes are placed around the thorax. Red electrodes are driving electrodes and green electrodes are voltage sensing electrodes.

A computed tomographic image reconstruction technique is EIT and a nonlinear inverse problem in which the electrical conductivity or resistivity of a conducting domain (Ω) is reconstructed from the surface electrical potentials developed by a low frequency constant amplitude sinusoidal current signal is injected (Figure 4.3) at the domain boundary ($\partial\Omega$)[32].An electronic instrument is used for boundary potential measurement.

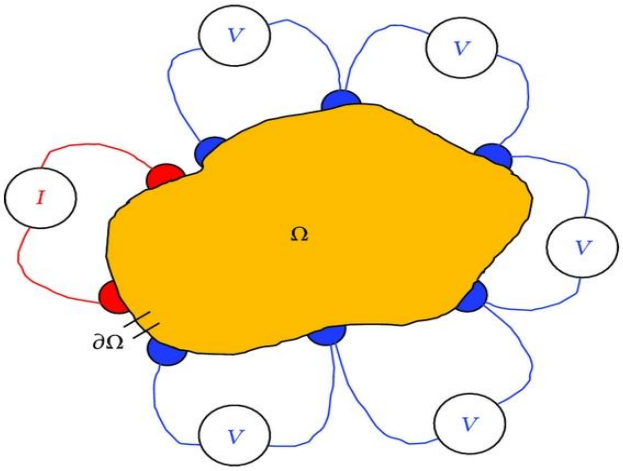

Figure 4.3: A low frequency constant amplitude sinusoidal current is injected through red electrodes (driving electrodes) and remaining electrodes are used for voltage calculations.

The calculated data are processed to reconstruct the spatial distribution of the electrical conductivity of the domain under test using a computer algorithm, called image reconstruction algorithm [32]. Electrical Impedance Tomography (EIT) measurements between inspiration and expiration are known as relative or functional EIT (f-EIT).

It has one major advantage over absolute EIT (a-EIT), which is the most artifacts will eliminate themselves due to simple image subtraction. It is found advantageous in several fields of applications compared to the X- ray CT, X-ray mammography, SPECT, PET computed tomographic methods [32].

4.2. Mathematical Formulation of Electrical Impedance Imaging

Henderson and Webster (1978) was proposed independently the electrical resistive tomography idea for medical imaging and by Lytle and Dines (1978) as a geophysical imaging tool (Daily and Ramirez 2000). Since 1978, computational power has increased drastically to allow for large three- dimensional EIT inversions, and computational time has decreased also due to the implementation of better methods of obtaining the inverse solution.

Figure 4.4 shows a simple EIT diagram with 16 electrodes around the perimeter of a circular medium. In this arrangement the current, I, is applied across a pair of electrodes on opposite sides of the core while the voltage distribution, $V_i$is measured between each set of neighboring electrodes. After the voltage around the entire perimeter has been measured, the current drive electrodes are rotated to the neighboring electrodes, such that they remain opposite, and the voltage at all electrodes is measured once again. This process continues until the 256 sets of voltage measurements are completed [44].

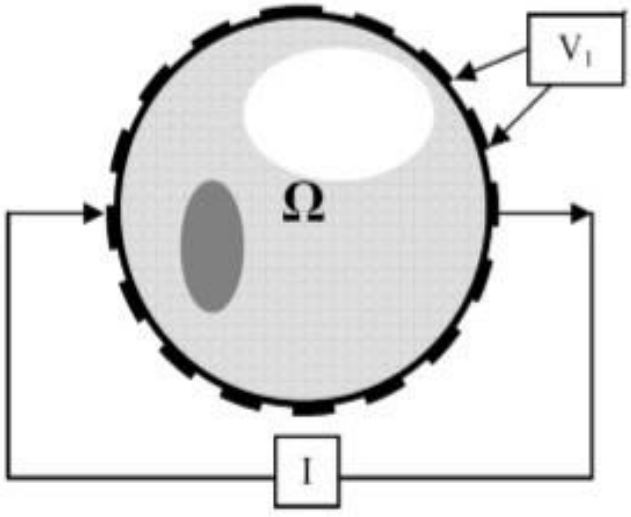

Figure 4.4: EIT experiment for 16 electrodes. The potential V_i is measured after a current I has been imposed across the coreΩ(Molinari 2003).

The governing equation for the voltage field produced by placing a current across a material is given in equation 4.2.1,

$\nabla.(\sigma + i\,\omega\epsilon)\nabla\emptyset = 0$ ----------(4.2.1)

Where $\sigma\ is$ the electrical impedance of the medium, $\emptyset$ is the electrical potential, ω is the frequency, and ϵ is the electric permittivity. When a low frequency or direct current is used, (≈ 0) (Molinari 2003), then equation 4.2.1 is reduced to equation 4.2.2

$\nabla.(\sigma\nabla\emptyset) = 0$ ----------(4.2.2)

The EIT inverse problem is simply a system stimulation problem. The stimulation and resulting effect (injected current i and measured voltage V) are known, but the internal physical system is unknown (impedance distribution,σ). The difficulty in solving this problem is in the nonlinearity that arises in σ, because the potential distribution $\emptyset$ is a function of impedance, $\emptyset = \emptyset\ (\sigma\ )$, and we cannot easily solve equation 4.2.2 for σ (Molinari 2003). The ill- posed nature of the problem is clearly apparent when observing the diffusive nature of electricity, coupled with inherent measurement errors.

The estimate of the electrical conductivity distribution, inside a heterogeneous body or object in EIT, is made by the resolution of a partial differential equation named Poisson's Equation (Borcea, 2002; Cheney et al., 1999) [45]:

$\nabla.\boldsymbol{D} = \rho$---------- (4.2.3)

Whereρ is the free electric charge in the interest region, and D is the electric elasticity given by the multiplication of the electrical conductive distribution $(\boldsymbol{u})$ in the point u **= u** (x, y, z) and the electric field **E**, given as

D= $\sigma(\boldsymbol{u})$ **E** ----------(4.2.4)

Electric field **E** can be written as

E = $-\nabla\emptyset\ (\boldsymbol{u})$ ---------- (4.2.5)

We consider that there is no free electric charge in the interest region (i.e. $\rho = 0$) for the reconstruction of EIT images. Now using equations (4.2.4) and (4.2.5) in equation (4.2.3), then we get

$-\nabla.[\sigma(\mathbf{u})\nabla\emptyset(\boldsymbol{u})] = 0$---------- (4.2.6)

Besides, we also need to consider the following boundary conditions (Borcea, 2002):

$\emptyset_{ext}(\mathbf{u}) = \emptyset(\mathbf{u}), \forall\, \mathbf{u} \in \partial\Omega$ ----------(4.2.7)

$I(\mathbf{u}) = -\sigma(\mathbf{u})\nabla\emptyset(\boldsymbol{u}).\hat{n}(\mathbf{u}), \forall\, \mathbf{u} \in \partial\Omega$ ----------(4.2.8)

where $\mathbf{u} = \mathbf{u}$ (x, y, z) is the position of a given object, $\emptyset$ ($\mathbf{u}$) is the potentials' global distribution, $\emptyset_{ext}(\mathbf{u})$ is the electric potentials distribution on the surface electrodes, $I(\mathbf{u})$ is the electric current applied on the interest region's surface, $\sigma(\mathbf{u})$ is the electric conductivity distribution (i.e., the goal image), Ω is the interest volume, $\partial\Omega$ is the volume border and $\hat{n}(\mathbf{u})$ is the border's normal vector on $\mathbf{u} \epsilon \partial\Omega$ position.

In EIT's Forward Problem the following relation is considered,

$\emptyset_{ext}(\mathbf{u}) = f(I(\boldsymbol{u}), \sigma(\mathbf{u}), \forall\, \mathbf{u} \in \partial\Omega \wedge \mathbf{u} \in \boldsymbol{\Omega}$----------(4.2.9)

The boundary condition in this case is

$\sigma \frac{\partial\phi}{\partial\hat{n}} = J$ ---------- (4.2.10)

where$\hat{n}$ is the surface's normal vector and J corresponds to the electric current density (Baker, 1989). For an arbitrary given domain Ω, there is no analytical solutions to (4.2.6) and (4.2.10). Finite Elements Method (FEM) is used to get an approximate solution to the boundary potential, converts the nonlinear system in (4.2.6) and (4.2.10) in the following linear equation's system (Bathe,2006; Castro Martins, Camargo, Lima, Amato, & Tsuzuki, 2012):

$$K(\sigma).\Phi - C = 0 \text{ ---------- (4.2.11)}$$

where $K(\sigma)$ is a conductivity – dependent (σ) coefficients matrix and C is a constant's values vector. In this way, it is possible to obtain an approximated value for the border potentialsΦ, known as conductivity distribution σ.

In the case of EIT inverse problem the conductivity distribution determination problem $\sigma(\mathbf{u})$(tomographic image), given $I(\mathbf{u})$ and $\emptyset_{ext}(\mathbf{u})$ and modeled given as:

$\sigma(\mathbf{u}) = f^{-1}(I(\mathbf{u}), \emptyset_{ext}(\mathbf{u})), \forall\, \mathbf{u} \in \partial\Omega \wedge \mathbf{u} \in \boldsymbol{\Omega}$ ----------(4.2.12)

By using Poisson's equation solution (4.2.6) to obtain the conductivity distribution $\sigma(\mathbf{u})$ and the contour conditions are considered, mentioned in equations (4.2.7) and (4.2.8) [45].

Electrical Impedance Tomography (EIT) is a comparatively new imaging technique. In 1826, a Norwegian physicist published the concept of tomography for the first time for an object with axi-symmetrical geometry [50]. In the mid to late 1980s, about a dozen groups have developed their own EIT systems and reconstruction software. The main areas of EIT imaging lung ventilation, cardiac function, gastric emptying, brain function and pathology, and screening for breast cancer [16]. An ideal system of EIT uses a box of electronics and a PC. Subject may sit on a movable trolley or a fixed position. Normally the subject is connected by co-axial cables a meter or two long. Electro Cardio Gram type electrodes are used in a ring or rings on the body part of the interest.

In current injection model EIT a small amount of ac current is injected into the body through a pair of electrodes and other pairs of electrodes used for voltage measurement. The pair of electrodes through which currents are injected called current pair, and the pair of electrodes by which voltages are measured, called voltage pair. In a single measurement current is injected through a current pair and voltages are measured through all others voltage pairs. Then the position of the current pair is changed and the voltage measurements are made like before. A data set is set to be complete for imaging when all the possible current pairs are used. These data set are then used to reconstruct impedance distribution, known as inverse problem.

Most single frequency systems apply a current at about 50 kHz. At this frequency, the properties of tissue are similar to those at dc in that the great majority of current travels in the extracellular space, but electrode impedance is much lower than at dc so there are less measurements errors.

4.3 Electrical Impedance Measurement Methods or Protocols

In Electrical Imlpedance Technique (EIT) currents are injected into the object under test and resulting electrical voltages are measured from the surface eletrodes. Two widely used EIT measurements methods or protocols are : Neighbouring Method or Adjacent Drive Method and Opposite Current Drive Method are desbrbed briefly.

Neighbouring Method or Adjacent Drive Method:

Brown and Segar (1987) suggested a method whereby the current is applied through a adjacent pairs of electrodes and the voltages are measured successively from all other adjacent electrode pairs [9]. Figure 4.5 illustrates the method with 16 equally spaced electrodes. The current is first applied through electrodes 1 & 2 shown in Figure 4.5, and voltages are measured through electrode pairs 3-4, 4-5, -----, 15-16. However , in practice voltage measumens are not made for current carriyng electordes (pair 2-3 and 16-1) to avoid contact impedance problem. Then the procedure is repeated for all other electrode pairs to complete all the measurements.

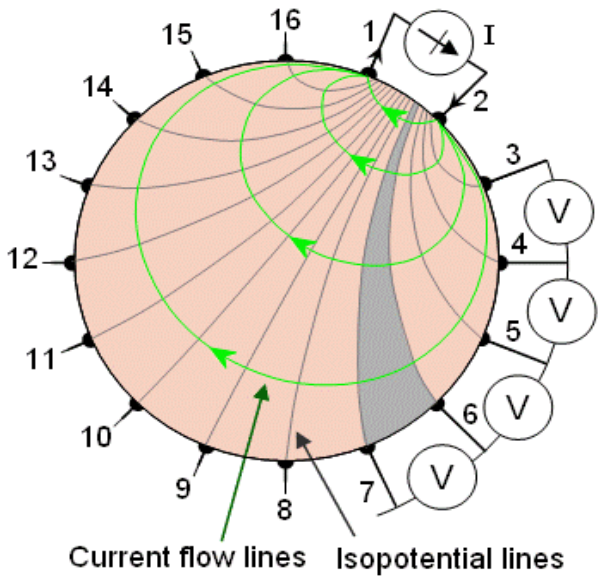

Fig 4.5: Neighbouring method of data collection.

Opposite Current Drive Method:

Currentsof this method are injected through two diametrically opposed electrodes (e.g. electrodes 16 & 8 in Figure 4.6), and volages are measured from the rest of the pairs of electodes.It is more uniform sensitivemethod due to its uniform current distribution.

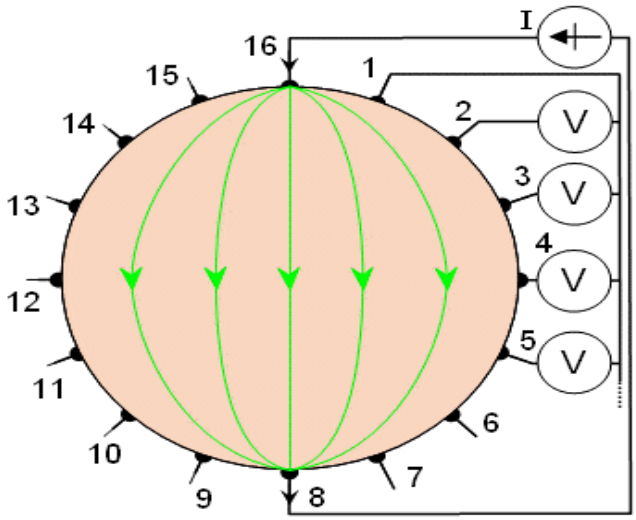

Fig 4.6 : Opposite method of impedance data collection.

4.4 Relative Advantages of Electrical Impedance Tomography

Electrical Impedance Tomography (EIT) is a non-ionizing tomographic imaging techniques being used in many areas of research and industry including health care ecosystem. In health care diagnostic and monitoring purposes generally an ac current of 1mA at 50KHz frequency is applied because at this level of low current and high frequency there is no electrical nerve stimulation nor skin burn. It also ensures patient safety and his/her satisfaction. Today there is no known harmful effect of EIT imaging, unlike x-ray and CT imaging. For this reason, the EIT technique can be used for continuous monitoring of patient's condition. In addition, the EIT instrument is relatively simple and portable unlike CT scan imaging system, therefore it can be used even at the bed side.

4.5 Application of EIT in Healthcare

Electrical Impedance Tomography (EIT) technique is being used to study the frequency response of the electrical impedance of biological tissues [10, 32]. Healthcare providers are repeatedly used absolute EIT (a-EIT) and functional EIT (f-EIT) for Lung, Breast Imaging, Brain Imaging, Cardiac, Hyperthermia, Cervix etc.

EIT imaging technique can be used for absolute impedance imaging and functional impedance imaging. Functional impedance imaging produces relative change of impedance for different condition of test subject/patient.

Absolute Electrical Impedance Tomography (a-EIT) is being used for the monitoring and assessment of the lung functions, because the lung tissues resistivity is five times higher than other soft tissues within the thorax. The electrical conductivity values are significantly changes during inspiration and expiration. Absolute EIT has the potential for clinical useful tool and also distinguish the lung conditions between the regions with lower resistivity (e.g., hemothorax, pleural effusion, atelectasis, lung edema) and those with higher resistivity (e.g., pneumothorax, emphysema).

Functional Electrical Impedance Tomography (f-EIT) can determine th**e** relative impedance changes that may be caused by either ventilation or changes of end-expiratory lung volume. The images of the functional EIT can be generated continuously and right at the bedside. These attributes make regional lung function monitoring particularly useful whenever there is a need to improve oxygenation or CO_2 elimination. The images of EIT lung function can resolve the changes in the regional distribution of lung volumes between e.g., dependent and non- dependent lung regions as ventilator parameters will be changed. Thus, EIT measurements may be used to control the specific ventilator settings to maintain lung protective ventilation for each patient.

Moreover, Electrical Impedance Tomography calculations provide raw data sets that can be used to measure the changes of intra thoracic gas volume during critical illness [10].

CHAPTER-5: COMPUTER SIMULATIONS FOR DIFFERENT LUNG CONDITIONSAND PHANTOM STUDY

Chapter-5: Computer Simulations for Different Lung Conditions and Phantom Study

5.1 Introduction to COMSOL Multiphysics Simulation Software

COMSOL Multiphysics (Version 4.3) simulation software is a potential and interactive situation for modeling and solving almost kind of scientific and physics related engineering problems. It gives two dimensional (2D) and three dimensional (3D) simulation situation and designed with real-world applications [85]. The COMSOL Multiphysics modeling in Version 4.3 simulation software provides a potential integrated desktop situation with a Model Builder where we get full overview of the model and access to all functionality. By using COMSOL Multiphysics we can easily extend usual models for one type of physics into Multiphysics models that solve coupled physics phenomena-and do so simultaneously [86]. We access the power of COMSOL Multiphysics as a standalone product through a flexible Graphical User Interface (GUI) or by script programming in Java or the MATLAB® language (requires the COMSOL Live Link for MATLAB).

COMSOL Multiphysics uses the proven Finite Element Method (FEM) for solving the models. The software runs the finite element analysis together with adaptive meshing (if selected) and error control using a variety of numerical solvers. It creates sequences to record all steps that create the geometry, mesh, studies and solver settings, and visualization and results presentation. It is therefore easy to parameterize any part of the model: Simply change a node in the model tree and re-run the sequences.

Partial differential equations (PDEs) form the basis for the laws of science and provide the foundation for modeling a wide range of scientific and engineering phenomena [86]. COMSOL Multiphysics may be used in many application areas like-Acoustics, Electromagnetics, Geophysics, Heat transfer, Quantum mechanics, Radio-frequency components, Semiconductor devices etc.

There are three Electrostatics, Electric Currents, and Magnetic Fields physical interfaces are present in COMSOL Multiphysics for simulating electromagnetic fields. Electrostatics and electric currents can perform static simulations to solve for electric properties. We have used powerful tool of AC/DC module and it provides

unparalleled simulation environment of AC/DC electromagnetics in 2D and 3D. By using this module, it can run static, quasi- static, transient, and time-harmonic simulation in an easy to use Graphical User Interface (GUI). Electrostatics, electric currents in conducting media, magneto statics and low-frequency electromagnetics are covered the electromagnetic field of simulations [84].

5.2 Arrangement of Simulation Environment in COMSOL Multiphysics

Electrical Impedance Tomography (EIT) are discussed in this chapter for the assessment of different lung conditions. The respiratory system is one of the most important organs, which includes lungs and airways. Electrical Impedance Tomography (EIT), being the screening tool for the assessment of lung functions, serves to be quite safe, non-invasive, non-hazardous, non- radiative and not harmful while considering the health issues of the lung patient. The simulation software COMSOL Multiphysics Version 4.3 has been used here for building human thorax/chest phantom, lungs, electrodes etc. Electrical impedance measurements also have the potential to detect and diagnose many disorders and diseases including localizing tumors in the lungs. In Electrical Impedance Imaging (EII) system two surface electrodes (SE) are used for small and safe current injection (1mA, 50 KHz assumed safe) through the center of anterior and the posterior side of the chest, and other eight SE at the posterior side following the shape (ellipsoid) of lungs, are used for surface potential calculation. Chest phantom has taken as a specimen [92]. Computer generated digital phantom has constructed according to the chest phantom. COMSOL compatible human thorax/chest phantom, right lung, left lung, connector of two lungs, tumors, electrodes figures are modeled according to the modeled tissues based on electrical properties of frequency 20 kHz to 200 kHz [Ref: Table-5.1].

5.2.1(a) Human Phantom

The structure of phantom is artificial and designed to emulate properties of the human body in matters such as, light scattering and optics, electrical conductivity, and sound wave reception. Experimentally Phantoms have been used as a supplement to human subjects to maintain the consistency and verify the reliability of technologies to reduce the experimental expenses. Male phantom and its dimension given below. According to the following phantom dimensions the geometry of the adult male subject chest/thorax is eccentric cone with the measurements of a- semiaxis or B_1 10 cm, b- semiaxis or A_1 is 20 cm and height 42 cm.

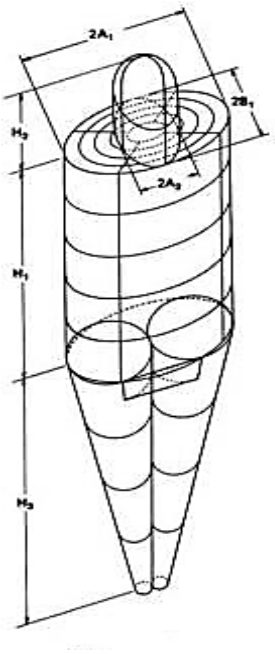

PHANTOM DIMENSIONS

Age (yr)	Weight (kg)	H_1 (cm)	H_2 (cm)	H_3 (cm)	A_1 (cm)	B_1 (cm)	A_2 (cm)
0	3.148	23	13	16	5.5	5	4.5
1	9.112	33	16	28.8	8	7	6.5
5	18.12	45	20	46	11	7.5	6.5
10	30.57	54	22	64	14	8	6.5
15	53.95	65	23	78	18	9	7
Adult	69.88	70	24	80	20	10	7

Figure-5.1: The adult male phantom and its dimension [92].

5.2.1(b) Electrical Properties of Modeled Tissues

For an adequate geometric model of the human thorax/chest phantom, lung, tumor (body fluid) different types of tissues were being modeled with different electrical conductivity and relative permittivity between the frequency 20 KHz to 200 KHz given as table-5.1[24,33].

Table 5-1: Modeled Tissues for the Electrical Properties of the frequency limit 20KHz to 200 KHz.

Tissue	Electrical Conductivity (σ) (Sm^{-1})	Relative Permittivity (∈)
Healthy Lung (inflated)	0.103	4272.50
Healthy Lung(deflated)	0.262	8531.40
Lung Collapsed (Pneumothorax)	0.600	1000.00
Muscle	0.352	10094.00
Body Fluid (Pulmonary Edema)	1.500	98.56
Blood	0.701	5197.70
Heart	0.195	16982.00

5.2.1 (c): Model Parameters for Existing Electrical Impedance Technique (EIT) Protocol

Table5.2: Model Parameters for Existing EIT Protocol

Geometrical Shape	Comsol Compatible Figures	Measurement (cm)	Electrical Conductivity Sm^{-1}	Relative Permittivity	Position (cm)
Eccentric Cone	Human Thorax/Chest Phantom	a-semiaxis : 10 b-semiaxis : 20 Height : 42 Ratio : 1 Top displacement1:0 Top displacement2:0	0.352	10094.00	(0,0,0)
Ellipsoid	Right Lung	a-semi principal axis: 4.5 b-semi principal axis: 6.0 c-semi principal axis: 16	0.103 (Inflated) 0.262 (Deflated)	4272.50 8531.40	(0,-8,23)
Ellipsoid	Left Lung	a-semi principal axis: 4.0 b-semi principal axis: 4.5 c-semi principal axis : 17	0.103 (Inflated) 0.262 (Deflated)	4272.50 8531.40	(0,6,23)
Cylinder	Connector of two lungs	Radius : 3 Height : 6	0.103 (Inflated) 0.262 (Deflated)	4272.50 8531.40	(0,-0.5,22)
Sphere	SE-1 (Silver)	Radius: 1.0	6.16×10^{7}	3.4	(0,-20,23)
Sphere	SE- 2 (Silver)	Radius: 1.0	6.16×10^{7}	3.4	(6.7,-14.5,23)
Sphere	SE- 3 (Silver)	Radius: 1.0	6.16×10^{7}	3.4	(9.7,-5,23)
Sphere	SE- 4 (Silver)	Radius: 1.0	6.16×10^{7}	3.4	(9.5,5,23)
Sphere	SE- 5 (Silver)	Radius: 1.0	6.16×10^{7}	3.4	(6.5,14.5,23)
Sphere	SE- 6 (Silver)	Radius: 1.0	6.16×10^{7}	3.4	(0,20,23)
Sphere	SE- 7 (Silver)	Radius: 1.0	6.16×10^{7}	3.4	(-6.5,14.5,23)
Sphere	SE- 8 (Silver)	Radius: 1.0	6.16×10^{7}	3.4	(-9.5,5,23)
Sphere	SE -9 (Silver)	Radius: 1.0	6.16×10^{7}	3.4	(-9.7,-5,23)
Sphere	SE -10 (Silver)	Radius: 1.0	6.16×10^{7}	3.4	(-6.75,-14,23)

5.2.1(d): Model Parameters for Proposed Anterior-Posterior Electrical Impedance Technique (APEIT)Protocol Applying through Right Lung

Table 5.3: Model Parameters for Proposed Anterior-Posterior EIT Protocol without presence of heart

Geometrical Shape	Comsol Compatible Figures	Measurement (cm)	Electrical Conductivity Sm^{-1}	Relative Permittivity	Position (cm)
Eccentric Cone	Human Thorax/Chest Phantom	a- semiaxis: 10 b- semiaxis: 20 Height : 42 Ratio : 1 Top displacement1:0 Top displacement2:0	0.352	10094.00	(0,0,0)
Ellipsoid	Right Lung	a-semi principal axis: 4.5 b-semi principal axis: 6 c-semi principal axis : 16	0.103 (Inflated) 0.262 (Deflated)	4272.50 8531.40	(0,-8,23)
Ellipsoid	Left Lung	a-semi principal axis: 4 b-semi principal axis: 4.5 c-semi principal axis : 17	0.103 (Inflated) 0.262 (Deflated)	4272.50 8531.40	(0,6,23)
Cylinder	Connector of two lungs	Radius : 3 Height : 6	0.103 (Inflated) 0.262 (Deflated)	4272.50 8531.40	(0,-0.5,22)
Sphere	SE- 1 (Silver)	Radius: 1.0	6.16×10^7	3.4	(9,-8,23)
Sphere	SE- 2 (Silver)	Radius: 1.0	6.16×10^7	3.4	(-9,-8,23)
Sphere	SE- 3 (Silver)	Radius: 1.0	6.16×10^7	3.4	(-9,-8,37)
Sphere	SE- 4 (Silver)	Radius: 1.0	6.16×10^7	3.4	(9.75,2.5,30)
Sphere	SE- 5 (Silver)	Radius: 1.0	6.16×10^7	3.4	(-9.75,-1.5, 23)
Sphere	SE- 6 (Silver)	Radius: 1.0	6.16×10^7	3.4	(-9.70,-3,16)
Sphere	SE- 7 (Silver)	Radius: 1.0	6.16×10^7	3.4	(-9,-8,10)
Sphere	SE- 8 (Silver)	Radius: 1.0	6.16×10^7	3.4	(-7.4,-13,16)
Sphere	SE -9 (Silver)	Radius: 1.0	6.16×10^7	3.4	(-7,-14,23)
Sphere	SE-10 (Silver)	Radius: 1.0	6.16×10^7	3.4	(-7.5,-13,30)

5.2.1(e): Model Parameters for Proposed Anterior-Posterior EIT Protocol Applying through Left Lung with the presence of heart

Table 5.4: Model Parameters for Proposed Anterior-Posterior EIT Protocol with presence of heart.

Geometrical Shape	Comsol Compatible Figures	Measurement (cm)	Electrical Conductivity Sm^{-1}	Relative Permittivity	Position (cm)
Eccentric Cone	Human Thorax/Chest Phantom	a- semiaxis: 10 b- semiaxis: 20 Height : 42 Ratio : 1 Top displacement1:0 Top displacement2:0	0.352	10094.00	(0,0,0)
Ellipsoid	Right Lung	a-semi principal axis: 4.5 b-semi principal axis: 6 c-semi principal axis : 16	0.103 (Inflated) 0.262 (Deflated)	4272.50 8531.40	(0,-8,23)
Ellipsoid	Left Lung	a-semi principal axis: 4 b-semi principal axis: 4.5 c-semi principal axis : 17	0.103 (Inflated) 0.262 (Deflated)	4272.50 8531.40	(0,6,23)
Cylinder	Connector of two lungs	Radius : 3 Height : 6	0.103 (Inflated) 0.262 (Deflated)	4272.50 8531.40	(0,-0.5,22)
Cylinder	Heart	Radius : 3 Height : 7	0.195	16982	(0,2,13)
Sphere	SE- 1 (Silver)	Radius: 1.0	6.16×10^7	3.4	(9.25,6.5,23)
Sphere	SE- 2 (Silver)	Radius: 1.0	6.16×10^7	3.4	(-9.25,6.5,23)
Sphere	SE- 3 (Silver)	Radius: 1.0	6.16×10^7	3.4	(-9.25,6.5,,37)
Sphere	SE- 4 (Silver)	Radius: 1.0	6.16×10^7	3.4	(-7.5,12.5,30)
Sphere	SE- 5 (Silver)	Radius: 1.0	6.16×10^7	3.4	(-7,-14, 23)
Sphere	SE- 6 (Silver)	Radius: 1.0	6.16×10^7	3.4	(-7.5,13,16)
Sphere	SE- 7 (Silver)	Radius: 1.0	6.16×10^7	3.4	(-9.25,6,10)
Sphere	SE- 8 (Silver)	Radius: 1.0	6.16×10^7	3.4	(-9.75,0,16)
Sphere	SE -9 (Silver)	Radius: 1.0	6.16×10^7	3.4	(-9.75,-1,23)
Sphere	SE-10 (Silver)	Radius: 1.0	6.16×10^7	3.4	(-9.75,0,30)

5.2.2 Construction of COMSOL Compatible Models

At first opening the COMSOL simulation window [Figure-5.2(a)], the model has been added in the model builder [Figure-5.2(b)] and its space dimension 3D has been selected from the model wizard [Figure-5.2(c)]. AC/DC module has been selected [Figure-5.2(d)] because Electrical Impedance Tomography (EIT) is operated with alternating current. Then model wizard is to select the Frequency Domain [Figure-5.2 (e)] where the simulation work will be performed. Hence here the selected physics is Electric Currents (ec) and the selected study type is Frequency Domain.

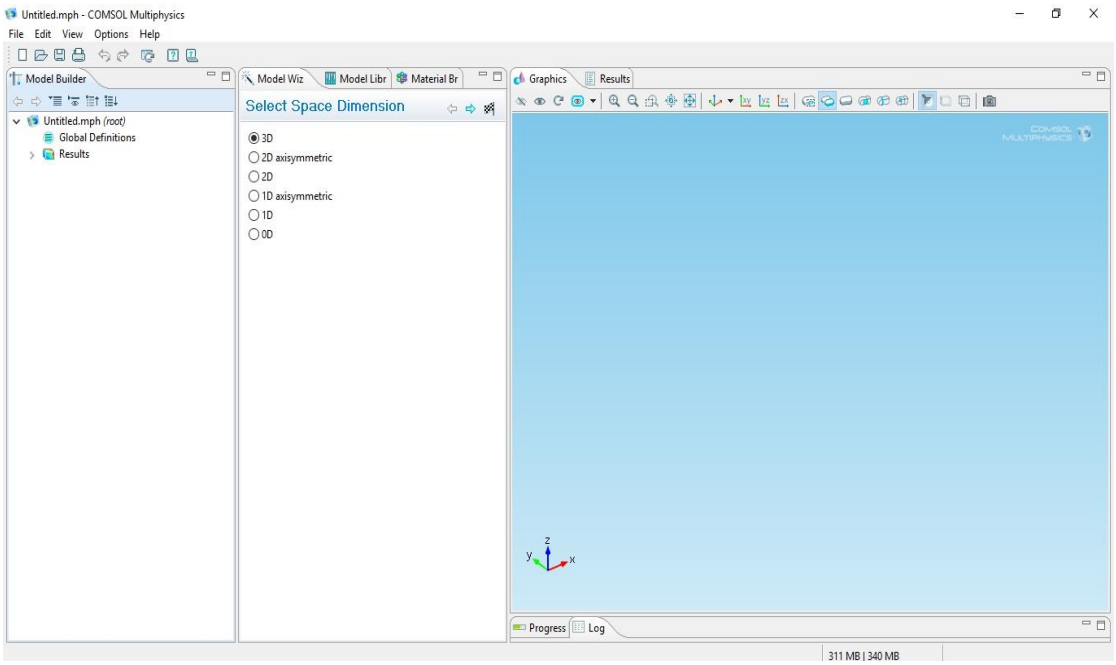

Figure- 5.2 (a): COMSOL Simulation window.

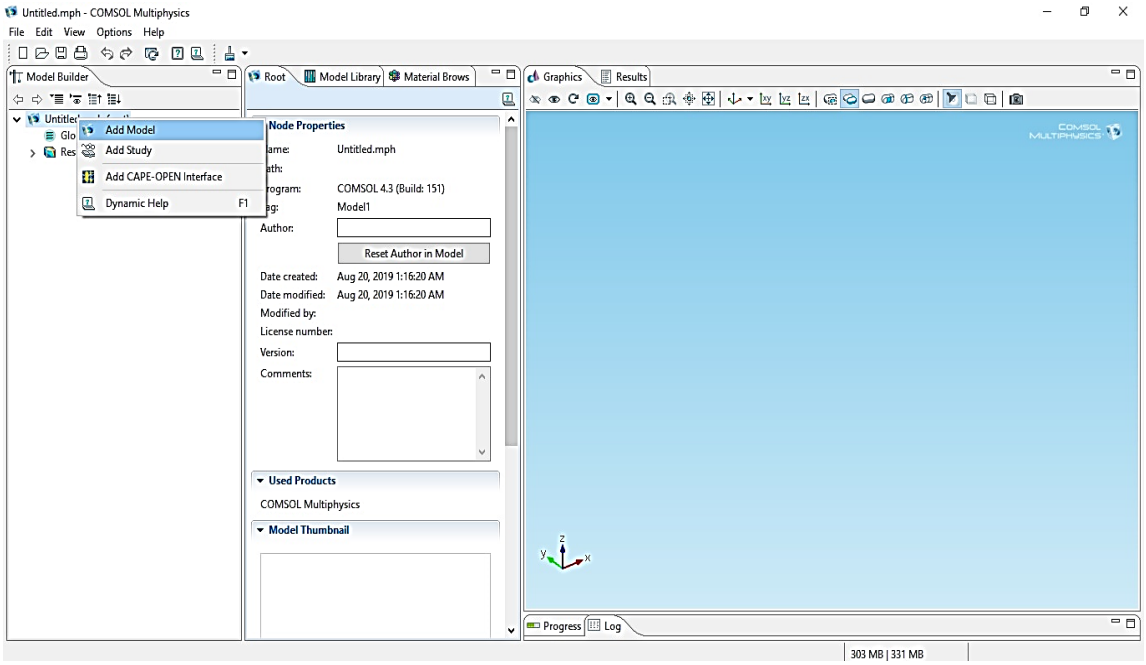

Figure-5.2(b): Add model in the model builder.

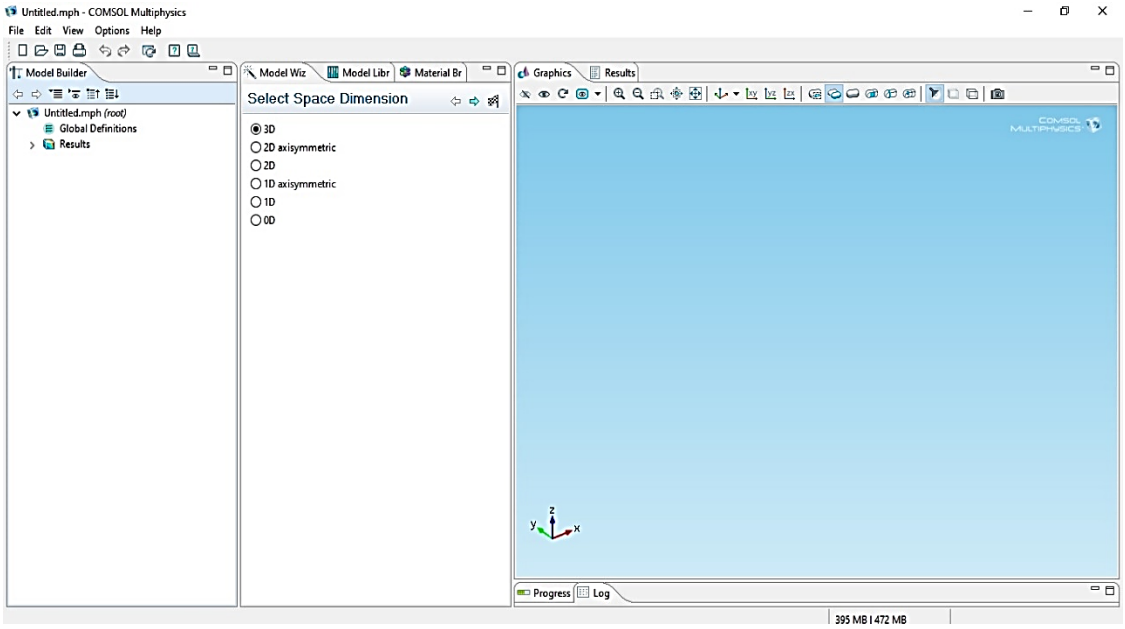

Figure-5.2(c): Selection of space dimension in 3D.

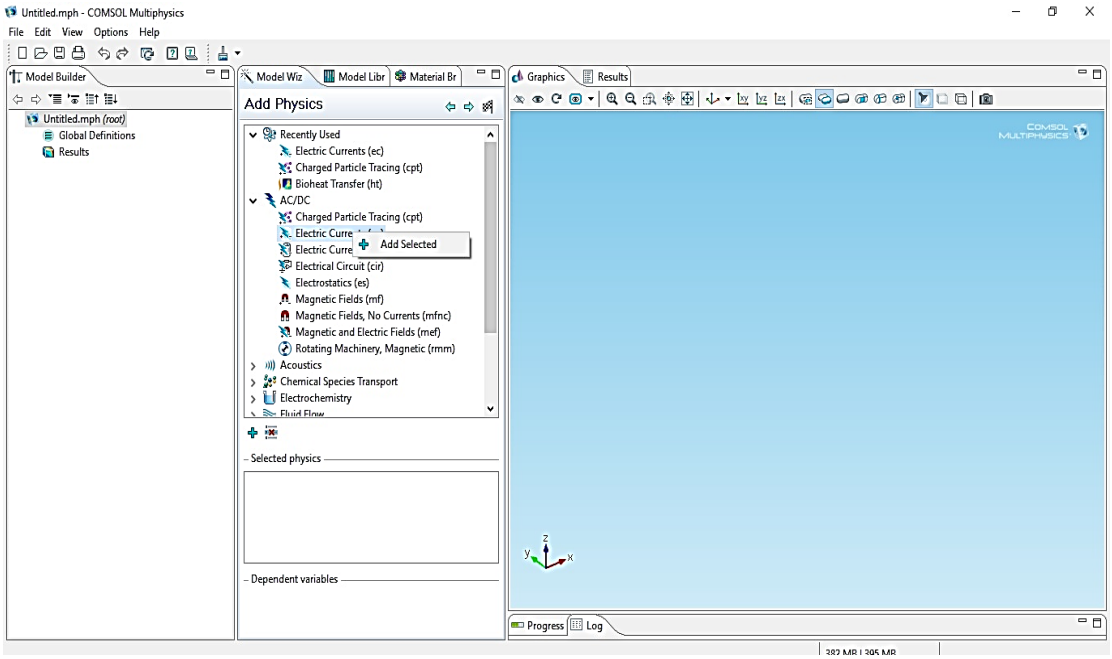

Figure- 5.2(d): Selection of AC/DC module from Add physics.

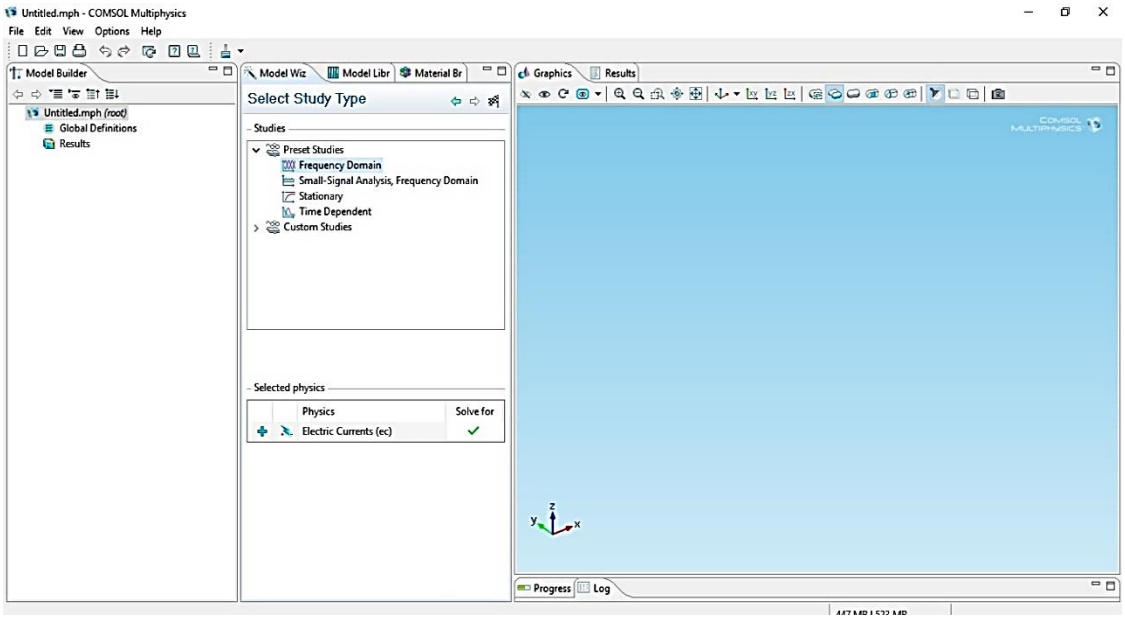

Figure-5.2(e): Selection of Frequency Domain from Select Study Type.

Now after selecting the study type, next Finish button is clicked, then need to define the units of Geometry. The unit of Length has been defined in cm and the Angular unit in degree. After setting these units, the windows view will be shown as Figure 5.2(f).

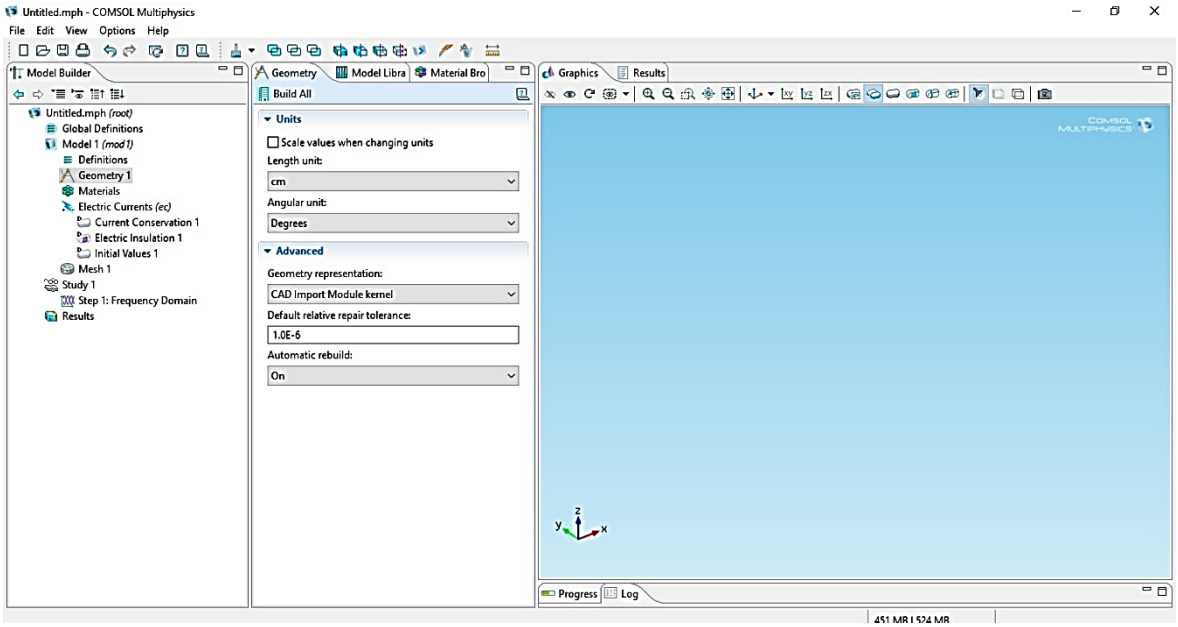

Figure-5.2(f): Selection of Units from Build All.

To make the similarity of Human Thorax/Chest Phantom Eccentric Cone geometrical shape is considered for Comsol compatible figure with the measurement of a-semiaxis:10 cm, b-semiaxis: 20 cm, Height: 42 cm, Ratio:1, Top displacement 1: 0 cm, Top displacement2: 0 cm and the position (0,0,0) cm [Figure-5.2(g)].

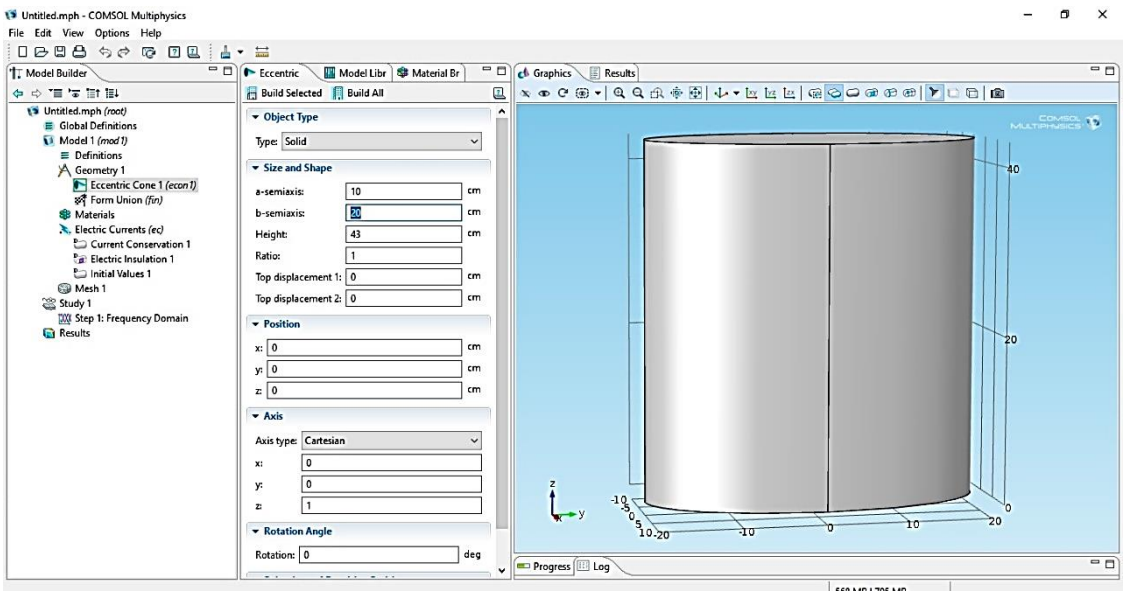

Figure-5.2(g): Computer generated Human Thorax/Chest Phantom.

Ellipsoid geometrical shapes are taken for right and left lung [Figure-5.2(h)]. Usually, the right lung is bigger than the left, which shares space in the chest with the heart [62]. Geometrical shape cylinder is taken for connecter of two lungs all measurement and positions are given in the tables 5.2 or 5.3. Connecter placed between two lungs by using two times Boolean operations.

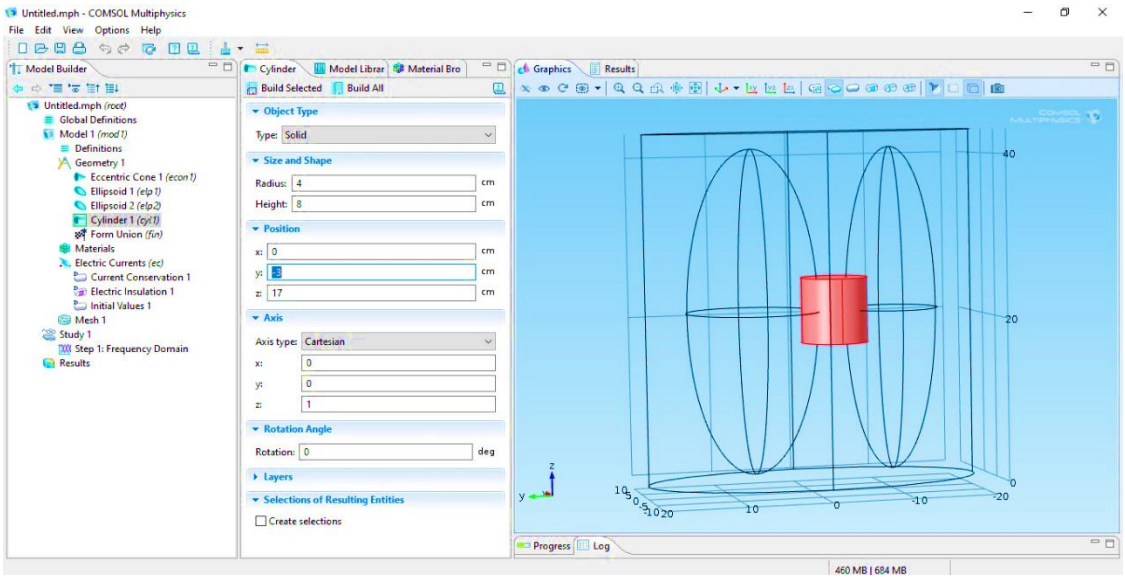

Figure-5.2(h): Computer generated Chest Phantom with Two Lungs and their connector.

Ten Surface Electrodes (SE) (Silver) are created from Sphere geometric shape with radius 1 cm and SEs are placed on Computer generated Chest Phantom for Existing Adjacent Current Drive EIT Protocol and Proposed Anterior-Posterior EIT Protocol with proper positions [Figures-5.2(i) & (j)]. All model parameters are tabulated in the table 5.2 for figure -5.2(i) and table 5.3 for figure- 5.2(j).

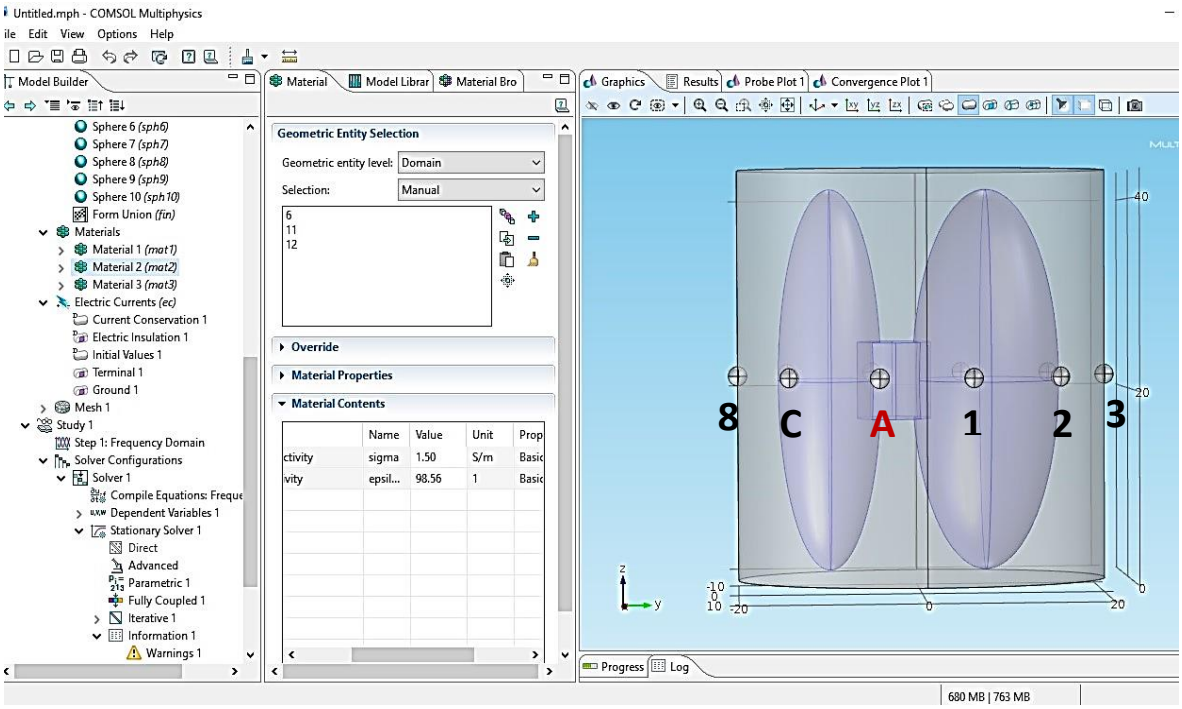

Figures-5.2(i): Computer generated Chest Phantom for Existing Adjacent Current Drive Electrical Impedance Tomography (EIT) Protocol.

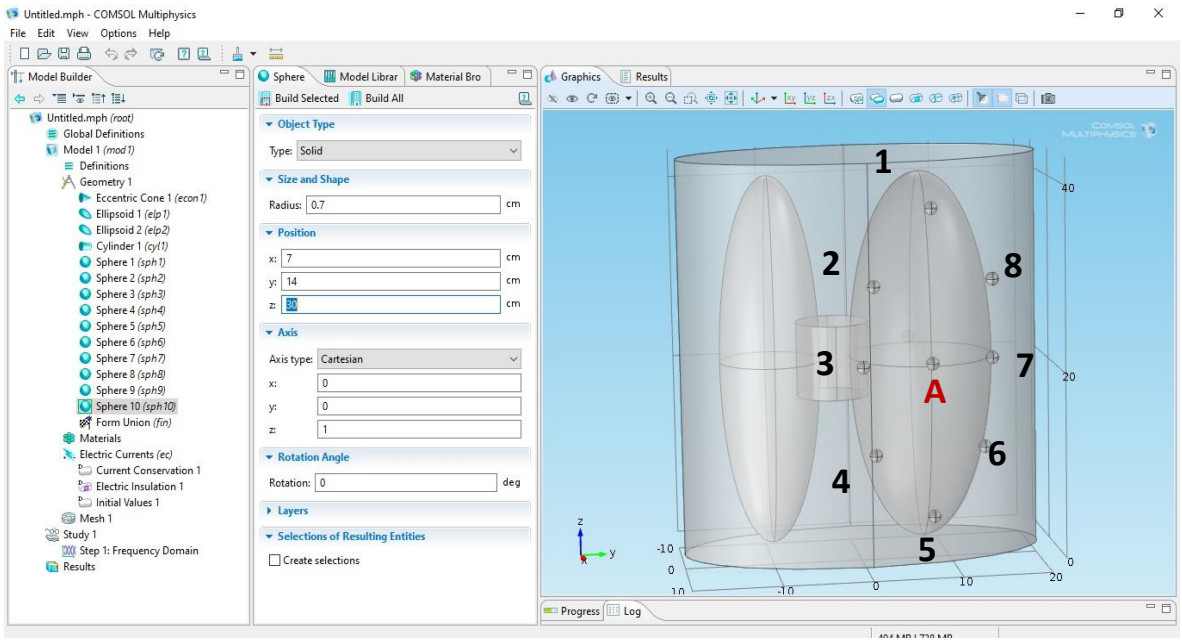

Figures-5.2(j): Computer generated Chest Phantom for Proposed Anterior-Posterior EIT Protocol.

For Existing Adjacent Current Drive Electrical Impedance Tomography (EIT) Protocol and Proposed Anterior-Posterior Electrical Impedance Tomography (EIT) Protocol. Both cases surface electrode C is used as a negative terminal and A as a positive terminal. Remaining eight SE (1 to 8) are used as a potential calculating electrodes.

5.3 Computer Simulation Studies on Existing All Electrical Impedance Technique (EIT) Protocols

In order to simulate healthy or diseased lung during breathing, electrical conductivity (σ) and relative permittivity (ϵ) of the lung were varied between deflated and inflated lung. Visceral movement (i.e., geometrical changes) during a breath cycle was not considered. Our studies were normal lung at inspiration and expiration conditions diseased lungs like- pneumothorax (collapsed lung) and pulmonary edema (excess fluid accumulation in the lungs) were taken due to their significant change of electrical conductivity [24].Bioelectrical Impedance Analysis (BIA) uses a low and constant amplitude (≤1mA) alternating current (generally 50 KHz) is injected through two current drive electrodes and voltages are measured on the other electrodes (named as voltage electrodes) [32]. As followed by the other Researchers of bioelectrical impedance analysis1mA a low and constant amplitude alternating current was injected through two current drive surface electrodes (SE) and another eight SE are used for voltage calculations of single frequency 50 KHz for computer simulation. Multi-frequency 20 KHz, 50 KHz, 100 KHz, 150 KHz and 200 KHz were also used for computer simulation studies for better tissue characterizations as well as for the assessment of lung functions. Simulation studies 1,2,3,4 and 5 were used 1 mA constant amplitude alternating current with 50 KHz frequency for two current drive surface electrodes.

Four existing EIT protocols (like-adjacent current drive, opposite current drive at the vertices of the semi-major axis of the chest cross section, opposite current drive at the vertices of the semi-minor axis of the chest cross section, opposite current drive along the right lung) by computer simulation for assessing lung functions of healthy lung at inspiration and expiration, diseased lungs of pneumothorax (collapsed lung) and pulmonary edema. Existing all types of EIT Protocols electrodes are placed on the chest cross section (horizontal plane).

5.3(A): Simulation Study Method -1: Existing Adjacent Current Drive EIT Protocol

Following the section 5.2.2 for construction of computer generated human chest phantom with two lungs and their connector and also ten placed electrodes, then material selections are very important for computer simulation. Material selections sequences are given as follows.

Step-1: Thorax material is selected with the electrical conductivity 0.352 Sm^{-1} and relative permittivity 10094 [Table-5-2] and the selection domains are 3,4,5,8,9,15,16,17,18,21,22 as shown in Figure-5.3(a-i).

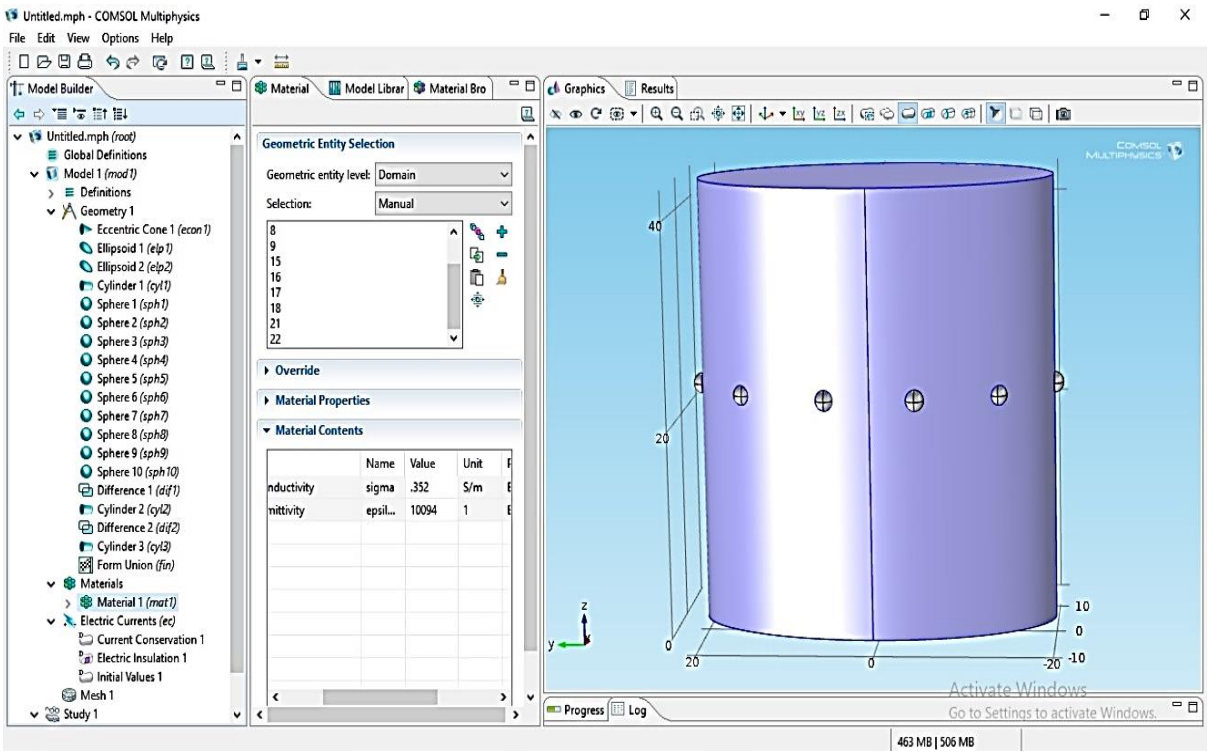

Figure-5.3 (a-i): Selection of Thorax material for Computer generated Chest Phantom.

Step-2: Lungs and connector of two lungs materials are selected with the electrical conductivity and relative permittivity for inflated lung 0.103Sm^{-1},4272.50 and for deflated lung 0.2620 Sm^{-1}, 8531.40 and the selection domains are 10,11,12 as shown in Figure-5.3(a-ii).

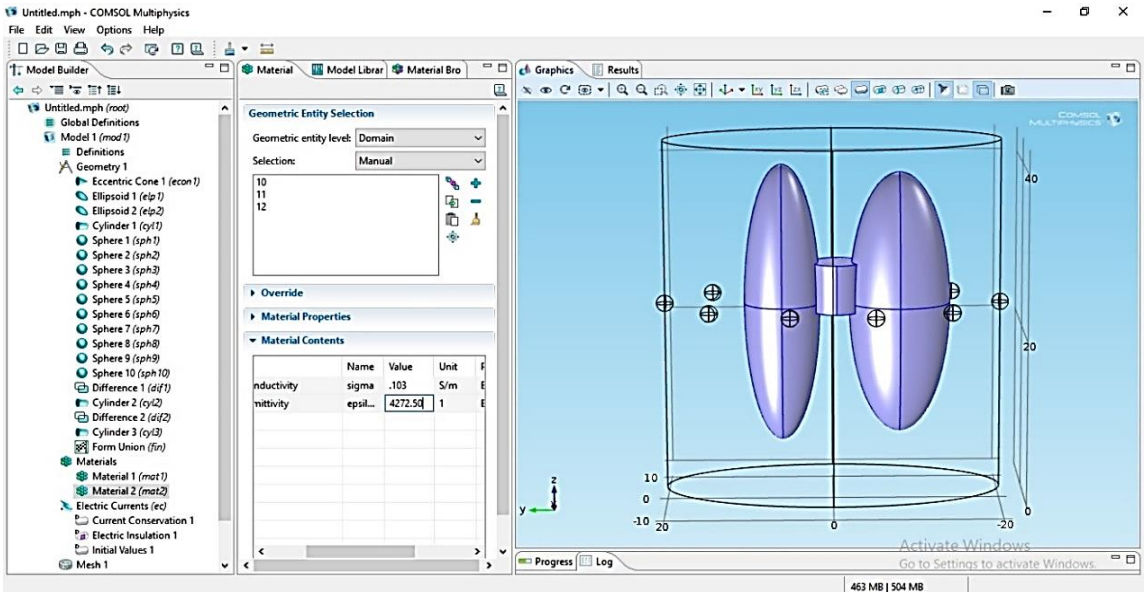

Figure-5.3(a-ii): Complete view of computer generated chest phantom with two lungs and their connector.

Step-3: Ten electrodes of Silver material are selected with electrical conductivity 6.16× 10^7 S/m and relative permittivity 3.4 and the selection domains are 1, 2,6,7,13, 14, 19, 20, 23, and 24 as shown in Figure-5.3 (a-iii).

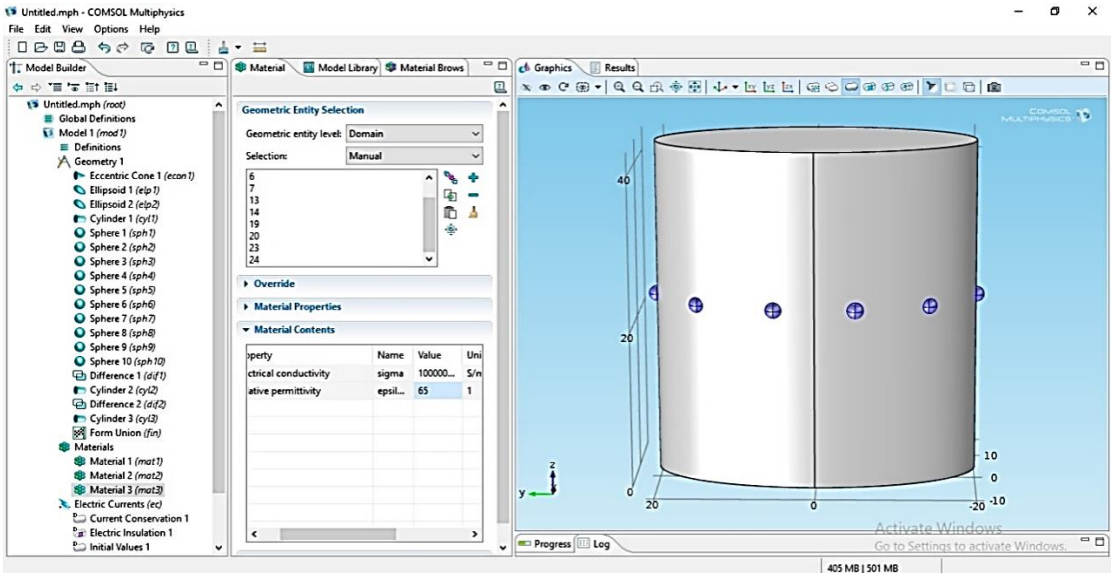

Figure-5.3(a-iii): Selection of10 surface electrodes Silver material for Computer generated Chest Phantom.

Step-4: In order to define the ten electrodes as ten boundary probes have been chosen the Definitions option in the model builder. Boundary probes renamed as Surface Electrodes (SE) have been selected from the electrodes one by one. Boundary elements are SE-1 (37-40), SE- 2 (5-8), SE-3 (1-4), SE-4 (33-36), SE- 5 (83,84,95,96), SE- 6 (143,144,145,150), SE-7 (175-178), SE- 8 (166,167,173,174), SE- 9 (141,142,151,152) &SE-10 (87,88,117,119) as shown in Figure-5.3(a-iv).

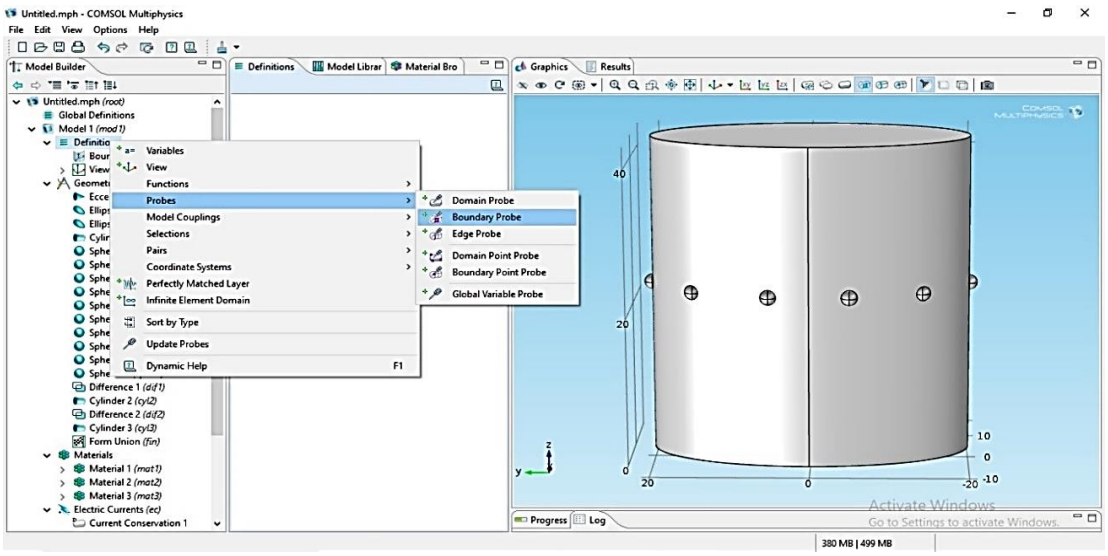

Figure-5.3(a-iv): Selection of SE from sub- menu probe.

Step-5: Terminal (source) and Ground are very important for simulation. Ground and Terminal have been added to the model builder of Electric Currents (ec). The current at the terminal has been set to 1 mA. The selected SE has set as a Ground and adjacent another SE as Terminal as shown in Figure-5.3(a-v).

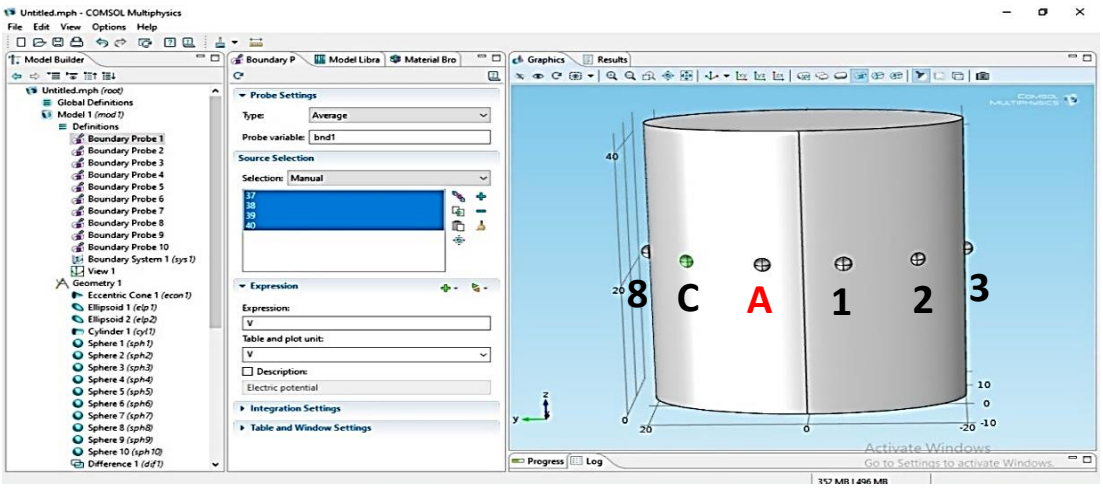

Figure-5.3(a-v): Selection of Surface Electrode (SE).

Surface Electrodes configuration of Existing Adjacent Current Drive EIT Protocol with computer generated digital chest phantom shown in the figure-5.3(a-vi) and 5.3(a-vii).

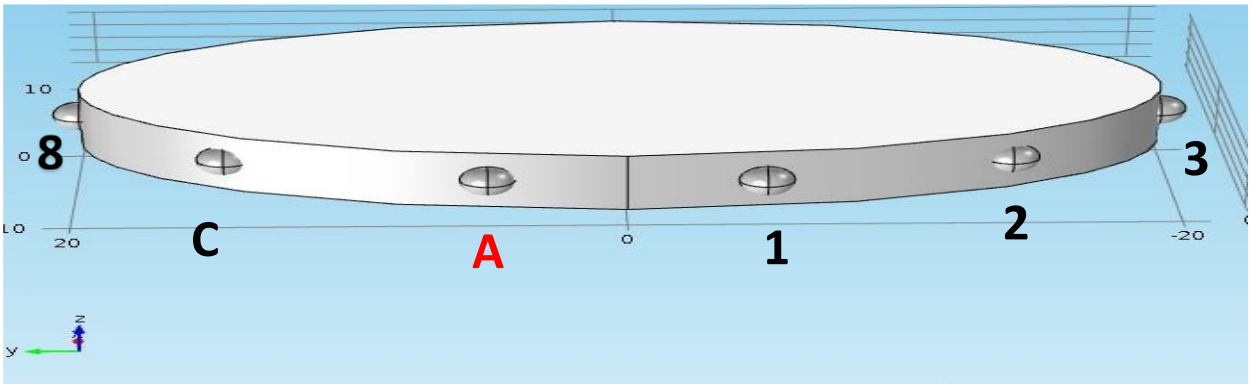

Figure 5.3(a-vi): Surface Electrodes Configuration of Adjacent Current Drive EIT Protocol.

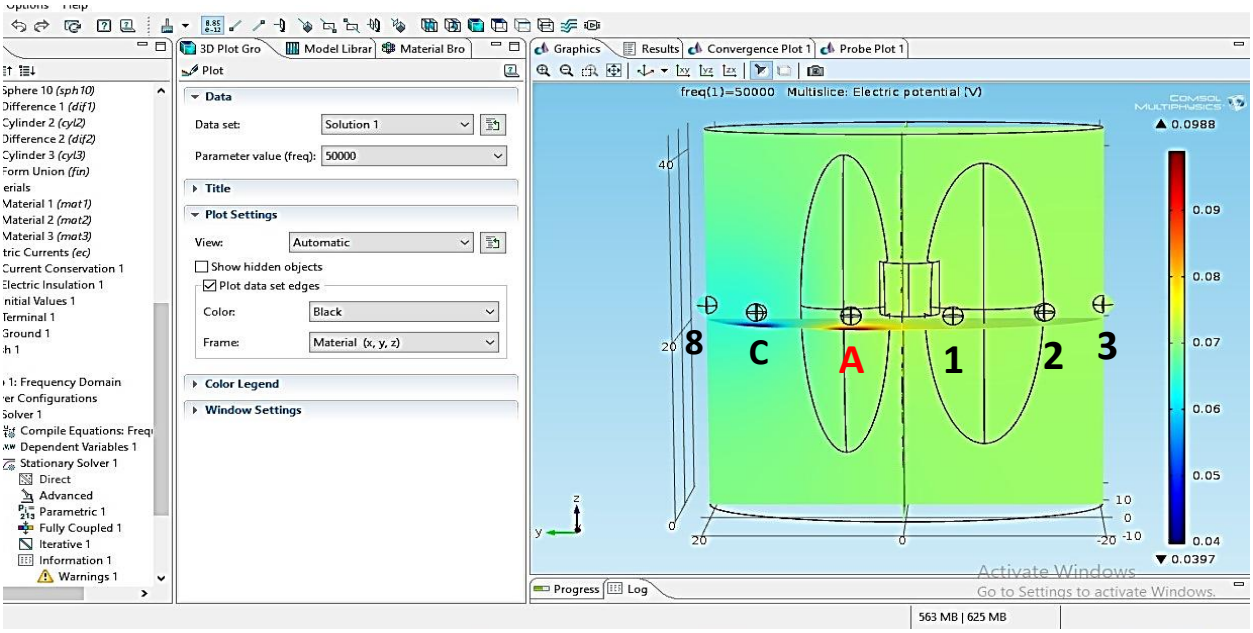

Figure 5.3(a-vii): Existing Adjacent Current Drive EIT Protocol with computer generated digital chest phantom.

Step-6: The frequency of the current has been specified as 50 KHz in the study settings from the section Study-1. Finally, Study-1 to select compute option to run the simulation. After this, the Result Window contains the data that shows the boundary potential at each of the surface electrodes [Figure- 5.3 (a-viii).

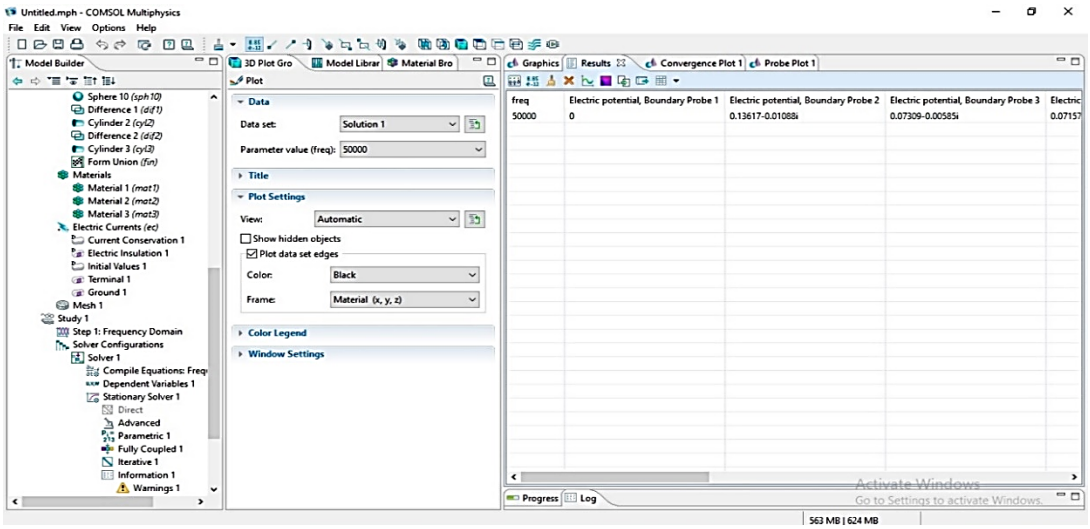

Figure-5.3 (a-viii): Result window shows the boundary potential at each of the surface electrodes.

Multi slice Electric Potential view window of Computer generated Chest Phantom as shown in figure-5.3(a-ix).

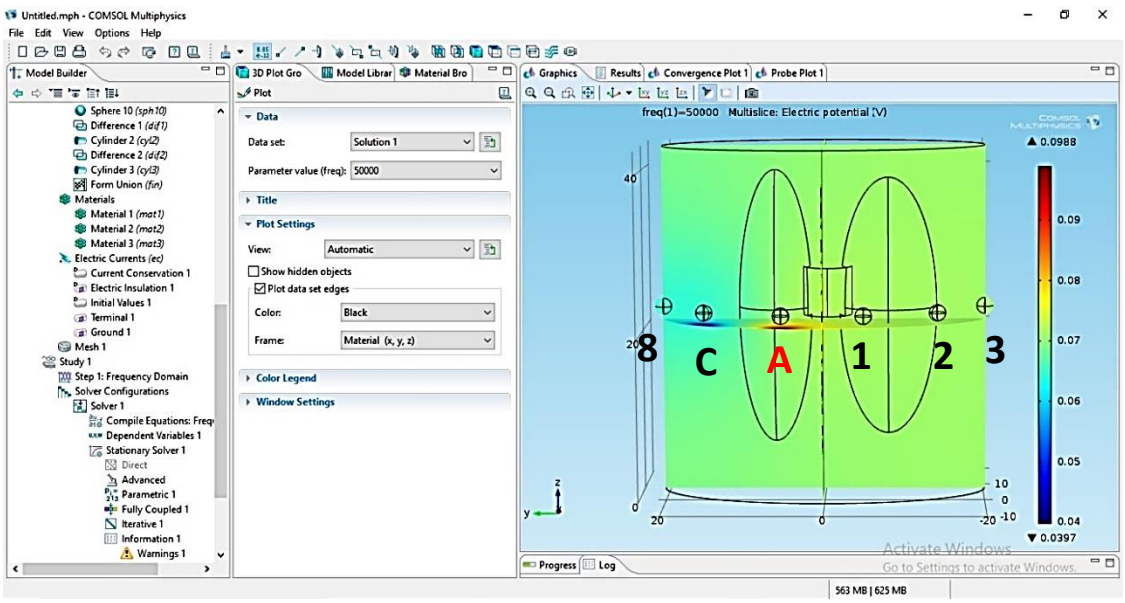

Figure-5.3(a-ix): Electric Potential view of Computer generated Chest Phantom.

Mesh view of Computer generated Chest Phantom as shown in Figure-5.3 (a-x).

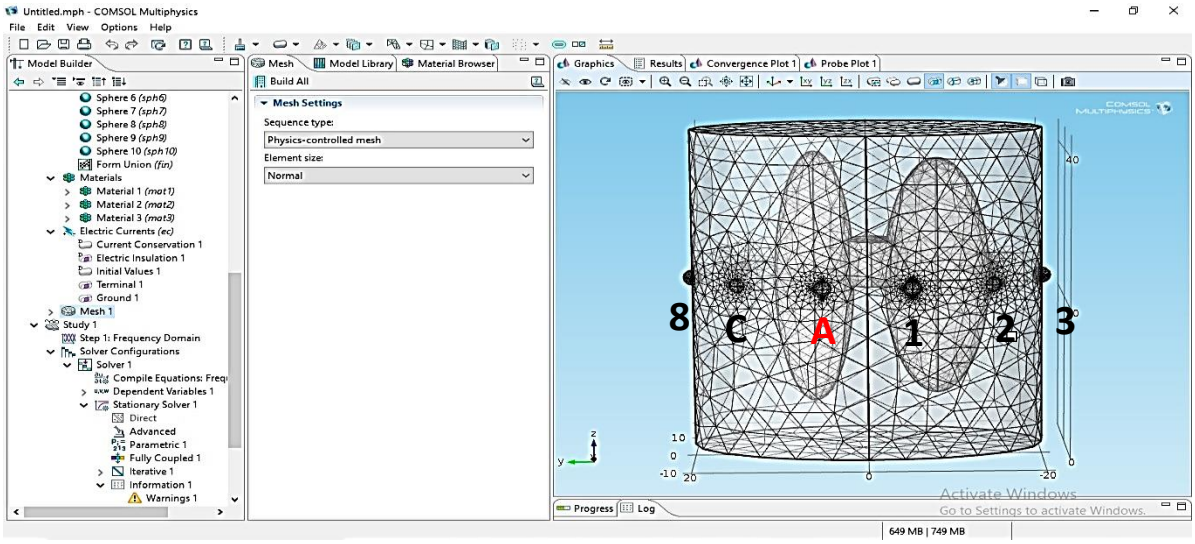

Figure-5.3(a-x): Mesh view of Computer generated Chest Phantom.

After mesh analysis number of vertex elements 150, number of edge elements 1218, number of boundary elements 8802, number of elements 49650, free meshing time 3.64 sec and minimum element quality 0.0002288.

After computer simulation we have got simulated data which have tabulated of the tables 5.4 (a& b) to 5.8(a& b).From these tables 5.4(a) to 5.4(e)figures are drawn to study the sensitivity and accuracy of the computer simulated data for existing adjacent current drive EIT protocol for assessing lung functions of **(a)**healthy lungs at inspiration and expiration condition,**(b)**healthy lungs at inspiration and diseased lungs pneumothorax (collapsed lung),**(c)**healthy lungs at expiration and diseased lungs pneumothorax (collapsed lung),**(d)** healthy lungs at inspiration and diseased lungs pulmonary edema, and**(e)** healthy lungs at expiration and diseased lungs pulmonary edema.

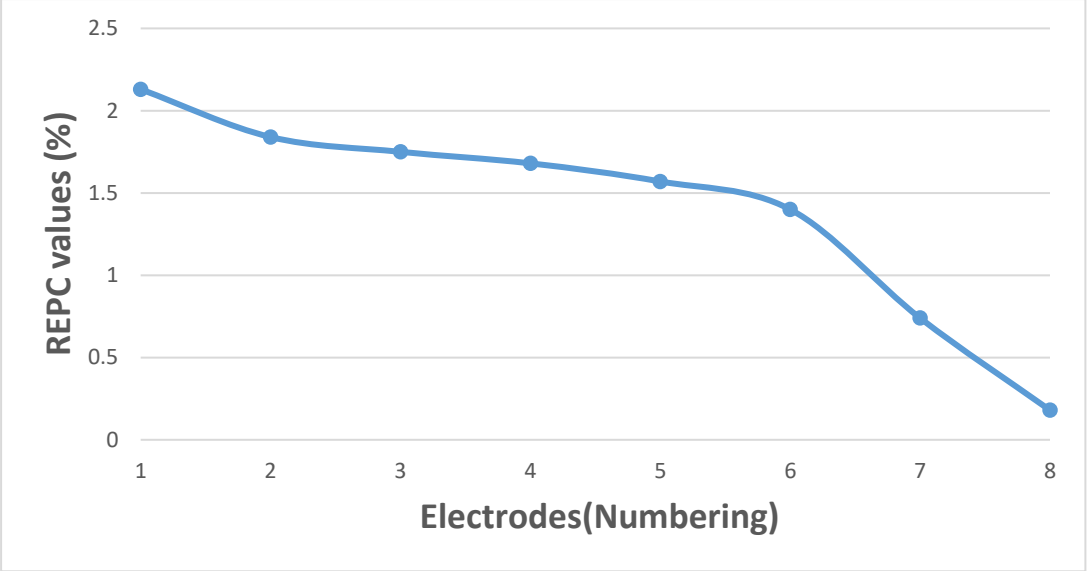

Figure 5.4(a)

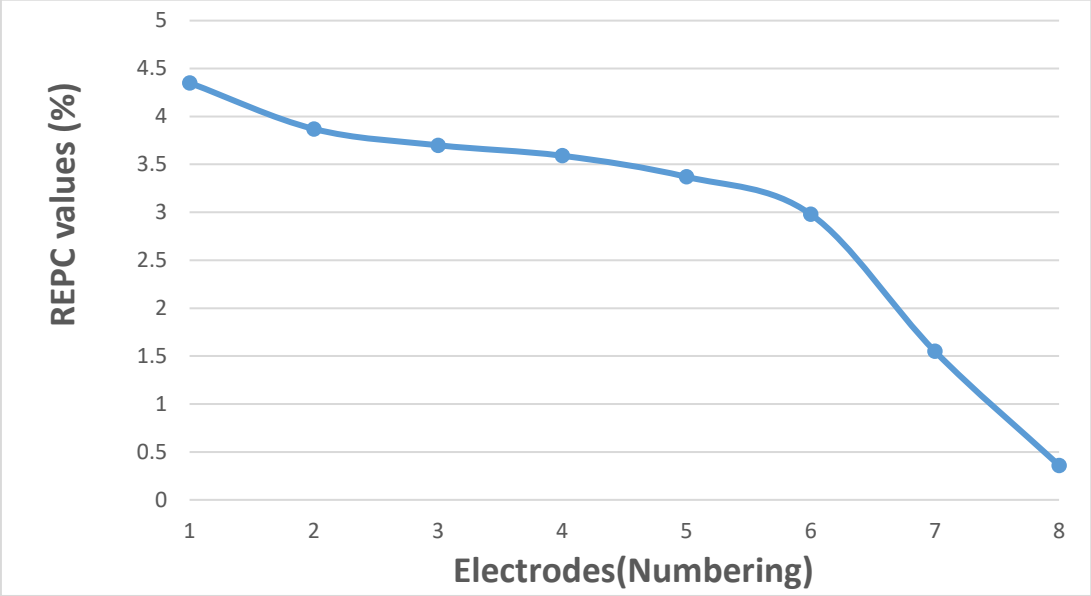

Figure 5.4(b)

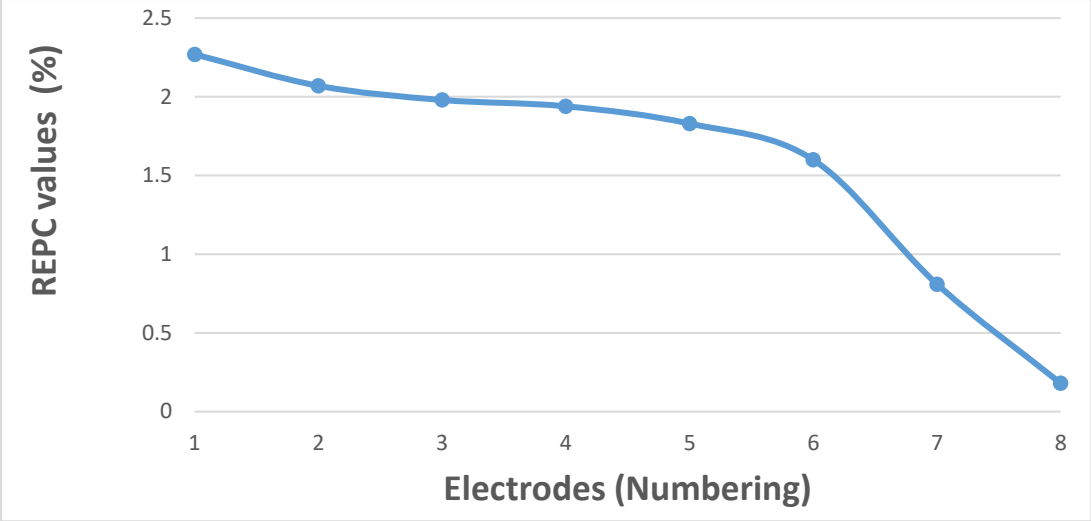

Figure 5.4(c)

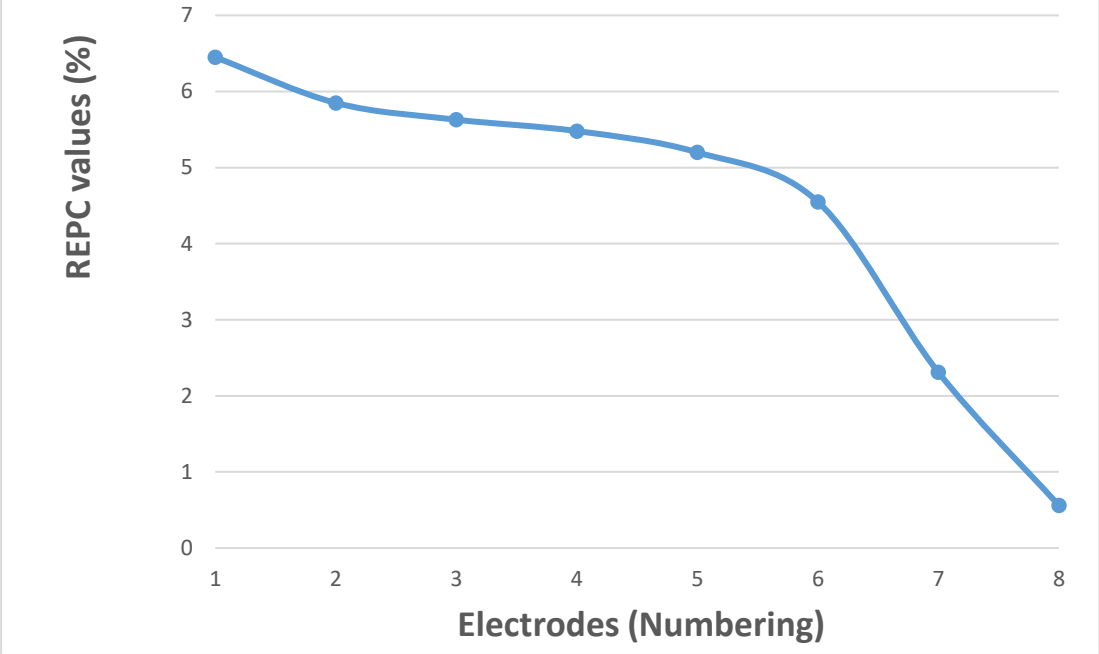

Figure 5.4(d)

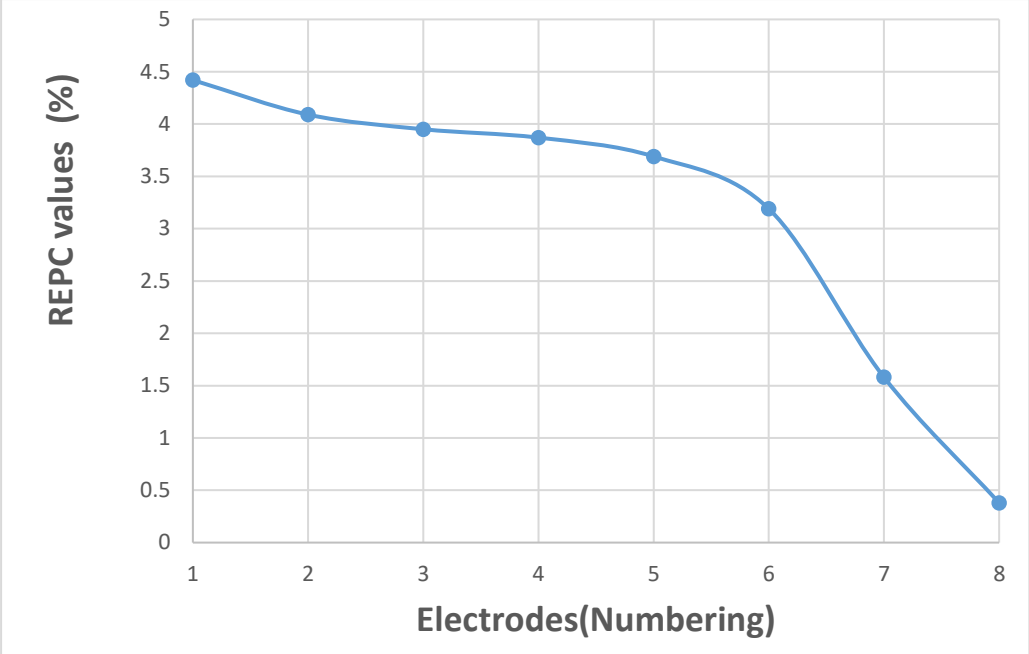

Figure 5.4(e)

Figure 5.4 Sensitivities and accuracies are obtained by using Comsol simulated data for existing adjacent current drive EIT protocol for assessing lung functions of **(a)** healthy lungs at inspiration and expiration condition, **(b)** healthy lungs at inspiration and diseased lungs pneumothorax (collapsed lung), **(c)** healthy lungs at expiration and diseased lungs pneumothorax (collapsed lung), **(d)**healthy lungs at inspiration and diseased lungs pulmonary edema, **(e)** healthy lungs at expiration and diseased lungs pulmonary edema ; where X and Y axes are indicates the electrodes (numbering) and relative electric potential change (REPC) values (%) respectively.

5.3(B) Simulation Study Method-2: Existing Opposite Current Drive at the vertices of the semi-major axis of the chest cross section EIT Protocol

Surface Electrodes configuration of Existing Opposite Current Drive at the vertices of the semi-major axis of the chest cross section EIT Protocol with computer generated digital chest phantom shown in the figure-5.5.

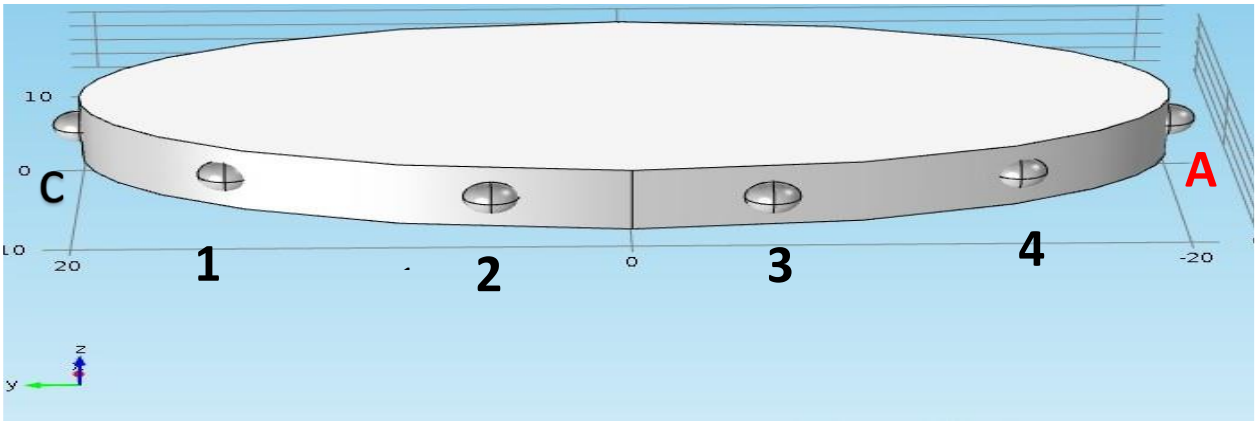

Figure 5.5(a): Surface Electrodes configuration of Existing Opposite Current Drive at the vertices of the semi-major axis of the chest cross section EIT Protocol.

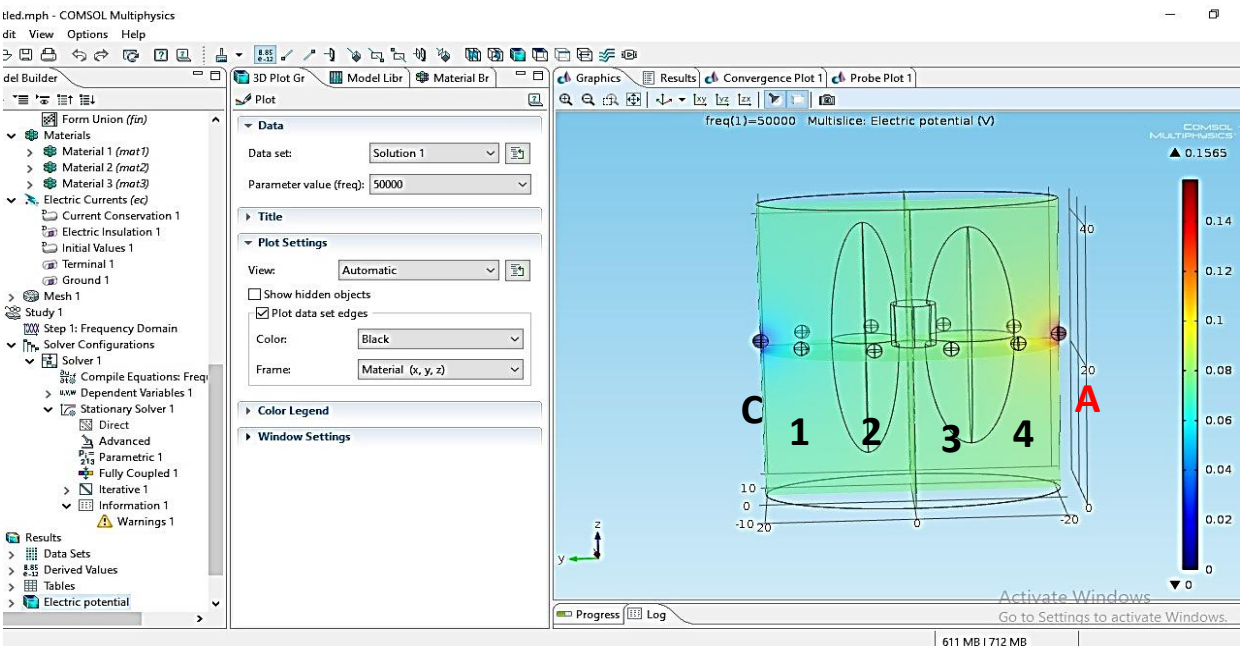

Figure 5.5(b): Existing Opposite Current Drive at the vertices of the semi-major axis of the chest cross section EIT Protocol with computer generated digital chest phantom.

Following the same simulation tasks of section 5.3(A) has been done for Existing Opposite Current Drive at the vertices of the semi-major axis of the chest cross section EIT Protocol. We have got computer simulated data which have tabulated of the tables 5.9 (a& b) to 5.13(a&b).From these tables 5.6(a) to 5.6(e) figures have drawn to study the sensitivity and accuracy of computer simulated data for existing opposite current drive at the vertices of the semi-major axis of the chest cross section EIT Protocol for assessing lung functions of **(a)** healthy lungs at inspiration and expiration condition, **(b)** healthy lungs at inspiration and diseased lungs pneumothorax (collapsed lung), **(c)** healthy lungs at expiration and diseased lungs pneumothorax (collapsed lung), **(d)** healthy lungs at inspiration and diseased lungs pulmonary edema, and **(e)** healthy lungs at expiration and diseased lungs pulmonary edema.

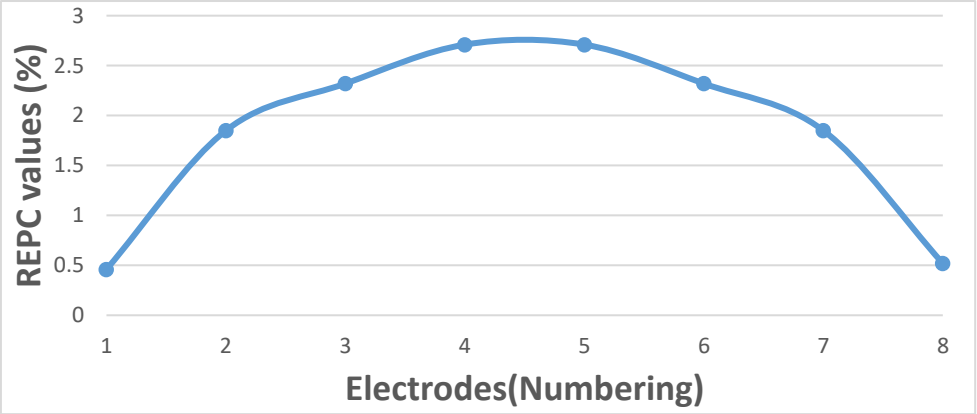

Figure 5.6(a)

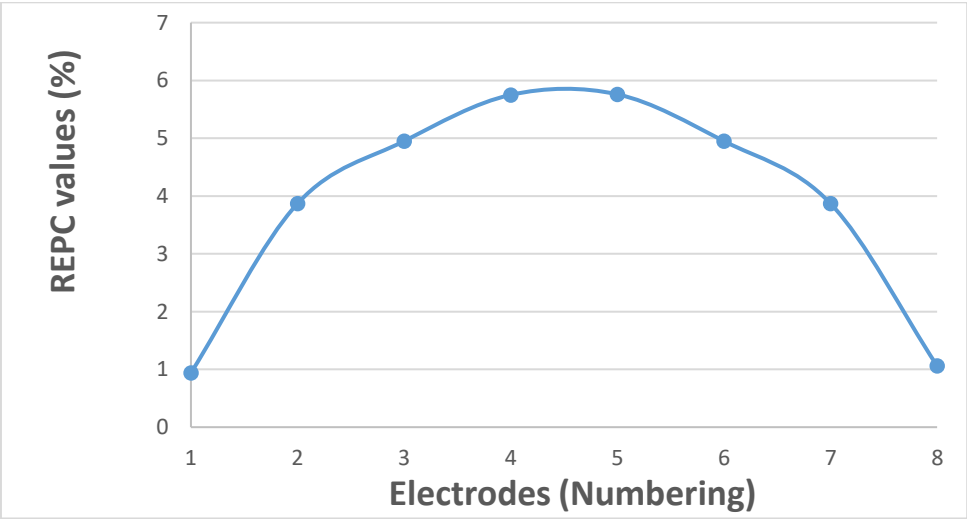

Figure 5.6(b)

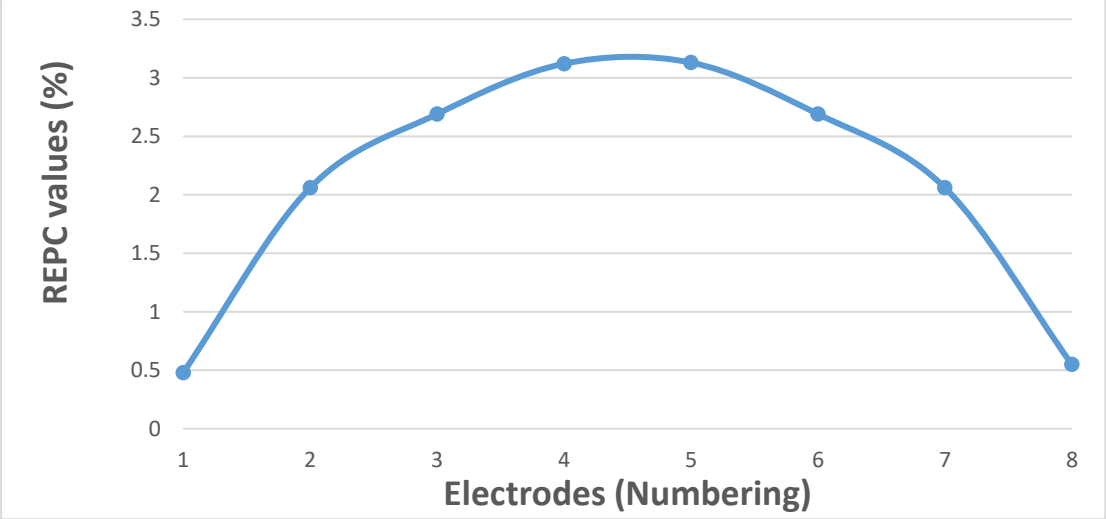

Figure 5.6(c)

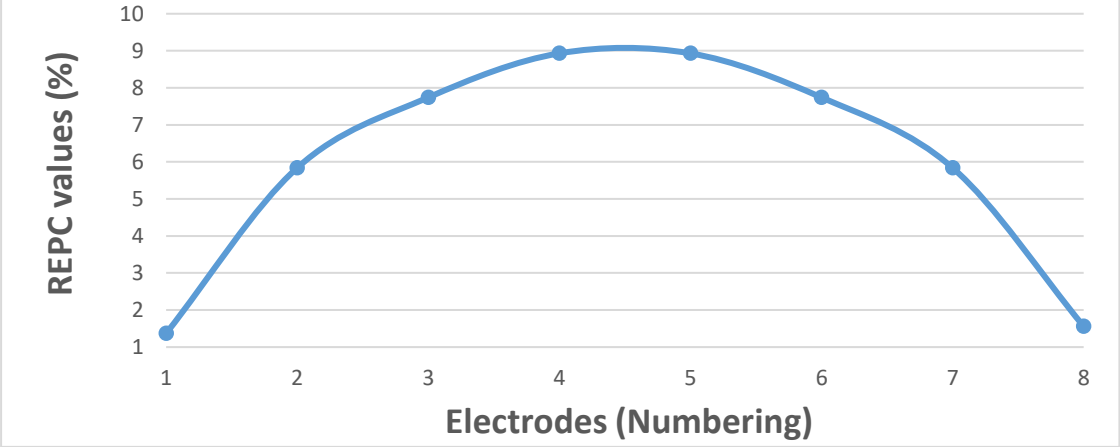

Figure 5.6(d)

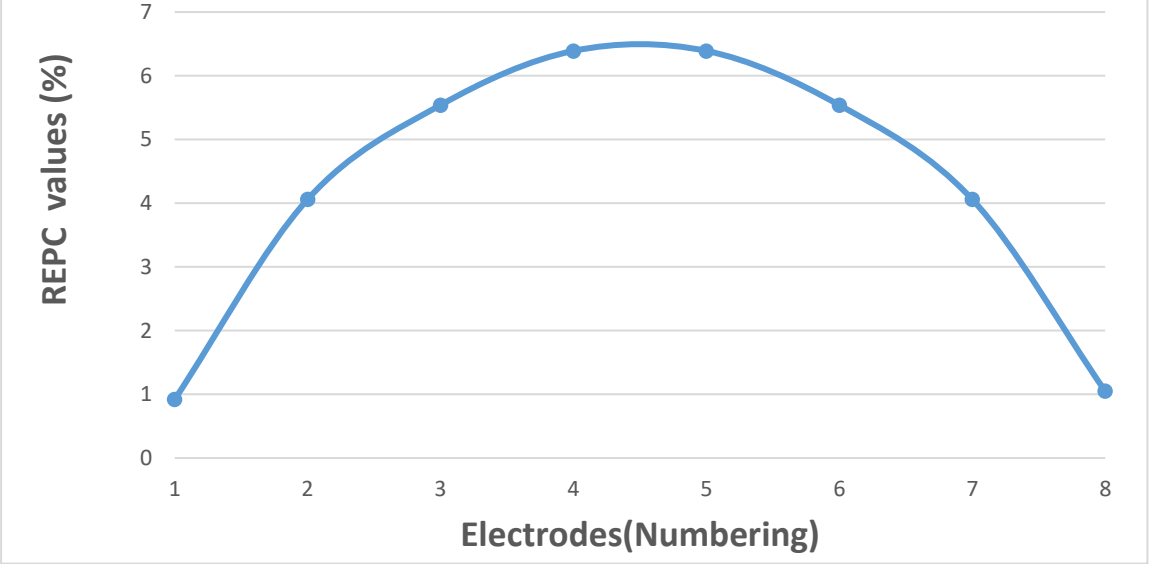

Figure 5.6(e)

Figure 5.6 Sensitivities and accuracies are obtained by using Comsol simulated data for existing opposite current drive at the vertices of the semi-major axis of the chest cross section EIT Protocol for assessing lung functions of **(a)** healthy lungs at inspiration and expiration condition, **(b)** healthy lungs at inspiration and diseased lungs pneumothorax (collapsed lung), **(c)** healthy lungs at expiration and diseased lungs pneumothorax (collapsed lung), **(d)** healthy lungs at inspiration and diseased lungs pulmonary edema, **(e)** healthy lungs at expiration and diseased lungs pulmonary edema ; where X and Y axes are indicates the electrodes (numbering) and relative electric potential change (REPC) values (%) respectively.

5.3(C) Simulation Study Method-3: Existing Opposite Current Drive at the vertices of the semi-minor axis of the chest cross section EIT Protocol

Surface Electrodes configuration of Existing Opposite Current Drive at the vertices of the semi-minor axis of the chest cross section EIT Protocol with computer generated digital chest phantom shown in the figure-5.7.

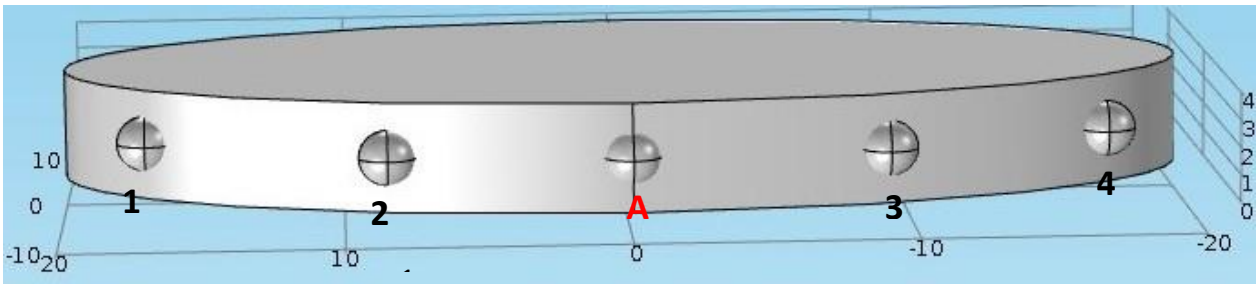

Figure 5.7(a): Surface Electrodes configuration of Existing Opposite Current Drive at the vertices of the semi-minor axis of the chest cross section EIT Protocol.

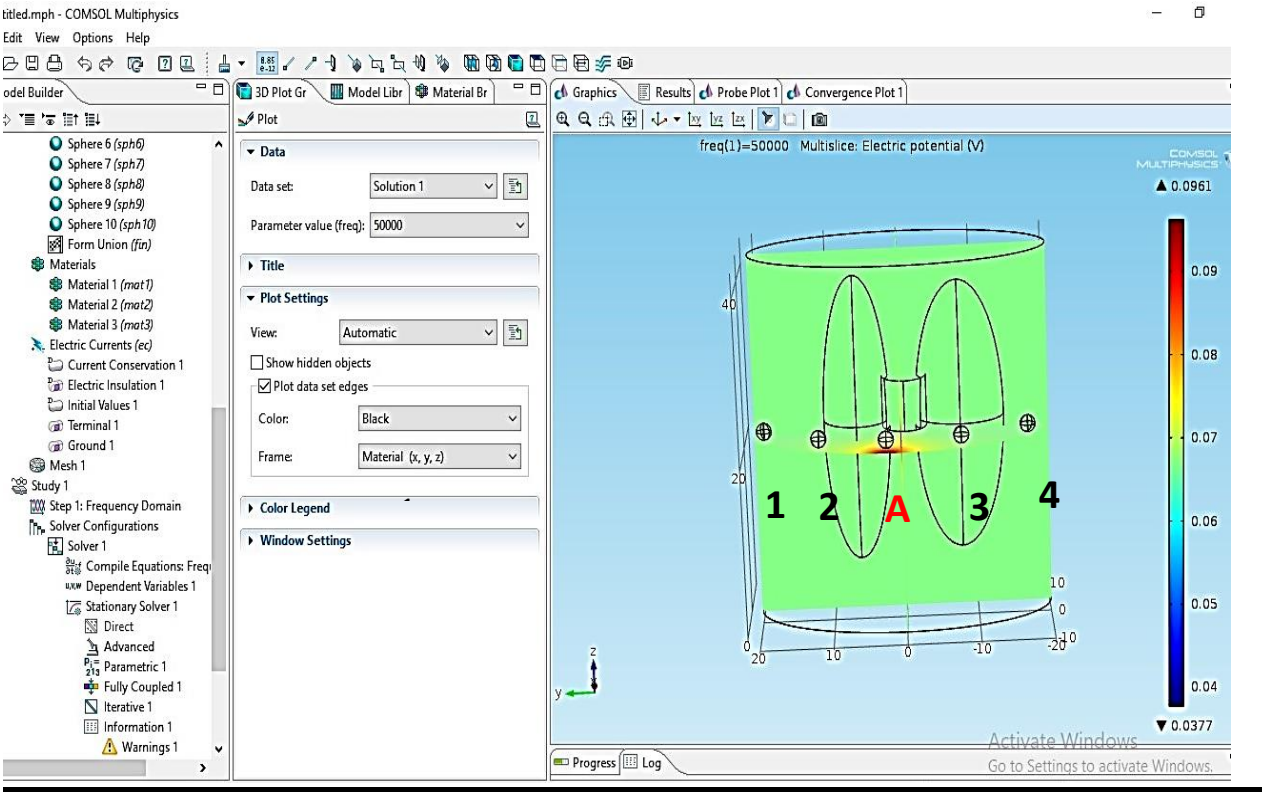

Figure 5.7(b): Existing Opposite Current Drive at the vertices of the semi-minor axis of the chest cross section EIT Protocol with computer generated digital chest phantom.

Following the same simulation tasks of section 5.3(A) for Existing Opposite Current Drive at the vertices of the semi-minor axis of the chest cross section EIT Protocol. We have got computer simulated data which has been tabulated of the tables 5.14 (a& b) to 5.18(a& b).From these tables 5.8(a) to 5.8(e) figures have been drawn to study the sensitivity and accuracy of computer simulated data for existing opposite current drive at the vertices of the semi-minor axis of the chest cross section EIT Protocol for assessing lung functions of **(a)** healthy lungs at inspiration and expiration condition, **(b)** healthy lungs at inspiration and diseased lungs pneumothorax (collapsed lung), **(c)** healthy lungs at expiration and diseased lungs pneumothorax (collapsed lung), **(d)** healthy lungs at inspiration and diseased lungs pulmonary edema, and **(e)** healthy lungs at expiration and diseased lungs pulmonary edema.

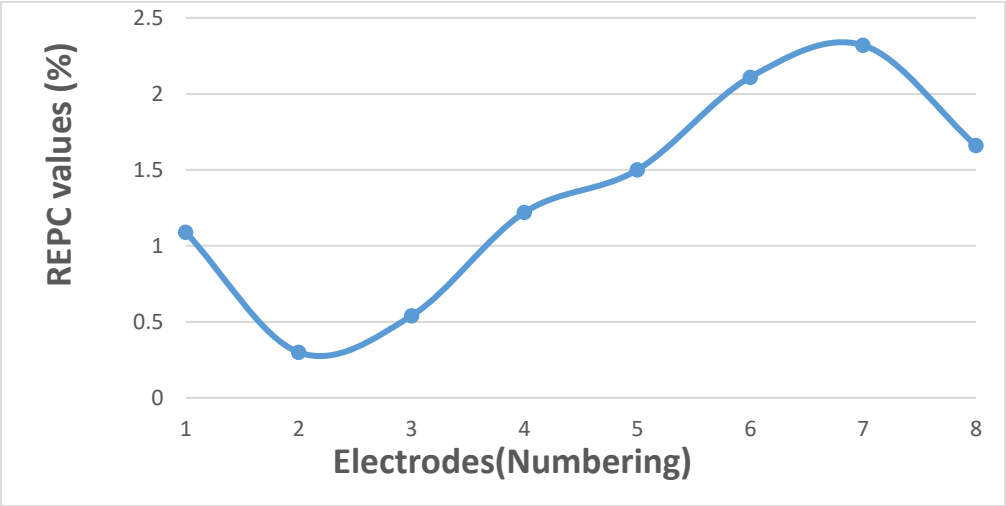

Figure 5.8(a)

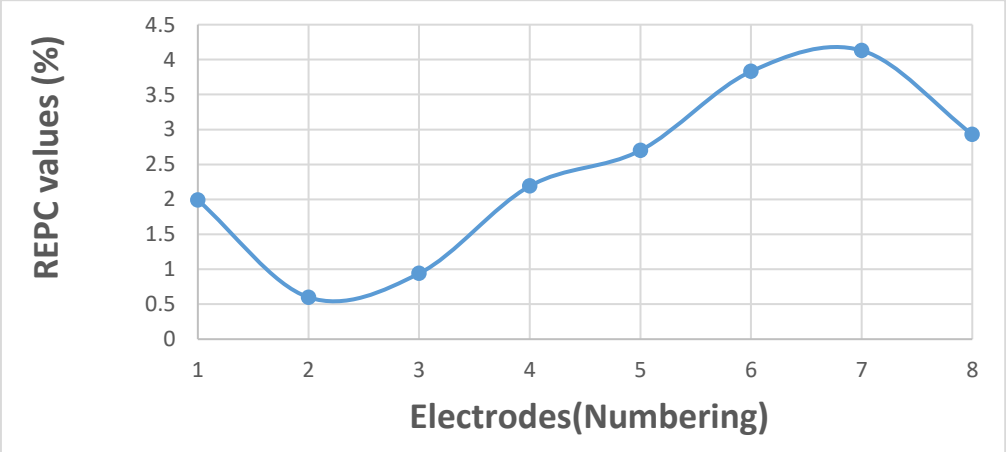

Figure 5.8(b)

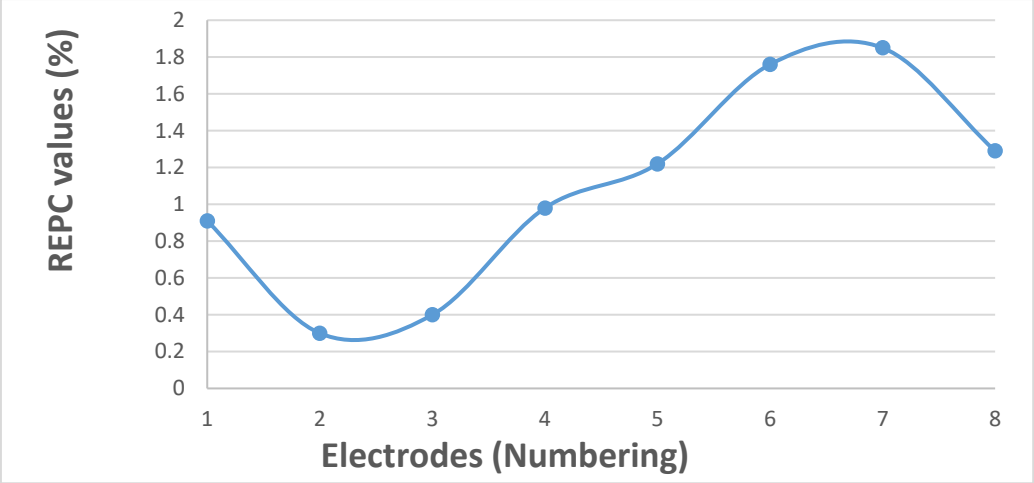

Figure 5.8(c)

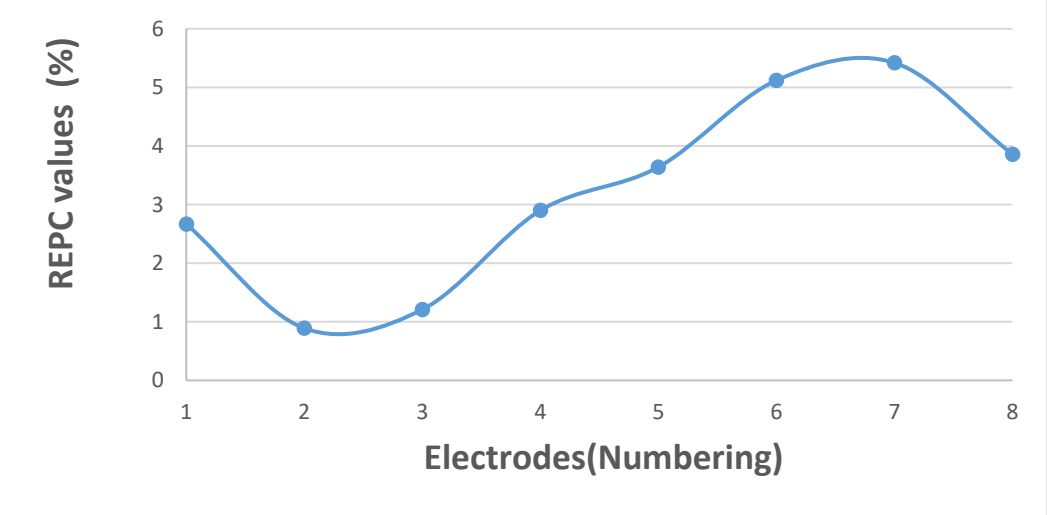

Figure 5.8(d)

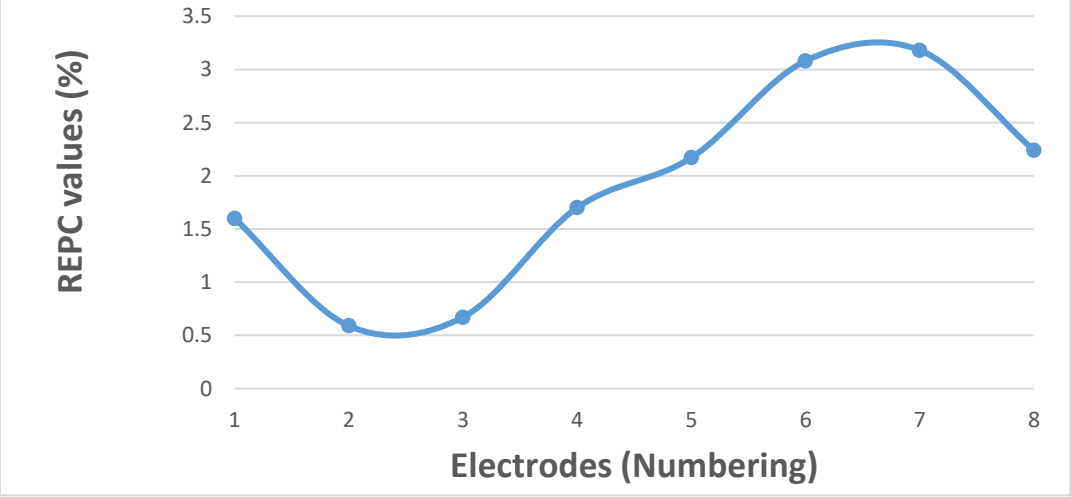

Figure 5.8(e)

Figure 5.8 Sensitivities and accuracies are obtained by using Comsol simulated data for existing opposite current drive at the vertices of the semi-minor axis of the chest cross section EIT Protocol for assessing lung functions of **(a)** healthy lungs at inspiration and expiration condition, **(b)** healthy lungs at inspiration and diseased lungs pneumothorax (collapsed lung), **(c)** healthy lungs at expiration and diseased lungs pneumothorax (collapsed lung), **(d)** healthy lungs at inspiration and diseased lungs pulmonary edema, **(e)** healthy lungs at expiration and diseased lungs pulmonary edema ; where X and Y axes are indicates the electrodes (numbering) and relative electric potential change (REPC) values (%) respectively.

5.3(D) Simulation Study Method-4: Existing Opposite Current Drive along the right lung EIT Protocol

Surface Electrodes configuration of Existing Opposite Current Drive along the right lung EIT Protocol with computer generated digital chest phantom shown in the figure-5.9.

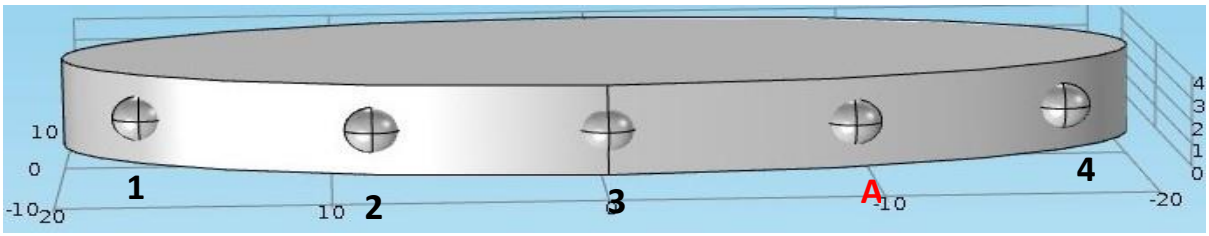

Figure 5.9(a): Surface Electrodes configuration of Existing Opposite Current Drive along the right lung EIT Protocol.

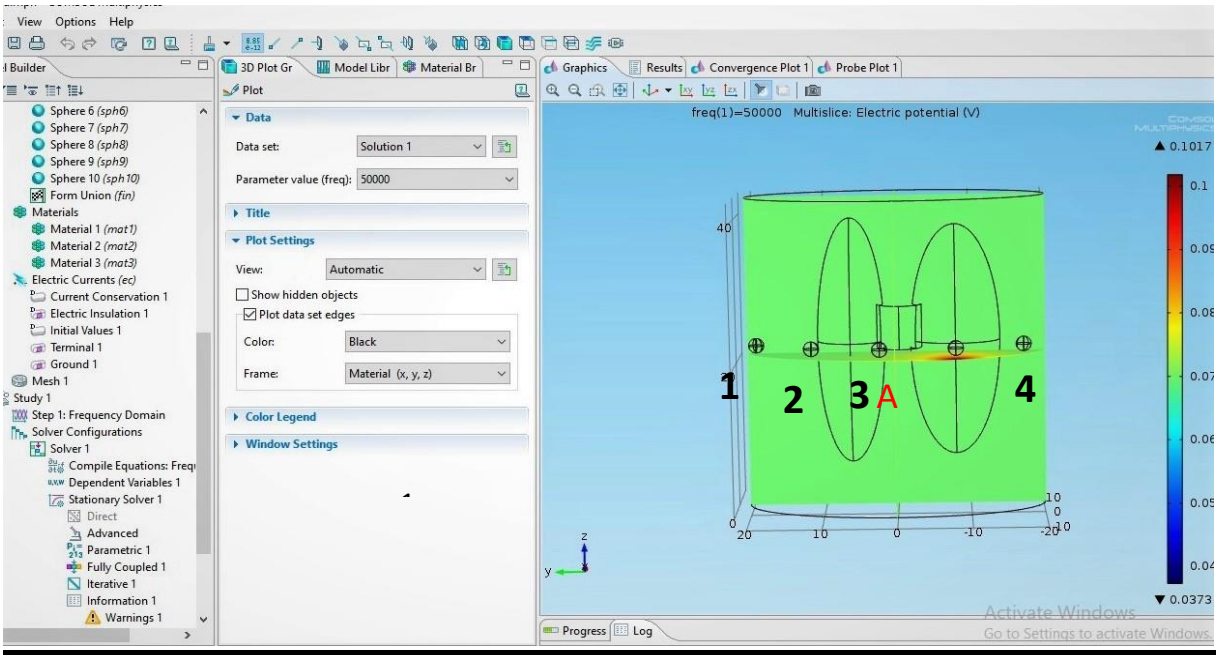

Figure 5.9(b): Existing Opposite Current Drive along the right lung EIT Protocol with computer generated digital chest phantom.

Following the same simulation tasks of section 5.3(A) for Existing Opposite Current Drive along the right lung EIT Protocol. We have got computer simulated data which has been tabulated of the tables 5.19 (a& b) to 5.23(a& b).From these tables 5.10(a) to 5.10(e) figures have drawn to study the sensitivity and accuracy of computer simulated data for existing opposite current drive along the right lung EIT Protocol for assessing lung functions of **(a)** healthy lungs at inspiration and expiration condition, **(b)** healthy lungs at inspiration and diseased lungs pneumothorax (collapsed lung), **(c)** healthy lungs at expiration and diseased lungs pneumothorax (collapsed lung), **(d)** healthy lungs at inspiration and diseased lungs pulmonary edema, and **(e)** healthy lungs at expiration and diseased lungs pulmonary edema.

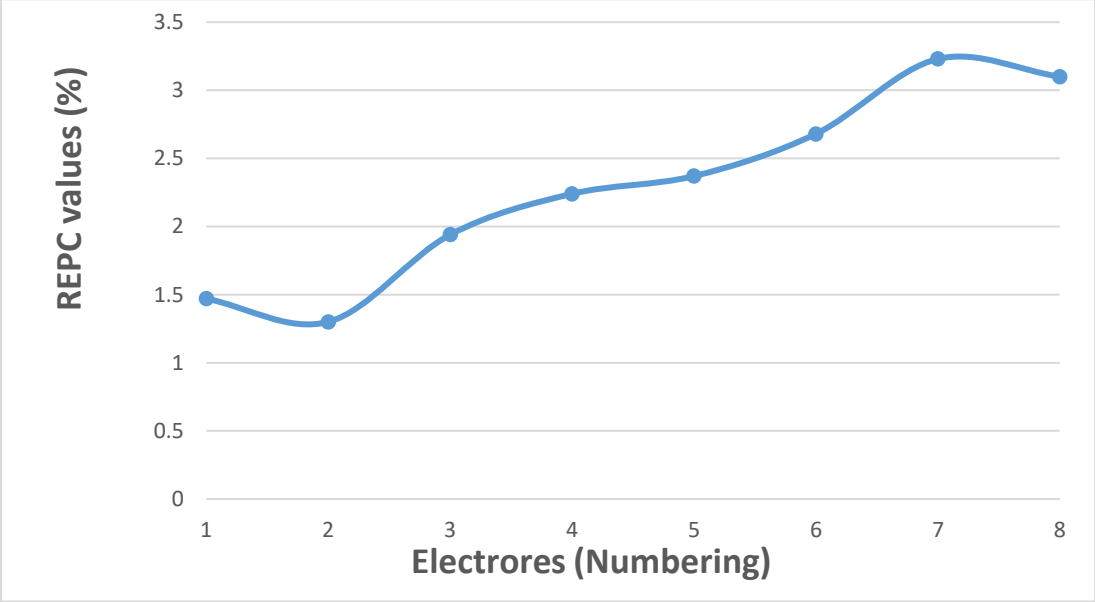

Figure 5.10(a)

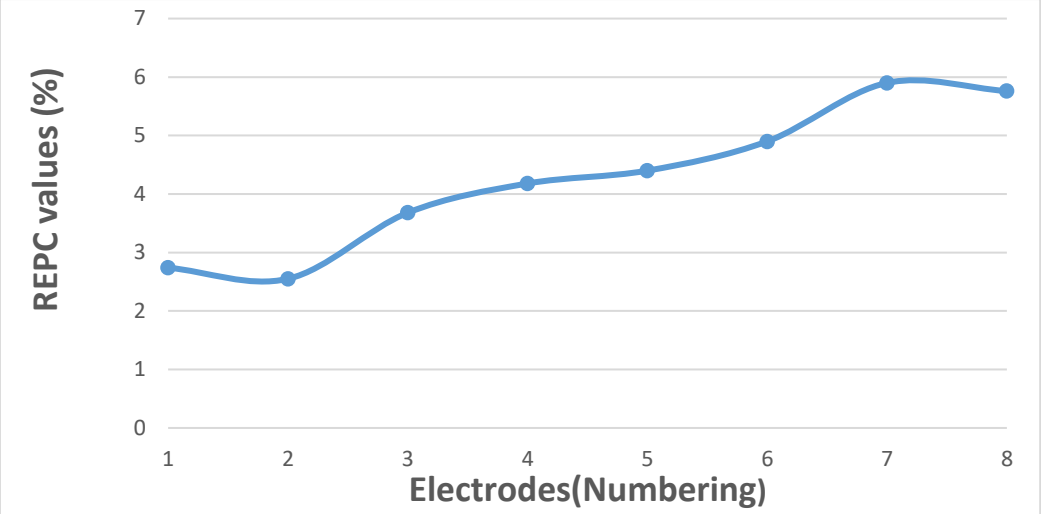

Figure 5.10(b)

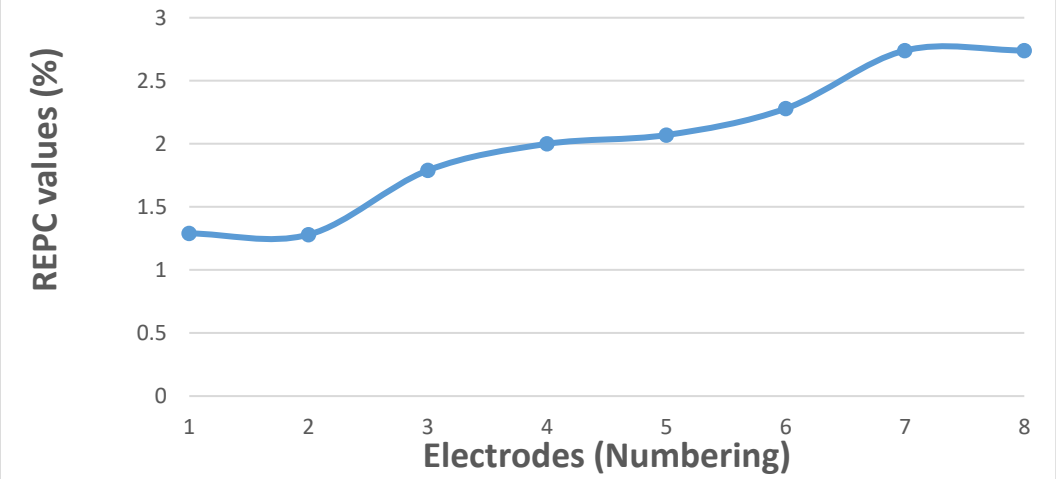

Figure 5.10(c)

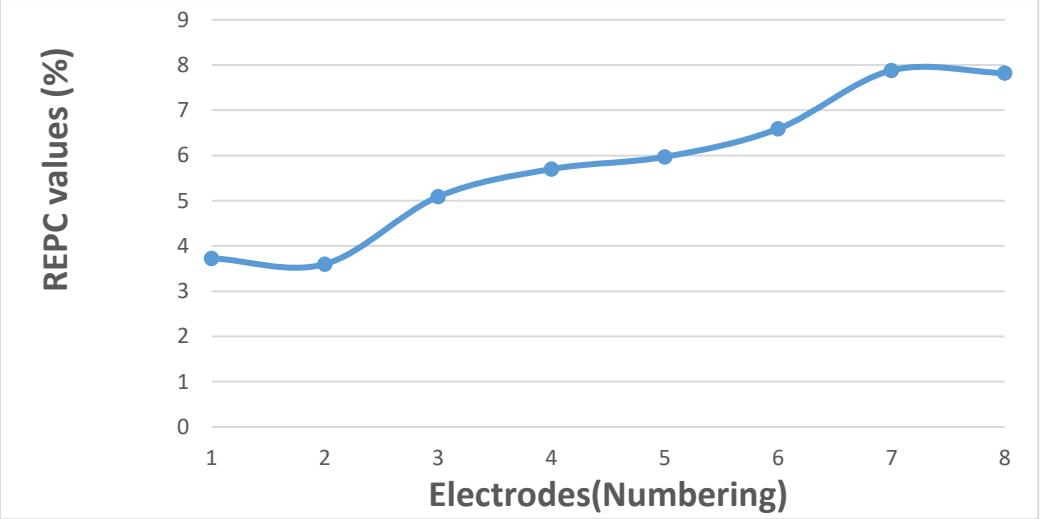

Figure 5.10(d)

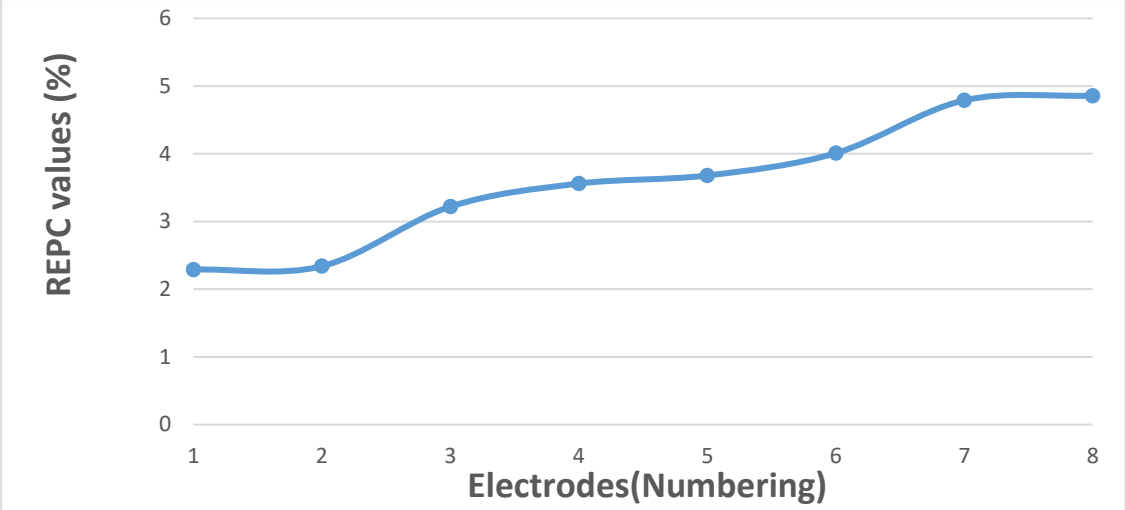

Figure 5.10(e)

Figure 5.10 Sensitivities and accuracies are obtained by using Comsol simulated data for existing opposite current drive along the right lung EIT protocol for assessing lung functions of **(a)** healthy lungs at inspiration and expiration condition, **(b)** healthy lungs at inspiration and diseased lungs pneumothorax (collapsed lung), **(c)** healthy lungs at expiration and diseased lungs pneumothorax (collapsed lung), **(d)** healthy lungs at inspiration and diseased lungs pulmonary edema, **(e)** healthy lungs at expiration and diseased lungs pulmonary edema ; where X and Y axes are indicates the electrodes (numbering) and relative electric potential change (REPC) values (%) respectively.

5.4 Simulation Study Method-5: Proposed Anterior-Posterior Electrical Impedance Technique (APEIT) Protocol

Following the section 5.2.2 construction of computer generated human chest phantom with two lungs and their connector and also placed ten surface electrodes, then material selections are very important for computer simulation. Material selections sequences are given as follows.

Step-1: Thorax material is selected with the electrical conductivity 0.352 Sm^{-1} and relative permittivity 10094 [Table-3] and the selection domains are 7,8,9,10,11,12,13,17,18,19,23 as shown in Figure-5.11(a-i).

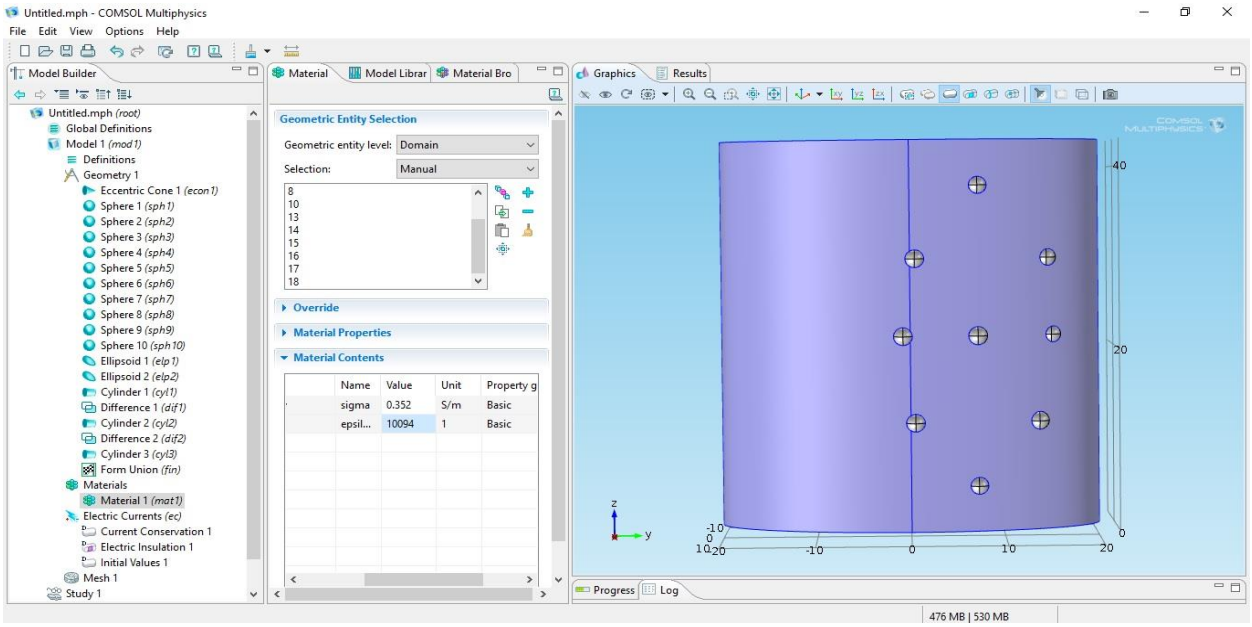

Figure-5.11(a-i): Selection of Thorax material for Computer generated Chest Phantom.

Step-2: Lungs and connector of two lungs materials are selected with the electrical conductivity and relative permittivity for inflated lung 0.103 Sm^{-1}, 4272.50 and for deflated lung 0.2620 Sm^{-1}, 8531.40 and the selection domains are 20,21,22 as shown in Figure-5.11(a-ii).

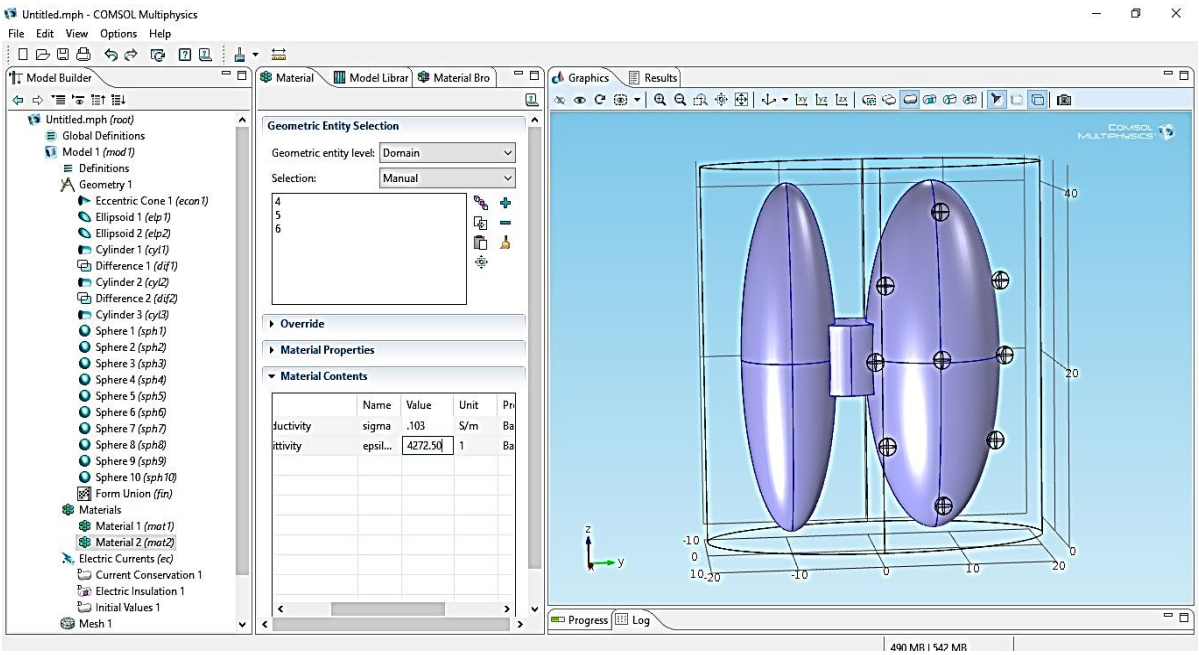

Figure-5.11(a-ii): Complete view of computer generated chest phantom with two lungs and their connector.

Step-3: Ten surface electrodes of Silver material are selected with electrical conductivity 6.16×10^{7} Sm^{-1} and relative permittivity 3.4 and the selection domains are 1, 2, 3, 4, 5, 6, 14, 15, 16, 24 as shown in Figure-5.11(a-iii).

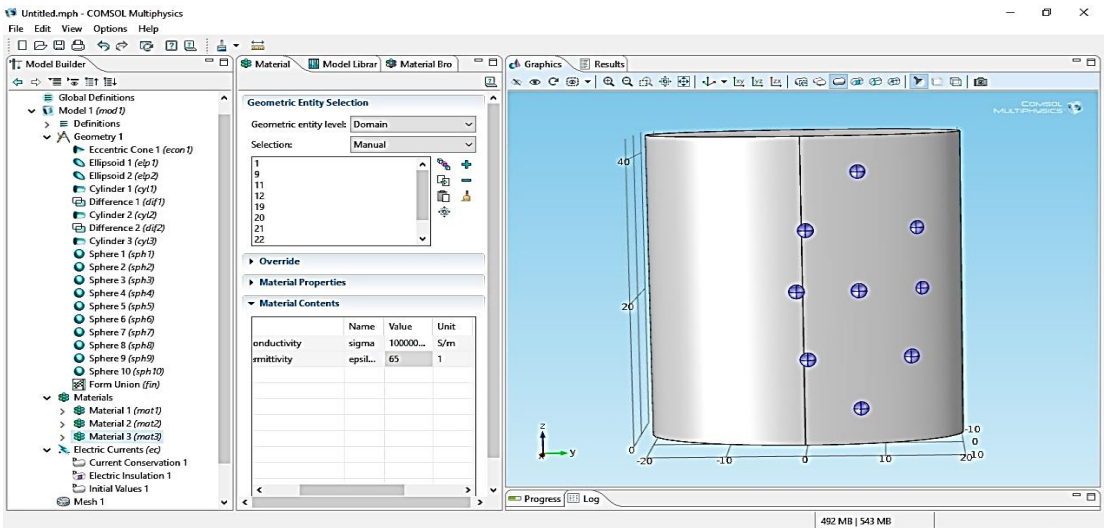

Figure-5.11(a-iii): Selection of the ten surface electrodes of Silver material for Computer generated Chest Phantom.

Step-4: In order to define the ten surface electrodes as ten boundary probes have been chosen the Definitions option in the model builder. Boundary probes renamed as Surface Electrodes (SE) have been selected from the electrodes one by one. Boundary elements are SE-1 (173,174,179,180), SE- 2 (17,18,19,20), SE-3 (21,22,23,24), SE-4 (1,2,3,4), SE- 5 (5,6,7,8), SE- 6 (9,10,11,12), SE-7 (13,14,15,16), SE- 8 (93,94,95,96), SE- 9 (97,98,99,100) and SE-10 (89,90,91,92) as shown in Figure-5.11(a-iv).

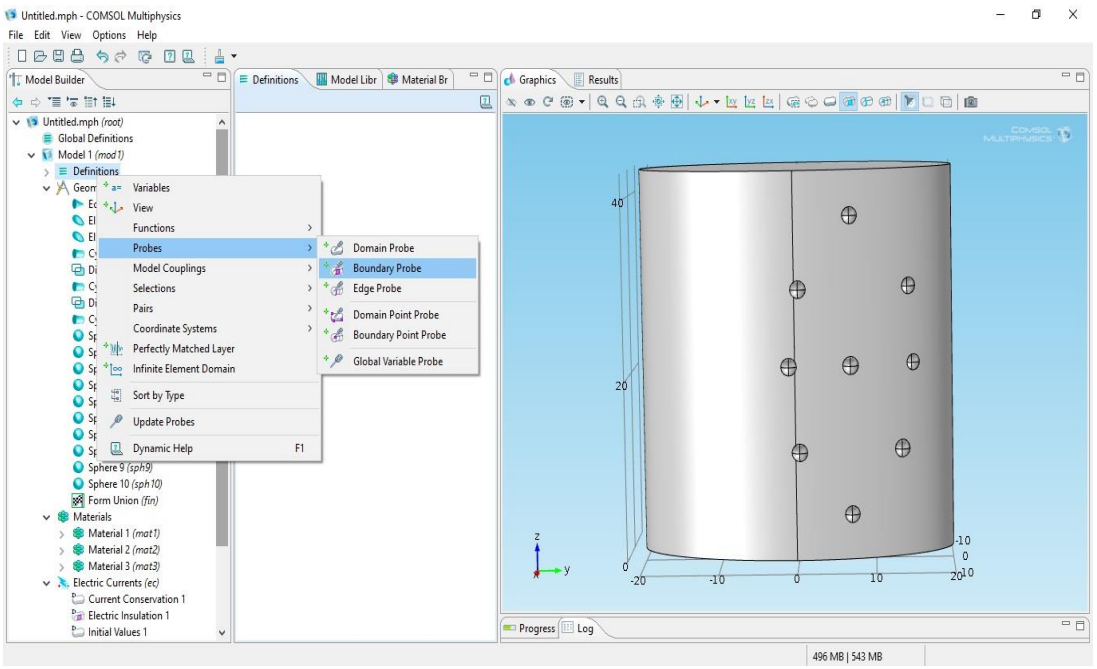

Figure-5.11(a-iv): Selection of Boundary Probe from sub- menu probe.

Step-5: Terminal (source) and Ground are very important for simulation. Ground and Terminal have been added to the model builder of Electric Currents (ec). The current at the terminal has been set to 1 mA. The selected SE has set as a Ground and another SE as Terminal as shown in Figure-5.11(a-v) and 5.11(a-vi).

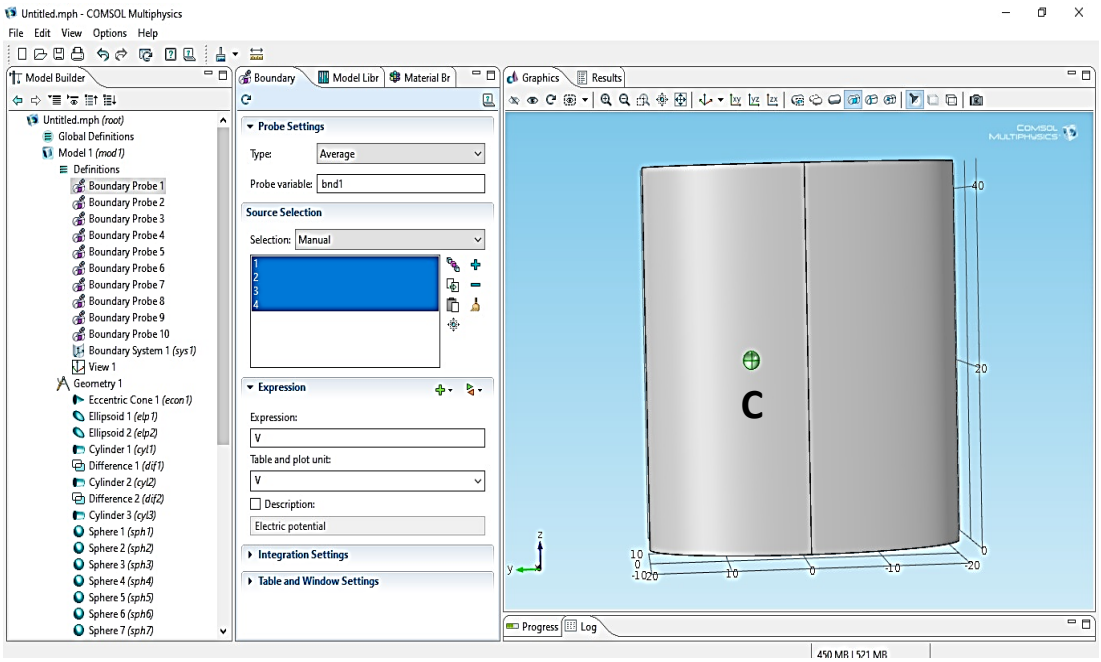

Figure-5.11(a-v): Selection of Surface Electrode (SE) as a Ground.

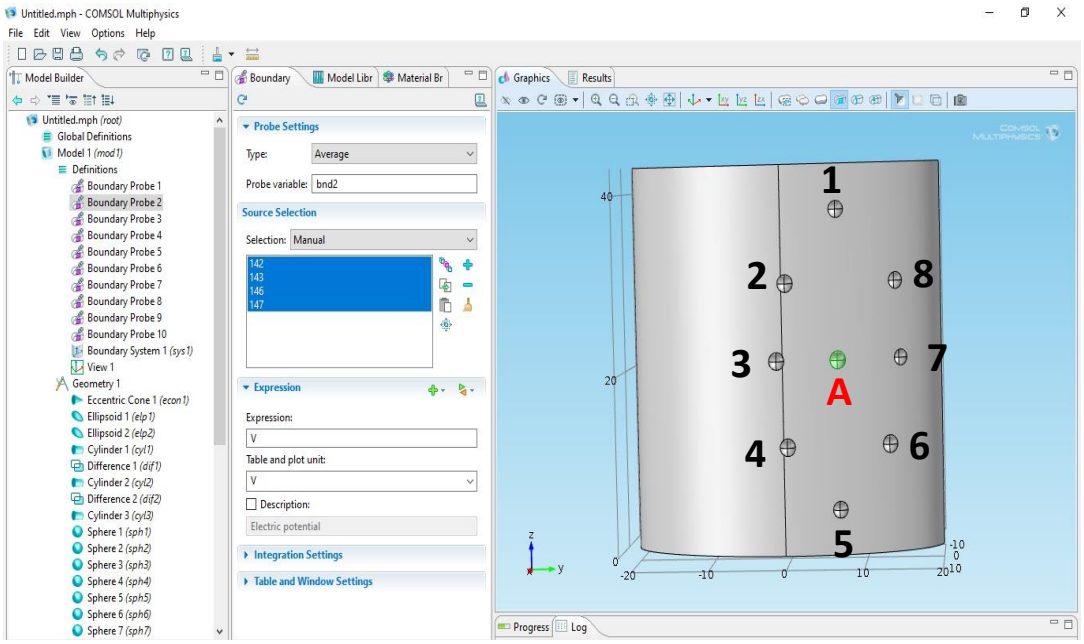

Figure-5.11(a-vi): Selection of Surface Electrode (SE) as a Terminal.

Step-6: The frequency of the current has been specified as 50 KHz in the study settings from the section Study-1. Finally, Study-1 to select compute option to run the simulation. After this, the Result Window contains the data that shows the boundary potential at each of the surface electrodes [Figure 5.11(a-vii)].

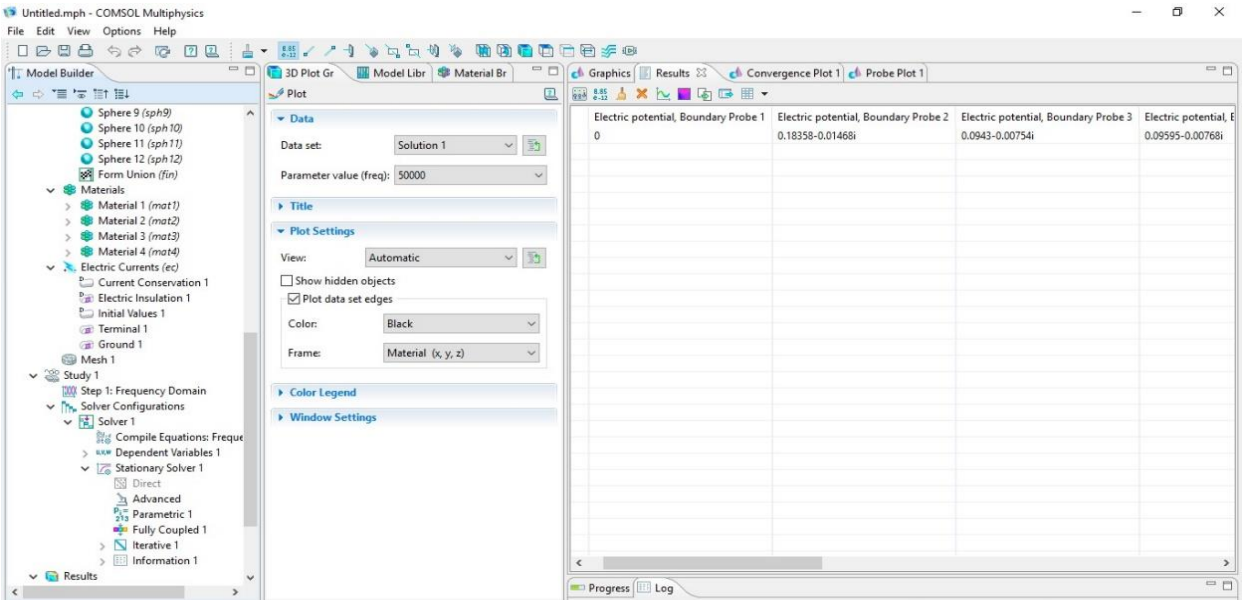

Figure-5.11 (a-vii): Result window shows the boundary potential at each of the surface electrodes.

Multi slice Electric Potential view window of Computer generated Chest Phantom as shown in figure-5.11(a-viii) and 5.11(a-ix).

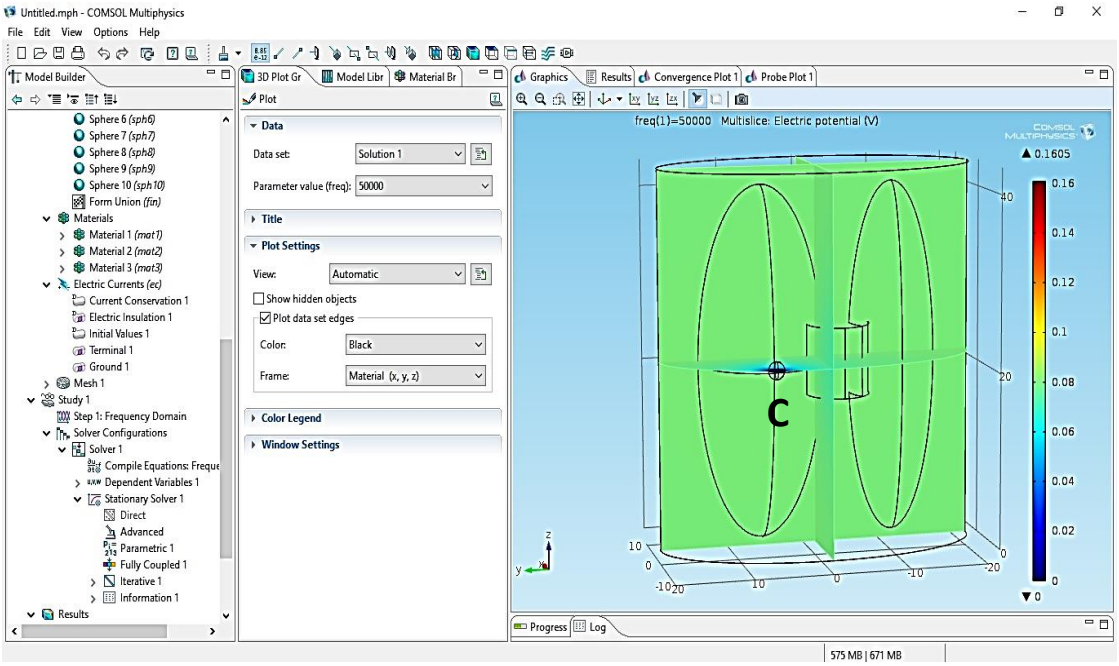

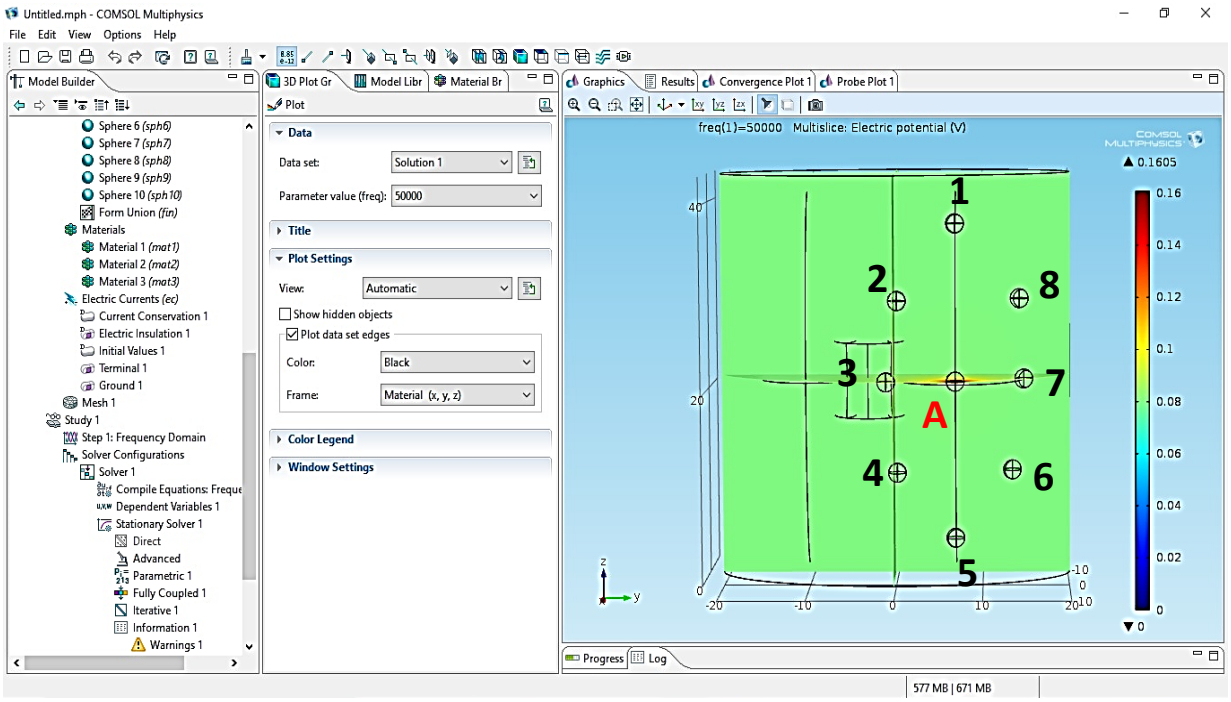

Figure-5.11 (a-viii): Anterior view of Computer generated Chest Phantom.

Figure-5.11(a-ix): Posterior view of Computer generated Chest Phantom.

Electrodes configuration of Proposed Anterior-Posterior Electrical Impedance Tomography (EIT) Protocol with computer generated digital phantom shown in the figure 5.11(a-x) and 5.11(a-xi).

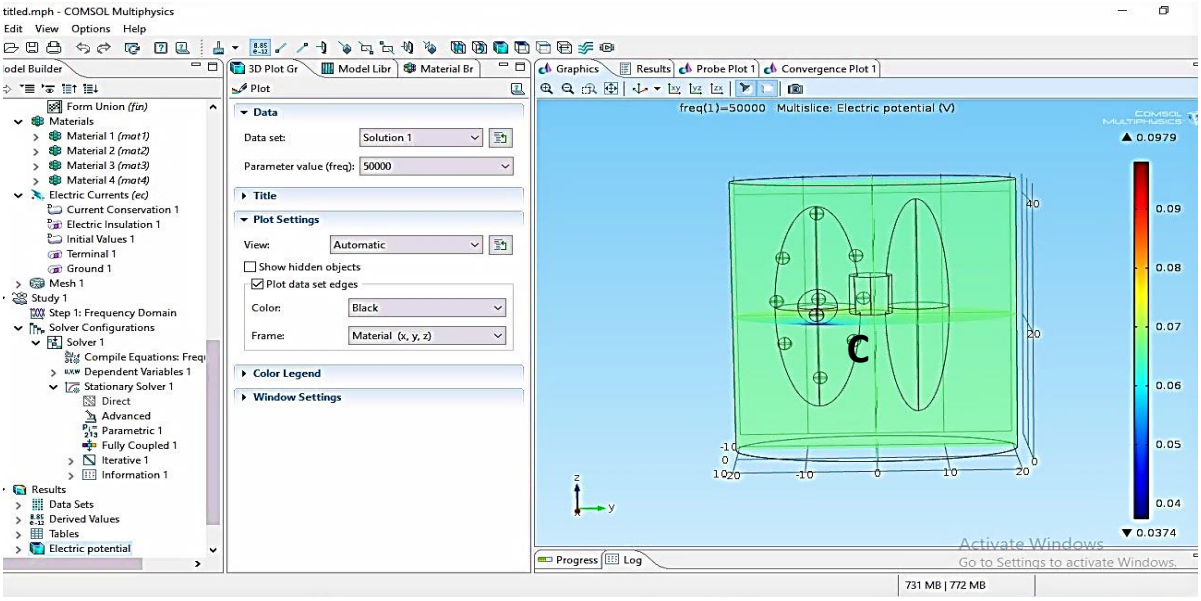

Figure 5.11(a-x): Anterior view of computer generated chest phantom.

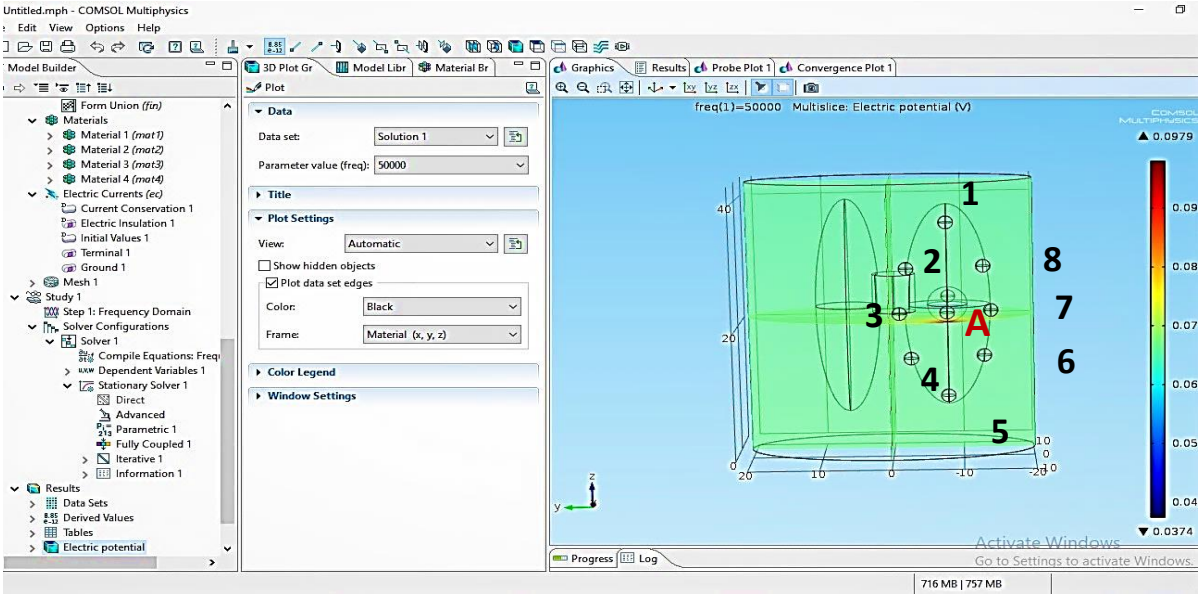

Figure 5.11(a-xi): Posterior view of computer generated chest phantom.

Figure 5.11: Surface Electrode-**C** (-ve electrode) placed anterior side of the right lung &surface electrode-**A** (+ve electrode) placed posterior side of the right lung for current driving electrodes. Remaining 1 to 8 surface electrodes are placed posterior side of right lung like ellipsoid shape and anticlockwise direction for voltage calculations.

Mesh view of Computer generated Chest Phantom as shown in Figure-5.11 (a-xii) and 5.11(a-xiii).

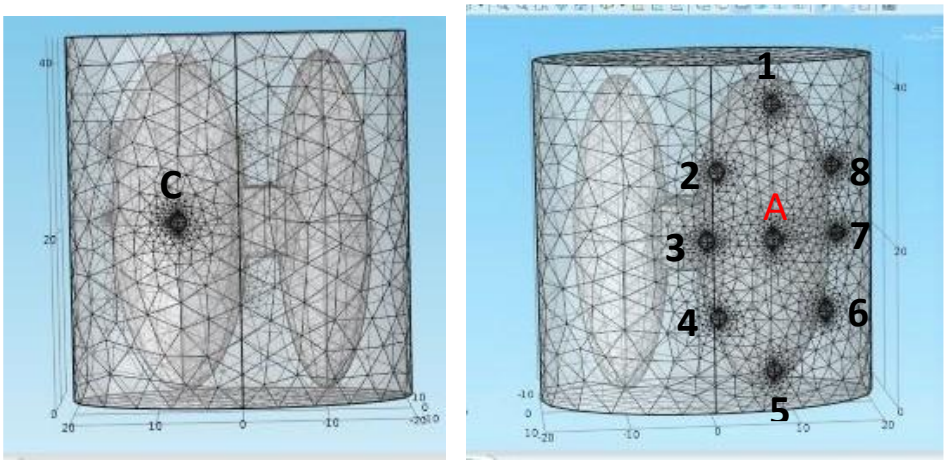

Fig-5.11(a-xii): Anterior mesh view. Fig-5.11(a-xiii): Posterior mesh view.

After mesh analysis number of vertex elements 156, number of edge elements 1275, number of boundary elements 9074, number of elements 53311, free meshing time 3.98 sec and minimum element quality 0.036.

Following the same simulation tasks of section 5.3(B) we have got computer simulated data which has tabulated in the tables 5.24 (a& b) to 5.28(a& b).From these tables 5.12(a) to 5.12(e) figures have drawn to study the sensitivity and accuracy of computer simulated data for Proposed Anterior-Posterior EIT Protocol for assessing lung functions of **(a)** healthy lungs at inspiration and expiration condition, **(b)** healthy lungs at inspiration and diseased lungs pneumothorax (collapsed lung), **(c)** healthy lungs at expiration and diseased lungs pneumothorax (collapsed lung), **(d)** healthy lungs at inspiration and diseased lungs pulmonary edema, and **(e)** healthy lungs at expiration and diseased lungs pulmonary edema.

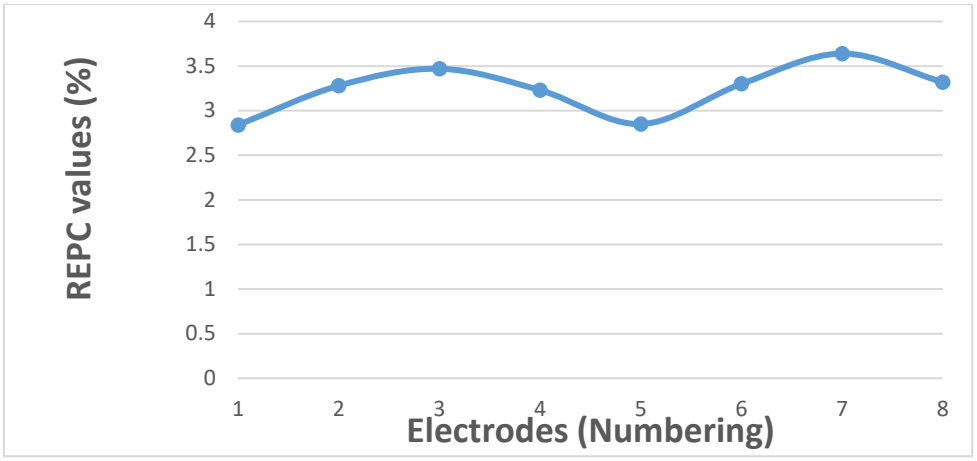

Figure 5.12(a)

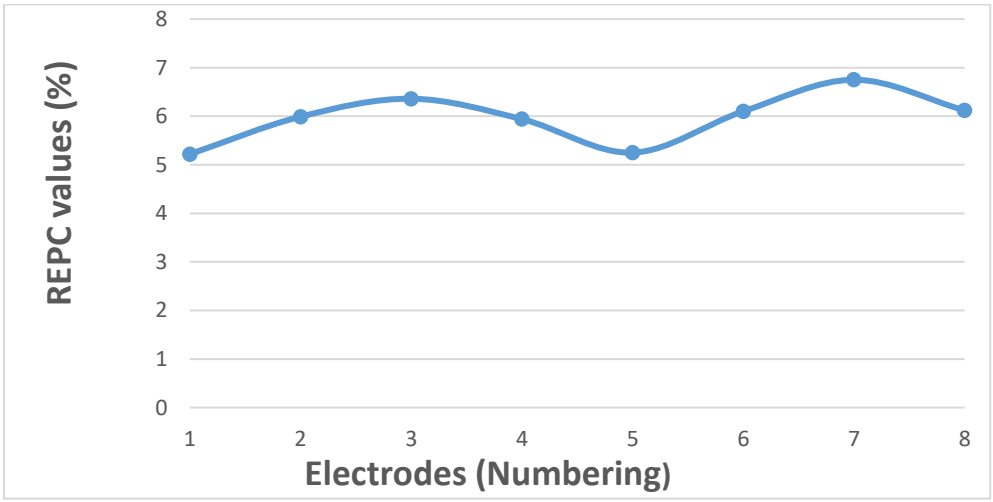

Figure 5.12(b)

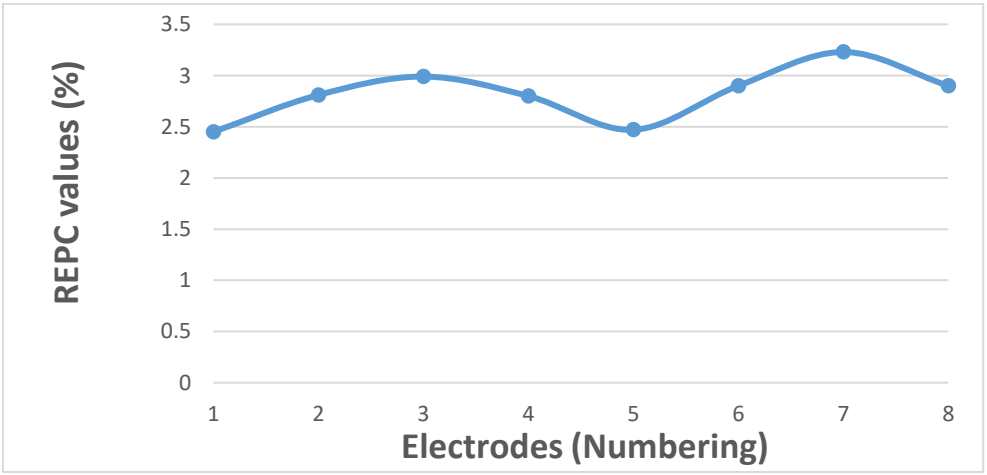

Figure 5.12(c)

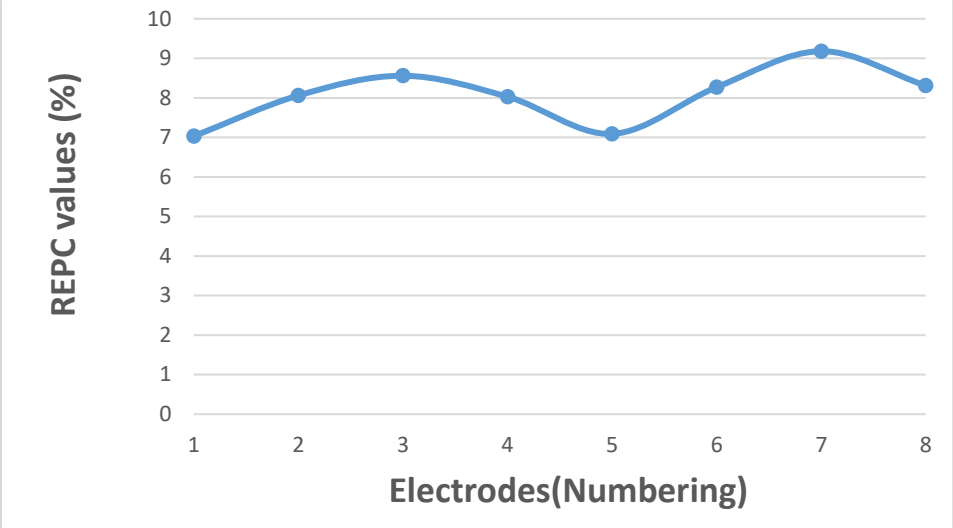

Figure 5.12(d)

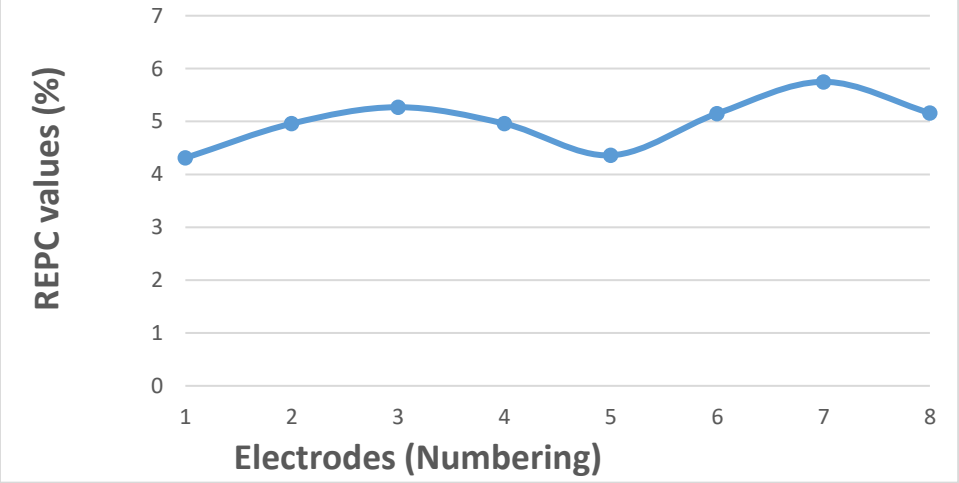

Figure 5.12(e)

Figure 5.12 Sensitivities and accuracies are obtained by using Comsol simulated data for Proposed Anterior- Posterior EIT protocol for assessing lung functions of **(a)** healthy lungs at inspiration and expiration condition, **(b)** healthy lungs at inspiration and diseased lungs pneumothorax (collapsed lung), **(c)** healthy lungs at expiration and diseased lungs pneumothorax (collapsed lung), **(d)** healthy lungs at inspiration and diseased lungs pulmonary edema, **(e)** healthy lungs at expiration and diseased lungs pulmonary edema ; where X and Y axes are indicates the electrodes (numbering) and relative electric potential change (REPC) values (%) respectively.

5.5 Comparison Statements of four Existing EIT Protocols and Proposed Anterior-Posterior EIT Protocol

Sensitivity curves for four existing EIT Protocols and proposed Anterior- Posterior EIT protocol have shown in figure-5.13 for healthy (normal) lungs at inspiration & expiration condition.

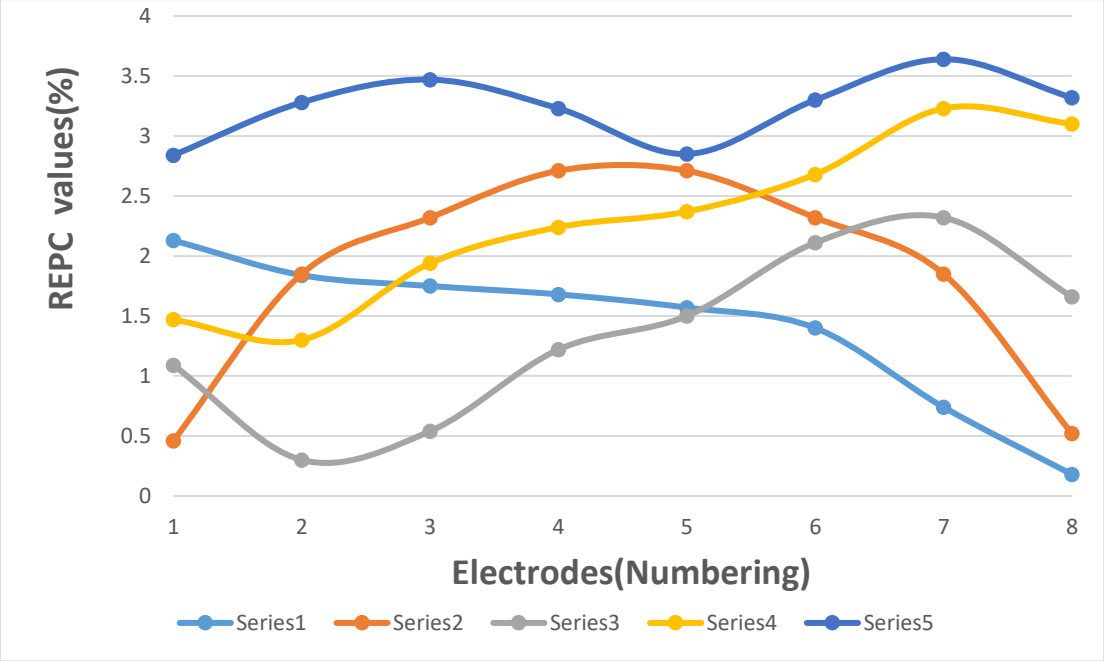

Figure-5.13: Relative Electric Potential Change (REPC) values (%) plotted against Electrodes (Numbering) for Existing Four Current Drive EIT Protocols and Proposed Anterior-Posterior EIT Protocol for Healthy lungs at Inspiration and Expiration. [Table Used 5.29]

Series-1: Existing Adjacent Current Drive EIT Protocol

Series-2: Existing Opposite Current Drive at the vertices of the semi-major axis of the chest cross section EIT Protocol

Series-3: Existing Opposite Current Drive at the vertices of the semi-minor axis of the chest cross section EIT Protocol

Series-4: Existing Opposite Current Drive along the right lung EIT Protocol

Series-5: Proposed Anterior-Posterior EIT Protocol

Average sensitivity values for four existing EIT Protocols and proposed Anterior-Posterior EIT protocol have shown in figure-5.14for healthy (normal) lungs at inspiration & expiration condition.

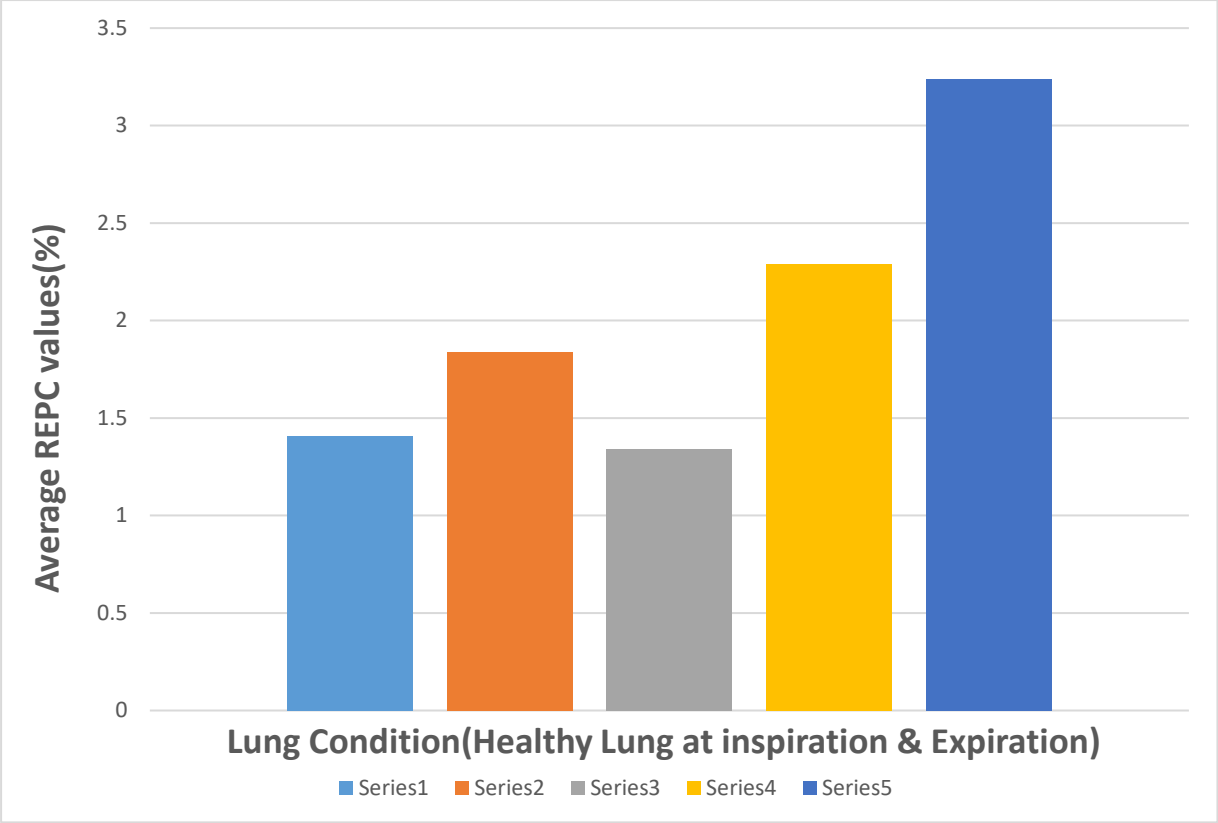

Figure-5.14: Average REPC values (%) for Existing Four Current Drive EIT Protocols and Proposed Anterior-Posterior EIT Protocol for Healthy Lungs at Inspiration and Expiration. [Table Used 5.29]

Series-1: Existing Adjacent Current Drive EIT Protocol

Series-2: Existing Opposite Current Drive at the vertices of the semi-major axis of the chest cross section EIT Protocol

Series-3: Existing Opposite Current Drive at the vertices of the semi-minor axis of the chest cross section EIT Protocol

Series-4: Existing Opposite Current Drive along the right lung EIT Protocol

Series-5: Proposed Anterior-Posterior EIT Protocol

Sensitivity curves for four existing EIT Protocols and proposed Anterior- Posterior EIT protocol have shown in figure-5.15 for healthy (normal) lungs at inspiration &pneumothorax (collapsed lung).

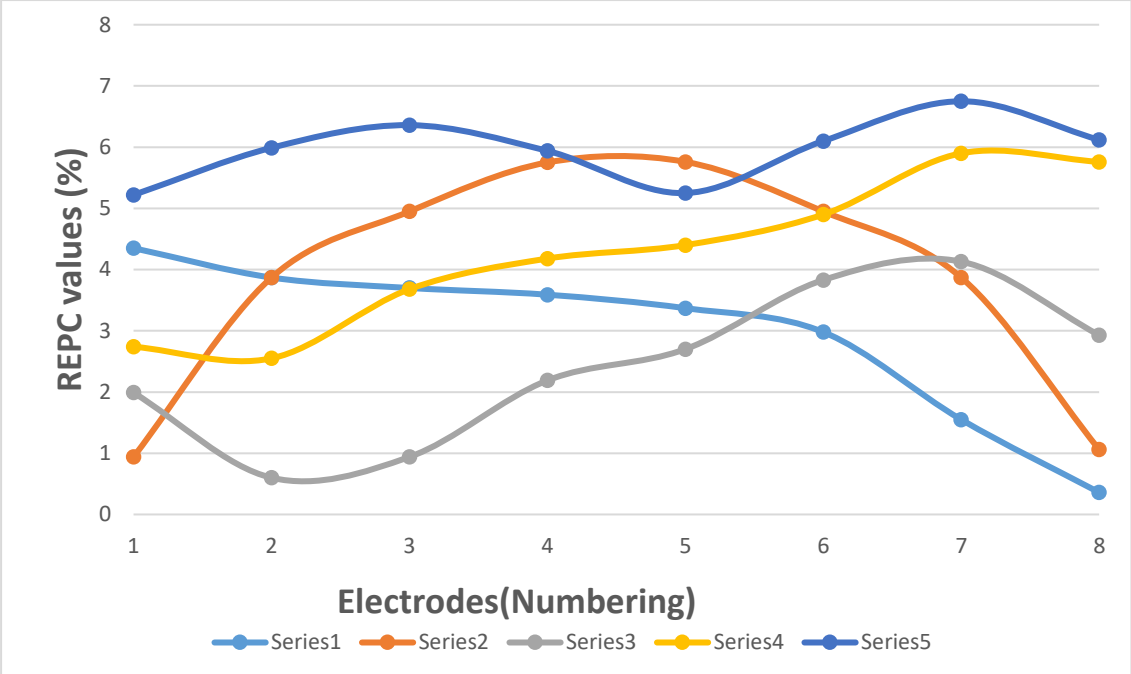

Figure- 5.15: Relative Electric Potential Change (REPC) values (%) plotted against electrodes (numbering) for Existing Four Current Drive EIT Protocols and Proposed Anterior-Posterior EIT Protocol for Healthy Lungs at Inspiration and Pneumothorax (Collapsed Lung). [Table Used 5.30]

Series-1: Existing Adjacent Current Drive EIT Protocol

Series-2: Existing Opposite Current Drive at the vertices of the semi-major axis of the chest cross section EIT Protocol

Series-3: Existing Opposite Current Drive at the vertices of the semi-minor axis of the chest cross section EIT Protocol

Series-4: Existing Opposite Current Drive along the right lung EIT Protocol

Series-5: Proposed Anterior-Posterior EIT Protocol

Average sensitivity values for four existing EIT Protocols and proposed Anterior-Posterior EIT protocol have shown in figure-5.16 for healthy (normal) lungs at inspiration & pneumothorax (collapsed lung).

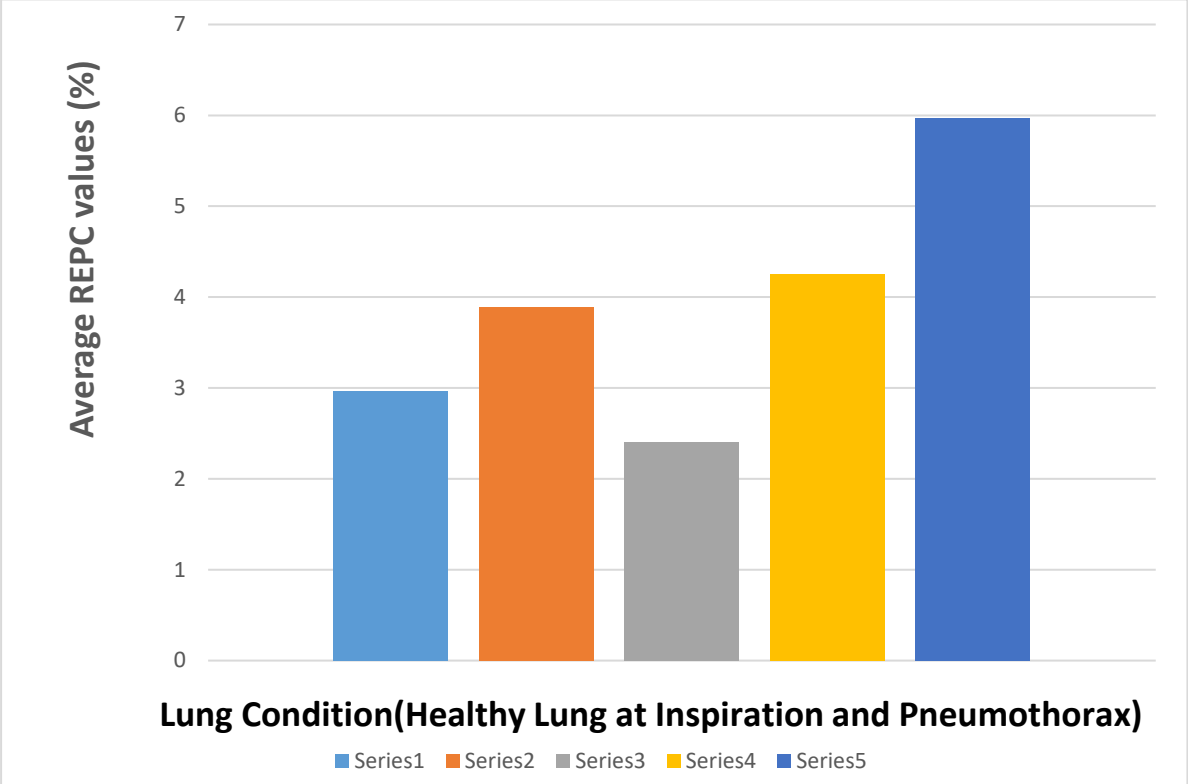

Figure-5.16: Average REPC value of the SE for Existing Four Current Drive EIT Protocols and Proposed Anterior-Posterior EIT Protocol for Healthy Lungs at Inspiration and Pneumothorax (Collapsed Lung). [Table Used 5.30]

Series-1: Existing Adjacent Current Drive EIT Protocol

Series-2: Existing Opposite Current Drive at the vertices of the semi-major axis of the chest cross section EIT Protocol

Series-3: Existing Opposite Current Drive at the vertices of the semi-minor axis of the chest cross section EIT Protocol

Series-4: Existing Opposite Current Drive along the right lung EIT Protocol

Series-5: Proposed Anterior-Posterior EIT Protocol

Sensitivity curves for four existing EIT Protocols and proposed Anterior- Posterior EIT protocol have shown in figure-5.17 for healthy (normal) lungs at expiration &pneumothorax (collapsed lung).

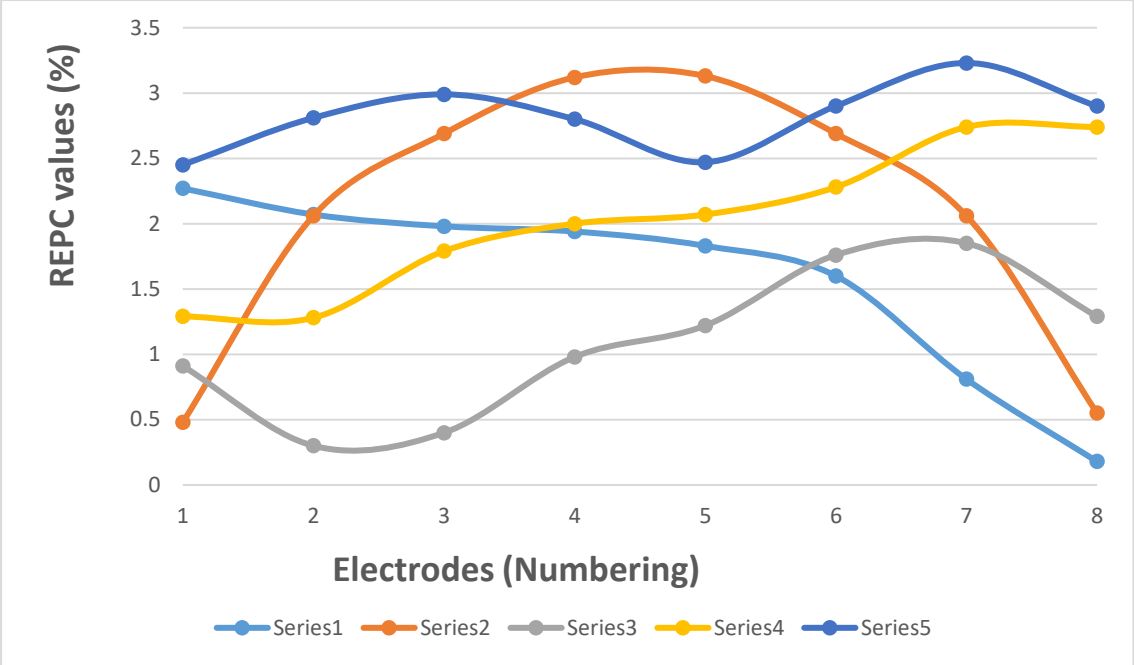

Figure- 5.17: Relative Electric Potential Change (REPC) values (%) plotted against electrodes (numbering) for Existing Four Current Drive EIT Protocols and Proposed Anterior-Posterior EIT Protocol for Healthy Lungs at Expiration and Pneumothorax (Collapsed Lung). [Table Used 5.31]

Series-1: Existing Adjacent Current Drive EIT Protocol

Series-2: Existing Opposite Current Drive at the vertices of the semi-major axis of the chest cross section EIT Protocol

Series-3: Existing Opposite Current Drive at the vertices of the semi-minor axis of the chest cross section EIT Protocol

Series-4: Existing Opposite Current Drive along the right lung EIT Protocol

Series-5: Proposed Anterior-Posterior EIT Protocol

Average sensitivity values for four existing EIT Protocols and proposed Anterior-Posterior EIT protocol have shown in figure-5.18 for healthy (normal) lungs at expiration &pneumothorax (collapsed lung).

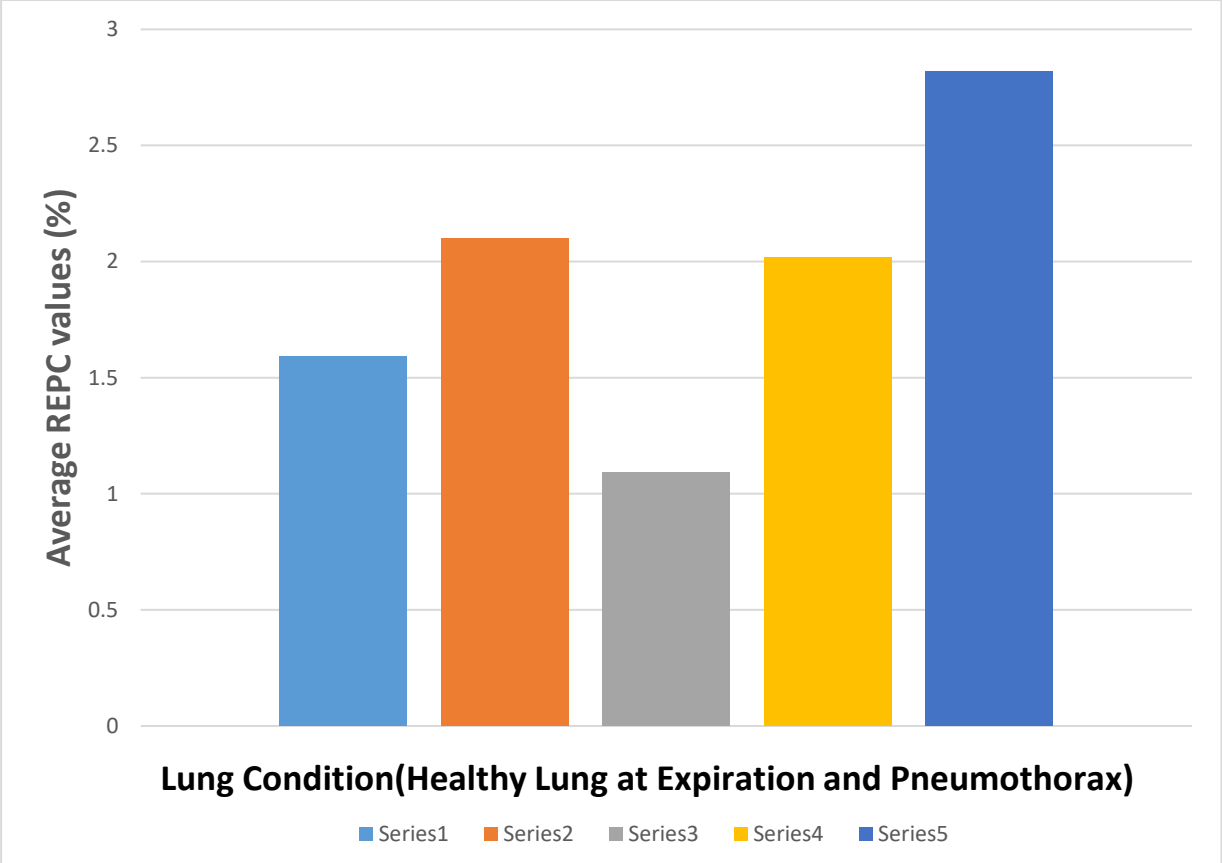

Figure-5.18: Average REPC value of the SE for Existing Four Current Drive EIT Protocols and Proposed Anterior-Posterior EIT Protocol for Healthy Lungs at Expiration and Pneumothorax (Collapsed Lung). [Table Used 5.31]

Series-1: Existing Adjacent Current Drive EIT Protocol

Series-2: Existing Opposite Current Drive at the vertices of the semi-major axis of the chest cross section EIT Protocol

Series-3: Existing Opposite Current Drive at the vertices of the semi-minor axis of the chest cross section EIT Protocol

Series-4: Existing Opposite Current Drive along the right lung EIT Protocol

Series-5: Proposed Anterior-Posterior EIT Protocol

Sensitivity curves for four existing EIT Protocols and proposed Anterior- Posterior EIT protocol have shown in figure-5.19 for healthy (normal) lungs at inspiration &pulmonary edema.

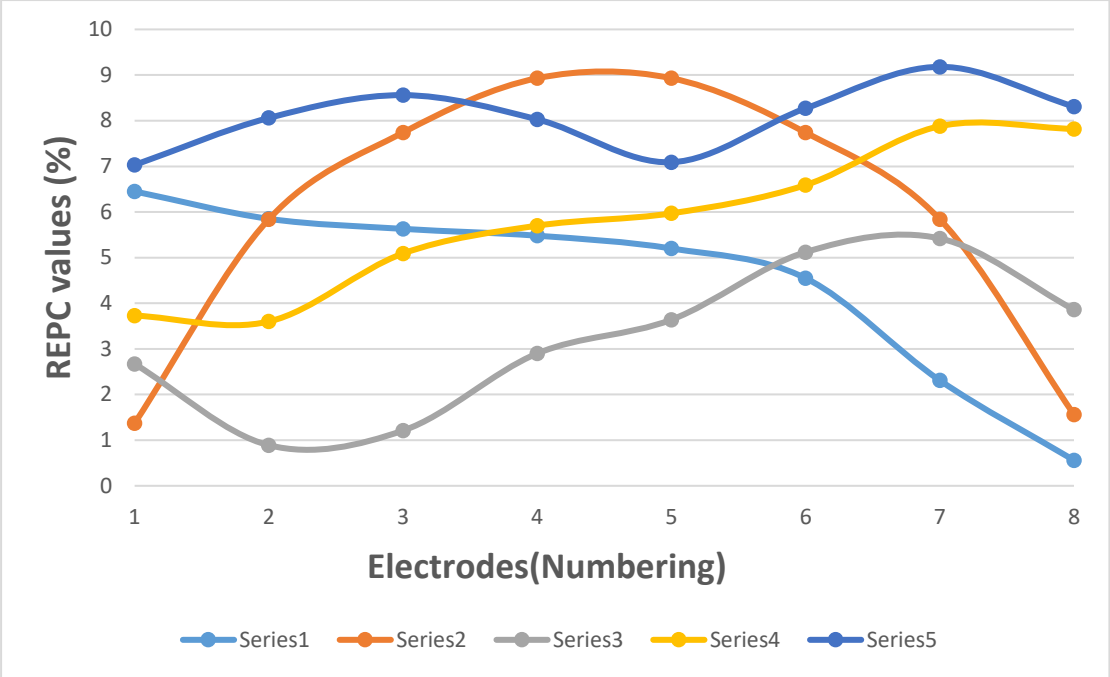

Figure-5.19: Relative Electric Potential Change (REPC) values (%) plotted against electrodes (numbering) for Existing Four Current Drive EIT Protocols and Proposed Anterior-Posterior EIT Protocol for Healthy Lungs at Inspiration and Pulmonary Edema. [Table Used 5.32]

Series-1: Existing Adjacent Current Drive EIT Protocol

Series-2: Existing Opposite Current Drive at the vertices of the semi-major axis of the chest cross section EIT Protocol

Series-3: Existing Opposite Current Drive at the vertices of the semi-minor axis of the chest cross section EIT Protocol

Series-4: Existing Opposite Current Drive along the right lung EIT Protocol

Series-5: Proposed Anterior-Posterior EIT Protocol

Average sensitivity values for four existing EIT Protocols and proposed Anterior-Posterior EIT protocol have shown in figure-5.20 for healthy (normal) lungs at inspiration &pulmonary edema.

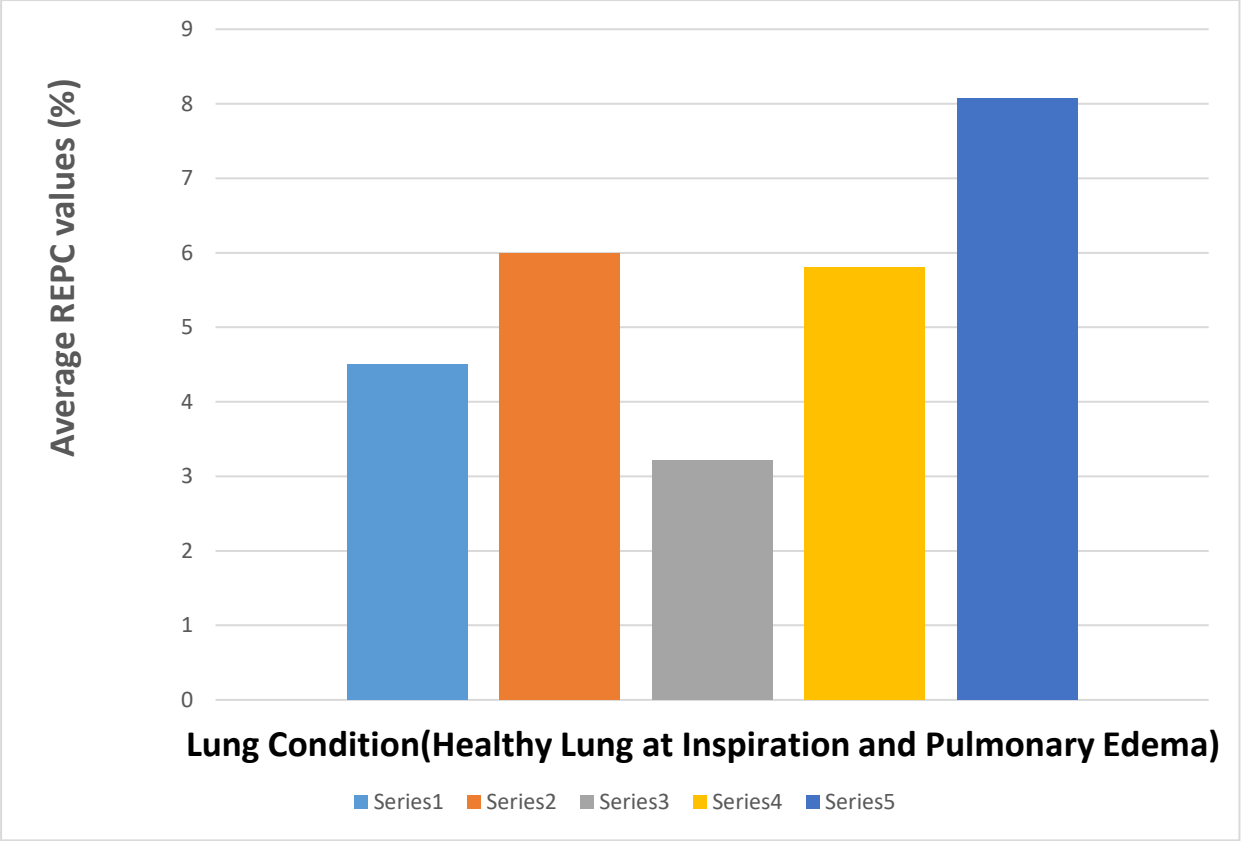

Figure-5.20: Average REPC value of the SE for Existing Four Current Drive EIT Protocols and Proposed Anterior-Posterior EIT Protocol for Healthy Lungs at Inspiration and Pulmonary Edema. [Table Used 5.32]

Series-1: Existing Adjacent Current Drive EIT Protocol

Series-2: Existing Opposite Current Drive at the vertices of the semi-major axis of the chest cross section EIT Protocol

Series-3: Existing Opposite Current Drive at the vertices of the semi-minor axis of the chest cross section EIT Protocol

Series-4: Existing Opposite Current Drive along the right lung EIT Protocol

Series-5: Proposed Anterior-Posterior EIT Protocol

Sensitivity curves for four existing EIT Protocols and proposed Anterior- Posterior EIT protocol have shown in figure-5.21 for healthy (normal) lungs at expiration &pulmonary edema.

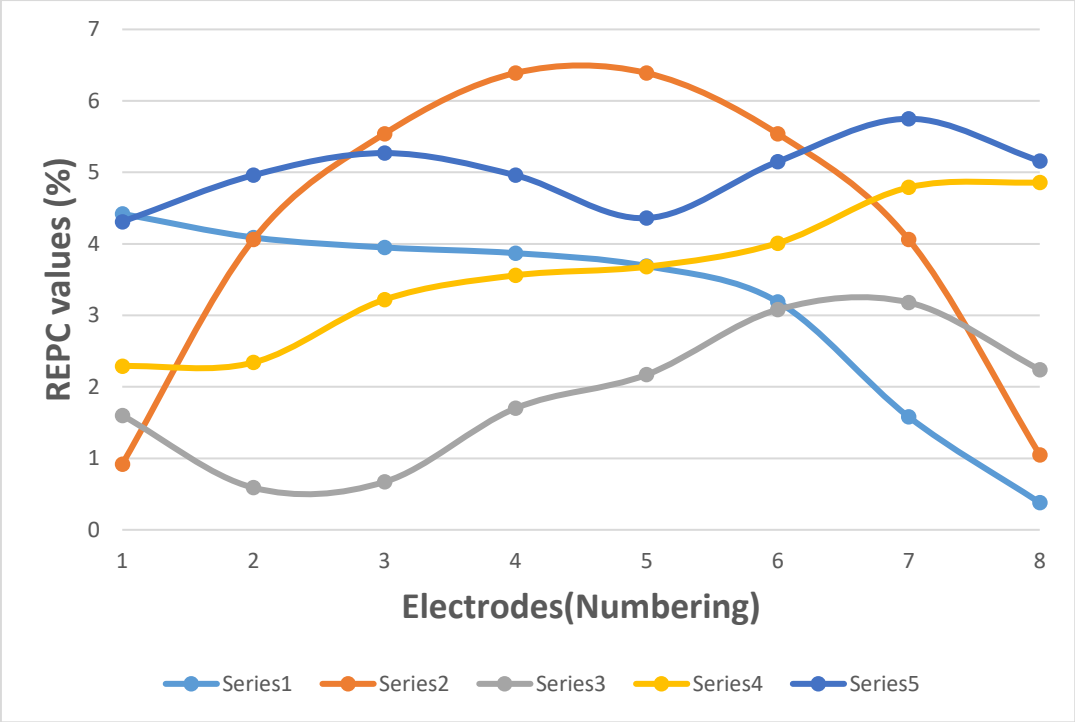

Figure-5.21: Relative Electric Potential Change (REPC) values (%) plotted against electrodes (numbering) for Existing Four Current Drive EIT Protocols and Proposed Anterior-Posterior EIT Protocol for Healthy Lungs at Expiration and Pulmonary Edema. [Table Used 5.33]

Series-1: Existing Adjacent Current Drive EIT Protocol

Series-2: Existing Opposite Current Drive at the vertices of the semi-major axis of the chest cross section EIT Protocol

Series-3: Existing Opposite Current Drive at the vertices of the semi-minor axis of the chest cross section EIT Protocol

Series-4: Existing Opposite Current Drive along the right lung EIT Protocol

Series-5: Proposed Anterior-Posterior EIT Protocol

Average sensitivity values for four existing EIT Protocols and proposed Anterior-Posterior EIT protocol have shown in figure-5.22 for healthy (normal) lungs at expiration &pulmonary edema.

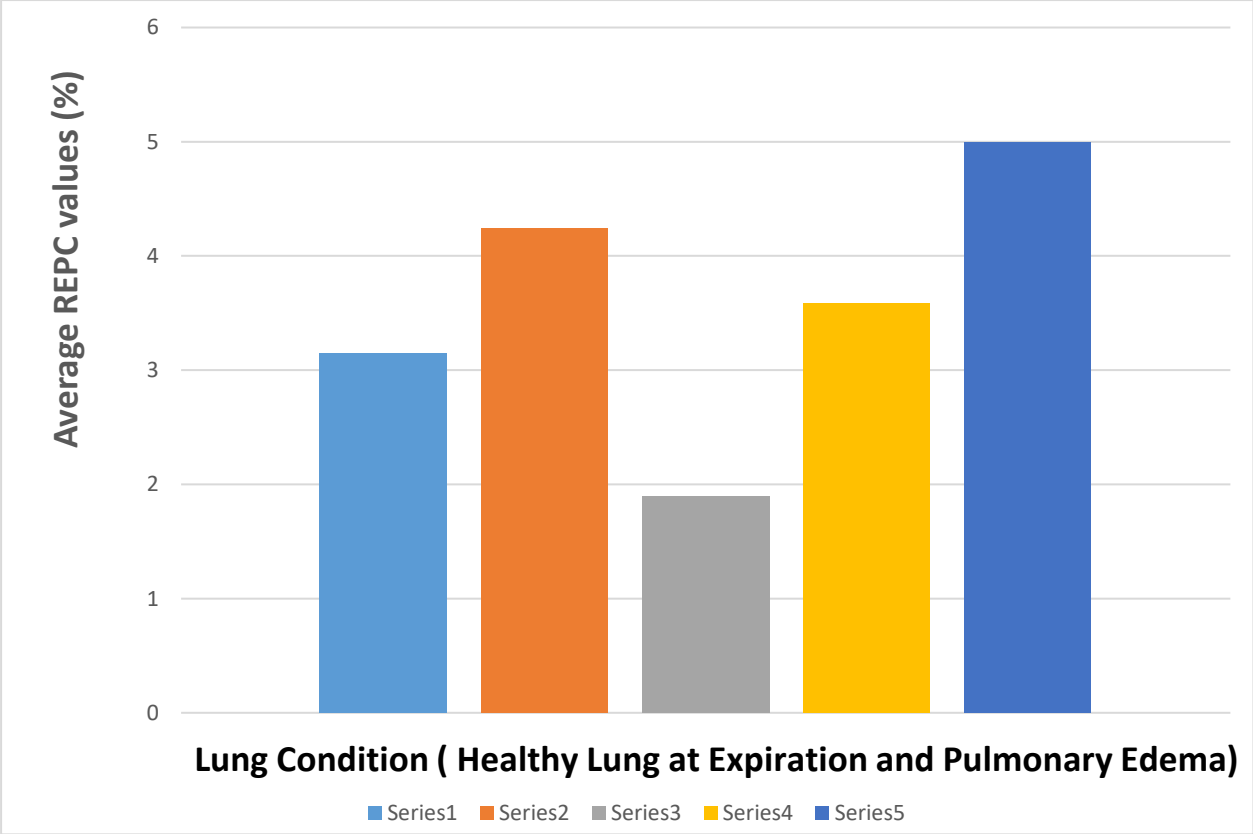

Figure-5.22: Average REPC value of the SE for Existing Four Current Drive EIT Protocols and Proposed Anterior-Posterior EIT Protocol for Healthy Lungs at Expiration and Pulmonary Edema. [Table Used 5.33]

Series-1: Existing Adjacent Current Drive EIT Protocol

Series-2: Existing Opposite Current Drive at the vertices of the semi-major axis of the chest cross section EIT Protocol

Series-3: Existing Opposite Current Drive at the vertices of the semi-minor axis of the chest cross section EIT Protocol

Series-4: Existing Opposite Current Drive along the right lung EIT Protocol

Series-5: Proposed Anterior-Posterior EIT Protocol

At a glance Average REPC values (%) for five different conditions of lungs- **(a)** healthy lung at inspiration and expiration, **(b)** healthy lung at inspiration and pneumothorax (collapsed lung), **(c)** healthy lung at expiration and pneumothorax (collapsed lung), **(d)** healthy lung at inspiration and pulmonary edema, and **(e)** healthy lung at expiration and pulmonary edema for four existing EIT protocols and proposed Anterior- Posterior EIT protocol are shown in the figure 5.23.

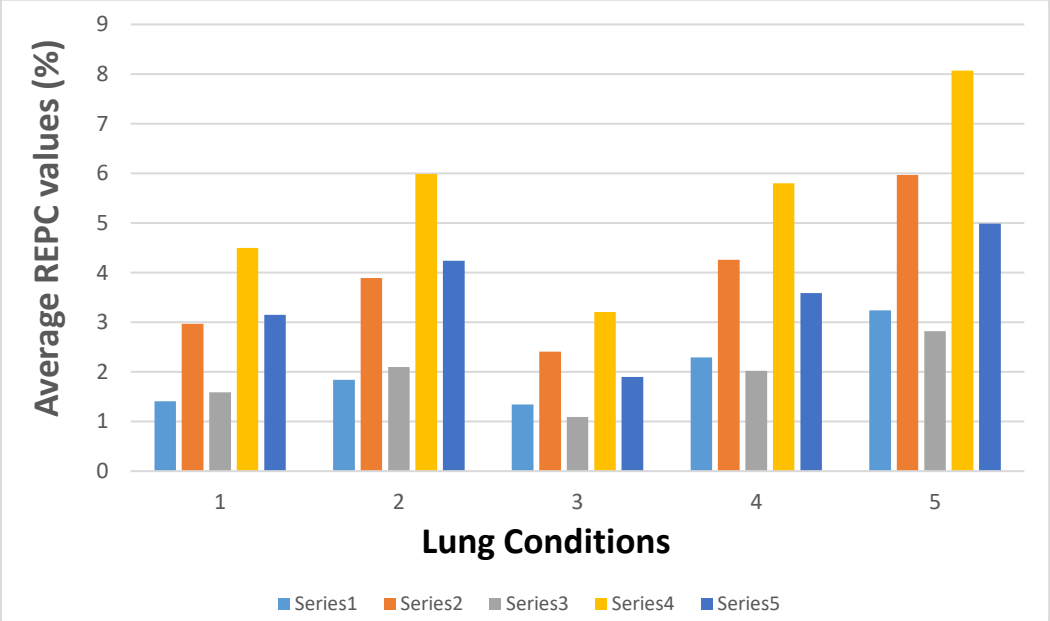

Figure-5.23: Average REPC values (%) for five different conditions of lungs for four existing EIT protocols and proposed Anterior- Posterior EIT protocol. [Table Used 5.34]

(1st bar from the left indicate for case (a), 2nd bar for (b), 3rd bar for (c), 4th bar for (d), and 5th bar for (e) respectively.)

Series-1: Existing Adjacent Current Drive EIT Protocol.

Series-2: Existing Opposite Current Drive at the vertices of the semi-major axis of the chest cross section EIT Protocol.

Series-3: Existing Opposite Current Drive at the vertices of the semi-minor axis of the chest cross section EIT Protocol.

Series-4: Existing Opposite Current Drive along the right lung EIT Protocol.

Series-5: Proposed Anterior-Posterior EIT Protocol.

5.6 Simulation Study Method-6: Tumor added Right Lung for different sizes (5%, 10%, and 20% volume of the right lung) of Tumors

After preparing computer generated human chest phantom with two lungs, tumor and ten placed electrodes, then material selections are very important for simulation [same as section 5.4].

Step-1: Thorax material is selected with the electrical conductivity 0.352 Sm^{-1} and relative permittivity 10094 [Table-6.3] and the selection domains are 7, 8, 9, 10, 11, 12,13,17,18, 19, and 24.

Step-2: Lungs and connector of two lungs materials are selected with the electrical conductivity and relative permittivity for inflated lung 0.103Sm^{-1}, 4272.50 and for deflated lung 0.2620Sm^{-1}, 8531.40 and the selection domains are 20, 21, and 22.

Step-3 : Tumor material is selected with the electrical conductivity 1.50$Sm^{-1}$and relative permittivity 98.56 and the selection domain is 23. Tumor placed on the position (0,-8,23)cm.

Step-4: Ten electrodes of Silver material are selected with electrical conductivity 6.16× $10^{7}Sm^{-1}$ and relative permittivity 3.4 and the selection domains are 1, 2, 3, 4, 5, 6, 14, 15, 16, and 25.

Step-5: In order to define the ten electrodes as ten boundary probes have been chosen the Definitions option in the model builder. Boundary probes renamed as Surface Electrodes (SE) have been selected from the electrodes one by one. Boundary elements are for SE-1 (181,182,187,188), SE- 2 (17,18,19,20), SE-3 (21,22,23,24), SE-4 (1,2,3,4), SE- 5 (5,6,7,8), SE- 6 (9,10,11,12), SE-7 (13,14,15,16), SE-8 (93,94,95,96), SE- 9 (97,98,99,100) and SE-10 (89,90,91,92).

Step-6: Terminal (source) and Ground are very important for simulation. Ground and Terminal have been added to the model builder of Electric Currents (ec). The current at the terminal has been set to 1 mA. The SE-1 has set as a Ground and SE-2 as Terminal.

Step-7: The frequency of the current has been specified as 50 KHz in the study settings from the section Study-1. Finally, Study-1 to select compute option to run the simulation. After this, the Result Window contains the data that shows the boundary potential at each of the surface electrodes.

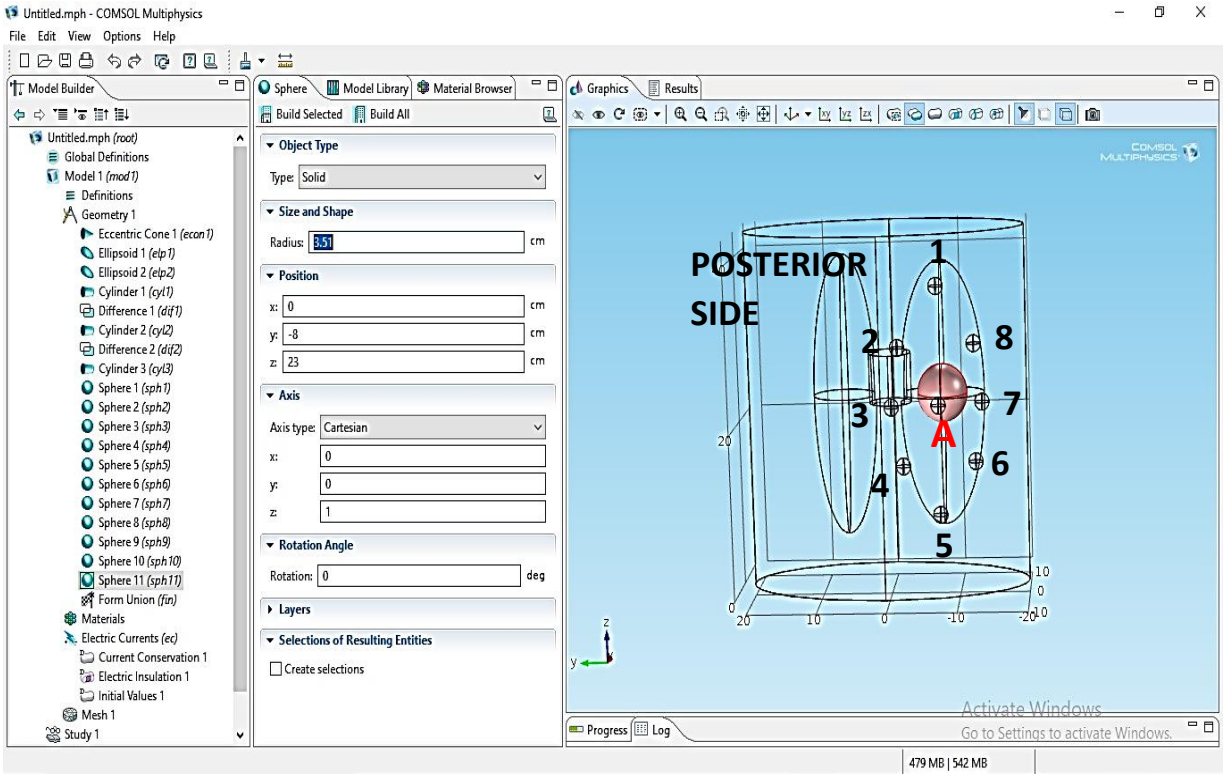

5.6 (A) Simulation study on Tumor Added Right Lung for Single Frequency (50 KHz) at Inspiration condition

Computer simulation of the Proposed Anterior-Posterior EIT Protocol computed average REPC values of the electrode (%) at constant current = 1mA, frequency = 50 KHz for healthy (normal) lungs with inspiration condition the electrical conductivity & the relative permittivity values were taken 0.1030Sm^{-1}& 4272.50 and for tumor these values were taken 1.50Sm^{-1}& 98.56 respectively is shown in the figure-5.24.

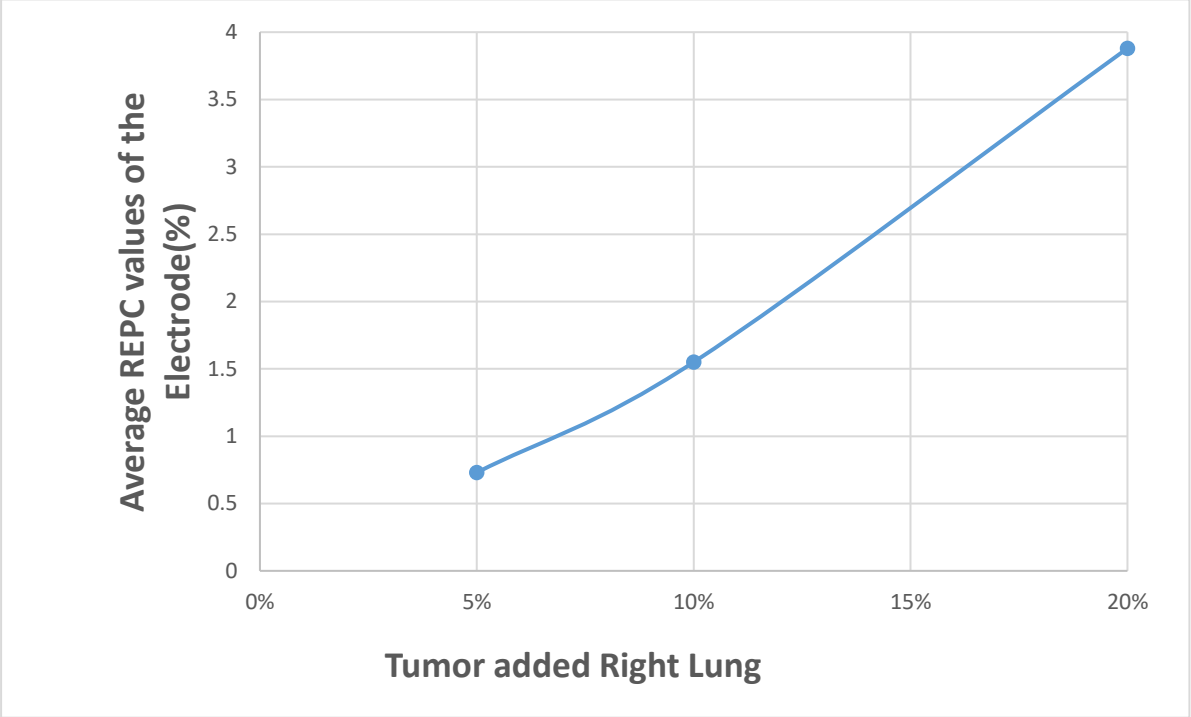

Figure- 5.24: Average REPC values of the electrode (%) plotted against different sizes (5%, 10%, and 20% volume of the right lung) tumor added Right Lung with inspiration condition. [Table Used 5.55-5.63]

5.6 (B) Simulation study on Tumor Added Right Lung for Single Frequency (50 KHz) at Expiration condition

Computer simulation of the Proposed Anterior-Posterior EIT Protocol computed average REPC values of the electrode (%) at constant current = 1mA, frequency = 50 KHz for healthy (normal) lungs with expiration condition the electrical conductivity & the relative permittivity values were taken 0.2620Sm^{-1}& 8531.40 and for tumor these values were taken 1.50 Sm^{-1}& 98.56 respectively is shown in the figure-5.25.

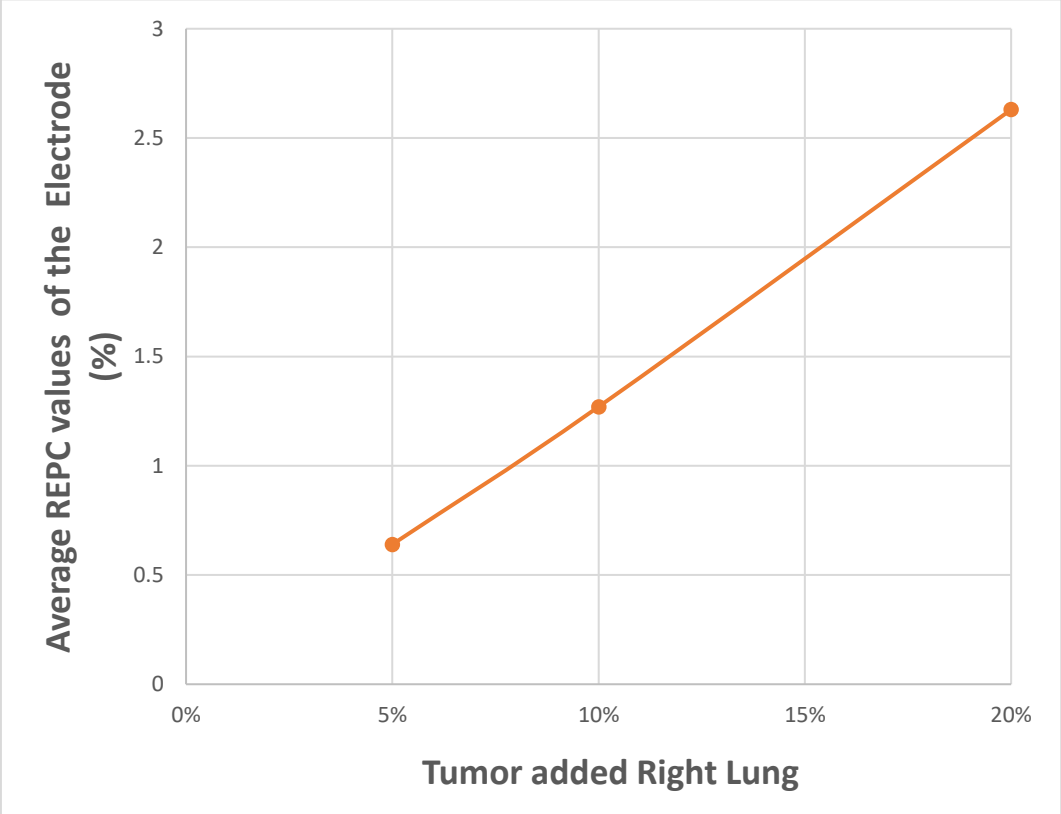

Figure- 5.25: Average REPC values of the Electrode (%) plotted against different sizes (5%, 10%, and 20% volume of the right lung) tumor added Right Lung with expiration condition. [Table Used 5.64-5.72]

5.6 (C): Comparison of the average REPC values for tumor added lungs at inspiration and expiration conditions.

Table-5.73: Comparison of the Average Relative Electric Potential Change (REPC) values of the Surface Electrode (%) for different sizes (5%, 10%, and 20% volume of the right lung) tumor of Right Lung with Inspiration and Expiration conditions.

Tumor sizes of the Right Lung volume (%)	Average REPC values of the SE with Inspiration (%)	Average REPC values of the SE with Expiration (%)
5	0.73	0.64
10	1.55	1.27
20	3.88	2.63

Comparison of the average REPC values of the electrode (%) for tumor added right lung with inspiration and expiration conditions are shown in the figure-5.26

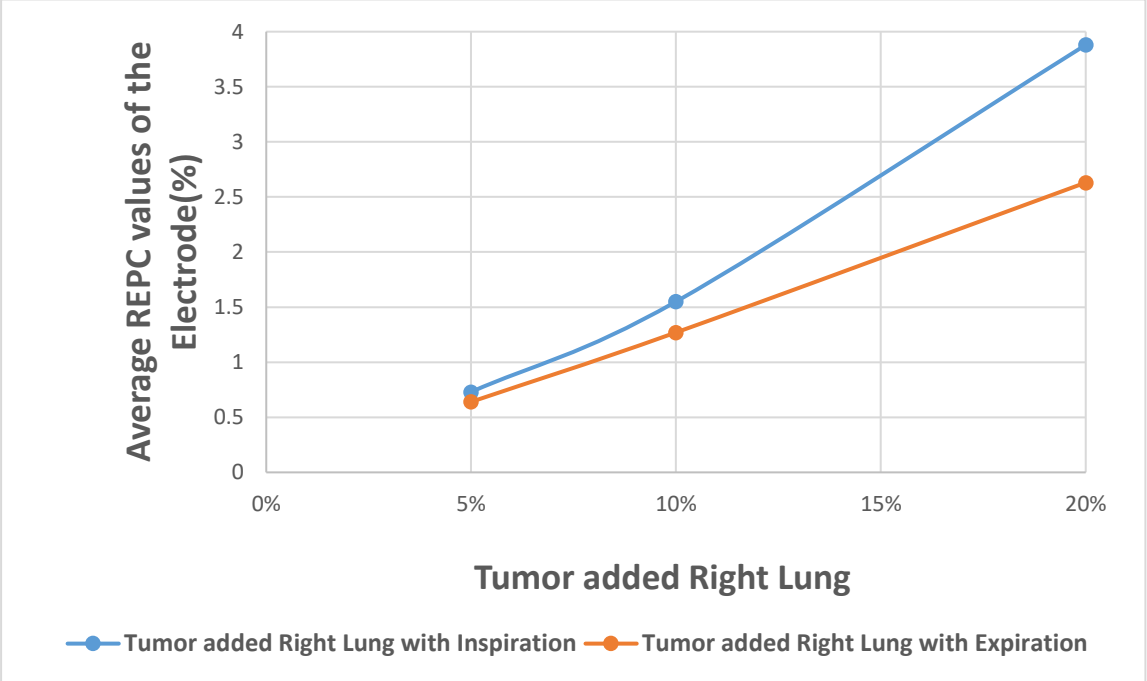

Figure- 5.26: Average REPC values of the Electrode (%) plotted against different sizes (5%, 10%, and 20% volume of the right lung) tumor added Right Lung at Inspiration and Expiration conditions. [Table used 5.73]

Table-5.74: Distinguishing Factor for Healthy (Normal) Lungs at inspiration condition and different sizes (5%, 10%, and 20% volume of the right lung) of Tumor added Right Lung.

Tumor sizes of the Right Lung volume (%)	Distinguishing Factor for uniform (healthy) and non-uniform (tumor) model considering the corresponding value of the surface electrode $\mathbf{D_1}=\sqrt{\frac{1}{N}\sum_{i=1}^{N}\left\{\frac{(Vu(i)-Vn(i)}{Vu(i)}\right\}^2}$	Distinguishing Factor for uniform (healthy) and non-uniform (tumor) model considering the consecutive difference value of the surface electrode $\mathbf{D_2}=\sqrt{\frac{1}{N}\sum_{i=1}^{N}\left\{\frac{(Vu(i)-Vn(i)}{Vu(i)}\right\}^2}$
5	0.74	4.18
10	1.56	8.57
20	3.89	20.79

Distinguishing Factor (D_1) for uniform (healthy) and non-uniform (tumor) model considering the corresponding value of the surface electrode with inspiration condition is shown in figure-5.27.

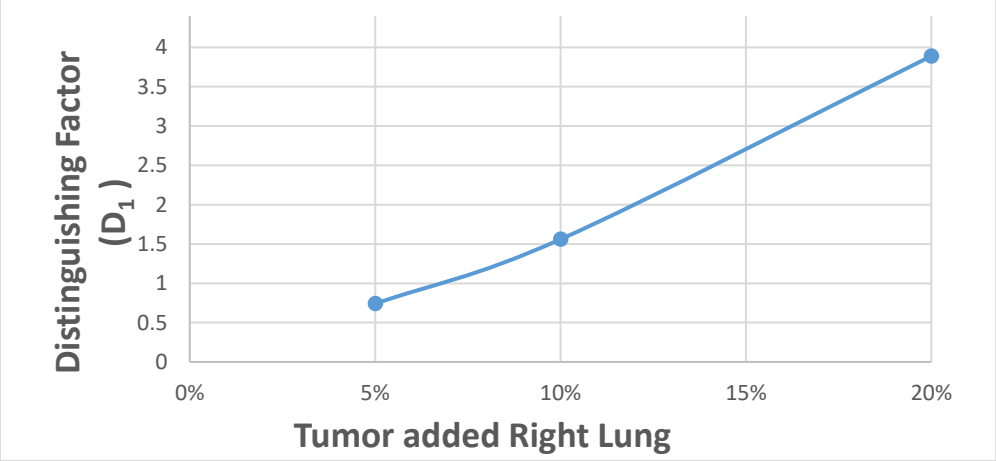

Figure- 5.27: Distinguishing Factor (D_1) plotted against different sizes (5%, 10%, and 20% volume of the right lung) of Tumor added Right Lung at inspiration condition. [Table Used-6.74]

Distinguishing Factor (D_2) for uniform (healthy) and non-uniform (tumor) model considering the consecutive difference value of the surface electrode at inspiration condition is shown in figure-5.28.

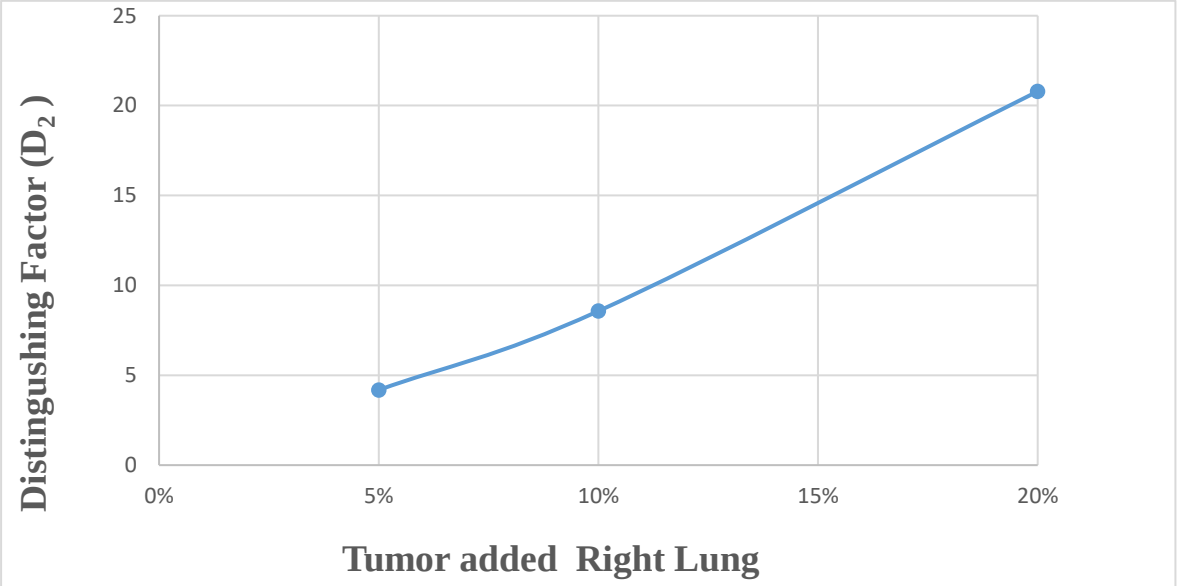

Figure- 5.28: Distinguishing Factor (D_2) plotted against different sizes (5%, 10%, and 20% volume of the right lung) of Tumor added Right Lung at inspiration condition. [Table Used 5.74]

Comparison of the distinguishing factors (D_1& D_2) for tumor added right lung at inspiration condition are shown in the figure-5.29.

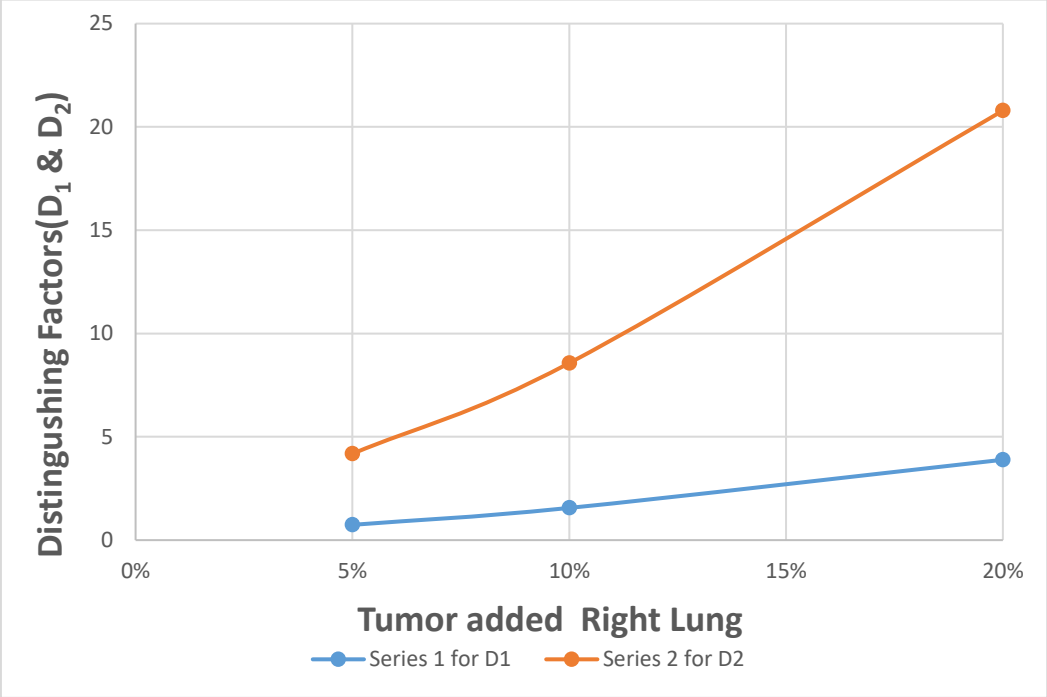

Figure -5.29: Distinguishing Factors (D_1& D_2) plotted against different sizes (5%, 10%, and 20% volume of the right lung) of tumor added Right Lung at inspiration condition.

Table-5.75: Distinguishing Factor for Healthy (Normal) Lungs at expiration condition and different sizes (5%, 10%, and 20% volume of the right lung) of Tumor added Right Lung.

Size of Tumor (%)	Distinguishing Factor for uniform (healthy) and non-uniform (tumor) model considering the corresponding value of the surface electrode $\mathbf{D_1}=\sqrt{\frac{1}{N}\sum_{i=1}^{N}\left\{\frac{(Vu(i)-Vn(i)}{Vu(i)}\right\}^2}$	Distinguishing Factor for uniform (healthy) and non-uniform (tumor) model considering the consecutive difference value of the surface electrode $\mathbf{D_2}=\sqrt{\frac{1}{N}\sum_{i=1}^{N}\left\{\frac{(Vu(i)-Vn(i)}{Vu(i)}\right\}^2}$
5	0.64	4.17
10	1.28	8.46
20	2.65	16.90

Distinguishing Factor ($D_{1)}$ for uniform (healthy) and non-uniform (tumor) model considering the corresponding value of the surface electrode at expiration condition is shown in figure-5.30.

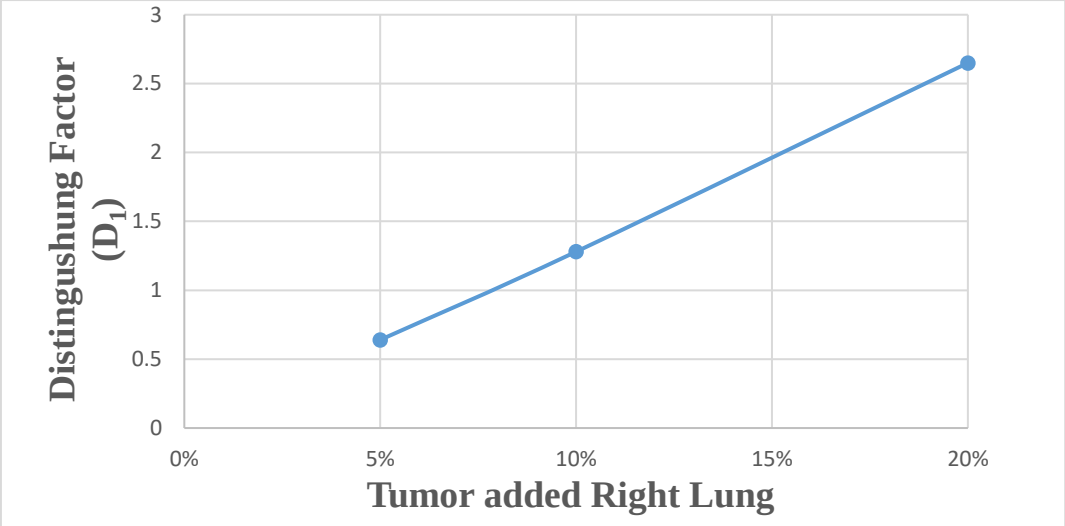

Figure-5.30: Distinguishing Factor (D_1) against different sizes (5%, 10%, and 20% volume of the right lung) of Tumor added Right Lung at expiration condition. [Table Used 6.75]

Distinguishing Factor (D_2) for uniform (healthy) and non-uniform (tumor) model considering the consecutive difference value of the surface electrode at expiration condition is shown in figure-5.31.

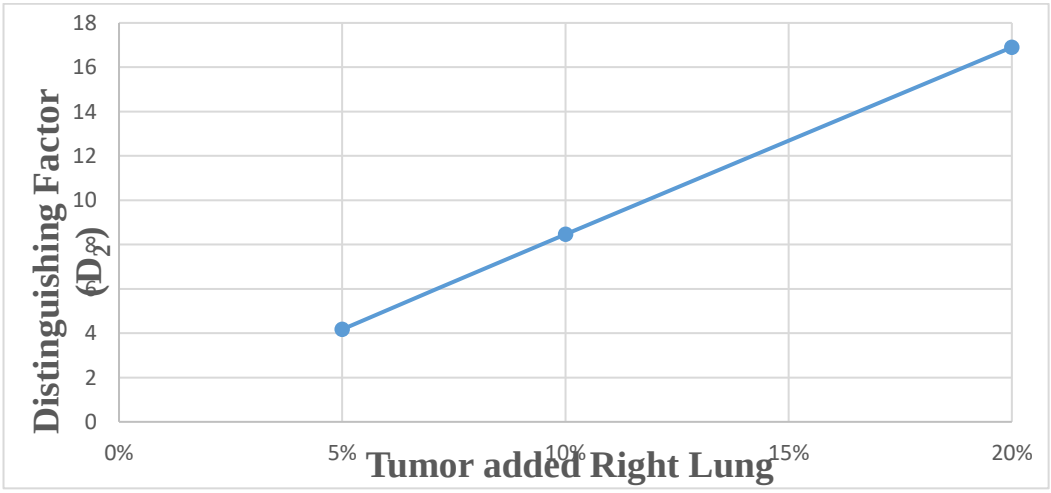

Figure- 5.31: Distinguishing Factor (D_2) against different sizes (5%, 10%, and 20% volume of the right lung) of Tumor added Right Lung at expiration condition. [Table Used 5.75]

Comparison of the distinguishing factors (D_1& D_2) for tumor added right lung at expiration condition are shown in the figure-5.32.

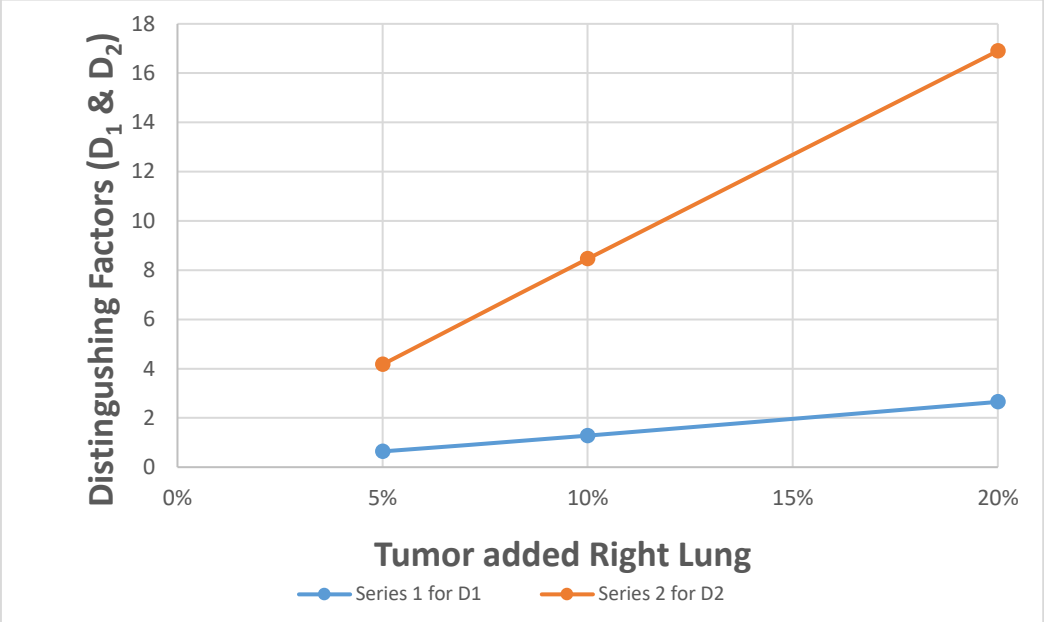

Figure-5.32: Distinguishing Factors (D_1& D_2) plotted against different sizes (5%, 10%, and 20% volume of the right lung) of tumor added Right Lung at expiration condition.

5.7 Simulation Study Method-7: Electrical impedance spectroscopy (EIS) i.e., imaging at multiple frequencies like-20 kHz, 50 kHz,100 kHz, 150 kHz, 200 kHz for fixed electrical conductivity for APEIT Protocol

5.7(A) At Inspiration Condition

Applying the Proposed Anterior-Posterior EIT Protocol for healthy lung at inspiration condition its electrical conductivity is 0.1030Sm^{-1}. Also took another four electrical conductivity values of ±10% steps of healthy lung at inspiration conditions i.e.,0.0824 Sm^{-1}, 0.0927 Sm^{-1}, 0.1133 Sm^{-1}, and 0.1236 Sm^{-1} for simulation of multi frequency or frequency spectrum 20 KHz, 50 KHz, 100 KHz, 150 KHz, and 200 KHz. All cases relative permittivity value was taken 4272.50 and constant alternating current 1mA (assumed to be safe).

Computer simulation of the Proposed Anterior-Posterior EIT Protocol computed electrical potential at each electrode for different frequencies 20 KHz, 50 KHz, 100 KHz, 150 KHz, and 200 KHz at constant current = 1mA, electrical conductivity=0.0824 $Sm^{-1}$and relative permittivity = 4272.50 are shown in figure-5.33.

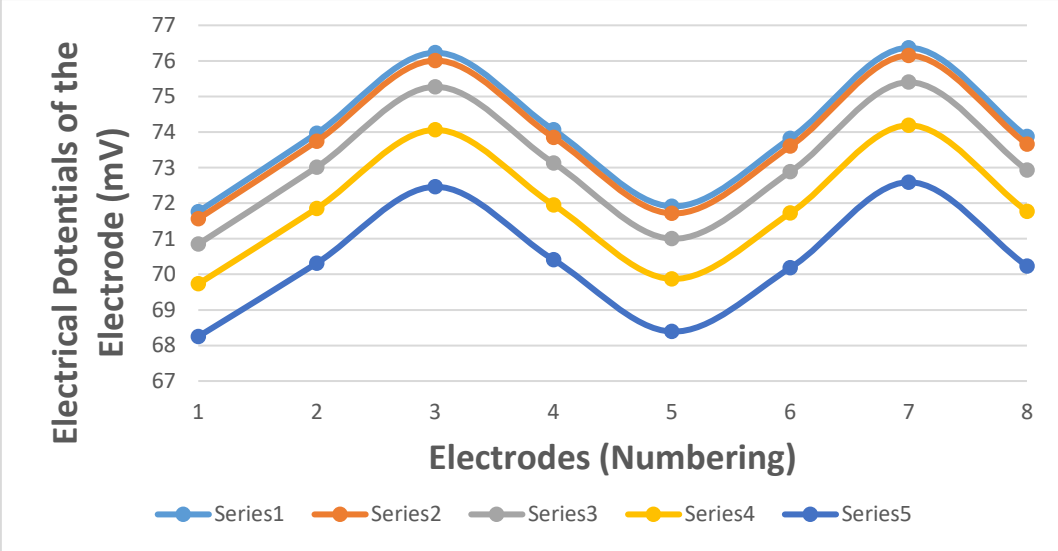

Figure-5.33: Electrical Potentials of the Electrode (mV) plotted against electrodes (numbering) for five different frequencies 20 KHz, 50 KHz, 100 KHz, 150 KHz, and 200 KHz at constant current = 1mA, electrical conductivity = 0.0824Sm^{-1}. [Table Used 5.45]

Series 1: For Frequency 20 KHz, Series 2: For Frequency 50 KHz, Series 3: For Frequency100 KHz, Series 4: For Frequency 150 KHz, and Series 5: For Frequency 200 KHz

Computer simulation of the Proposed Anterior-Posterior EIT Protocol computed sum of the eight electrodes electrical potential for different frequencies 20 KHz, 50 KHz, 100 KHz, 150 KHz, and 200 KHz at constant current = 1mA, electrical conductivity = 0.0824 Sm^{-1} and relative permittivity = 4272.50 is shown in figure-5.34.

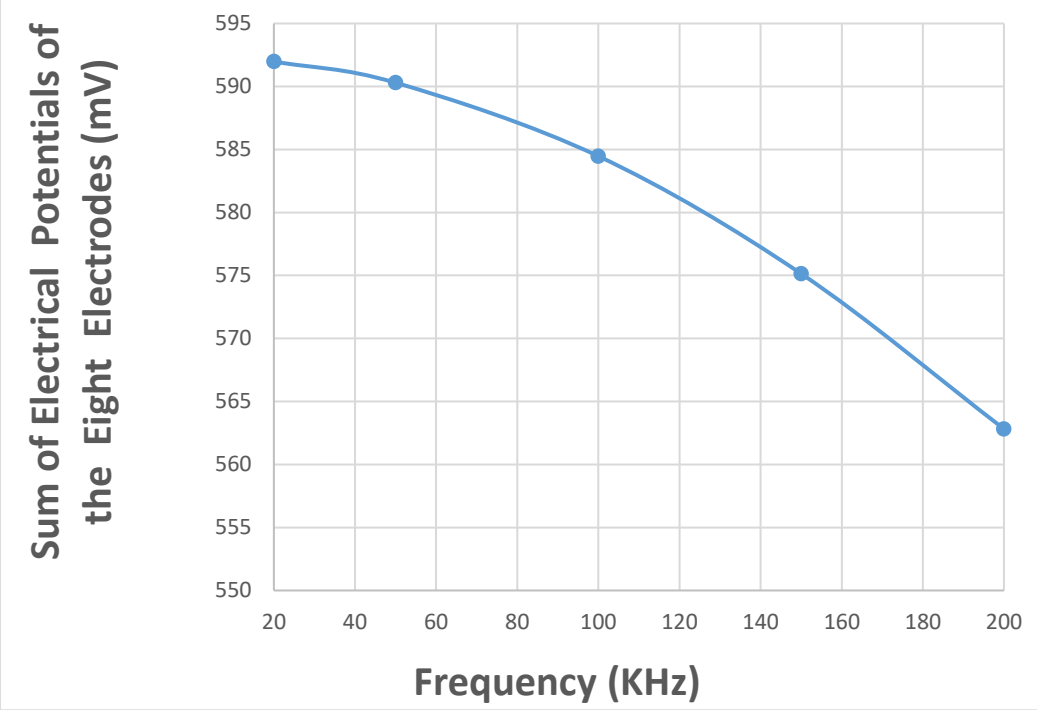

Figure-5.34: Sum of electrical potentials of the eight electrodes (mV) plotted against five different frequencies 20 KHz, 50 KHz, 100 KHz, 150 KHz, and 200 KHz at constant electrical conductivity = 0.0824 Sm^{-1}. [Table Used 5.45]

Computer simulation of the Proposed Anterior-Posterior EIT Protocol computed electrical potential at each electrode for different frequencies 20 KHz, 50 KHz, 100 KHz, 150 KHz, and 200 KHz at constant current = 1mA, electrical conductivity=0.0927 Sm^{-1} and relative permittivity = 4272.50 are shown in figure-5.35.

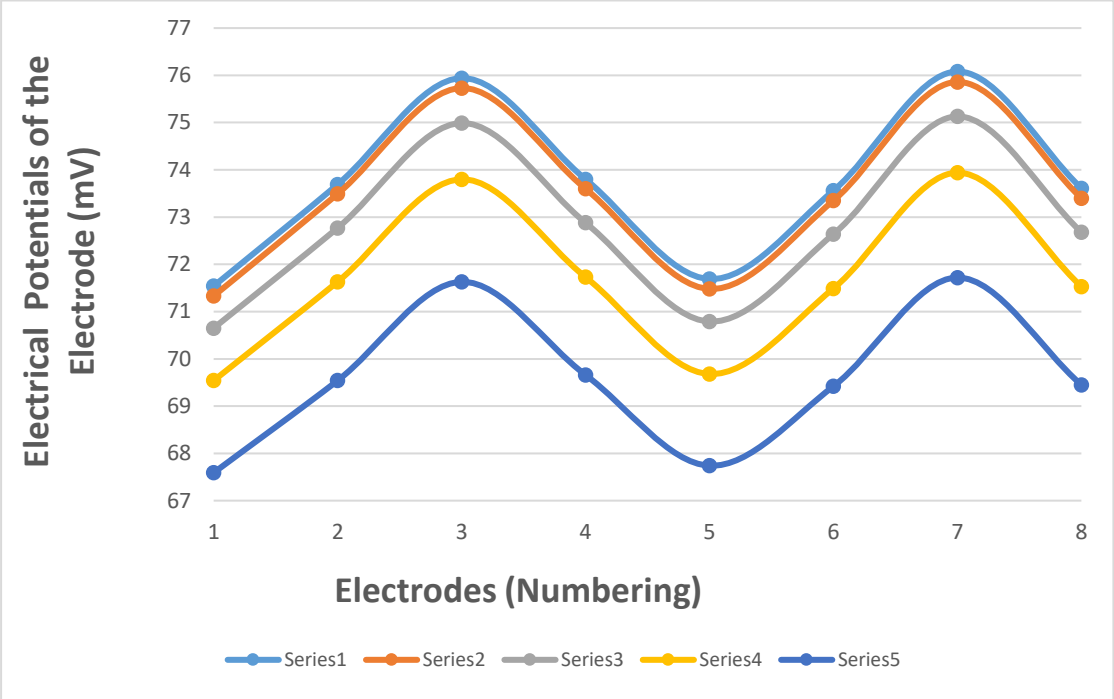

Figure-5.35: Electrical Potentials of the Electrode (mV) plotted against electrodes (numbering) for five different frequencies 20 KHz, 50 KHz, 100 KHz, 150 KHz, and 200 KHz at constant current = 1mA, electrical conductivity = 0.0927 Sm^{-1}. [Table Used 5.46]

Series 1: For Frequency 20 KHz, Series 2: For Frequency 50 KHz, Series 3: For Frequency100 KHz, Series 4: For Frequency 150 KHz, and Series 5: For Frequency 200 KHz.

Computer simulation of the Proposed Anterior-Posterior EIT Protocol computed sum of the electrodes electrical potential for different frequencies 20 KHz, 50 KHz, 100 KHz, 150 KHz, and 200 KHz at constant current = 1mA, electrical conductivity = 0.0927 Sm^{-1} and relative permittivity = 4272.50 is shown in figure-5.36.

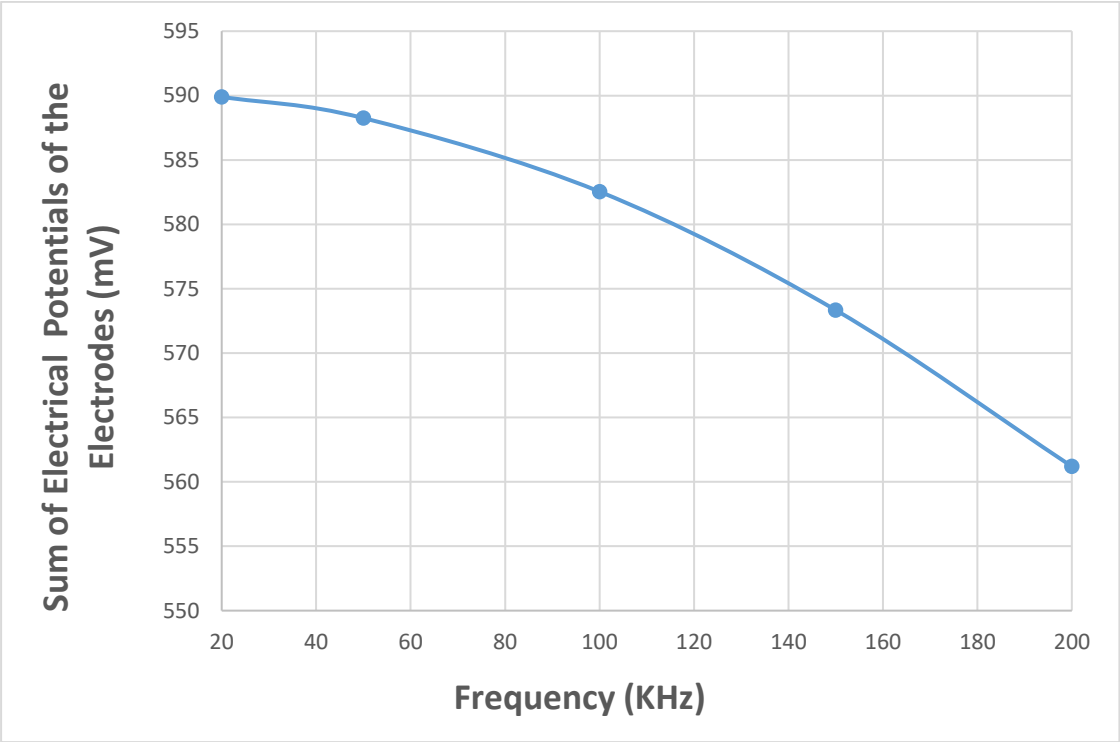

Figure-5.36: Sum of electrical potentials of the eight electrodes (mV) plotted against five different frequencies 20 KHz, 50 KHz, 100 KHz, 150 KHz, and 200 KHz at constant electrical conductivity = 0.0927 Sm^{-1}. [Table Used 5.46]

Computer simulation of the Proposed Anterior-Posterior EIT Protocol computed electrical potential at each electrode for different frequencies 20 KHz, 50 KHz, 100 KHz, 150 KHz, and 200 KHz at constant current = 1mA, electrical conductivity=0.1030 $Sm^{-1}$and relative permittivity = 4272.50 are shown in figure-5.37.

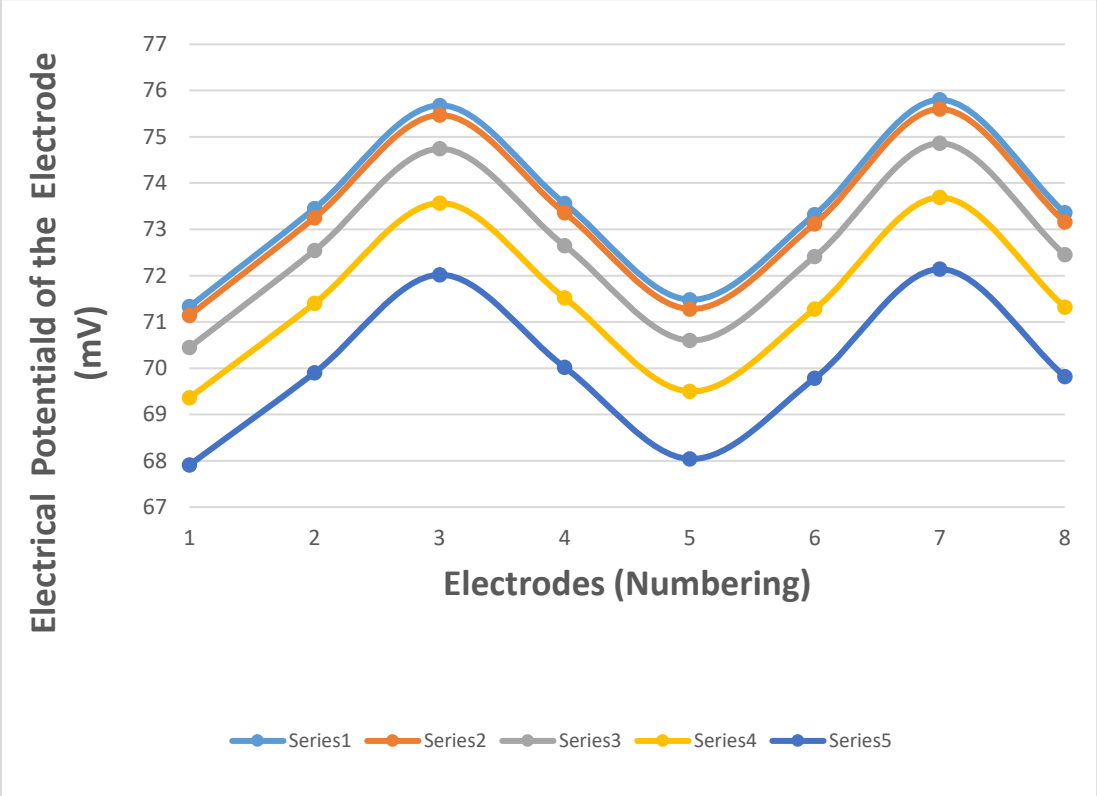

Figure-5.37: Electrical Potentials of the Electrode (mV) plotted against electrodes (numbering) for five different frequencies 20 KHz, 50 KHz, 100 KHz, 150 KHz, and 200 KHz at constant current = 1mA, electrical conductivity = 0.1030 Sm^{-1}. [Table Used 5.47]

Series 1: For Frequency 20 KHz, Series 2: For Frequency 50 KHz, Series 3: For Frequency100 KHz, Series 4: For Frequency 150 KHz, andSeries 5: For Frequency 200 KHz

Computer simulation of the Proposed Anterior-Posterior EIT Protocol computed sum of the eight electrodes electrical potential for different frequencies 20 KHz, 50 KHz, 100 KHz, 150 KHz, and 200 KHz at constant current = 1mA, electrical conductivity = 0.1030 Sm^{-1} and relative permittivity = 4272.50 is shown in figure-5.38.

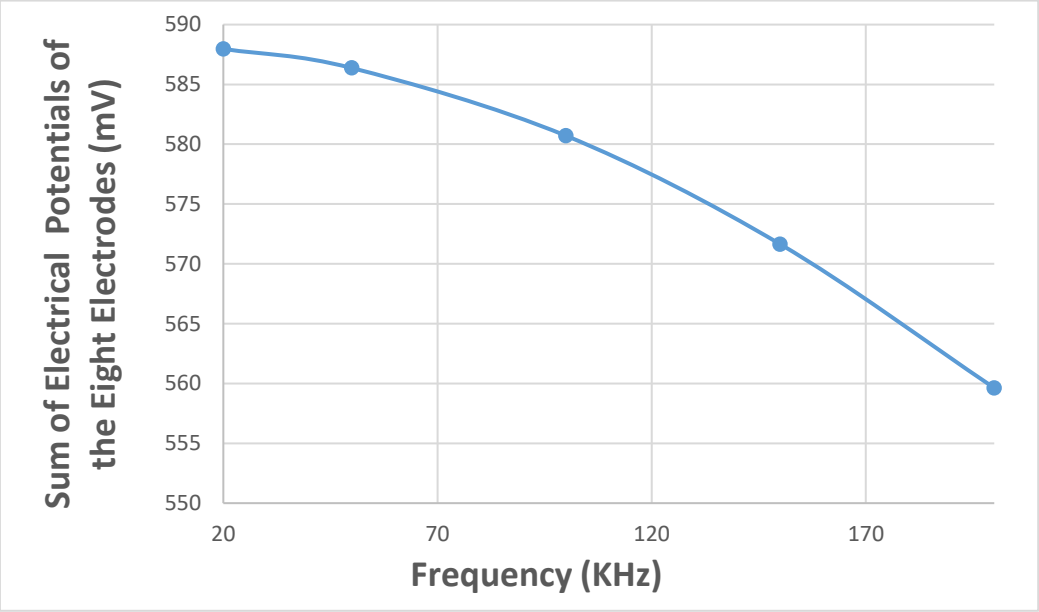

Figure-5.38: Sum of electrical potentials of the eight electrodes (mV) plotted against five different frequencies 20 KHz, 50 KHz, 100 KHz, 150 KHz, and 200 KHz at constant electrical conductivity = 0.1030 Sm^{-1}. [Table Used 5.47]

Computer simulation of the Proposed Anterior-Posterior EIT Protocol computed electrical potential at each electrode for different frequencies 20 KHz, 50 KHz, 100 KHz, 150 KHz, and 200 KHz at constant current = 1mA, electrical conductivity=0.1133 Sm^{-1} and relative permittivity = 4272.50 are shown in figure-5.39.

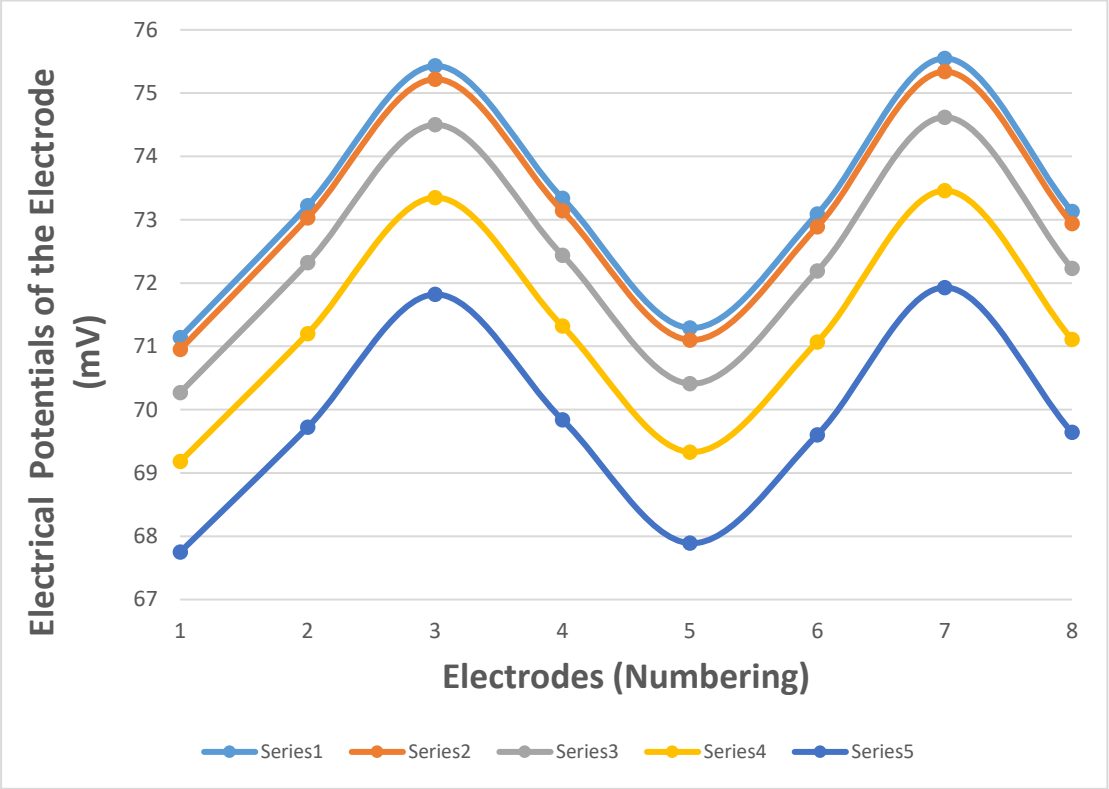

Figure-5.39: Electrical Potentials of the Electrode (mV) plotted against electrodes (numbering) for different frequencies 20 KHz, 50 KHz, 100 KHz, 150 KHz, and 200 KHz at constant current = 1mA, electrical conductivity = 0.1133Sm^{-1}. [Table Used 5.48]

Series 1: For Frequency 20 KHz, Series 2: For Frequency 50 KHz, Series 3: For Frequency100 KHz, Series 4: For Frequency 150 KHz, and Series 5: For Frequency 200 KHz

Computer simulation of the Proposed Anterior-Posterior EIT Protocol computed sum of the eight electrodes electrical potential for different frequencies 20 KHz, 50 KHz, 100 KHz, 150 KHz, and 200 KHz at constant current = 1mA, electrical conductivity = 0.1133 Sm^{-1} and relative permittivity = 4272.50 is shown in figure-5.40.

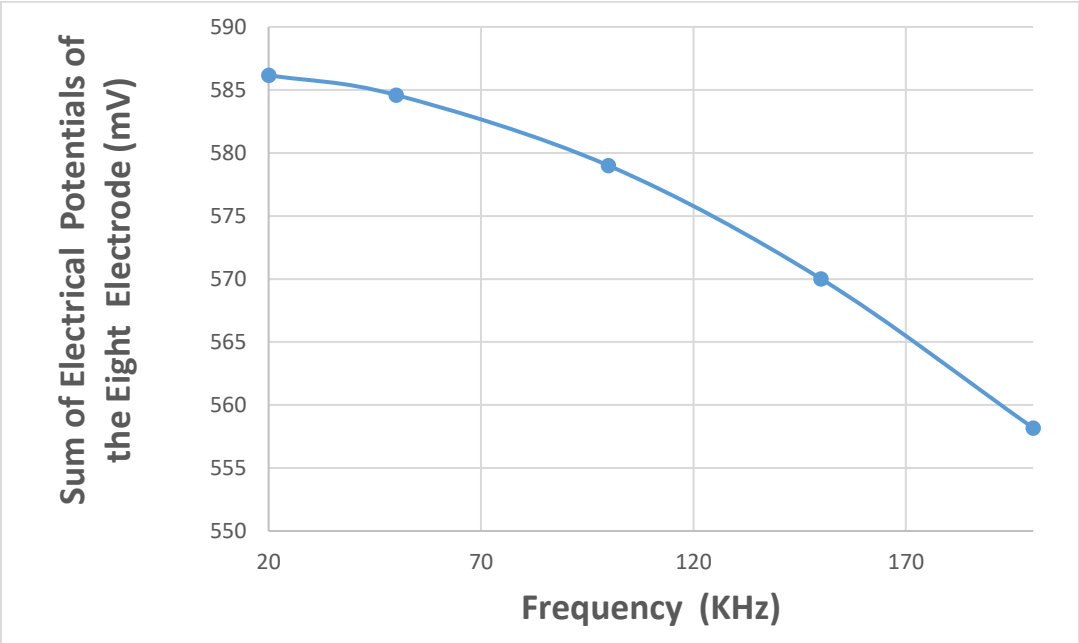

Figure-5.40: Sum of electrical potentials of the eight electrodes (mV) plotted against five different frequencies 20 KHz, 50 KHz, 100 KHz, 150 KHz, and 200 KHz at constant electrical conductivity = 0.1133 Sm^{-1}. [Table Used 5.48]

Computer simulation of the Proposed Anterior-Posterior EIT Protocol computed electrical potential at each electrode for different frequencies 20 KHz, 50 KHz, 100 KHz, 150 KHz, and 200 KHz at constant current = 1mA, electrical conductivity=0.1236 Sm^{-1} and relative permittivity = 4272.50 are shown in figure-5.41.

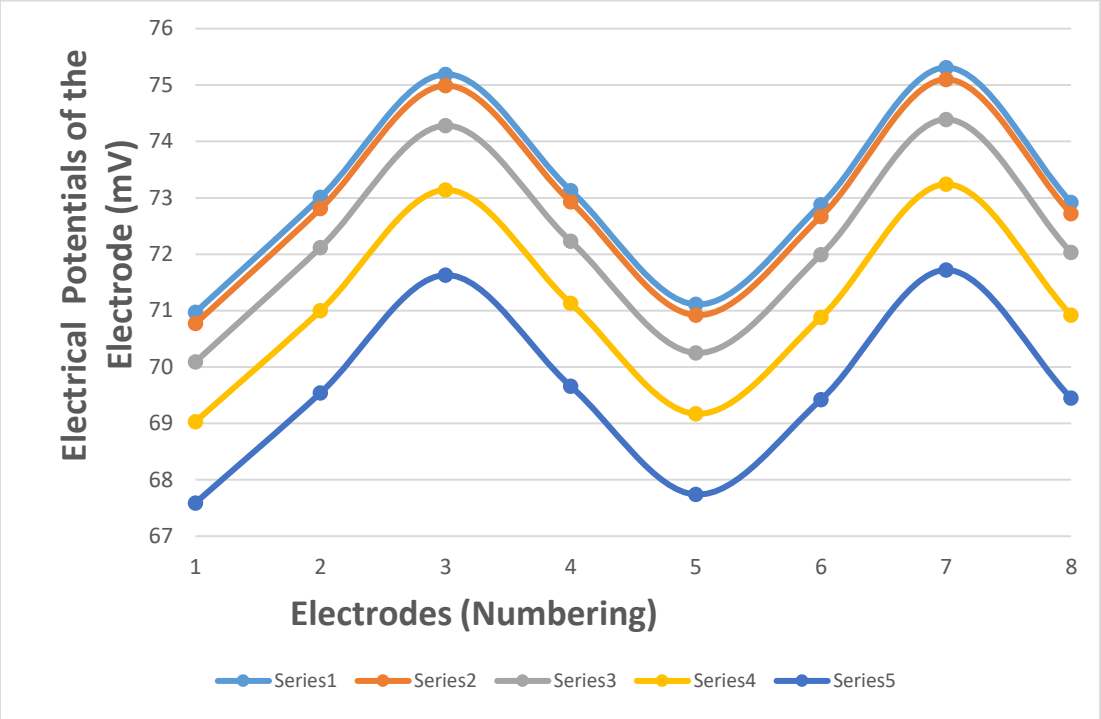

Figure-5.41: Electrical Potentials of the Electrode (mV) plotted against electrodes (numbering) for different frequencies 20 KHz, 50 KHz, 100 KHz, 150 KHz, and 200 KHz at constant current = 1mA, electrical conductivity = 0.1236 Sm^{-1}. [Table Used 5.49]

Series 1: For Frequency 20 KHz, Series 2: For Frequency 50 KHz, Series 3: For Frequency100 KHz, Series 4: For Frequency 150 KHz, and Series 5: For Frequency 200 KHz

Computer simulation of the Proposed Anterior-Posterior EIT Protocol computed sum of the eight electrodes electrical potential for different frequencies 20 KHz, 50 KHz, 100 KHz, 150 KHz, and 200 KHz at constant current = 1mA, electrical conductivity = 0.1236 Sm^{-1} and relative permittivity = 4272.50 is shown in figure-5.42.

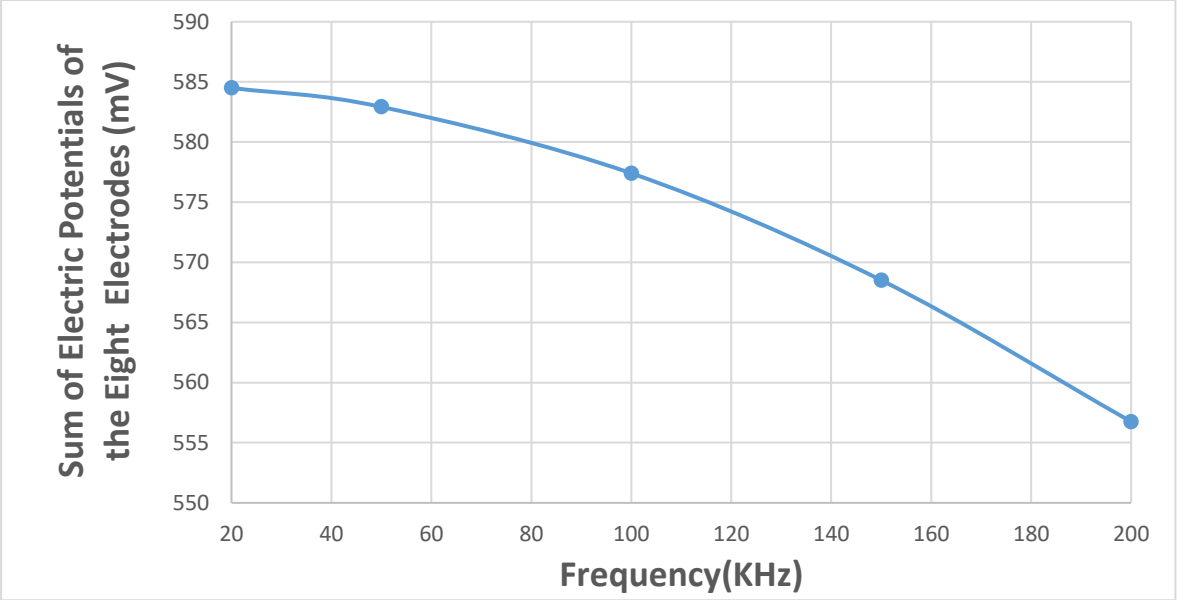

Figure-5.42: Sum of electrical potentials of the eight electrodes (mV) plotted against five different frequencies 20 KHz, 50 KHz, 100 KHz, 150 KHz, and 200 KHz at constant electrical conductivity = 0.1236 Sm^{-1}. [Table Used 5.49]

Computer simulation of the Proposed Anterior-Posterior EIT Protocol computed sum of the eight electrodes electrical potential for different frequencies 20 KHz, 50 KHz, 100 KHz, 150 KHz, and 200 KHz at constant current = 1mA, relative permittivity = 4272.50for different electrical conductivities 0.0824 Sm^{-1}, 0.0927 Sm^{-1}, 0.1030Sm^{-1}, 0.1133 Sm^{-1}, and 0.1236Sm^{-1} are shown in figure-5.43. [Table Used-5.45-5.49]

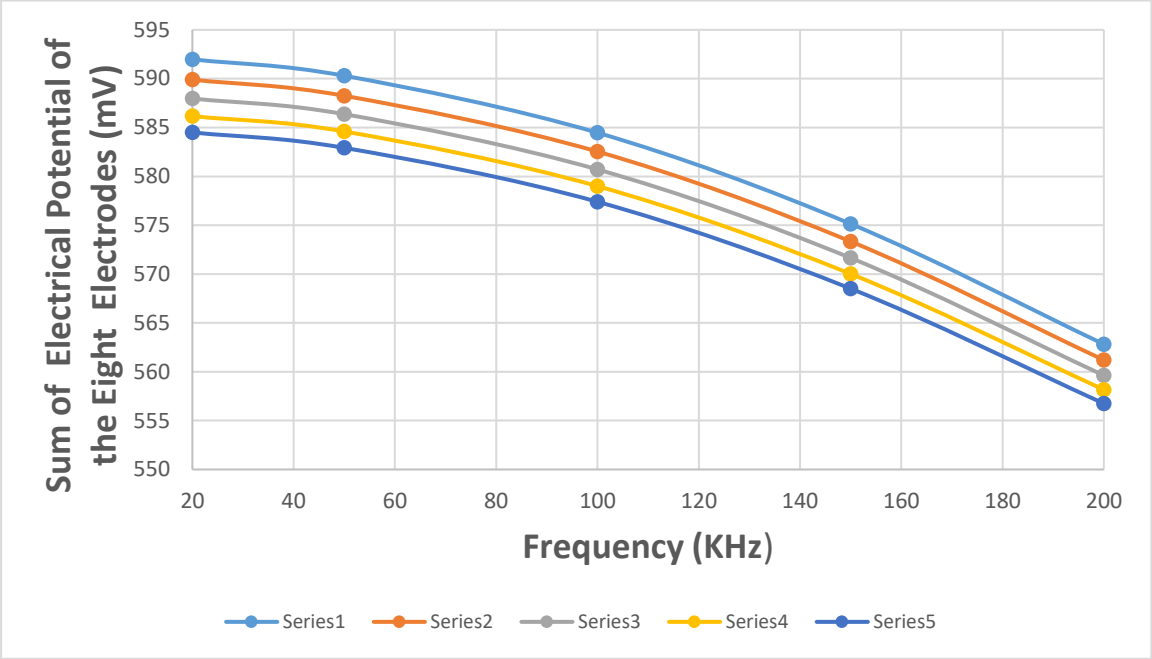

Figure-5.43: Sum of electrical potentials of the eight surface electrodes (mV) plotted against five different frequencies 20 KHz, 50 KHz, 100 KHz, 150 KHz, and 200 KHz for five electrical conductivity values 0.0824Sm^{-1}, 0.0927 Sm^{-1}, 0.1030Sm^{-1}, 0.1133 Sm^{-1}, and 0.1236 Sm^{-1}.

Series 1: For Electrical Conductivity 0.0824 Sm^{-1} at Frequency Spectrum (20 KHz, 50 KHz, 100 KHz, 150 KHz, and 200 KHz)

Series2: For Electrical Conductivity 0.0927 Sm^{-1} at Frequency Spectrum (20 KHz, 50 KHz, 100 KHz, 150 KHz, and 200 KHz)

Series3: For Electrical Conductivity 0.1030Sm^{-1} at Frequency Spectrum (20 KHz, 50 KHz, 100 KHz, 150 KHz, and 200 KHz)

Series4: For constant Electrical Conductivity 0.1133 Sm^{-1} at Frequency Spectrum (20 KHz, 50 KHz, 100 KHz, 150 KHz, and 200 KHz)

Series 5: For constant Electrical Conductivity 0.1236 Sm^{-1}at Frequency Spectrum (20 KHz, 50 KHz, 100 KHz, 150 KHz, and 200 KHz)

5.7 (B): At Expiration Condition

Applying the Proposed Anterior -Posterior EIT Protocol for healthy lung at expiration condition its electrical conductivity is 0.2620Sm^{-1}. Also took another four electrical conductivity values of ±10% steps of healthy lung at expiration conditions i.e. 0.2096 Sm^{-1}, 0.2358Sm^{-1}, 0.2882 Sm^{-1}, 0. 3144 Sm^{-1} for simulation of Multi Frequency (Frequency Spectrum). All cases relative permittivity value was taken 8531.40 and constant alternating current 1mA (assumed to be safe).

Computer simulation of the Proposed Anterior-Posterior EIT Protocol computed electrical potential at each surface electrode for different frequencies 20 KHz, 50 KHz, 100 KHz, 150 KHz, and 200 KHz at constant current = 1mA, electrical conductivity=0.2096 Sm^{-1} and relative permittivity = 8531.40 are shown in figure-5.44.

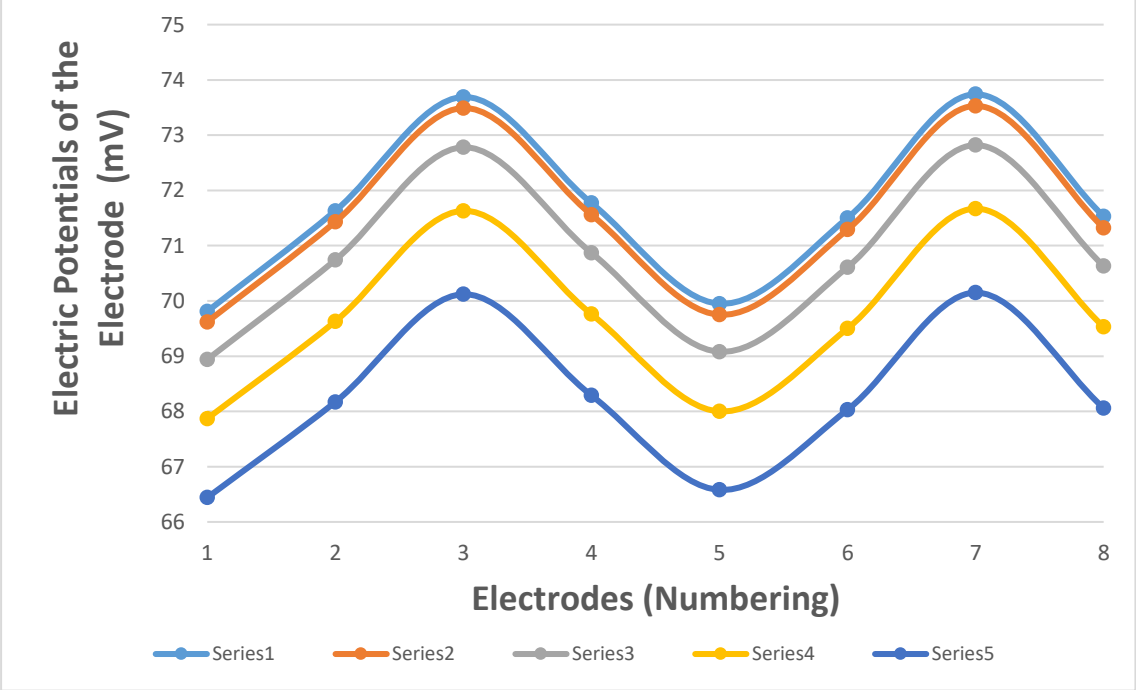

Figure-5.44: Electrical Potentials of the Surface Electrode (mV) plotted against electrodes (numbering) for different frequencies 20 KHz, 50 KHz, 100 KHz, 150 KHz, and 200 KHz at constant current = 1mA, electrical conductivity = 0.2096 Sm^{-1}. [Table Used 5.50]

Series 1: For Frequency 20 KHz, Series 2: For Frequency 50 KHz, Series 3: For Frequency100 KHz, Series 4: For Frequency 150 KHz, and Series 5: For Frequency 200 KHz

Computer simulation of the Proposed Anterior-Posterior EIT Protocol computed sum of the eight electrodes electrical potential for different frequencies 20 KHz, 50 KHz, 100 KHz, 150 KHz, and 200 KHz at constant current = 1mA, electrical conductivity = 0.2096 Sm^{-1} and relative permittivity = 8531.40 is shown in figure-5.45.

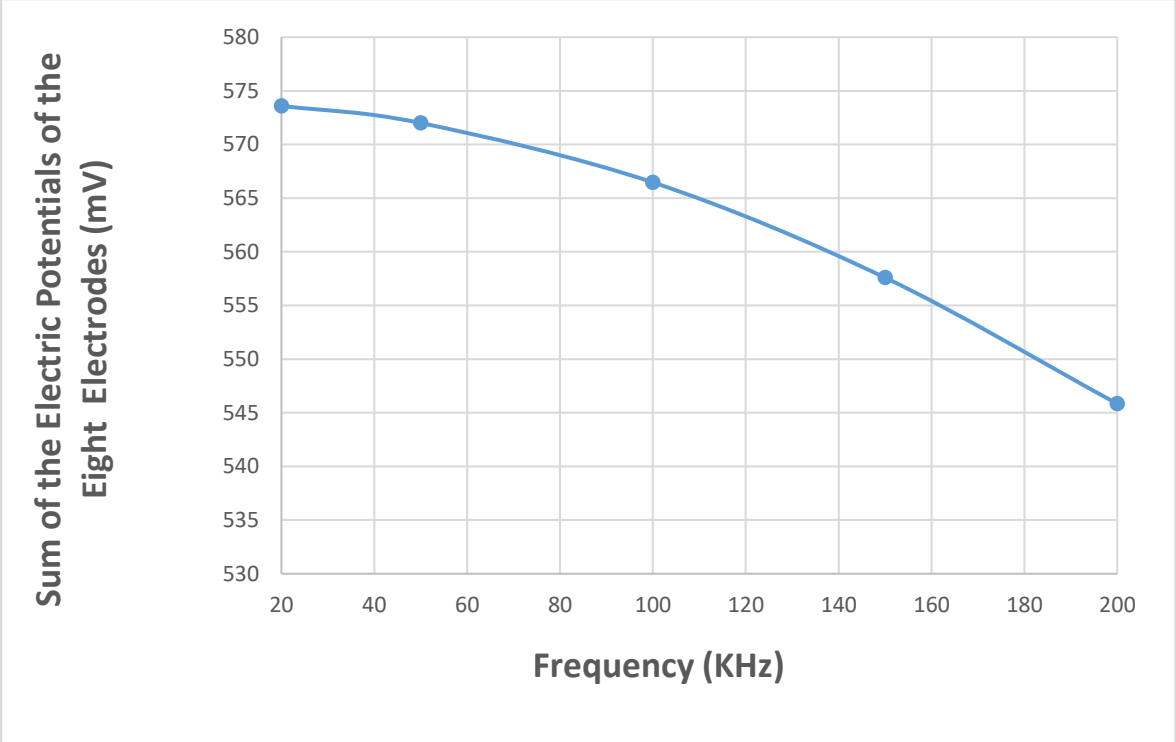

Figure-5.45: Sum of electrical potentials of the eight electrodes (mV) plotted against five different frequencies 20 KHz, 50 KHz, 100 KHz, 150 KHz, and 200 KHz at constant electrical conductivity = 0.2096 Sm^{-1}. [Table Used 5.50]

Computer simulation of the Proposed Anterior-Posterior EIT Protocol computed electrical potential at each electrode for different frequencies 20 KHz, 50 KHz, 100 KHz, 150 KHz, and 200 KHz at constant current = 1mA, electrical conductivity=0.2358 Sm^{-1} and relative permittivity = 8531.40 are shown in figure-5.46.

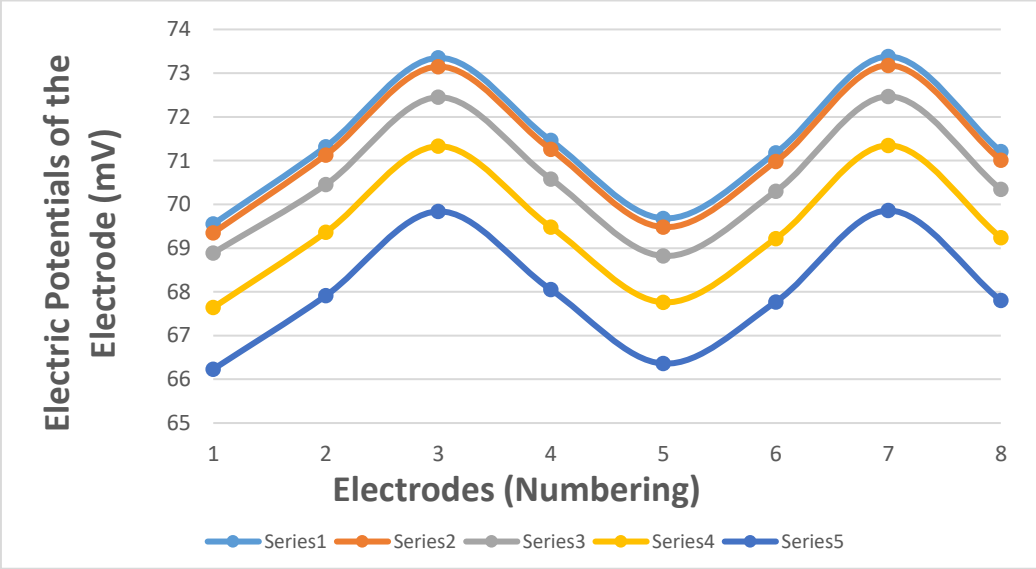

Figure-5.46: Electrical Potentials of the Electrode (mV) plotted against electrodes (numbering) for five different frequencies 20 KHz, 50 KHz, 100 KHz, 150 KHz, and 200 KHz at constant current = 1mA, electrical conductivity = 0.2358 Sm^{-1}. [Table Used 5.51]

Series 1: For Frequency 20 KHz, Series 2: For Frequency 50 KHz, Series 3: For Frequency100 KHz, Series 4: For Frequency 150 KHz, and Series 5: For Frequency 200 KHz

Computer simulation of the Proposed Anterior-Posterior EIT Protocol computed sum of the eight electrodes electrical potential for different frequencies 20 KHz, 50 KHz, 100 KHz, 150 KHz, and 200 KHz at constant current = 1mA, electrical conductivity = 0.2358 Sm^{-1} and relative permittivity = 8531.40 is shown in figure-5.47.

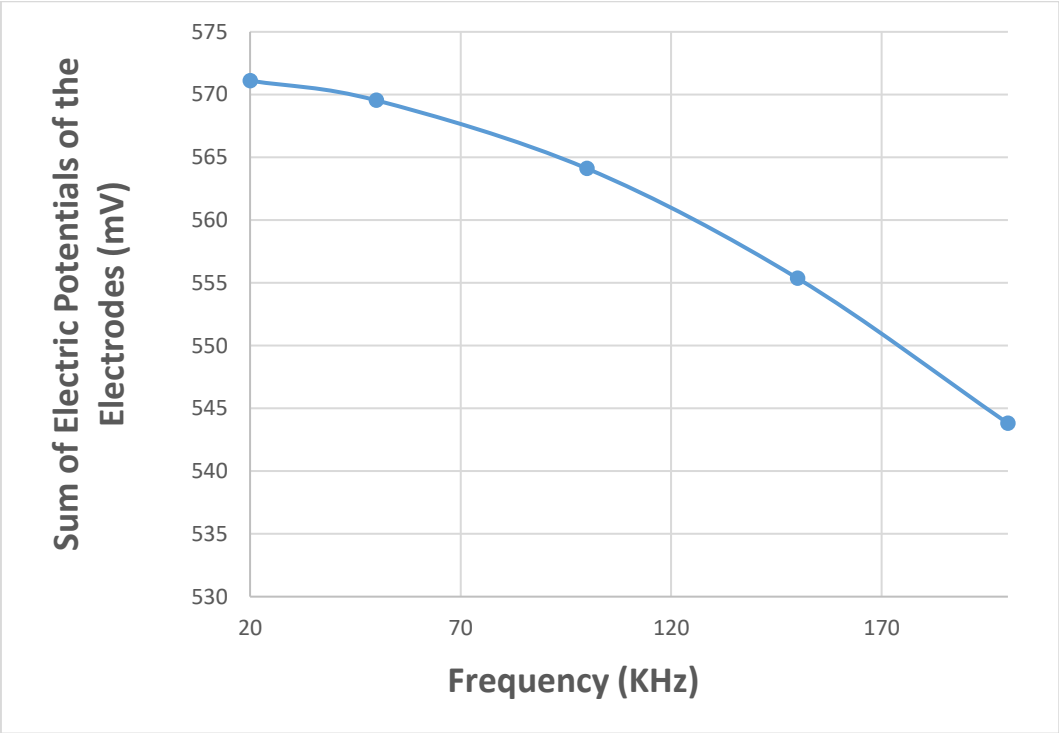

Figure-5.47: Sum of electrical potentials of the eight electrodes (mV) plotted against five different frequencies 20 KHz, 50 KHz, 100 KHz, 150 KHz, and 200 KHz at constant electrical conductivity = 0.2358 Sm^{-1}. [Table Used 5.51]

Computer simulation of the Proposed Anterior-Posterior EIT Protocol computed electrical potential at each electrode for different frequencies 20 KHz, 50 KHz, 100 KHz, 150 KHz, and 200 KHz at constant current = 1mA, electrical conductivity=0.2620 $Sm^{-1}$and relative permittivity = 8531.40 are shown in figure-5.48.

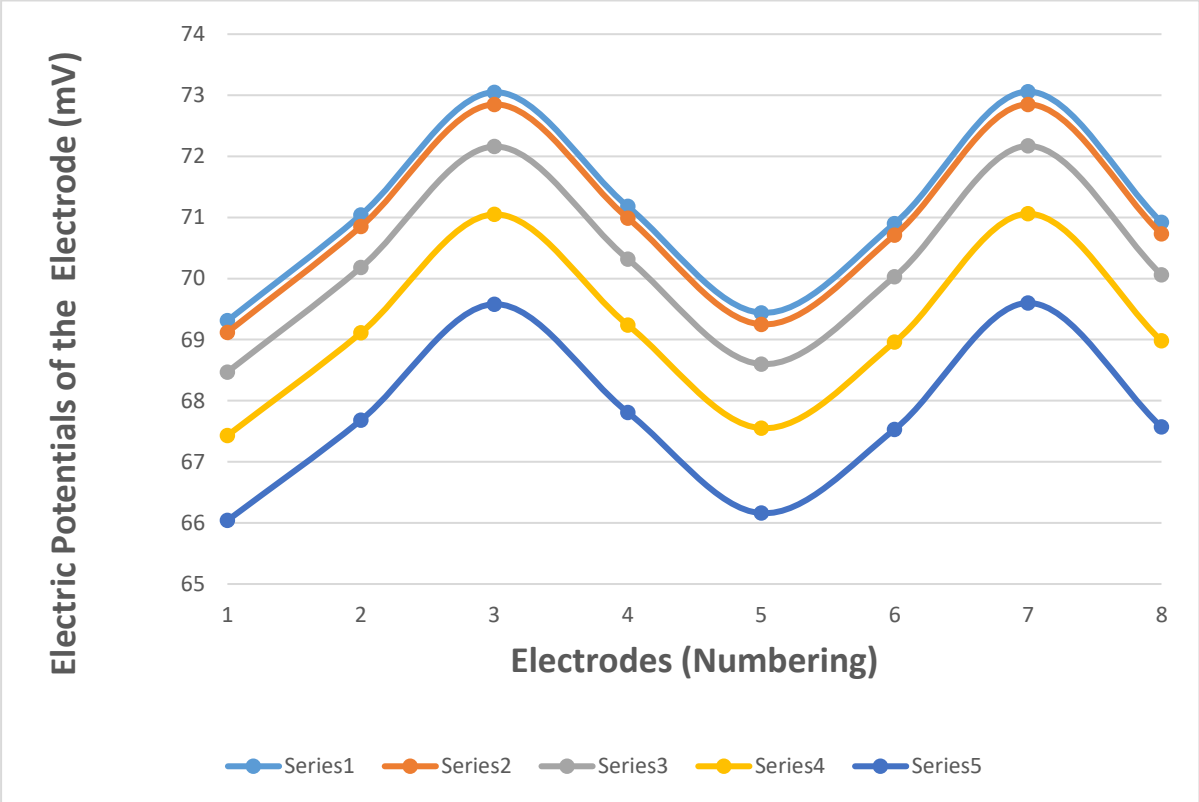

Figure-5.48: Electrical Potentials of the Electrode (mV) plotted against electrodes (numbering) for five different frequencies 20 KHz, 50 KHz, 100 KHz, 150 KHz, and 200 KHz at constant current = 1mA, electrical conductivity = 0.2620 Sm^{-1}. [Table Used 5.52]

Series 1: For Frequency 20 KHz, Series 2: For Frequency 50 KHz, Series 3: For Frequency100 KHz, Series 4: For Frequency 150 KHz, and Series 5: For Frequency 200 KHz

Computer simulation of the Proposed Anterior-Posterior EIT Protocol computed sum of the eight electrodes electrical potential for different frequencies 20 KHz, 50 KHz, 100 KHz, 150 KHz, and 200 KHz at constant current = 1mA, electrical conductivity = 0.2620 Sm^{-1} and relative permittivity = 8531.40 is shown in figure-5.49.

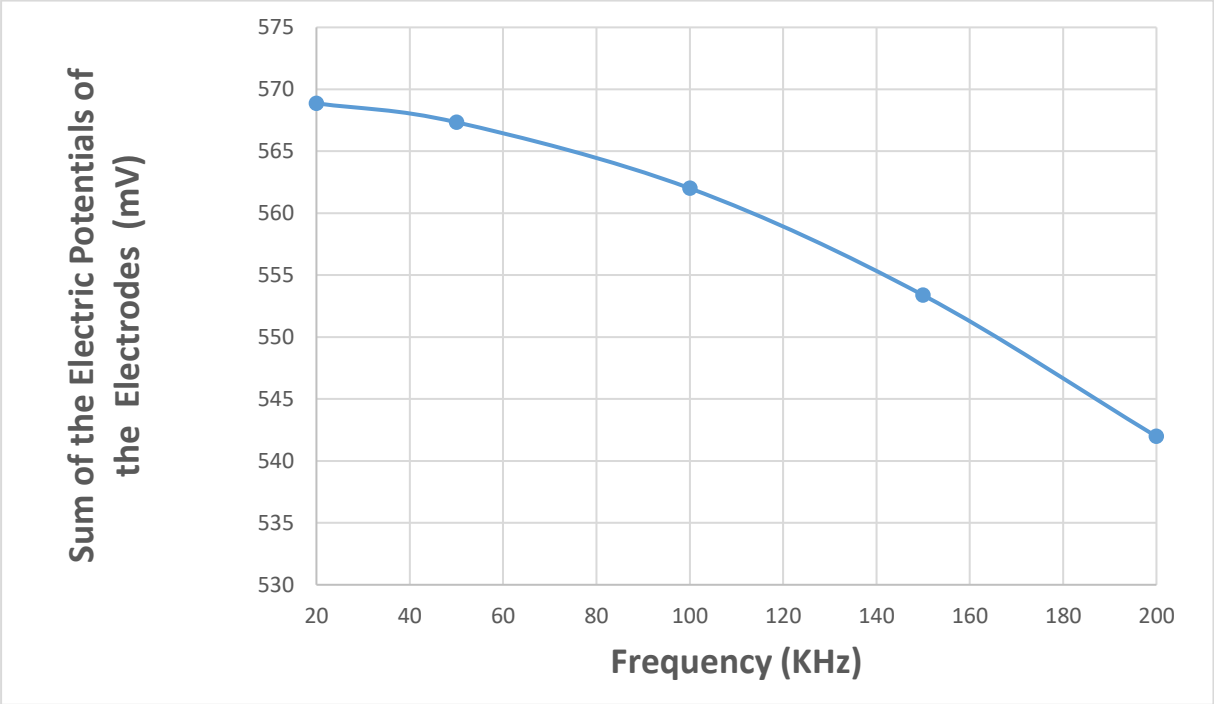

Figure-5.49: Sum of electrical potentials of the eight electrodes (mV) plotted against five different frequencies 20 KHz, 50 KHz, 100 KHz, 150 KHz, and 200 KHz at constant electrical conductivity = 0.2620 Sm^{-1}. [Table Used 5.52]

Computer simulation of the Proposed Anterior-Posterior EIT Protocol computed electrical potential at each electrode for different frequencies 20 KHz, 50 KHz, 100 KHz, 150 KHz, and 200 KHz at constant current = 1mA, electrical conductivity=0.2882 Sm^{-1} and relative permittivity = 8531.40 are shown in figure-5.50.

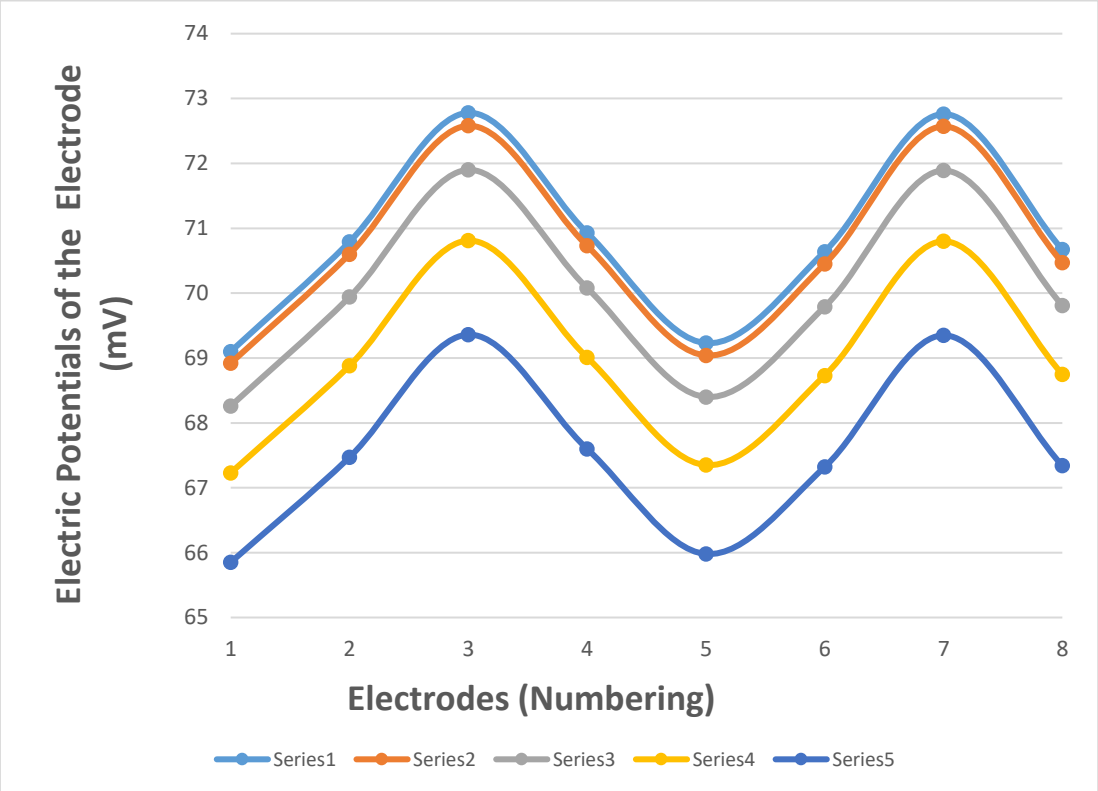

Figure-5.50: Electrical Potentials of the Electrode (mV) plotted against electrodes (numbering) for five different frequencies 20 KHz, 50 KHz, 100 KHz, 150 KHz, and 200 KHz at constant current = 1mA, electrical conductivity = 0.2882Sm^{-1}. [Table Used 5.53]

Series 1: For Frequency 20 KHz, Series 2: For Frequency 50 KHz, Series 3: For Frequency100 KHz, Series 4: For Frequency 150 KHz, and Series 5: For Frequency 200 KHz

Computer simulation of the Proposed Anterior-Posterior EIT Protocol computed sum of the eight electrodes electrical potential for different frequencies 20 KHz, 50 KHz, 100 KHz, 150 KHz, and 200 KHz at constant current = 1mA, electrical conductivity = 0.2882 Sm^{-1} and relative permittivity = 8531.40 is shown in figure-5.51.

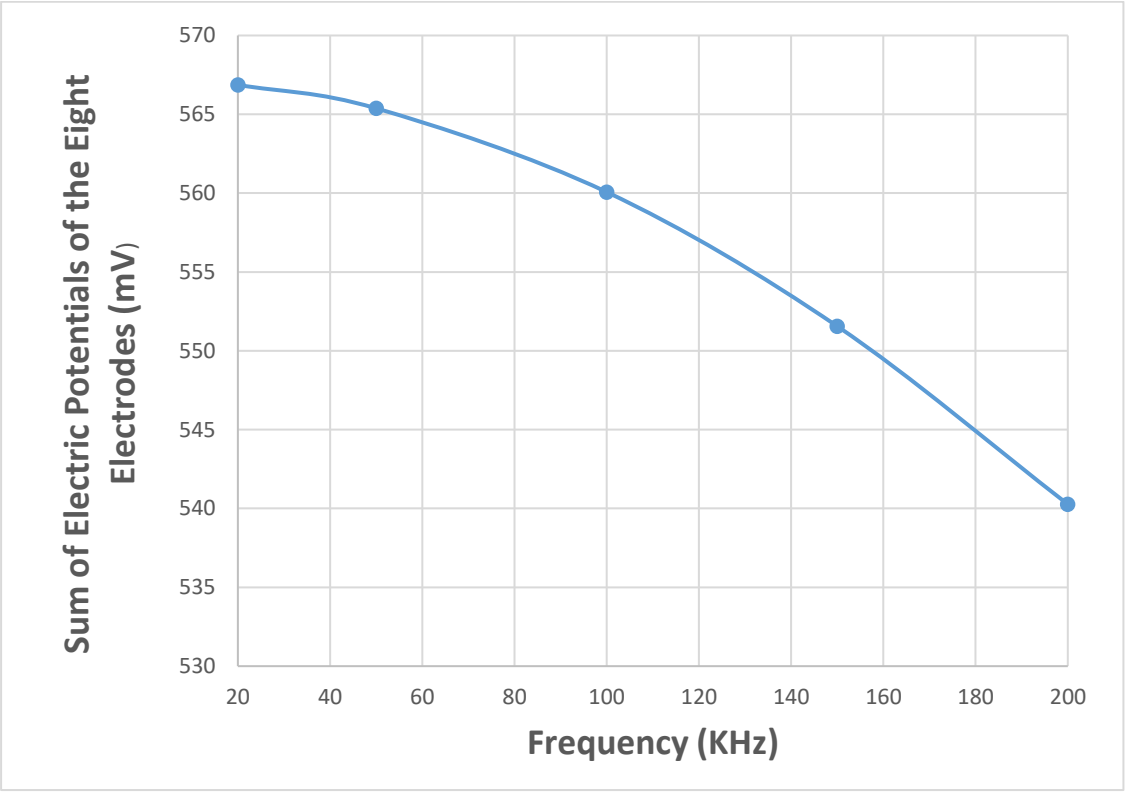

Figure-5.51: Sum of electrical potentials of the eight electrodes (mV) plotted against five different frequencies 20 KHz, 50 KHz, 100 KHz, 150 KHz, and 200 KHz at constant electrical conductivity = 0.2882Sm^{-1}. [Table Used 5.53]

Computer simulation of the Proposed Anterior-Posterior EIT Protocol computed electrical potential at each electrode for different frequencies 20 KHz, 50 KHz, 100 KHz, 150 KHz, and 200 KHz at constant current = 1mA, electrical conductivity=0.3144 Sm^{-1} and relative permittivity = 8531.40 are shown in figure-5.52.

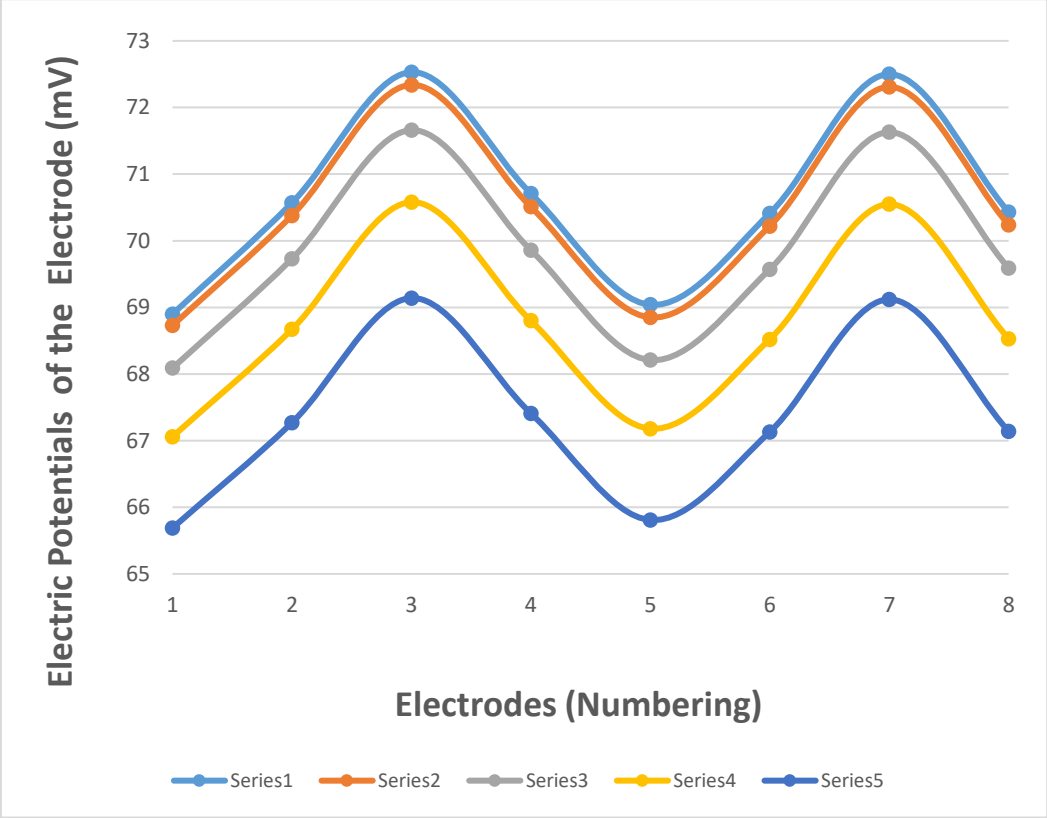

Figure-5.52: Electrical Potentials of the Electrode (mV) plotted against electrodes (numbering) for different frequencies 20 KHz, 50 KHz, 100 KHz, 150 KHz, and 200 KHz at constant current = 1mA, electrical conductivity = 0.3144Sm^{-1}. [Table Used 5.54]

Series 1: For Frequency 20 KHz, Series 2: For Frequency 50 KHz, Series 3: For Frequency100 KHz, Series 4: For Frequency 150 KHz, and Series 5: For Frequency 200 KHz

Computer simulation of the Proposed Anterior-Posterior EIT Protocol computed sum of the eight electrodes electrical potential for five different frequencies 20 KHz, 50 KHz, 100 KHz, 150 KHz, and 200 KHz at constant current = 1mA, electrical conductivity = 0.3144$Sm^{-1}$and relative permittivity = 8531.40 is shown in figure-5.53.

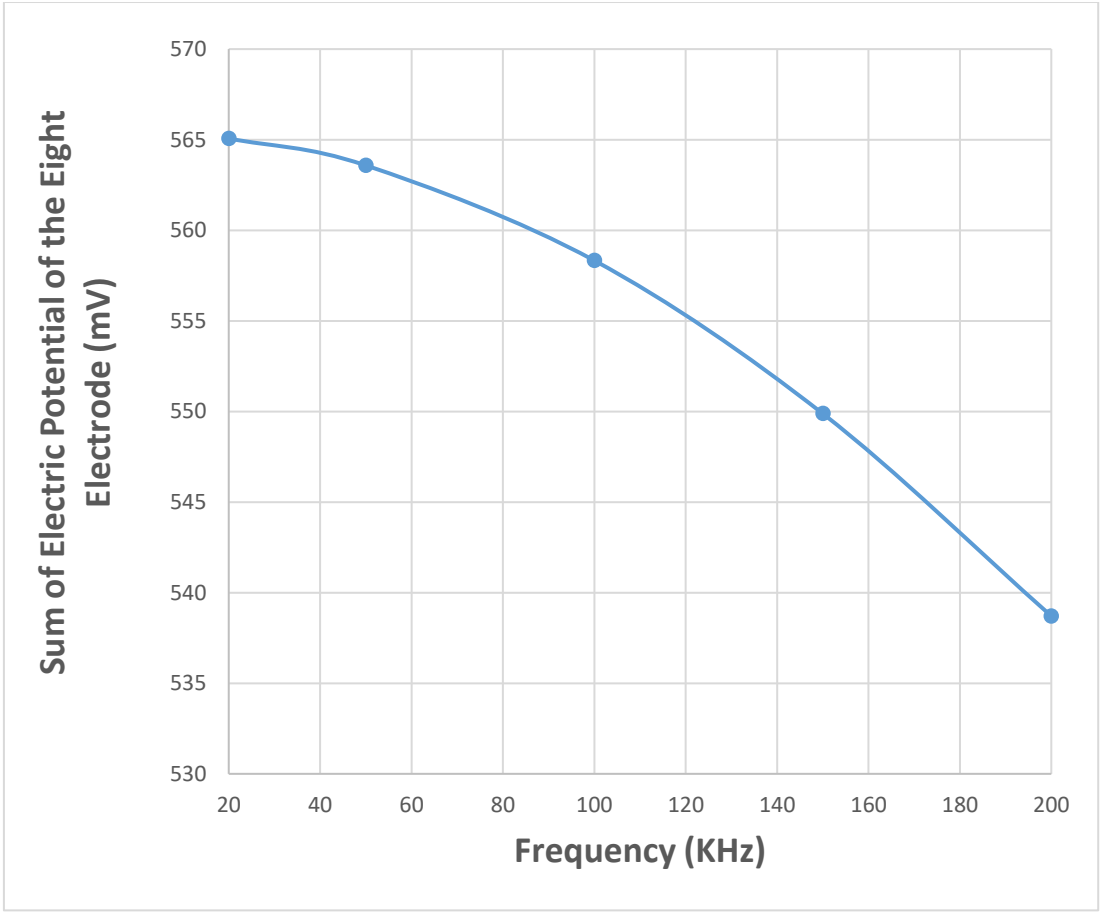

Figure-5.53: Sum of electrical potentials of the eight electrodes (mV) plotted against five different frequencies 20 KHz, 50 KHz, 100 KHz, 150 KHz, and 200 KHz at constant electrical conductivity = 0.3144 Sm^{-1}. [Table Used 5.54]

Computer simulation of the Proposed Anterior-Posterior EIT Protocol computed sum of the eight electrodes electrical potential for different frequencies 20 KHz, 50 KHz, 100 KHz, 150 KHz, and 200 KHz at constant current = 1mA, relative permittivity = 8531.40 for different electrical conductivities 0.2096Sm^{-1}, 0.2358 Sm^{-1}, 0.2620Sm^{-1}, 0.2882 Sm^{-1}, and 0.3144Sm^{-1} are shown in figure-5.54. [Table Used-5.50-5.54]

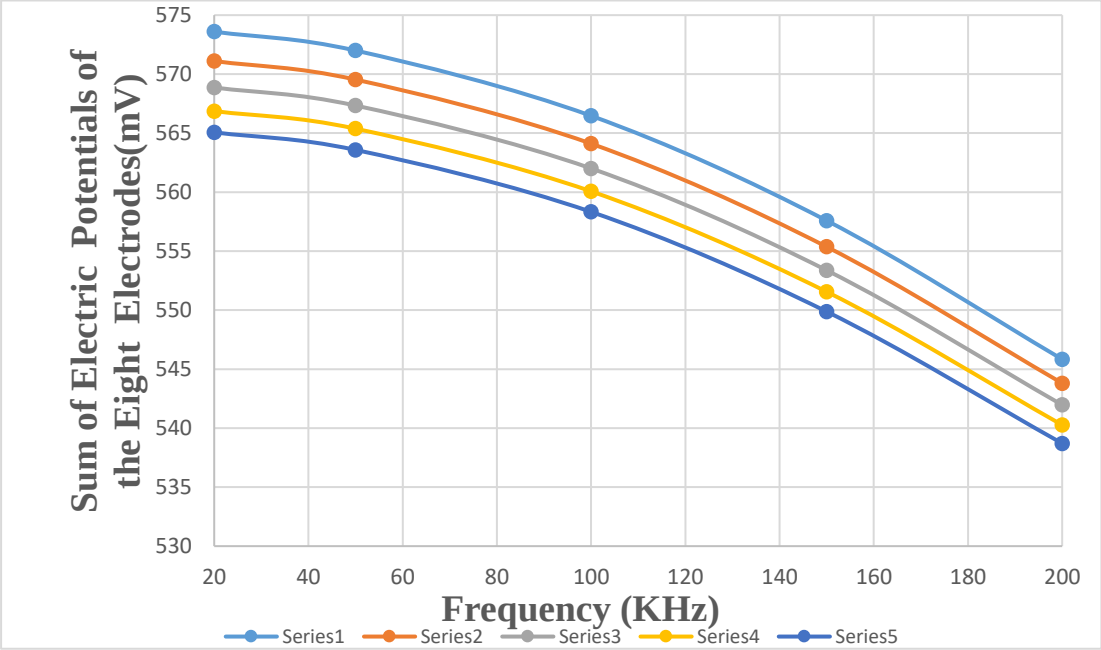

Figure-5.54: Sum of electrical potentials of the eight electrodes (mV) plotted against five different frequencies 20 KHz, 50 KHz, 100 KHz, 150 KHz, and 200 KHz for five electrical conductivity values 0.2096 Sm^{-1}, 0.2358Sm^{-1}, 0.2620Sm^{-1}, 0.2882Sm^{-1}, and 0.3144Sm^{-1}.

Series 1: For Electrical Conductivity 0.2096Sm^{-1}atFrequency Spectrum (20 KHz, 50 KHz, 100 KHz, 150 KHz, and 200 KHz)

Series2: For Electrical Conductivity 0.2358Sm^{-1}atFrequency Spectrum (20 KHz, 50 KHz, 100 KHz, 150 KHz, and 200 KHz)

Series3: For Electrical Conductivity 0.2620Sm^{-1}atFrequency Spectrum (20 KHz, 50 KHz, 100 KHz, 150 KHz, and 200 KHz)

Series4: For constant Electrical Conductivity 0.2882 Sm^{-1} at Frequency Spectrum (20 KHz, 50 KHz, 100 KHz, 150 KHz, and 200 KHz)

Series 5: For constant Electrical Conductivity 0.3144Sm^{-1}at Frequency Spectrum (20 kHz, 50 kHz, 100 kHz, 150 kHz, and 200 kHz)

5.8 Simulation Study Method -8: Electrical Impedance Imaging at Fixed Single Frequency (20 kHz or 50 kHz or 100 kHz or 150 kHz or 200 kHz) for different Electrical Conductivities for APEIT protocol

5.8 (A) At Inspiration Condition

Applying the Proposed Anterior-Posterior EIT Protocol for healthy lung at inspiration condition its electrical conductivity is 0.1030 Sm^{-1}. Also took another four electrical conductivity values of ±10% steps of healthy (normal) lungs at inspiration conditions i.e.0.0824 Sm^{-1}, 0.0927 Sm^{-1}, 0.1133 Sm^{-1}, 0.1236 Sm^{-1} for simulation of single frequency. All cases relative permittivity value was taken 4272.50 and constant alternating current 1mA (assumed to be safe).

Computer simulation of the Proposed Anterior-Posterior EIT Protocol computed electrical potential at each for different electrical conductivities 0.0824Sm^{-1}, 0.0927Sm^{-1}, 0.1030Sm^{-1}, 0.1133Sm^{-1}, and 0.1236 Sm^{-1}at constant current = 1mA, frequency =20 KHz and relative permittivity = 4272.50 are shown in figure-5.55

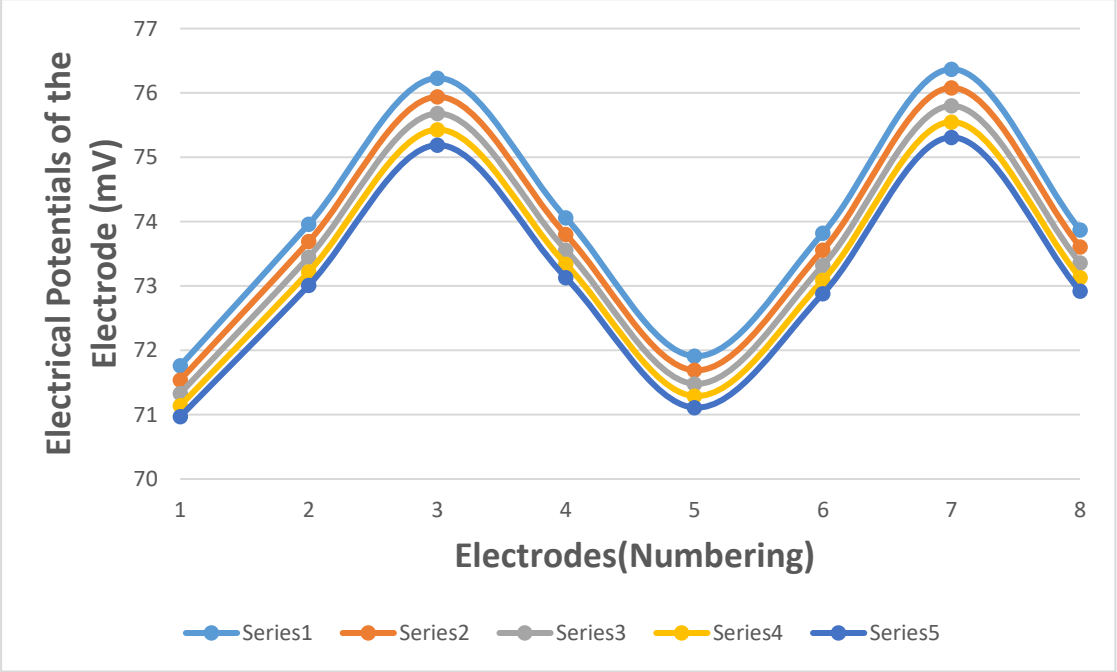

Figure-5.55: Electrical Potentials of the Electrode (mV) plotted against electrodes (numbering) for different electrical conductivities 0.0824Sm^{-1}, 0.0927Sm^{-1}, 0.1030Sm^{-1}, 0.1133Sm^{-1}, and 0.1236 Sm^{-1}at constant frequency 20 KHz. [Table Used-5.35]

Series 1: For electrical conductivity 0.0824 Sm^{-1}, Series 2: For electrical conductivity 0.0927 Sm^{-1}, Series 3: For electrical conductivity 0.1030 Sm^{-1}, Series 4: For electrical conductivity 0.1133 Sm^{-1}, and Series 5: For electrical conductivity: 0.1236 Sm^{-1}.

Computer simulation of the Proposed Anterior-Posterior EIT Protocol computed sum of the eight electrodes electrical potential for different electrical conductivities 0.0824Sm^{-1}, 0.0927 Sm^{-1}, 0.1030 Sm^{-1}, 0.1133 Sm^{-1}, and 0.1236 Sm^{-1} at constant current = 1mA, frequency =20 KHz and relative permittivity = 4272.50 is shown in figure-5.56

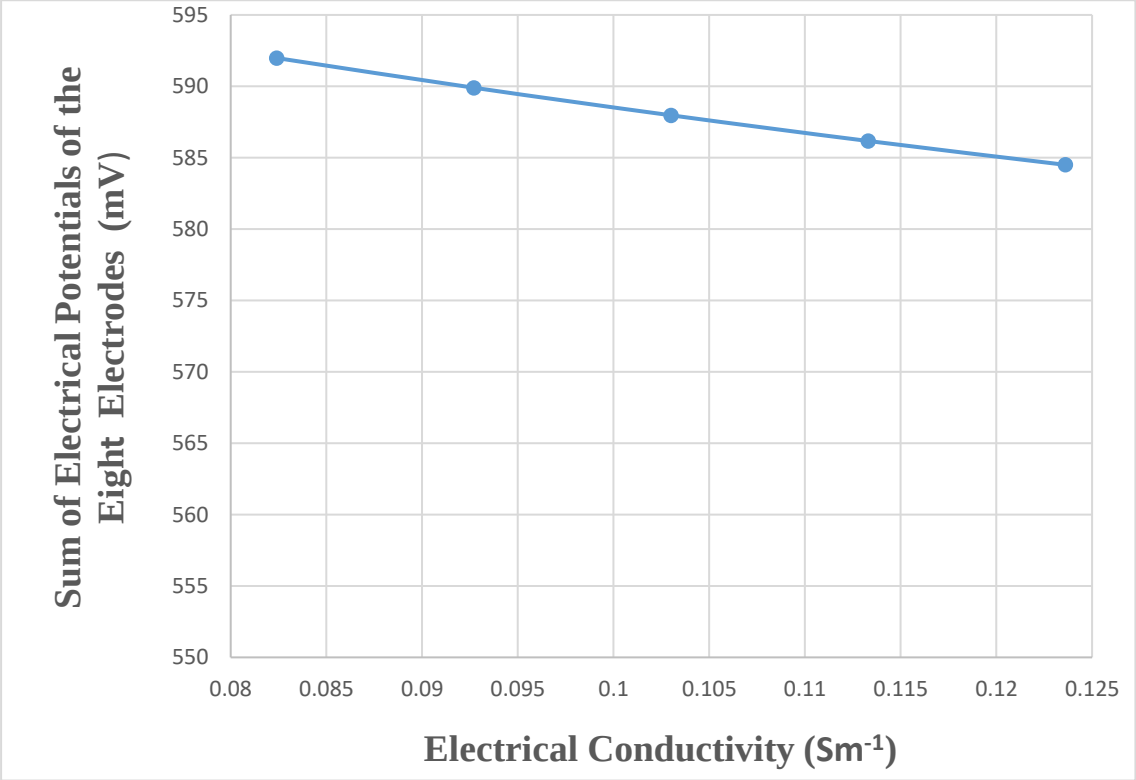

Figure-5.56Sum of electrical potentials of the eight electrodes (mV) plotted against five different electrical conductivity values (i.e., 0.0824 Sm^{-1}, 0.0927 Sm^{-1}, 0.1030 Sm^{-1}, 0.1133 Sm^{-1}, and0.1236 Sm^{-1}) at constant frequency=20 KHz. [Table Used-5.35]

Computer simulation of the Proposed Anterior-Posterior EIT Protocol computed electrical potential at each electrode for different electrical conductivities 0.0824 Sm^{-1}, 0.0927 Sm^{-1}, 0.1030 Sm^{-1}, 0.1133 Sm^{-1}, and 0.1236 Sm^{-1} at constant current = 1mA, frequency =50 KHz and relative permittivity = 4272.50 are shown in figure-5.57

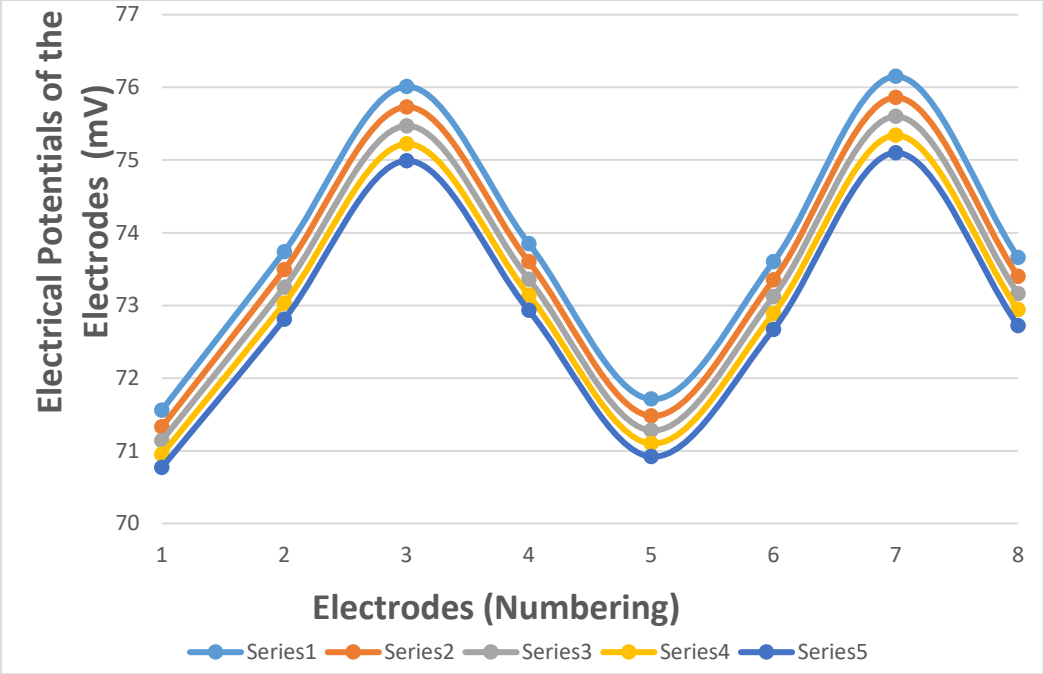

Figure-5.57. Electrical Potentials of the Electrode (mV) plotted against electrodes (numbering) for different electrical conductivities 0.0824Sm^{-1}, 0.0927 Sm^{-1}, 0.1030 Sm^{-1}, 0.1133 Sm^{-1}, and 0.1236 Sm^{-1} at constant frequency 50 KHz. [Table Used-5.36]

Series 1: For electrical conductivity 0.0824 Sm^{-1}, Series 2: For electrical conductivity 0.0927 Sm^{-1}, Series 3: For electrical conductivity 0.1030 Sm^{-1}, Series 4: For electrical conductivity 0.1133 Sm^{-1}, and Series 5: For electrical conductivity: 0.1236 Sm^{-1}.

Computer simulation of the Proposed Anterior-Posterior EIT Protocol computed sum of the eight electrodes electrical potential for different electrical conductivities 0.0824Sm^{-1}, 0.0927 Sm^{-1}, 0.1030 Sm^{-1}, 0.1133 Sm^{-1}, and 0.1236 Sm^{-1} at constant current = 1mA, frequency =50 KHz and relative permittivity = 4272.50 is shown in figure-5.58

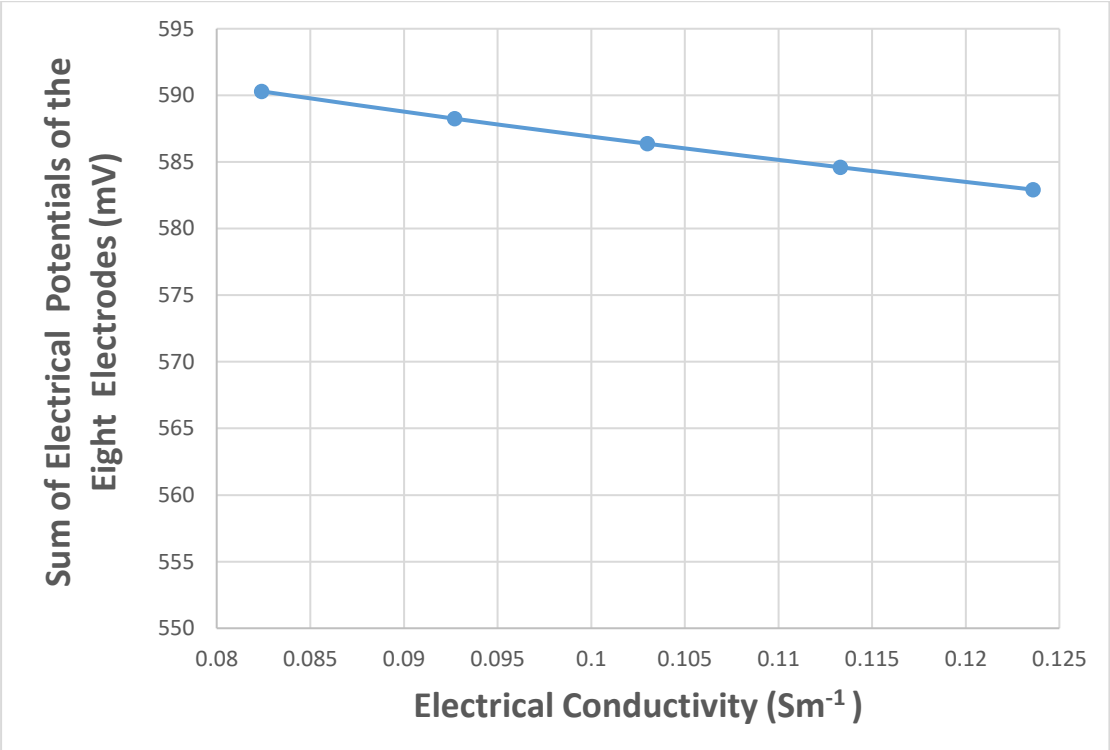

Figure-5.58 Sum of electrical potentials of the eight electrodes (mV) plotted against five different electrical conductivity values (i.e. 0.0824 Sm^{-1}, 0.0927 Sm^{-1}, 0.1030 Sm^{-1}, 0.1133 Sm^{-1}, and0.1236 Sm^{-1}) at constant frequency=50 KHz. [Table Used-5.36]

Computer simulation of the Proposed Anterior-Posterior EIT Protocol computed electrical potential at each electrode for electrical conductivities 0.0824 S/m, 0.0927 Sm^{-1}, 0.1030 Sm^{-1}, 0.1133 Sm^{-1}, and 0.1236 Sm^{-1}at constant current = 1mA, frequency =100 KHz and relative permittivity = 4272.50 are shown in figure-5.59

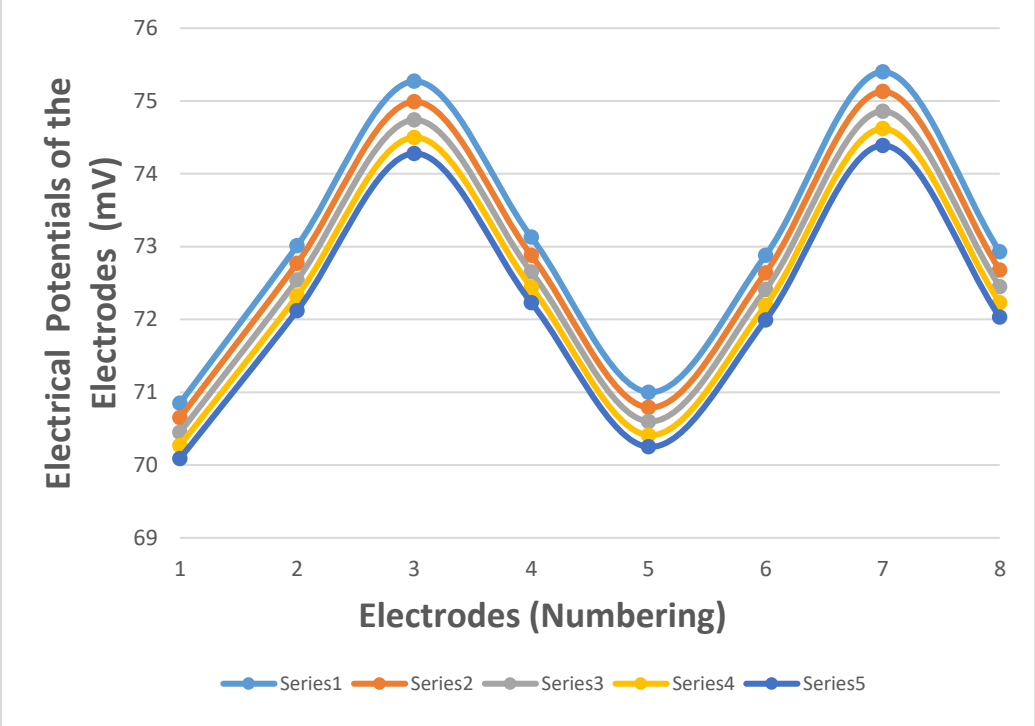

Figure-5.59 Electrical Potentials of the Electrode (mV) plotted against electrodes (numbering) for electrical conductivities 0.0824 Sm^{-1}, 0.0927 Sm^{-1}, 0.1030 Sm^{-1}, 0.1133 Sm^{-1}, and 0.1236 Sm^{-1} at constant frequency 100 KHz. [Table Used-5.37]

Series 1: For electrical conductivity 0.0824 Sm^{-1}, Series 2: For electrical conductivity 0.0927 Sm^{-1}, Series 3: For electrical conductivity 0.1030 Sm^{-1}, Series 4: For electrical conductivity 0.1133 Sm^{-1}, and Series 5: For electrical conductivity: 0.1236 Sm^{-1}.

Computer simulation of the Proposed Anterior-Posterior EIT Protocol computed sum of the eight electrodes electrical potential for electrical conductivities 0.0824 Sm^{-1}, 0.0927 Sm^{-1}, 0.1030 Sm^{-1}, 0.1133 Sm^{-1}, and 0.1236 Sm^{-1} at constant current = 1mA, frequency =100 KHz and relative permittivity = 4272.50 is shown in figure-5.60

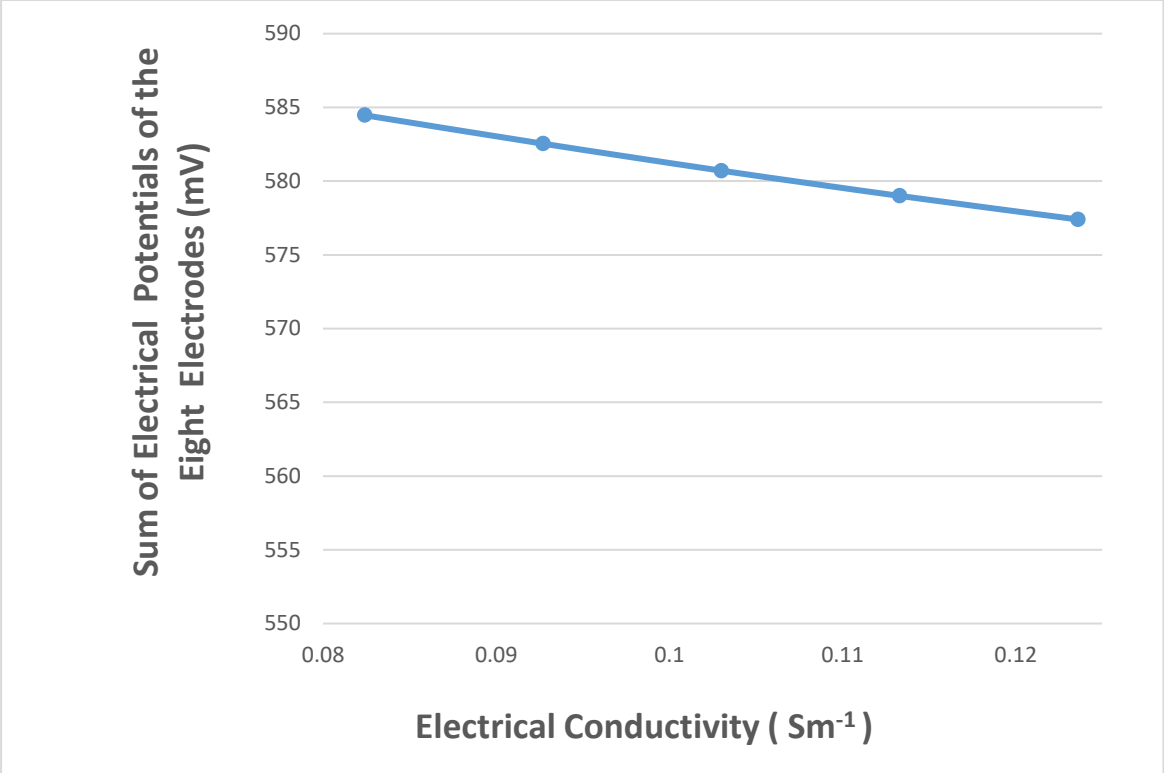

Figure-5.60: Sum of electrical potentials of the eight electrodes (mV) plotted against five different electrical conductivity values (i.e. 0.0824 Sm^{-1}, 0.0927 Sm^{-1}, 0.1030 Sm^{-1}, 0.1133 Sm^{-1}, and0.1236 Sm^{-1}) at constant frequency=100 KHz. [Table Used-5.37]

Computer simulation of the Proposed Anterior-Posterior EIT Protocol computed electrical potential at each electrode for electrical conductivities 0.0824 Sm^{-1}, 0.0927 Sm^{-1}, 0.1030 Sm^{-1}, 0.1133 Sm^{-1}, and 0.1236 Sm^{-1}at constant current = 1mA, frequency =150 KHz and relative permittivity = 4272.50 are shown in figure-5.61.

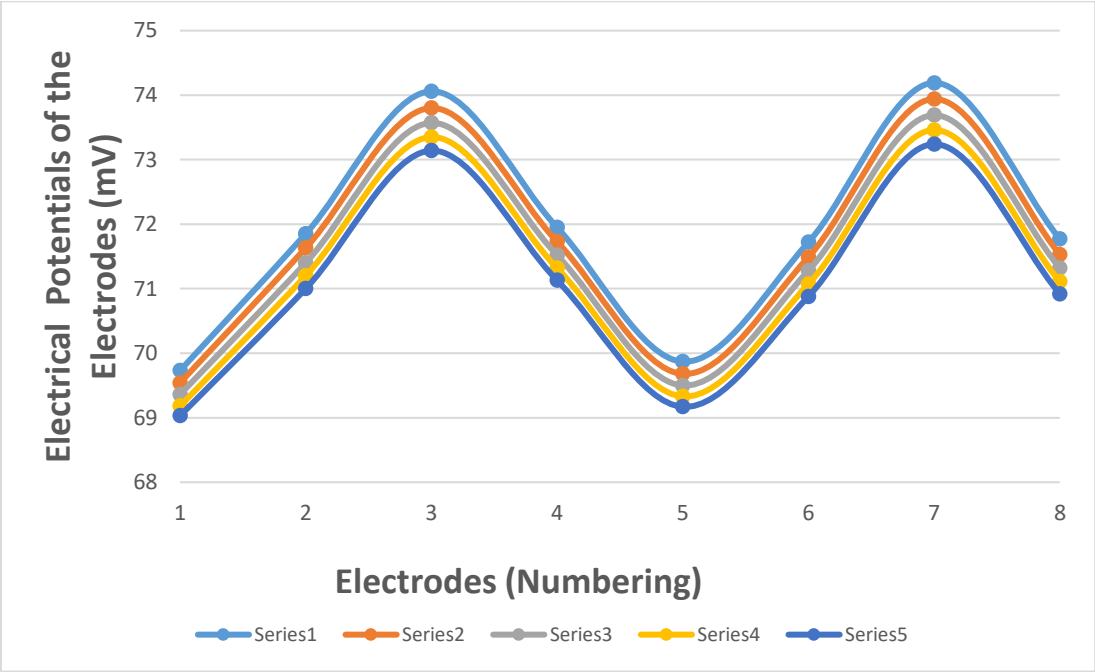

Figure-5.61 Electrical Potentials of the Electrode (mV) plotted against electrodes (numbering) for electrical conductivities 0.0824 Sm^{-1}, 0.0927 Sm^{-1}, 0.1030 Sm^{-1}, 0.1133 Sm^{-1}, and 0.1236 Sm^{-1} at constant frequency 150 KHz. [Table Used-5.38]

Series 1: For electrical conductivity 0.0824 Sm^{-1}, Series 2: For electrical conductivity 0.0927 Sm^{-1}, Series 3: For electrical conductivity 0.1030 Sm^{-1}, Series 4: For electrical conductivity 0.1133 Sm^{-1}, and Series 5: For electrical conductivity: 0.1236 Sm^{-1}.

Computer simulation of the Proposed Anterior-Posterior EIT Protocol computed sum of the eight electrodes electrical potential for electrical conductivities 0.0824 Sm^{-1}, 0.0927 Sm^{-1}, 0.1030 Sm^{-1}, 0.1133 Sm^{-1}, and 0.1236 Sm^{-1} at constant current = 1mA, frequency =150 KHz and relative permittivity = 4272.50 is shown in figure-5.62

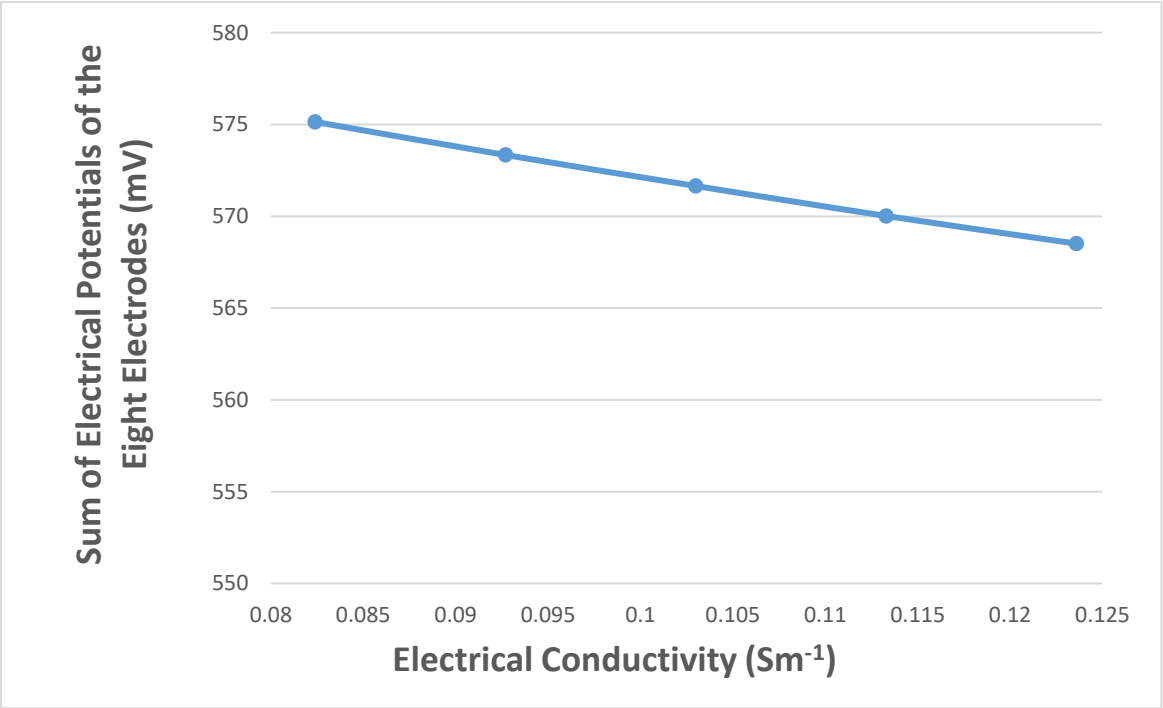

Figure-5.62 Sum of electrical potentials of the eight electrodes (mV) plotted against five different electrical conductivity values (i.e. 0.0824 Sm^{-1}, 0.0927 Sm^{-1}, 0.1030 Sm^{-1}, 0.1133 Sm^{-1}, and0.1236 Sm^{-1}) at constant frequency=150 KHz. [Table Used-5.38]

Computer simulation of the proposed Anterior-Posterior EIT Protocol computed electrical potential at each electrode for electrical conductivities 0.0824 Sm^{-1}, 0.0927 Sm^{-1}, 0.1030 Sm^{-1}, 0.1133 Sm^{-1}, and 0.1236 Sm^{-1} at constant current = 1mA, frequency =200 KHz and relative permittivity = 4272.50 are shown in figure-5.63

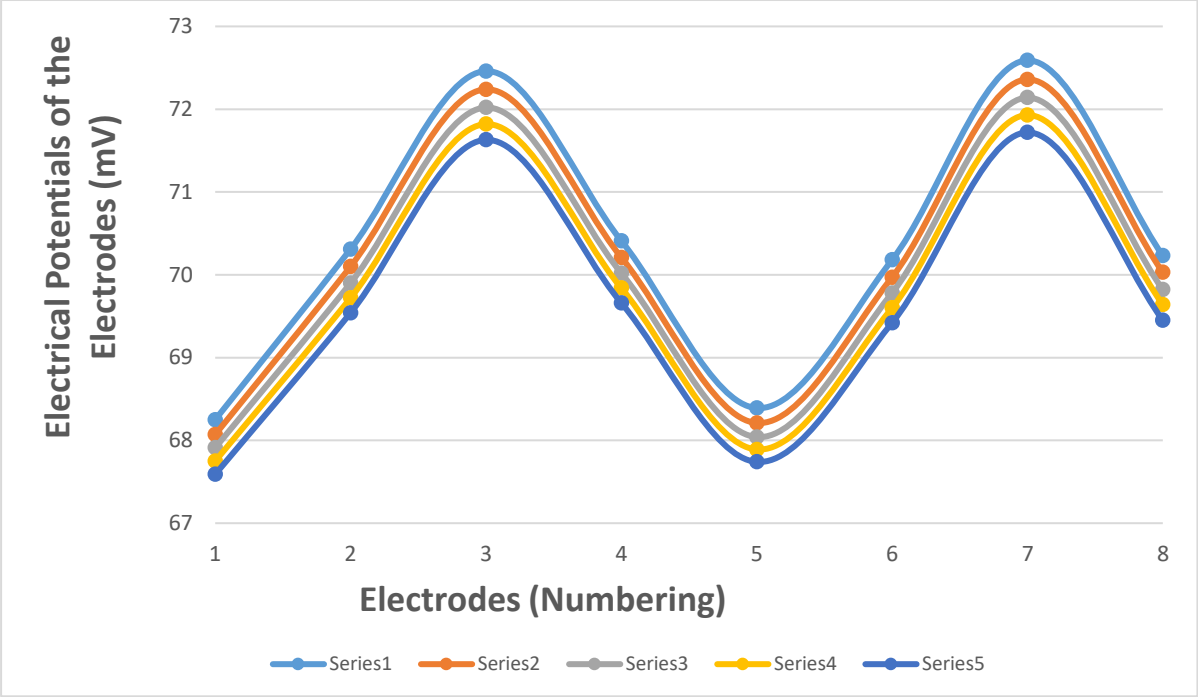

Figure-5.63 Electrical Potentials of the Electrode (mV) plotted against electrodes (numbering) for different electrical conductivities 0.0824 Sm^{-1}, 0.0927 Sm^{-1}, 0.1030 Sm^{-1}, 0.1133 Sm^{-1}, and 0.1236 Sm^{-1} at constant frequency 200 KHz. [Table Used-5.39]

Series 1: For electrical conductivity 0.0824 Sm^{-1}, Series 2: For electrical conductivity 0.0927 Sm^{-1}, Series 3: For electrical conductivity 0.1030 Sm^{-1}, Series 4: For electrical conductivity 0.1133 Sm^{-1}, and Series 5: For electrical conductivity: 0.1236 Sm^{-1}.

Computer simulation of the Proposed Anterior-Posterior EIT Protocol computed sum of the eight electrodes electrical potential for different electrical conductivities 0.0824Sm^{-1}, 0.0927 Sm^{-1}, 0.1030 Sm^{-1}, 0.1133 Sm^{-1}, and 0.1236 Sm^{-1} at constant current = 1mA, frequency =200 KHz and relative permittivity = 4272.50 is shown in figure-5.64.

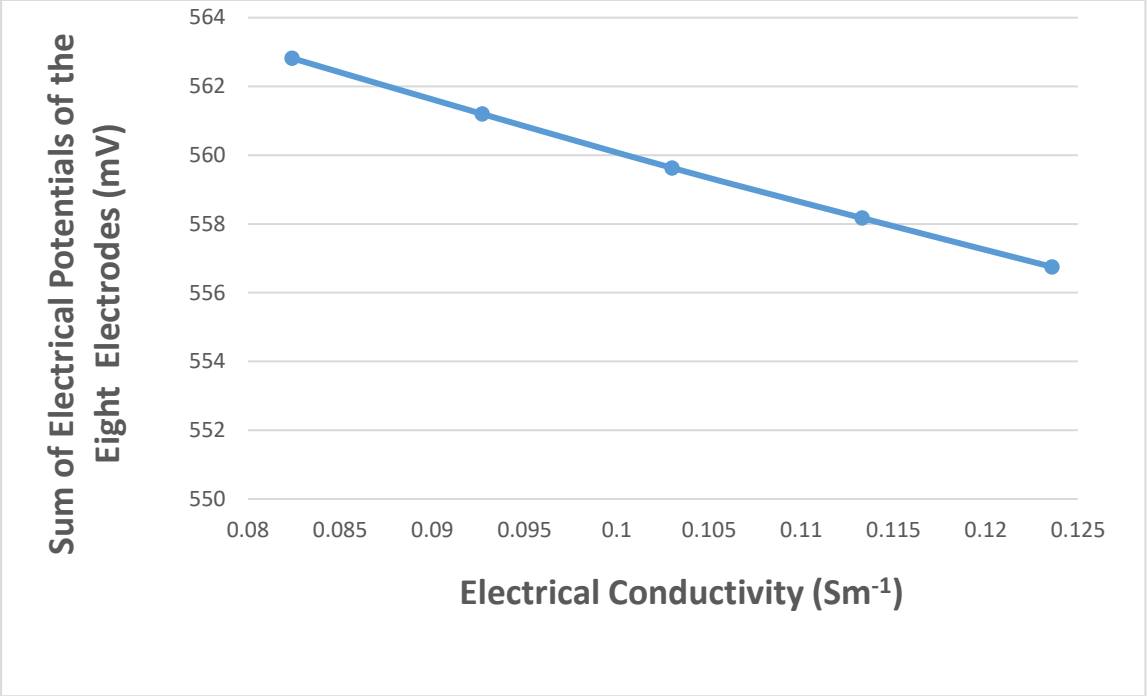

Figure-5.64: Sum of electrical potentials of the eight electrodes (mV) plotted against five different electrical conductivity values (i.e. 0.0824 Sm^{-1}, 0.0927 Sm^{-1}, 0.1030 Sm^{-1}, 0.1133 Sm^{-1}, and0.1236 Sm^{-1}) at constant frequency=200 KHz. [Table Used-5.39]

Computer simulation of Proposed Anterior-Posterior EIT Protocol computed sum of the eight electrodes electrical potential for different electrical conductivities 0.0824 Sm^{-1}, 0.0927 Sm^{-1}, 0.1030 Sm^{-1}, 0.1133 Sm^{-1}, and 0.1236 Sm^{-1} at constant current = 1mA, relative permittivity = 4272.50 for different frequencies 20 KHz,50 KHz. 100 KHz, 150 KHz, and 200 KHz are shown in figure-5.65 [Table Used-5.35-5.39]

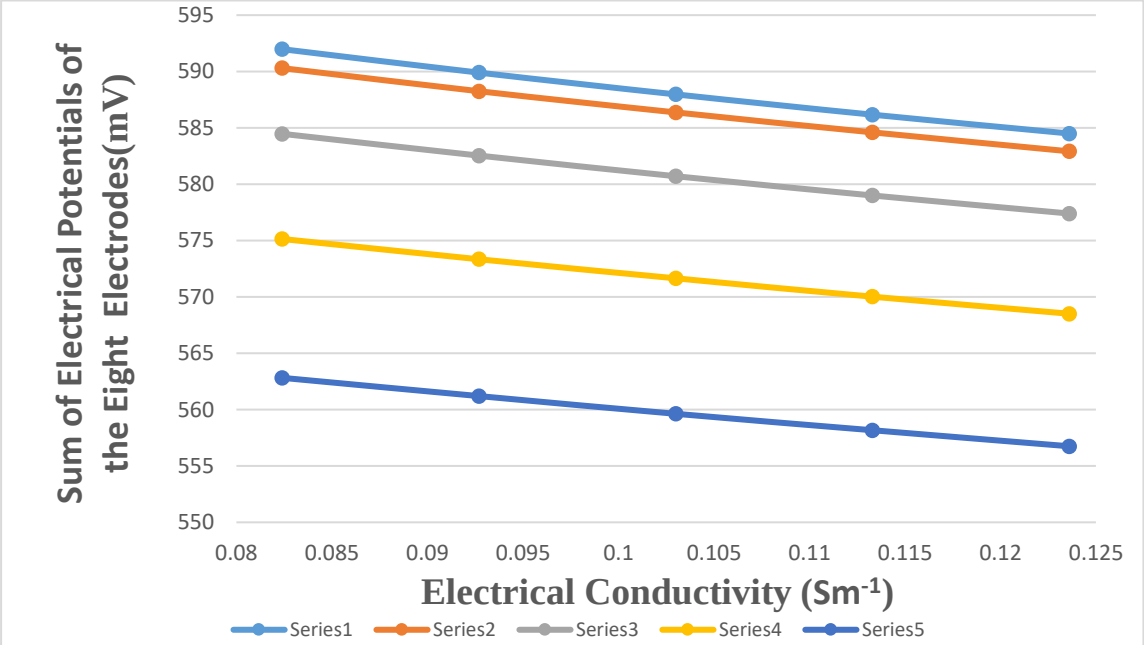

Figure-5.65Sum of electrical potentials of the eight electrodes (mV) plotted against five different electrical conductivity values (i.e. 0.0824 Sm^{-1}, 0.0927 Sm^{-1}, 0.1030 Sm^{-1}, 0.1133 Sm^{-1}, and0.1236 Sm^{-1}) for different frequencies 20 KHz, 50 KHz, 100 KHz, 150 KHz, and 200 KHz.

Series 1: For frequency 20 KHz at different electrical conductivities (0.0824 Sm^{-1}, 0.0927 Sm^{-1}, 0.1030 Sm^{-1}, 0.1133 Sm^{-1}, and 0.1236 Sm^{-1})

Series 2: For frequency 50 KHz at different electrical conductivities (0.0824 Sm^{-1}, 0.0927 Sm^{-1}, 0.1030 Sm^{-1}, 0.1133 Sm^{-1}, and 0.1236 Sm^{-1})

Series 3: For frequency 100 KHz at different electrical conductivities (0.0824 Sm^{-1}, 0.0927 Sm^{-1}, 0.1030 Sm^{-1}, 0.1133 Sm^{-1}, and 0.1236 Sm^{-1})

Series 4: For frequency 150 KHz at different electrical conductivities (0.0824 Sm^{-1}, 0.0927 Sm^{-1}, 0.1030 Sm^{-1}, 0.1133 Sm^{-1}, and 0.1236 Sm^{-1})

Series 5: For frequency 200 KHz at different electrical conductivities (0.0824 Sm^{-1}, 0.0927 Sm^{-1}, 0.1030 Sm^{-1}, 0.1133 Sm^{-1}, and 0.1236 Sm^{-1})

5.8(B): At Expiration Condition

Applying the Proposed Anterior -Posterior EIT Protocol for healthy (normal) lungs at expiration condition its electrical conductivity is 0.2620 Sm^{-1}. Also took another four electrical conductivity values of ±10% steps of healthy lungs at expiration conditions i.e.0.2096 Sm^{-1}, 0.2358 Sm^{-1}, 0.2882 Sm^{-1}, 0. 3144 Sm^{-1} for simulation. All cases relative permittivity value was taken 8531.40 and constant alternating current 1mA (assumed to be safe).

Computer simulation of Proposed Anterior-Posterior EIT Protocol computed electrical potential at each electrode for different electrical conductivities 0.2096 Sm^{-1}, 0.2358 Sm^{-1}, 0.2620 Sm^{-1}, 0.2882 Sm^{-1}, and 0.3144 Sm^{-1} at constant current = 1mA, frequency =20 KHz and relative permittivity = 8531.40 are shown in figure-5.66.

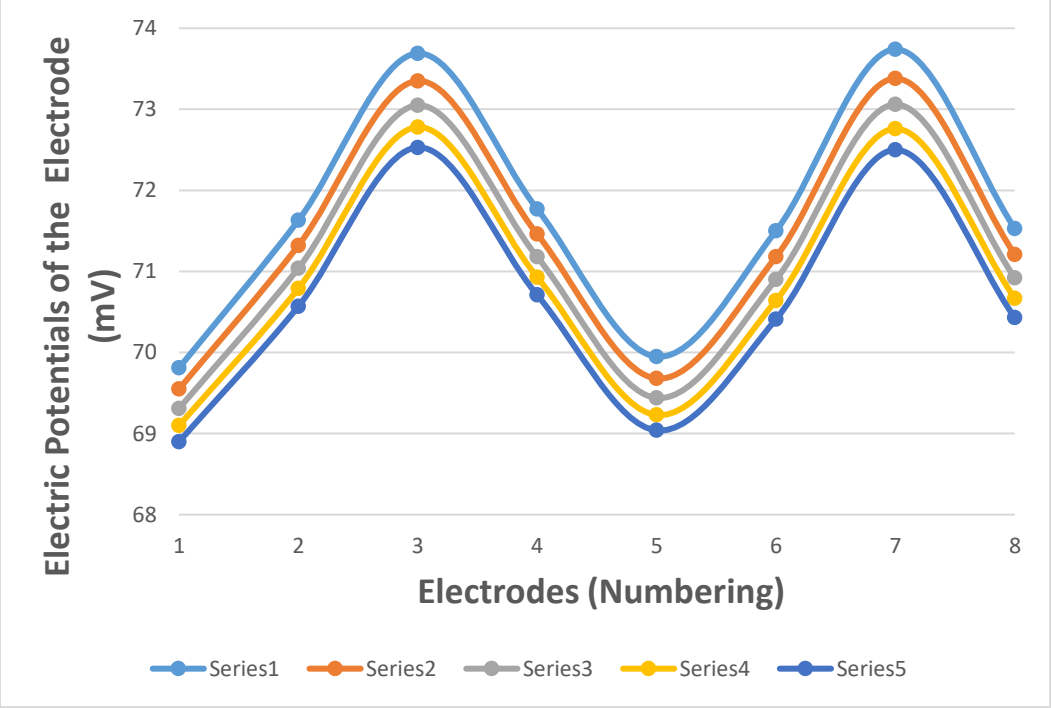

Figure-5.66 Electrical Potentials of the Electrode (mV) plotted against electrodes (numbering) for different electrical conductivities 0.2096 Sm^{-1}, 0.2358 Sm^{-1}, 0.2620 Sm^{-1}, 0.2882 Sm^{-1}, and 0.3144 Sm^{-1} at constant frequency 20 KHz. [Table Used 5.40]

Series 1: For electrical conductivity 0.2096 Sm^{-1}, Series 2: For electrical conductivity 0.2358 Sm^{-1}, Series 3: For electrical conductivity 0.2620 Sm^{-1}, Series 4: For electrical conductivity 0. 0.2882Sm^{-1}, and Series 5: For electrical conductivity:0.3144 Sm^{-1}.

Computer simulation of the Proposed Anterior-Posterior EIT Protocol computed sum of the eight electrodes electrical potential for different electrical conductivities 0.2096 Sm^{-1}, 0.2358 Sm^{-1}, 0.2620 Sm^{-1}, 0.2882 Sm^{-1}, and 0.3144 Sm^{-1} at constant current = 1mA, frequency =20 KHz and relative permittivity = 8531.40 is shown in figure-5.67

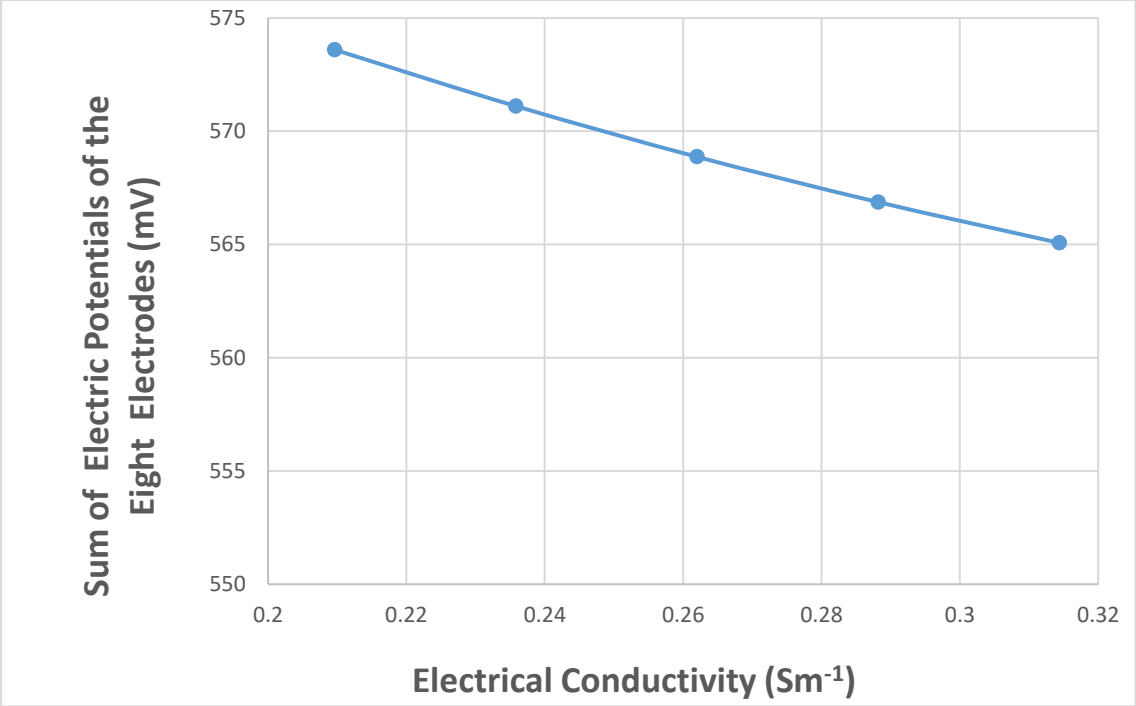

Figure-5.67: Sum of electrical potentials of the eight electrodes (mV) plotted against five different electrical conductivity values (i.e. 0.2096 Sm^{-1}, 0.2358 Sm^{-1}, 0.2620 Sm^{-1}, 0.2882 Sm^{-1}, and 0.3144 Sm^{-1}) at constant frequency=20 KHz. [Table Used 5.40]

Computer simulation of the Proposed Anterior-Posterior EIT Protocol computed electrical potential at each electrode for different electrical conductivities 0.2096 Sm^{-1}, 0.2358 Sm^{-1},0.2620 Sm^{-1}, 0.2882 Sm^{-1}, and 0.3144Sm^{-1} at constant current = 1mA, frequency =50 KHz and relative permittivity = 8531.40 are shown in figure-5.68.

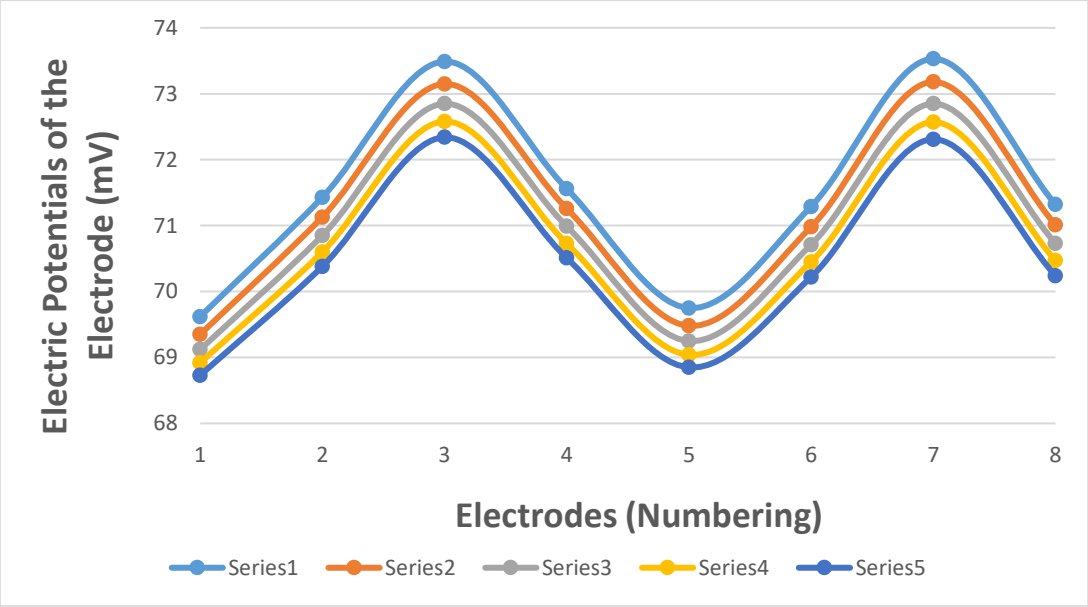

Figure-5.68 Electrical Potentials of the Surface Electrode (mV) plotted against electrodes (numbering) for different electrical conductivities 0.2096 Sm^{-1}, 0.2358Sm^{-1}, 0.2620 Sm^{-1}, 0.2882Sm^{-1}, and 0.3144 Sm^{-1} at constant frequency 50 KHz. [Table Used 5.41]

Series 1: For electrical conductivity 0.2096 Sm^{-1}, Series 2: For electrical conductivity 0.2358Sm^{-1}, Series 3: For electrical conductivity 0.2620 Sm^{-1}, Series 4: For electrical conductivity 0. 0.2882Sm^{-1}, and Series 5: For electrical conductivity:0.3144 Sm^{-1}.

Computer simulation of the Proposed Anterior-Posterior EIT Protocol computed sum of the eight electrodes electrical potential for different electrical conductivities 0.2096Sm^{-1}, 0.2358 Sm^{-1}, 0.2620 Sm^{-1}, 0.2882 Sm^{-1}, and 0.3144 Sm^{-1} at constant current = 1mA, frequency =50 KHz and relative permittivity = 8531.40 is shown in figure-5.69.

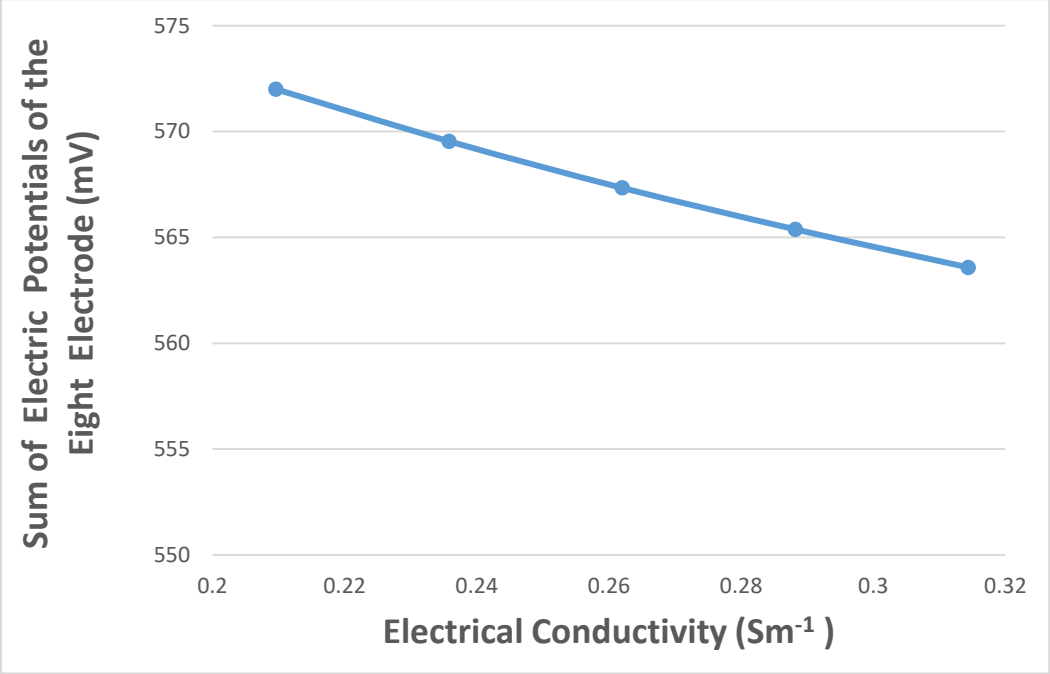

Figure-5.69: Sum of electrical potentials of the eight electrodes (mV) plotted against five different electrical conductivity values (i.e. 0.2096 Sm^{-1}, 0.2358 Sm^{-1}, 0.2620 Sm^{-1}, 0.2882 Sm^{-1}, and 0.3144 $Sm^{-1)}$ at constant frequency=50 kHz. [Table Used 5.41]

Computer simulation of the Proposed Anterior-Posterior EIT Protocol computed electrical potential at each electrode for different electrical conductivities 0.2096Sm^{-1}, 0.2358 Sm^{-1},0.2620 Sm^{-1}, 0.2882 Sm^{-1}, and 0.3144 Sm^{-1} at constant current = 1mA, frequency =50 KHz and relative permittivity = 8531.40 are shown in figure-5.70

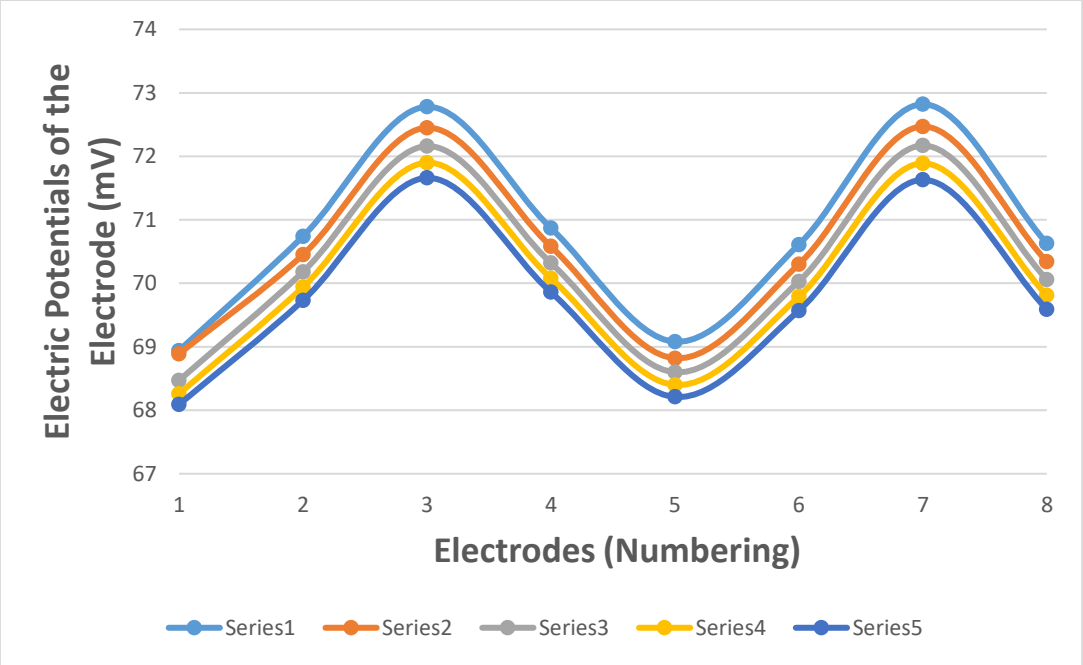

Figure-5.70: Electrical Potentials of the Electrode (mV) plotted against electrodes (numbering) for different electrical conductivities 0.2096 Sm^{-1}, 0.2358 Sm^{-1}, 0.2620Sm^{-1}, 0.2882 Sm^{-1}, and 0.3144 Sm^{-1} at constant frequency 100 KHz. [Table Used 5.42]

Series 1: For electrical conductivity 0.2096 Sm^{-1}, Series 2: For electrical conductivity 0.2358 Sm^{-1}, Series 3: For electrical conductivity 0.2620Sm^{-1}, Series 4: For electrical conductivity 0. 0.2882Sm^{-1}, and Series 5: For electrical conductivity:0.3144 Sm^{-1}.

Computer simulation of the Proposed Anterior-Posterior EIT Protocol computed sum of the eight electrodes electrical potential for different electrical conductivities 0.2096Sm^{-1}, 0.2358 Sm^{-1}, 0.2620 Sm^{-1}, 0.2882 Sm^{-1}, and 0.3144 Sm^{-1} at constant current = 1mA, frequency =100 KHz and relative permittivity = 8531.40 is shown in figure-5.71.

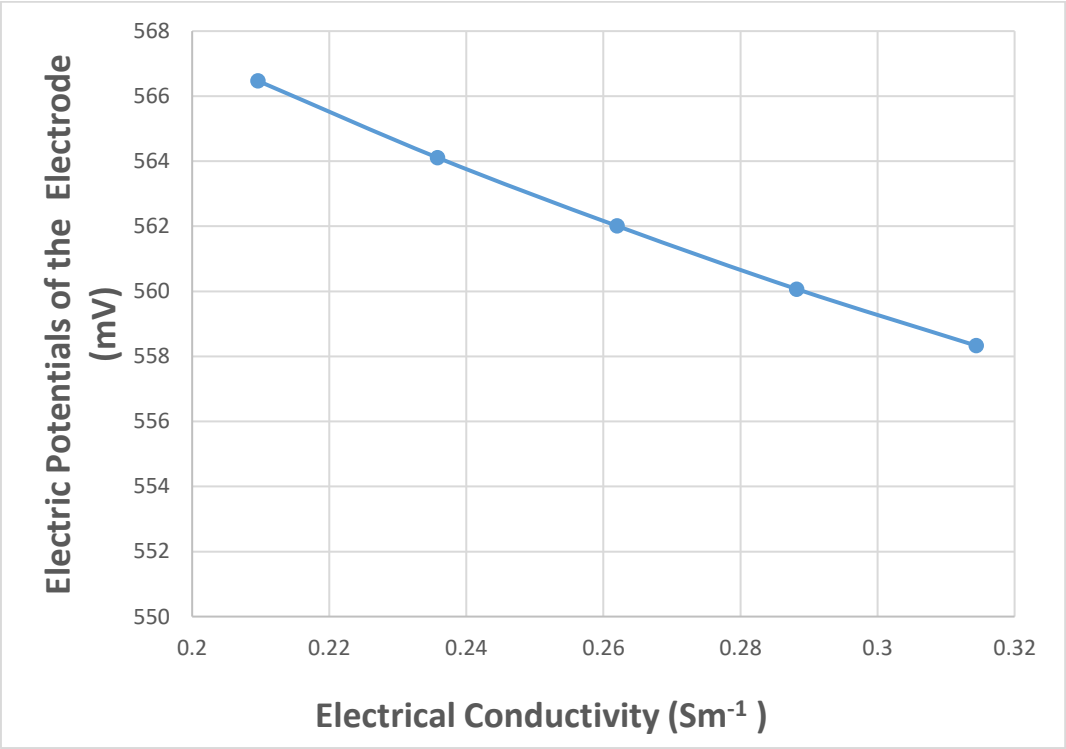

Figure-5.71: Sum of electrical potentials of the eight electrodes (mV) plotted against five different electrical conductivity values (i.e. 0.2096 Sm^{-1}, 0.2358 Sm^{-1}, 0.2620 Sm^{-1}, 0.2882 Sm^{-1}, and 0.3144 Sm^{-1}) at constant frequency=100 KHz. [Table Used 5.42]

Computer simulation of the Proposed Anterior-Posterior EIT Protocol computed electrical potential at each electrode for different electrical conductivities 0.2096 Sm^{-1}, 0.2358 Sm^{-1},0.2620 Sm^{-1}, 0.2882 Sm^{-1}, and 0.3144 Sm^{-1} at constant current = 1mA, frequency =150 KHz and relative permittivity = 8531.40 are shown in figure-5.72.

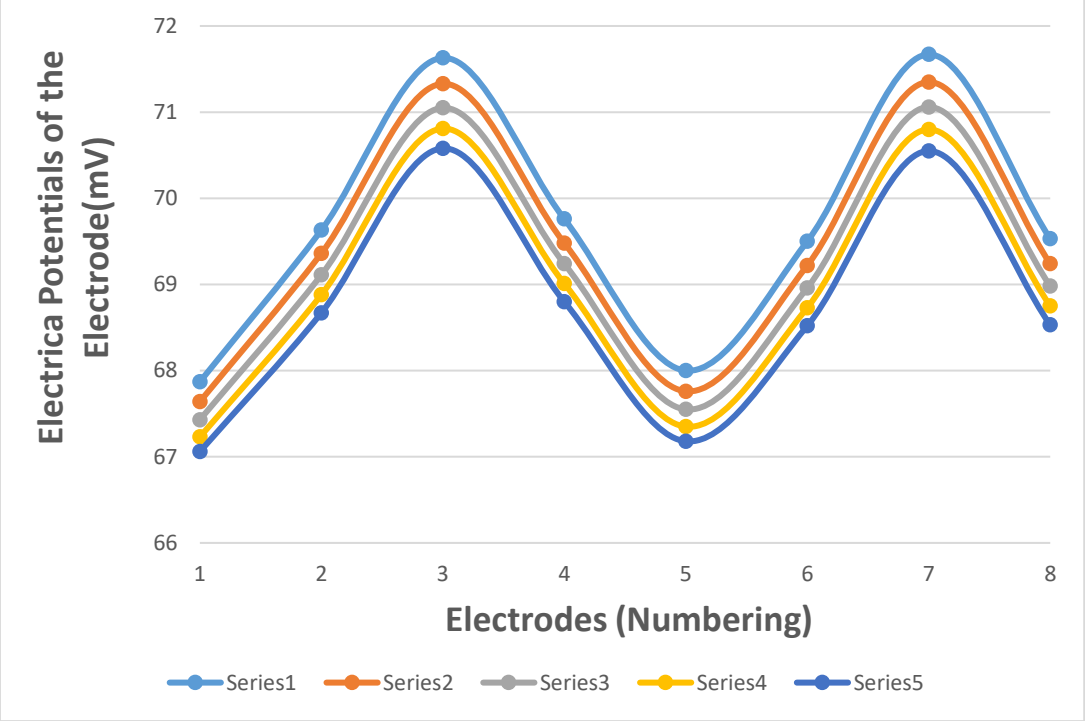

Figure-5.72: Electrical Potentials of the Electrode (mV) plotted against electrodes (numbering) for different electrical conductivities 0.2096 Sm^{-1}, 0.2358 Sm^{-1}, 0.2620 Sm^{-1}, 0.2882 Sm^{-1}, and 0.3144 Sm^{-1}at constant frequency 150 KHz. [Table Used 5.43]

Series 1: For electrical conductivity 0.2096 Sm^{-1}, Series 2: For electrical conductivity Sm^{-1}, Series 3: For electrical conductivity 0.2620 Sm^{-1}, Series 4: For electrical conductivity 0. 0.2882Sm^{-1}, and Series 5: For electrical conductivity:0.3144 Sm^{-1}.

Computer simulation of the Proposed Anterior-Posterior EIT Protocol computed sum of the eight electrodes electrical potential for different electrical conductivities 0.2096 Sm^{-1}, 0.2358 Sm^{-1}, 0.2620 Sm^{-1}, 0.2882 Sm^{-1}, and 0.3144 Sm^{-1} at constant current = 1mA, frequency =150 KHz and relative permittivity = 8531.40 is shown in figure-5.73.

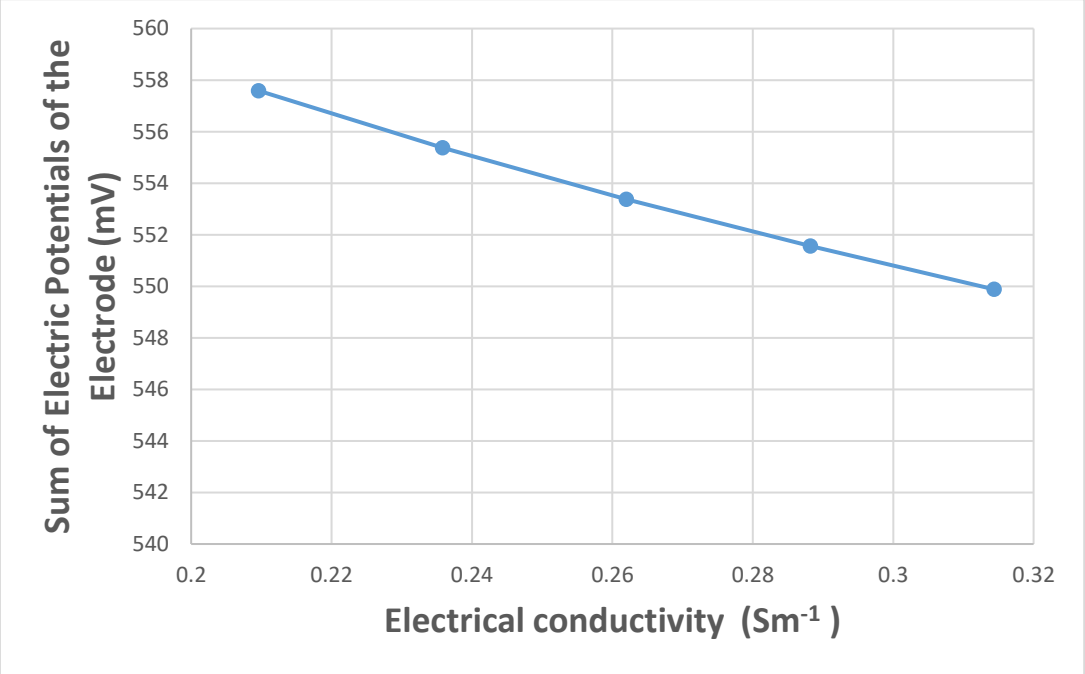

Figure-5.73: Sum of electrical potentials of the eight electrodes (mV) plotted against five different electrical conductivity values (i.e., 0.2096Sm^{-1}, 0.2358 Sm^{-1}, 0.2620 Sm^{-1}, 0.2882 Sm^{-1}, and 0.3144 Sm^{-1}) at constant frequency=150 KHz. [Table Used 5.43]

Computer simulation of the Proposed Anterior-Posterior EIT Protocol computed electrical potential at each electrode for different electrical conductivities 0.2096Sm^{-1}, 0.2358 Sm^{-1},0.2620 Sm^{-1}, 0.2882Sm^{-1}, and 0.3144 Sm^{-1} at constant current = 1mA, frequency =200 KHz and relative permittivity = 8531.40 are shown in figure-5.74.

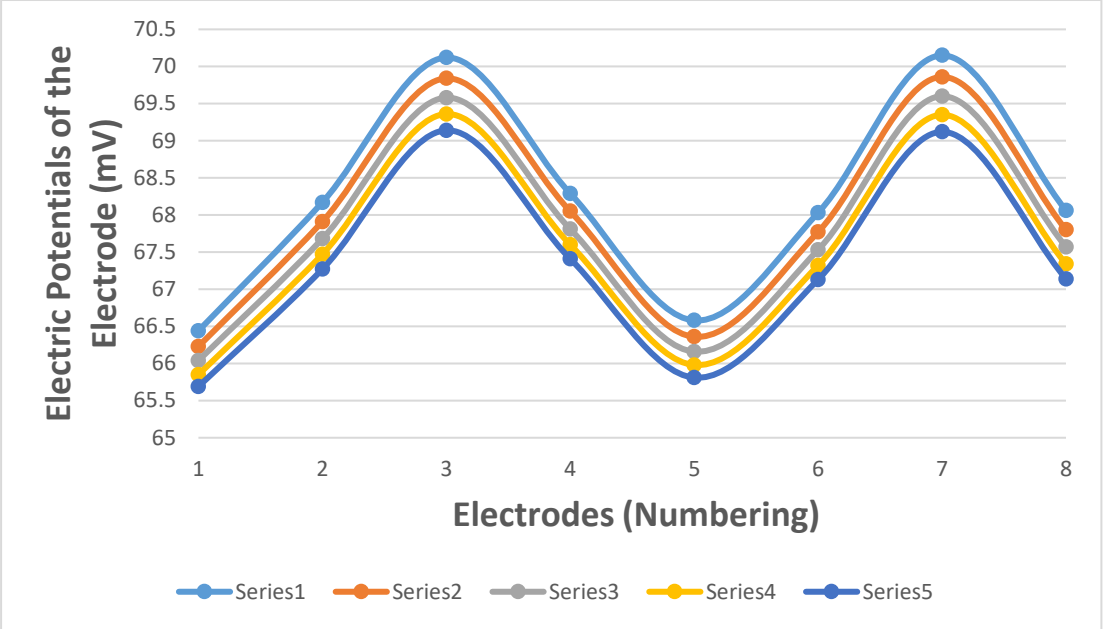

Figure-5.74: Electrical Potentials of the Electrode (mV) plotted against electrodes (numbering) for different electrical conductivities 0.2096Sm^{-1}, 0.2358 Sm^{-1}, 0.2620 Sm^{-1}, 0.2882 Sm^{-1}, and 0.3144Sm^{-1} at constant frequency 200 KHz. [Table Used 6.44]

Series 1: For electrical conductivity 0.2096 Sm^{-1}, Series 2: For electrical conductivity 0.2358 Sm^{-1}, Series 3: For electrical conductivity 0.2620Sm^{-1}, Series 4: For electrical conductivity 0. 0.2882Sm^{-1}, and Series 5: For electrical conductivity:0.3144 Sm^{-1}.

Computer simulation of the Proposed Anterior-Posterior EIT Protocol computed sum of the eight electrodes electrical potential for different electrical conductivities 0.2096Sm^{-1}, 0.2358 Sm^{-1}, 0.2620 Sm^{-1}, 0.2882Sm^{-1}, and 0.3144 Sm^{-1}at constant current = 1mA, frequency =200 KHz and relative permittivity = 8531.40 is shown in figure-5.75.

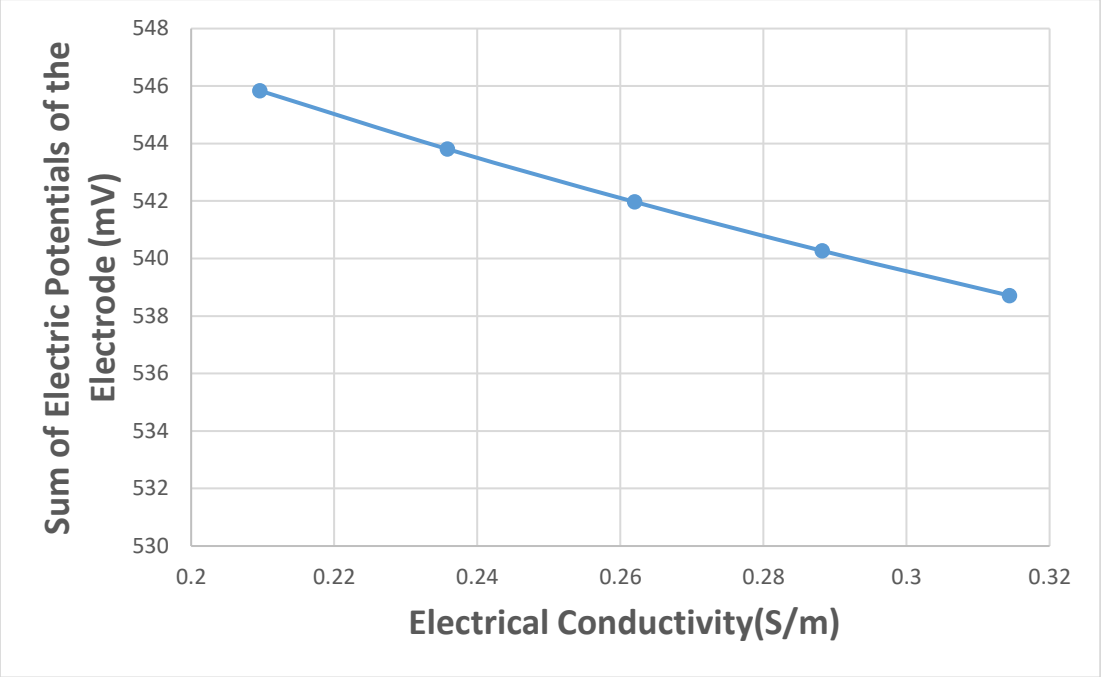

Figure-5.75 Sum of electrical potentials of the eight electrodes (mV) plotted against five different electrical conductivity values (i.e., 0.2096Sm^{-1}, 0.2358Sm^{-1}, 0.2620Sm^{-1}, 0.2882 Sm^{-1}, and 0.3144 Sm^{-1}) at constant frequency=200 KHz. [Table Used 5.44]

Computer simulation of the Proposed Anterior-Posterior EIT Protocol computed sum of the eight electrodes electrical potential for different electrical conductivities 0.2096Sm^{-1}, 0.2358 Sm^{-1}, 0.2620 Sm^{-1}, 0.2882 Sm^{-1}, and 0.3144Sm^{-1} at constant current = 1mA, relative permittivity = 8531.40 for different frequencies 20 kHz,50 KHz. 100 KHz, 150 KHz, and 200 KHz are shown in figure-5.76. [Table Used 5.40-5.44]

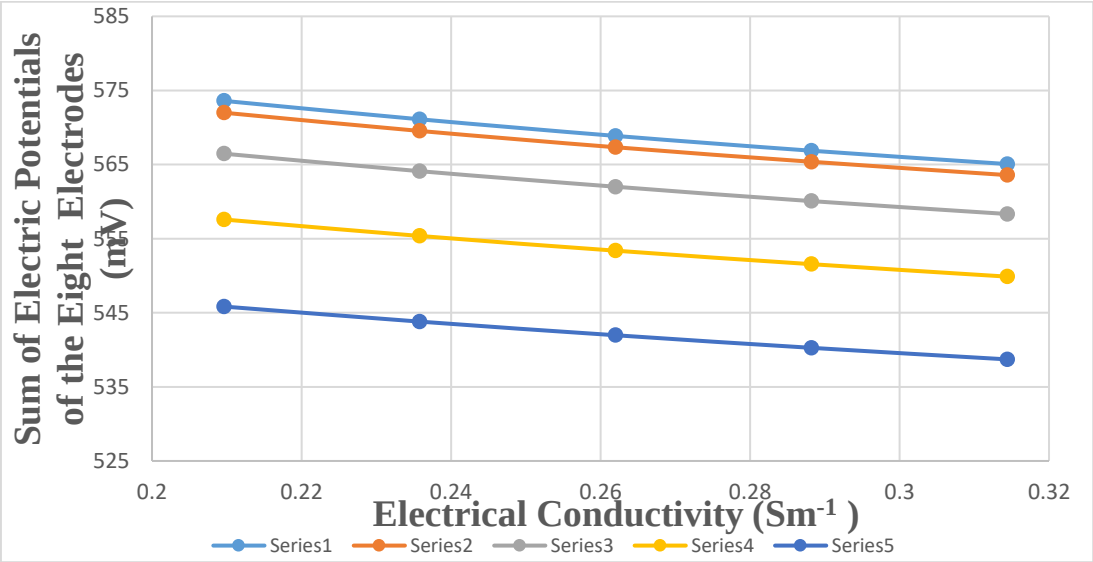

Figure-5.76 Sum of electrical potentials of the eight electrodes (mV) plotted against five different electrical conductivity values (i.e. 0.2096 Sm^{-1}, 0.2358 Sm^{-1}, 0.2620 Sm^{-1}, 0.2882 Sm^{-1}, and 0.3144 Sm^{-1}) for different frequencies 20 KHz, 50 KHz, 100 KHz, 150 KHz, and 200 KHz.

Series 1: For frequency 20 KHz at different electrical conductivities (0.2096 Sm^{-1}, 0.2358 Sm^{-1}, 0.2620 Sm^{-1}, 0.2882 Sm^{-1}, and 0.3144Sm^{-1})

Series 2: For frequency 50 KHz at different electrical conductivities (0.2096 Sm^{-1}, 0.2358 Sm^{-1}, 0.2620 Sm^{-1}, 0.2882 Sm^{-1}, and 0.3144Sm^{-1})

Series 3: For frequency 100 KHz at different electrical conductivities (0.2096 Sm^{-1}, 0.2358 Sm^{-1}, 0.2620 Sm^{-1}, 0.2882 Sm^{-1}, and 0.3144Sm^{-1})

Series 4: For frequency 150 KHz at different electrical conductivities (0.2096 Sm^{-1}, 0.2358 Sm^{-1}, 0.2620 Sm^{-1}, 0.2882 Sm^{-1}, and 0.3144Sm^{-1})

Series 5: For frequency 200 KHz at different electrical conductivities (0.2096 Sm^{-1}, 0.2358 Sm^{-1}, 0.2620 Sm^{-1}, 0.2882 Sm^{-1}, and 0.3144Sm^{-1})

5.9 Human Thorax Phantom Study using Maltron Bio Scan 920-11 Analyzer

Maltron- BioScan 920-11is an indispensable measuring instrument in the field of Medical Science. Maltron Instruments use scientific method of measuring Bioelectrical Impedance. Its technique is Bioelectrical Impedance analyzer and it has multi-frequency (5 KHz, 50 KHz, 100 KHz, and 200KHz) and Impedance Range 2 Ohms to 1200 Ohms. A total of four or eight electrodes are used (tetra polar). It can operate in one channel (4 electrodes) or 2 channel (8 electrodes) mode. A low-level battery current is passed through the body and the absolute measurement of impedance, phase, resistance, reactance and capacitance are measured. Bio Scan 920-11 offers a totally non-invasive method of assessing patients in many clinical settings, providing quick analysis of over 45 different parameters [102].

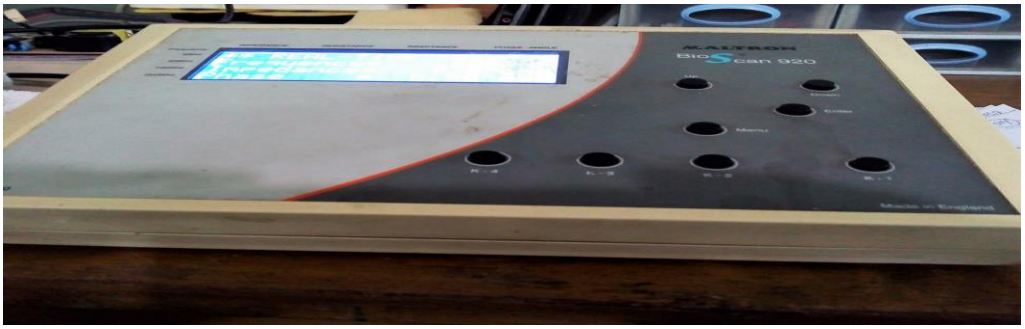

The advance circuitry and processing power of the BioScan 920-11 allows it to measure Extracellular (ECF) and Intracellular Fluid (ICF) volume without the need of complex clinical techniques like radioisotope dilution. In addition to estimating the standard parameters this advanced system is the world is first to provide estimation of mineral content. All data is recorded and displayed immediately for analysis by the system. Results can be viewed on the large graphic LCD display [www.maltronint.com][102]

Human Thorax Phantom has designed following the dimensions of Multipurpose Digital Chest Phantom

[Ref. https://www.ncbi.nlm.nih.gov/pmc/articles/PMC4169876]

Figure5.77: Prepared Human Thorax Phantom.

Maltron BioScan 920-11 system (Ref. www.maltronint.com) is used for measurement of impedance or electric potential following the same protocol as simulation studies. Maltron uses single channel four electrodes, where two electrodes are used for current injecting (driving) and another two electrodes are used for electric potential measurement. Maltron BioScan 929-11 uses a small alternating current 1mA and frequency of 50 kHz for injection of current into the object. The different conductive material and ellipsoid shape with porous foam lung (2.5cm × 9cm× 22 cm) was inserted at 8cm (fixed) away from the frontal of chest surface in the phantom of the different concentrations solution. Saline water of different concentrations of NaCl (%) were used in phantom to simulate the different conductive tissues of lungs.

Maltron Bio-Scan System

Electrical Conductivity measurement for different NaCl (%) solution is essential for this experiment. So, Extech Waterproof p^H / Conductivity/TDS (Total Dissolved Solids)/Salinity/Temperature Meter, Model ExStik EC500 is used here. With the EC 500's dynamic cell-constant technology it is possible to measure a wide range of Conductivity, TDS, and Salinity with same electrode [83]. 0.90% gm NaCl / Liter pure water is a normal concentration whose electrical conductivity is 1.52 S/m. Another 0.54 %, 0.72%, 1.08%,1.26% gm NaCl / Liter pure water concentration have taken for ±20%, ±40% on the basis of normal concentrations. Measured all electrical conductivities values are tabulated in the table-5.76.

Figure-5.78: pH/Conductivity/TDS (Total Dissolved Solids)/Salinity/Temperature Meter.

The relationship between the electrical conductivity (Sm^{-1}) for the concentrations of NaCl (%) in Phantom solution is shown in the figure-5.57.

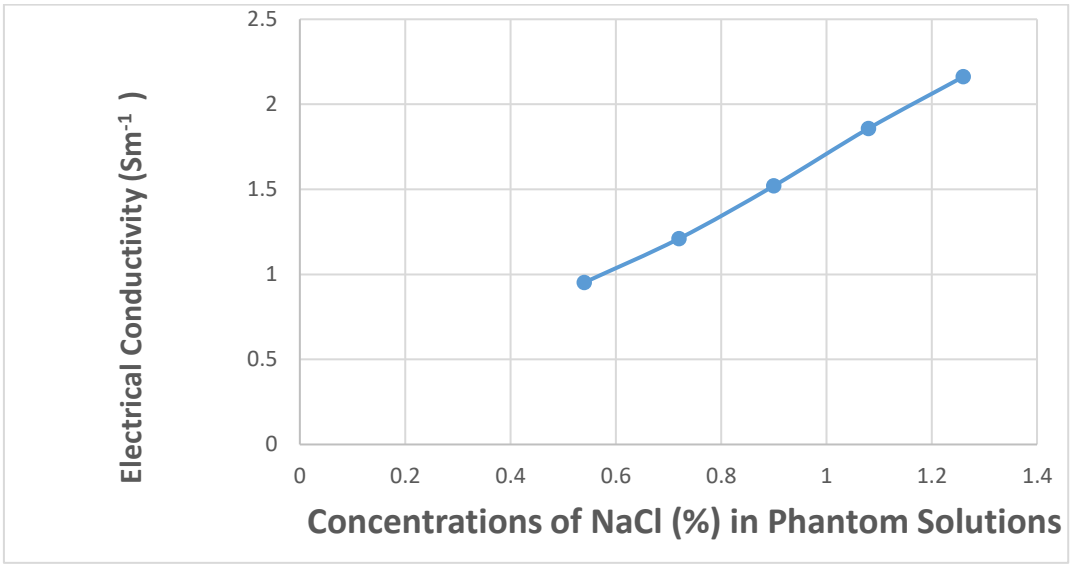

Figure- 5.57: Electrical Conductivity ((Sm^{-1}) plotted against different concentrations of NaCl (%) in Phantom solution. [Table Used 5.76]

Applying the Proposed Anterior-Posterior EIT Protocol in the prepared human thorax Phantom and measuring electrical potential at each electrode by using Maltron BioScan 920-11 system for different electrical conductivities 0.952Sm^{-1}, 1.210Sm^{-1}, 1.520Sm^{-1}, 1.858Sm^{-1}, and 2.162Sm^{-1} at constant current = 1mA, frequency =50KHz and relative permittivity = 15 are shown in figure-5.79

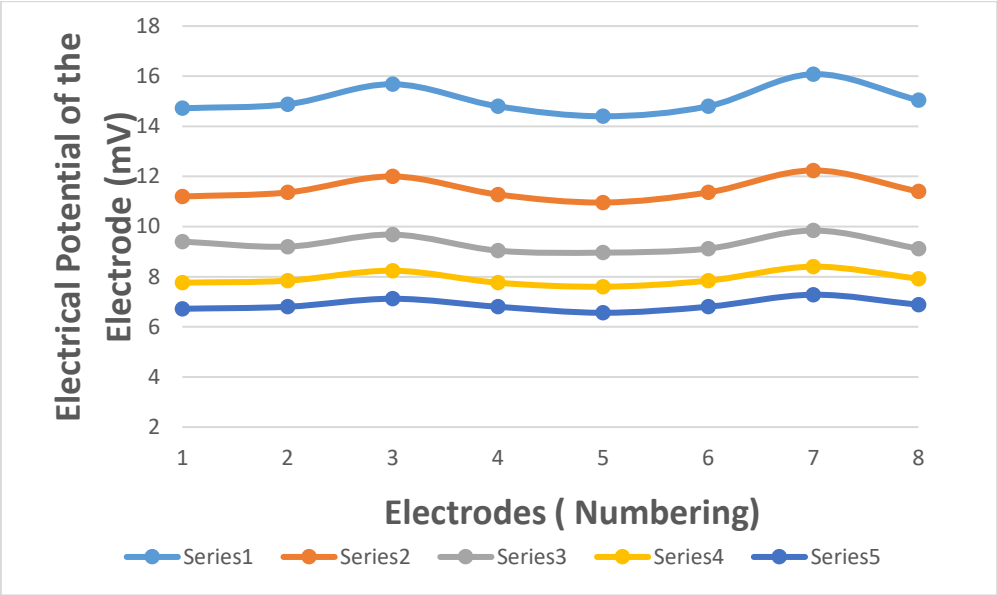

Figure- 5.79: Electrical Potentials of the Electrodes (mV) plotted against Electrodes (Numbering) for different electrical conductivities 0.952 Sm^{-1}, 1.210 Sm^{-1}, 1.520Sm^{-1}, 1.858 Sm^{-1}, and 2.162Sm^{-1}at frequency 50 KHz. [Table Used 5.77]

Series 1: For Electrical Conductivity 0.952Sm^{-1}, Series 2: For Electrical Conductivity 1.210Sm^{-1}, Series 3: For Electrical Conductivity 1.520Sm^{-1}, Series 4: For Electrical Conductivity 1.858Sm^{-1}, and Series 5: For Electrical Conductivity 2.162Sm^{-1}.

Applying the Proposed Anterior-Posterior EIT Protocol in the prepared human thorax Phantom and measuring and adding electrical potential of the eight electrodes by using Maltron BioScan 920-11 system for different NaCl (%) concentrations 0.54, 0.72, 0.90,1.08, and 1.26 at constant current = 1mA, frequency =50 KHz and relative permittivity = 15 is shown in figure-5.80

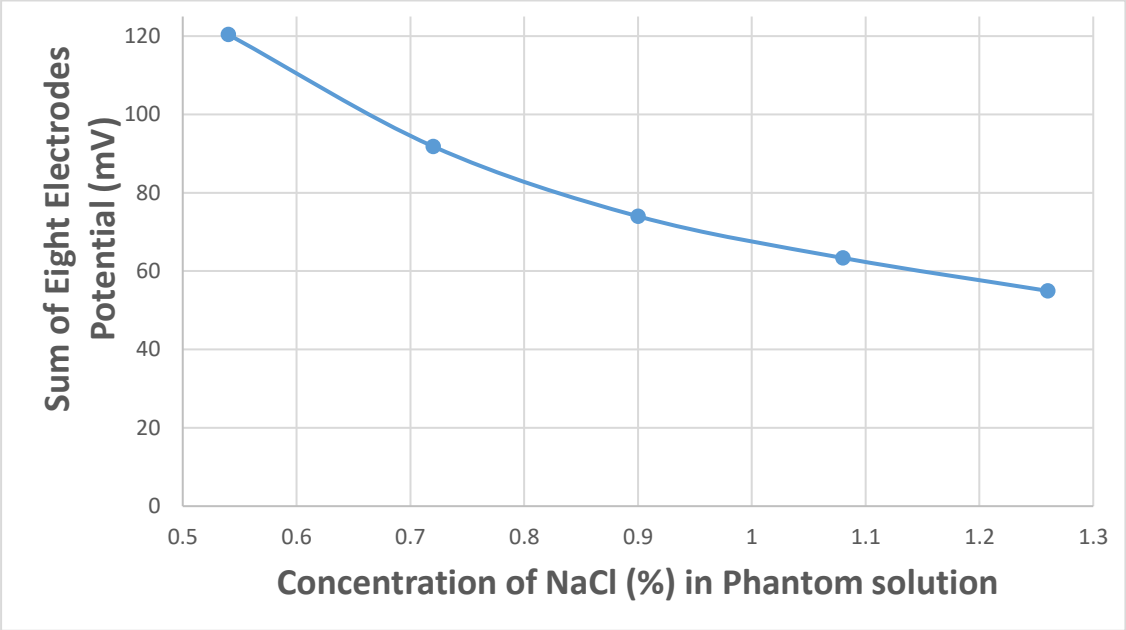

Figure-5.80: Sum of Eight Surface Electrodes Potential (mV) plotted against different concentrations of NaCl (%) in Phantom solution at frequency 50 KHz. [Table Used 5.78]

Applying the Proposed Anterior-Posterior EIT Protocol in the prepared human thorax Phantom and measuring electrical potential of the eight electrodes by using Maltron BioScan 920-11 system for different electrical conductivities 0.952Sm^{-1}, 1.210 Sm^{-1}, 1.520 Sm^{-1}, 1.858Sm^{-1}, and 2.162 Sm^{-1} at constant current = 1mA, frequency =50 KHz and relative permittivity = 15 is shown in figure-5.81.

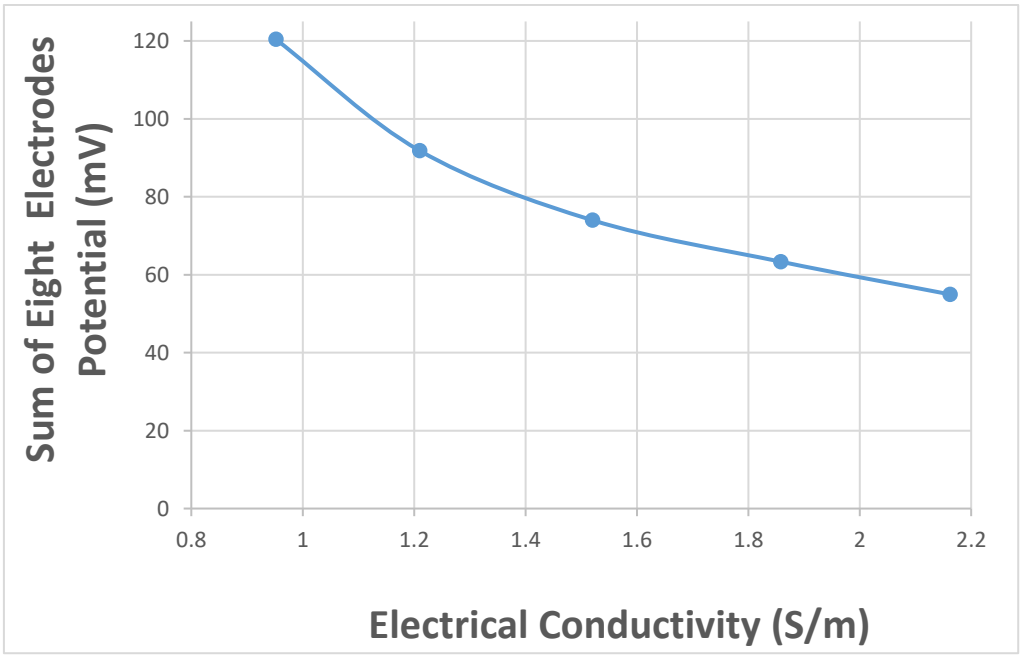

Figure-5.81: Sum of Eight Electrodes Electrical Potential (mV) plotted against five different electrical conductivities 0.952Sm^{-1}, 1.210Sm^{-1}, 1.520Sm^{-1}, 1.858Sm^{-1}, and 2.162Sm^{-1}at frequency 50 KHz [Table Used 5.78]

CHAPTER-6

DISCUSSION AND CONCLUSION

(164-172)

Chapter-6: Discussion and Conclusion

The biological tissues and organs have different electrical conductivities, relative permittivity and capacitive properties. These values do change due to structural and physiological changes of human tissues and organs. Therefore, electrical impedance measurement can be used for human disease diagnosis and monitoring purposes. This PhD research conducted computer simulation and phantom studies on different lung conditions such as- healthy lung at inspiration and expiration, Pneumothorax, Pulmonary Edema, different sizes of tumors, electrical impedance imaging spectroscopy.

The objectives of this PhD research to see the sensitivity of the existing four protocols and the proposed APEIT protocol for healthy lung, pneumothorax and pulmonary edema at inspiration and expiration. To see the detection ability/sensitivity of tumors in the lungs as a distinguish factor using the proposed APEIT protocol. To see the effectiveness of the proposed APEIT protocol for electrical spectroscopy imaging (20 kHz up to 200 kHz) for lung functions and diseases monitoring. Design and construct a human thorax for phantom study to see the sensitivity of the proposed APEIT protocol, using Maltron Bio-Scan 920-11 system.

There are four Existing Electrical Impedance Technique (EIT) Protocols namely-**(P-1)** adjacent current drive, **(P-2)** opposite current drive at the vertices of the semi-major axis of the chest cross section**, (P-3)** opposite current drive at the vertices of the semi-minor axis of the chest cross section**, (P-4)** opposite current drive along the right lung. In these existing EIT protocols the current drive electrodes and voltage sensing electrodes are placed on the chest cross section at horizontal plane. The proposed impedance measurement protocol for lung function is **Anterior- Posterior Electrical Impedance Technique (APEIT)**, where two current drive electrodes are placed at the anterior and posterior side of lungs and other eight voltage sensing electrodes at equal spacing in ellipsoid shape at vertical plane at the posterior side following the lung shape and size. In computer simulation studies 1mA current at 50 KHz was used as a single frequency for sections 5.3,5.4 & 5.6. To see the sensitivity of above five electrical impedance imaging protocols. The computer simulation was conducted by using COMSOL Multiphysics software for assessing lung functions at two conditions, lung at inspiration (electrical conductivity= $0.1030 Sm^{-1}$& relative permittivity =

4272.50) and expiration (electrical conductivity= 0. [1]2620Sm^{-1} & relative permittivity = 8531.40) for healthy lung, the lungs with Pneumothorax and Pulmonary Edema have electrical conductivity and relative permittivity 0.60 Sm^{-1} and 1000, 1.5 Sm^{-1} and 98.56 respectively. **[Section 5.3 & 5.4]**

Simulation Study-1: Healthy Lung at inspiration and at Expiration

In the computer simulation study, we have computed the Relative Electric Potential Change (REPC) values for eight voltage sensing electrodes to see the sensitivity between inspiration and expiration of healthy lungs for all protocols. The average REPC values were 1.41%, 1.84%, 1.34%, 2.29%, and **3.24%** for adjacent current drive EIT protocol, opposite current drive at the vertices of the semi-major axis of the chest cross section EIT protocol, opposite current drive at the vertices of the semi-minor axis of the chest cross section EIT protocol, opposite current drive along the right lung EIT protocol, and Anterior- Posterior Electrical Impedance Technique (APEIT) protocol respectively. The highest average REPC value for the APEIT protocol clearly indicates that this protocol is most sensitive among all existing protocols for electrical impedance measurement of lung functions. It is also been seen that the sensitivity of eight voltage sensing electrodes is more smoothly distributed than all other EIT protocols. In both counts our proposed APEIT protocol is the best amongst all the protocols for electrical impedance measurement and imaging for lung functions and lung diseases.

Then we computed REPC values for all above five EIT protocols using same current & same frequency for the following lung conditions-(a) lung at inspiration and pneumothorax (collapsed lung) (b) lung at expiration and pneumothorax (collapsed lung) (c) lung at inspiration and pulmonary edema (d) lung at expiration and pulmonary edema. **[Section 5.3 & 5.4]**

Simulation Study-2: Lung at inspiration and pneumothorax (collapsed lung)

We computed and found the average REPC value 2.97% for adjacent current drive EIT protocol, 3.89% for opposite current drive at the vertices of the semi-major axis of the chest cross section EIT protocol, 2.41% for opposite current drive at the vertices of the semi-minor axis of the chest cross section EIT protocol**,**4.26% for

opposite current drive along the right lung EIT protocol and **5.97%** for our proposed APEIT protocol.

Simulation Study-3: Lung at expiration and pneumothorax (collapsed lung)

We computed and found the average REPC value 1.59 % for adjacent current drive EIT protocol, 2.10 % for opposite current drive at the vertices of the semi-major axis of the chest cross section EIT protocol, 1.09 % for opposite current drive at the vertices of the semi-minor axis of the chest cross section EIT protocol**,**2.02% for opposite current drive along the right lung EIT protocol and **2.82 %** for our proposed APEIT protocol.

Simulation Study -4: Lung at inspiration and pulmonary edema

We computed and found the average REPC value 4.50 % for adjacent current drive EIT protocol, 5.99 % for opposite current drive at the vertices of the semi-major axis of the chest cross section EIT protocol, 3.21 % for opposite current drive at the vertices of the semi-minor axis of the chest cross section EIT protocol**,**5.80 % for opposite current drive along the right lung EIT protocol and **8.07 %** for our proposed APEIT protocol.

Simulation Study-5: Lung at expiration and pulmonary edema

We computed and found the average REPC value 3.15 % for adjacent current drive EIT protocol, 4.24 % for opposite current drive at the vertices of the semi-major axis of the chest cross section EIT protocol, 1.90 % for opposite current drive at the vertices of the semi-minor axis of the chest cross section EIT protocol**,**3.59 % for opposite current drive along the right lung EIT protocol and **4.99 %** for our proposed APEIT protocol.

We also computed distinguishing factors for APEIT protocol for (a) tumor of different sizes (5%, 10%, and 20% of lung volume) at the center of the right lung at inspiration and (b) tumor of different sizes at the center of the right lung at expiration. Electrical conductivity and relative permittivity values for tumor are taken 1.50 S/m and 98.56 respectively. **[Section 5.6]**

Simulation Study-6: Distinguishing factors for APEIT protocol for tumor of different sizes (5%,10%, and 20% of lung volume) at the center of the right lung at inspiration.

Computer simulation have conducted for APEIT protocol for 5%,10%, and 20% of lung volume sizes tumors at inspiration and found the average REPC values were 0.73%,1.55%, and 3.88% respectively. Also, the corresponding distinguishing factors were 4.18%,8.57% and 20.79 % respectively.

Simulation Study-7: Distinguishing factors for APEIT protocol for tumor of different sizes (5%,10%, and 20% of lung volume) at the center of the right lung at expiration

Computer simulation have conducted for APEIT protocol for 5%,10%, and 20% of lung volume sizes tumors at inspiration and found the average REPC values were 0.64%, 1.27%, and 2.63% respectively. Also, the corresponding distinguishing factors were 4.17%, 8.46% and 16.90 % respectively.

Distinguishing factors indicates whether a new condition in a lung like a tumor is present or not and its impact. In both cases for simulation 5 &6 even the size of the tumors around 5% can be detect by using our APEIT protocol. Furthermore, the tumor detection of lung will be more accurate at inspiration than at expiration.

Electrical impedance imaging spectroscopy i.e. imaging at multiple frequencies like- 20 kHz, 50 kHz, 100 kHz, 150 kHz, 200 kHz of 1 mA current is used for lung at inspiration for fixed conductivity value 0.0824 Sm^{-1} or 0.0927 Sm^{-1} or **0.103 Sm^{-1}** or 0.1133 Sm^{-1} or 0.1236 Sm^{-1} (i.e**. 0.103 Sm^{-1}± 10% steps**) and at expiration for fixed conductivity value .0.2096 Sm^{-1}or 0.2358 Sm^{-1} or **0.2620 Sm^{-1}** or 0.2882Sm^{-1} or 0.3144 Sm^{-1}(i.e. **0.2620 Sm^{-1}± 10% steps**) to see the sensitivity to our APEIT protocol.**[Section 5.7]**

Simulation Study -8: Lung at inspiration for above frequencies and fixed electrical conductivity 0.0824 Sm^{-1} & relative permittivity=4272.50.

We computed eight voltage sensing electrodes potential for the above range of frequencies, and found that the electric potentials at each electrode were decreasing as the frequencies were increased from 20 kHz to 200 kHz. The said relation is negatively correlated. The sum of the eight surface electrodes potential decreased almost linearly from 591.98 mV to 562.82 mV for frequencies from 20 kHz to 200 kHz as expected.

Simulation Study-9: Lung at inspiration for above frequencies and fixed electrical conductivity 0.0927 Sm^{-1} & relative permittivity=4272.50.

We computed eight voltage sensing electrodes potential for the above range of frequencies, and found that the electric potentials at each electrode were decreasing as the frequencies were increased from 20 kHz to 200 kHz. The said relation is negatively correlated. The sum of the eight surface electrodes potential decreased almost linearly from 589.90 mV to 561.20 mV for frequencies from 20 kHz to 200 kHz as expected.

Simulation Study-10: Lung at inspiration for above frequencies and fixed electrical conductivity value 0.103 Sm^{-1} & relative permittivity=4272.50.

We computed eight voltage sensing electrodes potential for the above range of frequencies, and found that the electric potentials at each electrode were decreasing as the frequencies were increased from 20 kHz to 200 kHz. The said relation is negatively correlated. The sum of the eight surface electrodes potential decreased almost linearly from 587.97 mV to 559.63 mV for frequencies from 20 kHz to 200 kHz as expected.

Simulation Study-11: Lung at inspiration for above frequencies for fixed electrical conductivity value 0.1133 Sm^{-1}, current & relative permittivity=4272.50.

We computed eight voltage sensing electrodes potential for the above range of frequencies, and found that the electric potentials at each electrode were decreasing as the frequencies were increased from 20 kHz to 200 kHz. The said relation is negatively correlated. The sum of the eight surface electrodes potential decreased almost linearly from 586.17 mV to 558.17 mV for frequencies from 20 kHz to 200 kHz as expected.

Simulation Study-12: Lung at inspiration for above frequencies for fixed electrical conductivity value 0.1236 Sm^{-1} & relative permittivity=4272.50

We computed eight voltage sensing electrodes potential for the above range of frequencies, and found that the electric potentials at each electrode were decreasing as the frequencies were increased from 20 kHz to 200 kHz. The said relation is negatively correlated. The sum of the eight surface electrodes potential decreased almost linearly from 584.50 mV to 556.75 mV for frequencies from 20 kHz to 200 kHz as expected.

Simulation Study-13: Lung at expiration for above frequencies for fixed electrical conductivity value 0.2096 Sm^{-1} & relative permittivity=8531.40

We computed eight voltage sensing electrodes potential for the above range of frequencies, and found that the electric potentials at each electrode were decreasing as the frequencies were increased from 20 kHz to 200 kHz. The said relation is negatively correlated. The sum of the eight surface electrodes potential decreased almost linearly from 573.60 mV to 545.84 mV for frequencies from 20 kHz to 200 kHz as expected.

Simulation Study-14: Lung at expiration for above frequencies for fixed electrical conductivity value 0.2358 Sm^{-1} & relative permittivity=8531.40

We computed eight voltage sensing electrodes potential for the above range of frequencies, and found that the electric potentials at each electrode were decreasing as the frequencies were increased from 20 kHz to 200 kHz. The said relation is negatively correlated. The sum of the eight surface electrodes potential decreased almost linearly from 571.11 mV to 543.81 mV for frequencies from 20 kHz to 200 kHz as expected.

Simulation Study. Case-15: Lung at expiration for above frequencies for fixed electrical conductivity value 0.2620 Sm^{-1} & relative permittivity=8531.40

We computed eight voltage sensing electrodes potential for the above range of frequencies, and found that the electric potentials at each electrode were decreasing as the frequencies were increased from 20 kHz to 200 kHz. The said relation is negatively correlated. The sum of the eight surface electrodes potential decreased almost linearly from 568.87 mV to 541.97 mV for frequencies from 20 kHz to 200 kHz as expected.

Simulation Study-16: Lung at expiration for above frequencies for fixed electrical conductivity value 0.2882 Sm^{-1} & relative permittivity=8531.40

We computed eight voltage sensing electrodes potential for the above range of frequencies, and found that the electric potentials at each electrode were decreasing as the frequencies were increased from 20 kHz to 200 kHz. The said relation is negatively correlated. The sum of the eight surface electrodes potential decreased almost linearly from 566.87 mV to 540.27 mV for frequencies from 20 kHz to 200 kHz as expected.

Simulation Study-17: Lung at expiration for above frequencies for fixed electrical conductivity value 0.3144 Sm^{-1} & relative permittivity=8531.40

We computed eight voltage sensing electrodes potential for the above range of frequencies, and found that the electric potentials at each electrode were decreasing as the frequencies were increased from 20 kHz to 200 kHz. The said relation is negatively correlated. The sum of the eight surface electrodes potential decreased almost linearly from 565.07mV to 538.71 mV for frequencies from 20 kHz to 200 kHz as expected.

The sum of eight surface electrodes potential value of lung at inspiration condition have significantly higher than at expiration condition.

Similar results were found from for the frequencies at 20 kHz or 50 kHz or, 100 kHz or, 150 kHz or, 200 kHz for the range of the following conduct ivies0.0824 Sm^{-1} o, 0.0927 Sm^{-1} o, **0.103 Sm^{-1}** o, 0.1133 Sm^{-1} o, 0.1236 Sm^{-1} (i.e**., 0.103 Sm^{-1}± 10% steps**) at inspiration and values.0.2096 Sm^{-1}, 0.2358 Sm^{-1} o, **0.2620 Sm^{-1}** o, 0.2882Sm^{-1} o, 0.3144 Sm^{-1}(i.e., **0.2620 Sm^{-1}± 10% steps**) at expiration as expected.

[Section 5.8]

Human Thorax Phantom study using Maltron Bio Scan 920-11 Analyzer **[Ref. Section 5.9]**

Maltron Bio-Scan 920-11 system is used for electrical impedance measurement. In this study a human thorax phantom has been designed following the dimensions of multipurpose digital chest phantom [Ref. https://www.ncbi.nlm.nih.gov/pmc/articles/PMC4169876].In this study we have used our proposed more sensitive Anterior- Posterior Electrical Impedance Technique (APEIT) protocol .Here a single channel with four electrodes of Maltron Bio-Scan 920-11 system is used, where two driving electrodes are used for injecting 1 mA alternating current at 50 kHz and another two electrodes are used for electrical potential measurement. The different conductive material and ellipsoid shape with porous foam like lung (2.5cm × 9cm× 22 cm) was inserted at 8cm (fixed) away from the frontal of the chest surface in the phantom for different concentration solutions.

Saline water of 0.54%,0.72%,0.90%,1.08 %,1.26%NaCl concentrations and the corresponding electrical conductivity 0.952 S/m,1.210S/m,1.520S/m,1.858S/m,2.162S/m were used in phantom to simulate the different conductive tissues of lungs. We computed eight voltage sensing electrodes potentials and found they have distinct electric potentials and the sum of the eight voltage sensing electric potential were 120.40 mV to 54.96 mV at 50 kHz frequency. Electrical conductivity (S/m) for different concentrations of NaCl (%) in Phantom solutions have linear relationship and gave a straight line through origin.

We found the sum of eight voltage sensing electrodes electrical potentials (mV) against the above mentioned concentrations of NaCl (%) in Phantom solutions or its corresponding electrical conductivity (Sm^{-1}) is negatively correlated, which is similar to computer simulation studies of our proposed Anterior- Posterior Electrical Impedance Technique (APEIT) protocol.

Computing the electrical impedances of the above mentioned different computer simulations for five (5) protocols for different lung conditions and diseases. It is found that the proposed Anterior-Posterior Electrical Impedance Technique (APEIT) protocol is the most sensitive method for the measurements of electrical impedances for the assessment the lung functions and diseases. Phantom study was also conducted and the result was similar to computer simulations.

Before the applications of this proposed APEIT protocol in real life, a computerized EIT data collection and image reconstruction software to be design, and implemented.

Preclinical and clinical trials using the above mentioned APEIT computer system to be tested, validated before practical use in clinics and hospitals.

Chapter-7: References (Bibliography)

(174-182)

Chapter-7: References (Bibliography)

[1] Grimnes S, Martinsen Ø G (2008): Bioimpedance and Bioelectricity Basics 2nd ed (San Diego: Academic)

[2] Martinsen, Ø. G. & Grimnes, S. (2009): The concept of transfer impedance in bioimpedance measurements. 4th European Conference of the International Federation for Medical and Biological Engineering, Springer, 1078-1079

[3] Mayer, M. Brunner, P., Merwa, R. & Scharfetter, H. (2005): Monitoring of lung edema using focused impedance spectroscopy- a feasibility study. Physiological measurement, **26**,185

[4] Carr Joseph J, Brown John M (2012): Introduction to Biomedical Equipment Technology Fourth Edition Pearson Education, Inc. pages 324-335

[5] www.worldlifeexpectancy.com>bangladesh-lifeexpectancy

[6] www.merckmanuals.com/home/fundamentals/the-human-body/introduction

[7] www.sciencekids.co.nz/pictures/human body/human organs.htm!

[8] Vatter A. F Barbosa, Victor L. B.A. Silva et.al: Reconstruction of Electrical Impedance Tomography Using Fish School Search, Non-Blind Search and Genetic Algorithm. International Journal of Swarm Intelligence Research, Volume 8, Issue 2, 2017.

[9] Holder D.S. (2004): Electrical Impedance Tomography: Methods, History and Applications, Institute of Physics Publishing, ISBN 0-7503- 0952-0

[10] https:// en.wikipedia.org/wiki/Electrical impedance tomography

[11] https:// www.slideshare.net/sharif_genius/electrical -impedance-tomography

[12] Brown B.H. (2003): "Electrical Impedance Tomography (EIT)- A Review". J. Med. Eng. Technol. 27(3); 97-108.

[13] Barber D.C, Brown B. H and Frceston I. L. (1983): "Imaging spatial distribution of resistivity using Applied Potential Tomography". Electronics Letters, 19, 93-95.

[14] Uhlmann G. (1999): "Developments in inverse problems since Calderon's fundamental paper", Harmonic Analysis and Partial Differential Equations: Essays in

Honor of Alberto P. Calderon, (editors ME Christ and CE Kenig), University of Chicago Press, ISBN 0-226-10455-9

[15] Bodenstein M., David M., Markstaller K. (2009): “Principles of electrical impedance tomography and its clinical application.” Crit. Care Med. 37(2): 713-724

[16] Noop, P, Rapp, E., Pfutzner, H., Nakesh, H.& Rusham,C. (1993): Dielectric properties of lung tissue as a function of air content ,physics in medicine and biology ,**38** ,699

[17] http://www.bbc.co.uk/news/science-environment-13751783

[18] Henderson, R.P.,Webster, J.G.(1978): “An Impedance Camera for Spatially Specific Measurements of the Thorax. ” IEEE Trans. Biomed. Eng. 25 (3): 250-254

[19] Barber, D.C.; Brown, B.H. (1984): “Applied Potential Tomography”. J. Phys. E: Sci. Instrum 17 (9): 723-733

[20] M. S. Beck and R.Williams, Process Tomography: Principles, Techniques and Applications, Butterworth- Heinemann (July 19, 1995), ISBN 0-7506-0744-0

[21] Alan Fein M D, Ronald F, Grossman M D, J Gareth Jones M D, Philip C Goodman M D, and John F Murray M D (1979): Evaluation of Transthoracic Electrical Impedance in the Diagnosis of Pulmonary Edema. American Heart Association Circular **60**, No. 5, 1156-1160

[22] Campbell J.H, Harris N. D., Z hang F., Morice A. H., and Brown B. H. (1994): Detection of changes in intrathoracic fluid in man using electrical impedance tomography. Clinical Science **87 ,**97-101

[23] Nebuya S, Kitamura K, Kobayashi H, Noshiro M and Brown B H (2007): Measurement accuracy in pulmonary function test using electrical impedance tomography. IFMBE Proceedings **17**, 539-542

[24] Henning Luepschen, Dirk van Riesen, Lisa Beckmann, Kay Hameyer, and Steffen Leonhardt (2008): Modeling of Fluid Shifts in the Human Thorax for Electrical Impedance Tomography. IEEE Transactions on Magnetics, Vol. **44**, No.6

[25] Rene Werner, Jan Ehrhardt, Rainer Schmidt, and Heinz Handels (2008): Modeling Respiratory Lung Motion- a Biological Approach using Finite Element Methods. Proc. Of SPIE Vol. **6916**, 69160 N

[26] Eduardo LV Costa, Raul Gonzalez Lima and Marcelo BP Amato (2009): Electrical Impedance Tomography. Respiratory Intensive Care Unit, **15,** 18-24

[27] Satoru Nebuya, Tomotaka Koike, Hiroshi Imai, Makoto Noshiro, Brain H. Brown, Kazui Soma (2010): Measurement of lung function using Electrical Impedance Tomography (EIT) during mechanical ventilation. Phys. Conf.Ser. **224** 012029

[28] Inez Frerichs, Sven Pulletz, Gunnar Elke, Gunther Zick and Norbert Weiler (2010): Electrical Impedance Tomography in Acute Respiratory Distress Syndrome. Nuclear Medicine Journal **2**, 110-118

[29] Mouloud A. Denai, Mahdi Mahfouf, Suzani Mohamad Samuri, George Panoutsos, Brain H. Brown and Gary H. Mills (2010): 'Absolute electrical impedance tomography (an EIT) guided ventilation therapy in critical care patients: simulations and future trends,' IEEE Transactions on Information Technology in Biomedicine.**14(3),** pp 641- 649

[30] Pikkemaat R, Tenbrock K, Lehmann S, Leonhardt S (2012): Electrical impedance tomography: New diagnostic possibilities using regional time constant maps. Applied Cardiopulmonary Pathophysilogy**16**, 212-225

[31] Wojciech Durlak and Przemko Kwinta (2013): Role of Electrical Impedance Tomography in Clinical Practice in Pediatric Respiratory Medicine. ISRN Pediatrics vol. **2013**, Article ID 529038, 5 pages

[32] Tusher Kanti Bera (2014): Bioelectrical Impedance Methods for Noninvasive Health Monitoring: A Review Journal of Medical Engineering Volume **2014**, Article ID 381251, 28 pages.

[33] Deborshi Chakrabotry, Madhurima Chattopadhyay (2014): "Monitoring of the lung fluid movement and estimation of lung area using Electrical Impedance Tomography: A Simulation Study." Proceedings of the 8th International Conference of Sensing Technology, Sep. 2-4, Liverpool, UK

[34] Brain K Walsh PhD RRT-NPS FAARC and Craig D Smallwood RRT (2016): Electrical Impedance Tomography During Mechanical Ventilation. Respiratory Care vol. **61** No.10

[35] Gong B, Schullck B, Krueger- Ziolek S, Moeller K (2016): EIT Image Reconstruction by Modified Data. J. Biomedical Science and Engineering, **9,** 99-106

[36] Inez Frerichs, Marcelo BP Amato, Anton H Van Kaam et al. (2017): Chest electrical impedance tomography examination, data analysis, terminology, clinical use and recommendations: Consensus statement of the Translational EIT development StuDy group. Thorax **72**, 83-93

[37] Szymon Bialka, Maja Copik, Katarzyna Rybczyk, Hanna Misiolek (2017): Electrical impedance tomography for diagnosis and monitoring of pulmonary function disorders in the intensive care unit- case report and feview of literature vol. 49, No. **3**, 222-226

[38] Beatriz Lobo, Cecilia Hermosa, Ana Abella, Federico Gordo (2017): Electrical Impedance Tomography. A Review Article.

http://dx.doi.org/10.21037/atm.2017.12.06

[39] Schullcke B., Krueger-Ziolek S., Gong B., Moeller K. (2017): A simulation study on the ventilation inhomogeneity measured with Electrical Impedance Tomography. Science Direct Hosting by Elsevier Ltd. IFAC Papers Online 50-1(2017)8781-8785

[40] Bachmann MC, Caio Morais, Guillermo Bugedo, Alejandro Bruhn, Arturo Morales, Joao B Borges, Eduardo Costa and Jaime Retamal (2018): A Review Article. https://doi.org/10.1186/s 13054-018-2195-6

[41] Alessandro Santini, Elena Spinelli, Thomas Longer, Savino- Spadaro, Giacomo Grasselli, Tommaso Mauri (2018): Thoracic electrical impedance tomography: an adaptive monitor for dynamic organs. A Review Article. http://dx.doi.org/10.21037/jeccm.2018.08.08

[42] http://dx.doi.org/10.1155/2013/529038 ISRN Pediatrics Volume 2013 (2013), Article ID 529038, 5 pages

[43] Humayra Ferdous (2014): Study of changes in Lung Transfer Impedance due to Ventilation Using Focused Impedance Measurement (FIM) Technique.

[44] http:// earthsci.stanford.edu/ERE/research/geoth/ publication/SGP-TR-182 pdf

[45] Vatter A. F Barbosa et.al, Reconstruction of Electrical Impedance Tomography Using Fish School Search, Non-Blind Search and Genetic Algorithm. Department de Biomedica, Universidade F ederal de Pernambuco, Cidade Universitaria, Recife, PE, 50670-901-, Brazil.

[46] www.research gate.net/publication/321334050

[47] Brown BH and Seagar AD. The Sheffield data collection system. Clin. Phys. Physiol. Meas., vol.8, Suppl. A, 91-97, 1987.

[48] Venkatratnam Chitturi and Nagi Farrukh. Spatial resolution in electrical impedance tomography: A topical review. J Electro Bioimp, vol. 8, pp. 66-78, 2017

[49]www.biologydiscussion.com/essay/human-respiratory-system-and-its-mechanism-with-diagram/1548

[50] https:// www.livescience.com/52250-lung.htm! Lungs: Facts, Function and Diseases (By Alina Bradford, Live Science Contributor).

[51] Herman. I P 2007: Physics of the Herman Body; Biological and Medical Physics, Biomedical Engineering. Springer-Verlag Berlin Heidelberg New York, USA. Pages 525-537

[52] https://www.liverpool.ac.uk/~gdwill/hons/gul_lect. pdf

[53] http://philschatz.com/anatomy-book/contents/m46548htm!

[54] https://byjus.com/biology/respiration-gas-exchange

[55] https://bio.libretexts.org/Under-Construction/BioStuff/BIO-102/ Reading- and-Lecture-Notes/ Respiratory System

[56] https://www.britannica.com/Science/respiratory -disease

[57] https://www.webmd.com/lung/obstructive-and-restrictive-lungdisease

[58] https://lung institute.com/blog/the-difference-between-obstructive-and – restrictive-lung-disease

[59] https:// my.clevelandclinic.org/health/diseases/15305-collapsed lung

[60] https://en.wikipedia.org/wiki/Obstructive_lung_disease

[61] www.goldcopd.org

[62]https://en.wikipedia.org/wiki/Obstructive_lung_disease#Chronic_obstructive_pulmonary_disease

[63]https://pulmonary fibrosis news.com/2017/05/09/8-common-lung-diseaseswomen

[64]https://www.mayoclinic.org/disease-conditions/asthma/symptons-causes/syc-20369653

[65] https://floridachest.com/cystic-fibrosis

[66] https://emedicine.medscape.com/article/296961-overview

[67]www.ugr.es/~jhuertas/EvaluacionFisiologica/Espirometria /restobst.htm

[68] https://en.wikipedia.org/wiki/Lung-Complance

[69]https://www.mayoclinic.org/diseases-conditions/pulmonary fibrosis/Symptoms-Causes/Syc-20353690

[70]https://www.mayoclinic.org/diseases-conditions/pulmonary fibrosis/Symptoms-Causes/Syc-20353690https://www.mayoclinic.org/diseases-conditions/pneumonia /Symptoms-Causes/Syc-203534204

[71]https://www.mayoclinic.org/diseases-conditions/pulmonary -edema/Symptoms-Causes/Syc-20377009

[72]https://www.thoracic.org/patients/patient-resources/resources/pulmonary-function-tests.pdf

[73] https://www.ncbi.nlm.nih.gov/pmc/articles/PMC 3229853

[74]https://www.clinicaladvisor/pulmonary-medicine/pulmpnary-function-testing/article/625268

[75]https://www.hopkinsmedicine.org/healthlibrary/test_procedures/pulmonary/pulmonary_function_tests_92,P07759

[76] https://www.docdoc.com/info/procedure/pulmonary-function -testing

[77] https://www.ncbi.nlm.gov/pubmed/9769260

[78]http://www.beckdhop.de/fachbuch/leseprobe/9783540746577_Excerpt-001.pdf

[79] https://lung foundation.com.au/lung-health/lung-testing

[80] Brown BH, Smallwood RH, Barber DC, Lawford PV and Hose DR 1999: Medical Physics and Biomedical Engineering; Taylor & Francis Group 270 Madison Avenue, New York, NY 10016

[81] https:// clinicalgate .com/ pulmonary-function-testing-equipment

[82]www.clevelandclinicmeded.com/medicalpubs/disease management/pulmonary/pulmonary-function-testing

[83] www.burntec.com

[84] www.comsol.com

[85] https://www.comsol.dk/video/what-is-comsol-multiphysics.

[86] www.ComsolMultiphysics Users Guide (1)

file://c:/Users/User/Downloads/ComsolMultiphysics Users Guide (1).pdf

[87] https://www.comsol.com/products/4.3#acdc

[88] https://www.comsol.com/models/acdc-module

[89] https:// www.comsol.com/model/e-core-transformer-14123

[90]https://www.comsol.com/model/multi-turn-coil-winding-around-a- ferromagnet-23641

[91] https://www.comsol.com/products

[92] https://www.comsol.com/rf.module

[93] D.K. Cheng 1989: Field and Wave Electromagnetics, Addison- Wesley, Reading, Massachusetts.

[94] J. Jin 1993: The Finite Element Method in Electromagnetics, John Wiely & Sons, New York.

[95] B.D. Popovic 1971: Introductory Engineering Electromagnetics, Addison-Wesley, Reading, Massachusetts, USA.

[96] https://medlineplus.gov/ency/article/000087.htm

[97] Adler A, Amato MB, Arnold JH, Bayford R, Bodenstein M, Bohm SH, et al. (2012), Whither Lung EIT? Physiol Meas 33, 679-694.

[98] www.imagingpathways-health.wa.gov.au/index.php/consumer.info

[99] www.medicalnewstoday.com.articles/219970.php

[100] www.nrpb.org.uk

[101] www.radiologyinfo.org/patients safety-radiation dose in X ray and CT exams

[102] www.maltronint.com

[103] https://www.researchgate.net/figure/A-Simplified-Cole-Cole -model-for-biological tissue

[104] https://www.who.int> health – topics

[105] https://www.researchgate.net/figure/current-flow-in-tissue and -electrical -equivalent-circuit

[106] https// www.courses: lumen learning .com/ physics/chapter/20-6-electric-hazards-and-the –human-body

[107] Trainito C.I., Francais O., Le Pioufle B, 2015: Analysis of pulsed electric field effects on cellular tissue with Cole-Cole model: Monitoring permeabilization under inhomogeneous electric field with bioimpedance parameter variations. ELSEVIER Innovative Food Science & Emerging Technologies Volume **29**, pages 193-200

[108] www.who.int (medical devices)

[109] Rangaraj M. Rangayyan 2005: Biomedical Signal Analysis. A Case-Study Approach, IEEE (Institute of Electrical and Electronics Engineers) Press, Wiley-Interscience, John Wiley & Sons, INC.

[110] Vinko Tomicic, Rodrigo Cornejo 2019: Lung monitoring with electrical impedance tomography: technical considerations and clinical applications, Journal of Thoracic Disease, vol. **11,** No. 7

[111]https://www.analog.com/ru/technical-articles/bioelectrical-

impedance-analysis-in-monitoring-of-the-clinical-status-and-diagnosis-of -diseases.

[112] Numan Celik, Nadarajah Manivannan, Andrew Strudwick and Wamadeva Balachandran 2016: Graphene-Enabled Electronics for Electrocardiogram Monitoring, 6, 156; doi: 10.3390/nano6090156

[113] https://www.thoughtco.com/electrical-conductivity-in-metals-2340117

[114]https://www.thoughtco.com/table-of-electricalresistivity-conductivity-608499

[115]https://www.thoughtco.com/definition-of-element-conductivity-605064

[116] https://www.en.wikipedia.org/wiki/Relative Permittivity

[117]https://www.en.wikipedia.org/wiki/Electricalresistivityand conductivity

[118] www.massgeneral.org

[119] Antoni Ivorra 2014: Tissue Electroporation as a Bioelectric Phenomenon: Basic Concepts, Department of Information and Communication Technology, University Pompeu Fabra, Barcelona, Catalunya, Spain

[120] https://www.heartfailure.org/heart-failure/lungs

[121]www.lung.org/lung-heaith-and-diseases/warning-sign-of-lung-disease,American Lung Association.

[122] Yan Shi,Zhi Guo Yang, Fei Xie, Shual Ren and Shao Feng Xu (2021):The Research Progrress of Electrical Impedance Tomography for Lung Monitoring, A Review Article. Frontiers in Bioengineering and Biotechnology. Volume 9, Article 726652.

[123] Fedi Zouari, Wei YiOon, Dipyaman Modak, Wing Hang Lee, Wang Chun Kwok, Peng Cao, Wei-Ning Lee, Terence Chi Chun Tam, Eddie C. Wong & Russell W. Chan (2022): Affordable, portable and self-administrable electrical impedance tomography enables global and regional lung function assessment. www.nature.com/scientificreportshtps://doi.org/10.1038*/s41598-022-24330-2.

Appendix

5.3(A). Simulation Study-1: Existing Adjacent Current Drive EIT Protocol

5.3(A-1) Case-1: For Healthy Lung at Inspiration & Expiration

Table 5-4(a): Electric Potentials of 8 different Surface Electrode (SE) due to different Electrical Conductivities & Relative Permittivity of Healthy Lung Tissues for inspiration and expiration at Constant Current =1mA and Frequency=50 KHz.

Electrical Conductivity (Sm^{-1}) & Relative Permittivity	SE-1 Potential (mV)	SE-2 Potential (mV)	SE-3 Potential (mV)	SE-4 Potential (mV)	SE-5 Potential (mV)	SE-6 Potential (mV)	SE-7 Potential (mV)	SE-8 Potential (mV)	Sum of SE Potential (1 to 8) (mV)
Inspiration 0.103 & 4272.50	70.58	69.02	68.75	68.61	68.22	67.11	64.53	61.18	538.00
Expiration 0.262 & 8531.40	69.08	67.75	67.55	67.46	67.15	66.17	64.05	61.07	530.28

Table 5-4(b): Relative Electric Potential Change (REPC) value of the same Surface Electrode (SE) between Healthy Lung at Inspiration and Expiration.

$\frac{V_i - V_e}{V_i} \times 100\%$	SE-1 (%)	SE-2 (%)	SE-3 (%)	SE-4 (%)	SE-5 (%)	SE-6 (%)	SE-7 (%)	SE-8 (%)	Average of REPC value (%)
	2.13	1.84	1.75	1.68	1.57	1.40	0.74	0.18	1.41

5.3(A-2): Case-2: For Healthy Lung at Inspiration and Pneumothorax (Collapsed Lung)

Table 5-5(a): Electric Potentials of 8 different Surface Electrode (SE) due to different Electrical Conductivities & Relative Permittivity of Healthy Lung Tissue for Inspiration and Pneumothorax (Collapsed Lung) at Constant Current =1mA and Frequency=50 KHz.

Electrical Conductivity (Sm^{-1}) & Relative Permittivity	SE-1 Potential (mV)	SE-2 Potential (mV)	SE-3 Potential (mV)	SE-4 Potential (mV)	SE-5 Potential (mV)	SE-6 Potential (mV)	SE-7 Potential (mV)	SE-8 Potential (mV)	Sum of SE Potential (1 to 8) (mV)
Inspiration 0.103 & 4272.50	70.58	69.02	68.75	68.61	68.22	67.11	64.53	61.18	538.00
Pneumoth-orax (Colla-psed Lung) 0.60 & 1000	67.51	66.35	66.21	66.15	65.92	65.11	63.53	60.96	521.74

Table-5-5(b): Relative Electric Potential Change (REPC) value of the same Surface Electrode (SE) between Healthy Lung at Inspiration and Pneumothorax (Collapsed Lung).

$\frac{V_i - V_{pn}}{V_i} \times 100\%$	SE-1 (%)	SE-2 (%)	SE-3 (%)	SE-4 (%)	SE-5 (%)	SE-6 (%)	SE-7 (%)	SE-8 (%)	Average of REPC value (%)
	4.35	3.87	3.70	3.59	3.37	2.98	1.55	0.36	2.97

5.3 (A-3) Case-3: For Healthy Lung at Expiration and Pneumothorax (Collapsed Lung)

Table 5-6(a): Electric Potentials of 8 different Surface Electrode (SE) due to different Electrical Conductivities & Relative Permittivity of Lung Tissues for Expiration and Pneumothorax (Collapsed Lung) at Constant Current =1mA and Frequency=50 KHz.

Electrical Conductivity (Sm^{-1}) & Relative Permittivity	SE-1 Potential (mV)	SE-2 Potential (mV)	SE-3 Potential (mV)	SE-4 Potential (mV)	SE-5 Potential (mV)	SE-6 Potential (mV)	SE-7 Potential (mV)	SE-8 Potential (mV)	Sum of SE Potential (1 to 8) (mV)
Expiration 0.262 & 8531.40	69.08	67.75	67.55	67.46	67.15	66.17	64.05	61.07	530.28
Pneumotho-rax (Collapsed Lung 0.60 & 1000	67.51	66.35	66.21	66.15	65.92	65.11	63.53	60.96	521.74

Table-5.6(b): Relative Electric Potential Change (REPC) value of the same Surface Electrode (SE) between Healthy Lung at Expiration and Pneumothorax (Collapsed Lung).

$\frac{V_e - V_{pn}}{V_e} \times 100\%$	SE-1 (%)	SE-2 (%)	SE-3 (%)	SE-4 (%)	SE-5 (%)	SE-6 (%)	SE-7 (%)	SE-8 (%)	Average REPC value (%)
	2.27	2.07	1.98	1.94	1.83	1.60	0.81	0.18	1.59

5.3(A-4) Case-4: For Healthy Lung at Inspiration and Pulmonary Edema.

Table-5.7(a): Electric Potentials of 8 different Surface Electrode (SE) due to different Electrical Conductivities & Relative Permittivity of Healthy Lung Tissue for Inspiration and Pulmonary Edema at Constant Current =1mA and Frequency=50 KHz.

Electrical Conductivity (Sm^{-1}) & Relative Permittivity	SE-1 Potential (mV)	SE-2 Potential (mV)	SE-3 Potential (mV)	SE-4 Potential (mV)	SE-5 Potential (mV)	SE-6 Potential (mV)	SE-7 Potential (mV)	SE-8 Potential (mV)	Sum of SE Potential (1to 8) (mV)
Inspiration 0.103 & 4272.50	70.58	69.02	68.75	68.61	68.22	67.11	64.53	61.18	538.00
Pulmonary Edema 1.50 & 98.56	66.03	64.98	64.88	64.85	64.67	64.06	63.04	60.84	513.35

Table-5.7(b): Relative Electric Potential Change (REPC) of the same Surface Electrode (SE) between Healthy Lung at Inspiration and Pulmonary Edema.

$\frac{V_i - V_{pe}}{V_i} \times 100\%$	SE-1 (%)	SE-2 (%)	SE-3 (%)	SE-4 (%)	SE-5 (%)	SE-6 (%)	SE-7 (%)	SE-8 (%)	Average REPC value (%)
	6.45	5.85	5.63	5.48	5.20	4.55	2.31	0.56	4.50

5.3(A-5) Case-5: For Healthy Lung at Expiration and Pulmonary Edema.

Table-5.8(a): Electric Potentials of 8 different Surface Electrode (SE) due to different Electrical Conductivities & Relative Permittivity of Healthy Lung Tissue for Expiration and Pulmonary Edema at Constant Current =1mA and Frequency=50 KHz.

Electrical Conductivity (Sm^{-1}) & Relative Permittivity	SE-1 Potential (mV)	SE-2 Potential (mV)	SE-3 Potential (mV)	SE-4 Potential (mV)	SE-5 Potential (mV)	SE-6 Potential (mV)	SE-7 Potential (mV)	SE-8 Potential (mV)	Sum of SE Potential (1to 8) (mV)
Expiration 0.262 & 8531.40	69.08	67.75	67.55	67.46	67.15	66.17	64.05	61.07	530.28
Pulmonary Edema 1.50 & 98.56	66.03	64.98	64.88	64.85	64.67	64.06	63.04	60.84	513.35

Table-5.8(b): Relative Electric Potential Change (REPC) value of the same Surface Electrode (SE) between Healthy Lung at Expiration and Pulmonary Edema.

$\frac{V_e - V_{pe}}{V_e} \times 100\%$	SE-1 (%)	SE-2 (%)	SE-3 (%)	SE-4 (%)	SE-5 (%)	SE-6 (%)	SE-7 (%)	SE-8 (%)	Average REPC value (%)
	4.42	4.09	3.95	3.87	3.69	3.19	1.58	0.38	3.15

5.3(B). Simulation Study-2: Opposite Current Drive at the vertices of the semi-major axis of the chest cross section EIT Protocol

5.3(B-1) Case-1: For Healthy Lung at Inspiration and Expiration.

Table-5.9(a): Electric Potentials of 8 different Surface Electrode (SE) due to different Electrical Conductivities and Relative Permittivity of Healthy Lung Tissues for inspiration and expiration at Constant Current =1mA and Frequency=50 KHz.

Electrical Conductivity (Sm^{-1}) & Relative Permittivity	SE-1 Potential (mV)	SE-2 Potential (mV)	SE-3 Potential (mV)	SE-4 Potential (mV)	SE-5 Potential (mV)	SE-6 Potential (mV)	SE-7 Potential (mV)	SE-8 Potential (mV)	Sum of SE Potential (1 to 8) (mV)
Inspiration 0.103 & 4272.50	69.20	76.77	81.44	88.25	88.26	81.44	76.77	69.73	631.86
Expiration 0.262 & 8531.40	68.88	75.35	79.55	85.86	85.87	79.55	75.35	69.37	619.78

Table-5.9(b): Relative Electric Potential Change (REPC) value of the same Surface Electrode (SE) between Healthy Lung at Inspiration and Expiration.

$\frac{V_i - V_e}{V_i} \times 100\%$	SE-1 (%)	SE-2 (%)	SE-3 (%)	SE-4 (%)	SE-5 (%)	SE-6 (%)	SE-7 (%)	SE-8 (%)	Average REPC value (%)
	0.46	1.85	2.32	2.71	2.71	2.32	1.85	0.52	1.84

5.3(B-2) Case-2: For Healthy Lung at Inspiration and Pneumothorax (Collapsed Lung)

Table-5.10(a): Electric Potentials of 8 different Surface Electrode (SE) due to different Electrical Conductivities and Relative Permittivity of Healthy Lung Tissue for Inspiration and Pneumothorax (Collapsed Lung) at Constant Current =1mA and Frequency=50 KHz.

Electrical Conductivity (Sm^{-1}) & Relative Permittivity	SE-1 Potential (mV)	SE-2 Potential (mV)	SE-3 Potential (mV)	SE-4 Potential (mV)	SE-5 Potential (mV)	SE-6 Potential (mV)	SE-7 Potential (mV)	SE-8 Potential (mV)	Sum of SE Potential (1 to 8) (mV)
Inspiration 0.103 & 4272.50	69.20	76.77	81.44	88.25	88.26	81.44	76.77	69.73	631.86
Pneumotho-rax (Collapsed Lung 0.60 & 1000	68.55	73.80	77.41	83.18	83.18	77.41	73.80	68.99	606.32

Table-5.10(b): Relative Electric Potential Change (REPC) value of the same Surface Electrode (SE) between Healthy Lung at Inspiration and Pneumothorax (Collapsed Lung).

$\frac{V_i - V_{pn}}{V_i} \times 100\%$	SE-1 (%)	SE-2 (%)	SE-3 (%)	SE-4 (%)	SE-5 (%)	SE-6 (%)	SE-7 (%)	SE-8 (%)	Average REPC value (%)
	0.94	3.87	4.95	5.75	5.76	4.95	3.87	1.06	3.89

5.3(B-3) Case-3: For Healthy Lung at Expiration and Pneumothorax (Collapsed Lung)

Table-5.11(a): Electric Potentials of 8 different Surface Electrode (SE) due to different Electrical Conductivities and Relative Permittivity of Lung Tissues Lung Tissues for Expiration and Pneumothorax (Collapsed Lung) at Constant Current =1mA and Frequency=50 KHz.

Electrical Conductivity (Sm^{-1}) & Relative Permittivity	SE-1 Potential (mV)	SE-2 Potential (mV)	SE-3 Potential (mV)	SE-4 Potential (mV)	SE-5 Potential (mV)	SE-6 Potential (mV)	SE-7 Potential (mV)	SE-8 Potential (mV)	Sum of SE Potential (1 to 8) (mV)
Expiration 0.262 & 8531.40	68.88	75.35	79.55	85.86	85.87	79.55	75.35	69.37	619.78
Pneumothor-ax (Collapsed Lung) 0.60 & 1000	68.55	73.80	77.41	83.18	83.18	77.41	73.80	68.99	606.32

Table-5.11(b): Relative Electric Potential Change (REPC) value of the same Surface Electrode (SE) between Healthy Lung at Expiration and Pneumothorax (Collapsed Lung).

$\frac{V_e - V_{pn}}{V_e} \times 100\%$	SE-1 (%)	SE-2 (%)	SE-3 (%)	SE-4 (%)	SE-5 (%)	SE-6 (%)	SE-7 (%)	SE-8 (%)	Average REPC value (%)
	0.48	2.06	2.69	3.12	3.13	2.69	2.06	0.55	2.10

5.3(B-4) Case-4: For Healthy Lung at Inspiration and Pulmonary Edema.

Table-5.12(a): Electric Potentials of 8 different Surface Electrode (SE) due to different Electrical Conductivities and Relative Permittivity of Healthy Lung Tissue for Inspiration and Pulmonary Edema at Constant Current =1mA and Frequency=50 KHz.

Electrical Conductivity (Sm^{-1}) & Relative Permittivity	SE-1 Potential (mV)	SE-2 Potential (mV)	SE-3 Potential (mV)	SE-4 Potential (mV)	SE-5 Potential (mV)	SE-6 Potential (mV)	SE-7 Potential (mV)	SE-8 Potential (mV)	Sum of SE Potential (1to 8) (mV)
Inspiration 0.103 & 4272.50	69.20	76.77	81.44	88.25	88.26	81.44	76.77	69.73	631.86
Pulmonary Edema 1.50 & 98.56	68.25	72.29	75.14	80.37	80.38	75.14	72.29	68.64	592.50

Table-5.12(b): Relative Electric Potential Change (REPC) value of the same Surface Electrode (SE) between Healthy Lung at Inspiration and Pulmonary Edema.

$\frac{V_i - V_{pe}}{V_i} \times 100\%$	SE-1 (%)	SE-2 (%)	SE-3 (%)	SE-4 (%)	SE-5 (%)	SE-6 (%)	SE-7 (%)	SE-8 (%)	Average REPC value (%)
	1.37	5.84	7.74	8.93	8.93	7.74	5.84	1.56	5.99

5.3(B-5) Case-5: For Healthy Lung at Expiration and Pulmonary Edema

Table-5.13(a): Electric Potentials of 8 different Surface Electrode (SE) due to different Electrical Conductivities and Relative Permittivity of Healthy Lung Tissue for Expiration and Pulmonary Edema at Constant Current =1mA and Frequency=50 KHz.

Electrical Conductivity (Sm^{-1}) & Relative Permittivity	SE-1 Potential (mV)	SE-2 Potential (mV)	SE-3 Potential (mV)	SE-4 Potential (mV)	SE-5 Potential (mV)	SE-6 Potential (mV)	SE-7 Potential (mV)	SE-8 Potential (mV)	Sum of SE Potential (1to 8) (mV)
Expiration 0.262 & 8531.40	68.88	75.35	79.55	85.86	85.87	79.55	75.35	69.37	619.78
Pulmonary Edema 1.50 & 98.56	68.25	72.29	75.14	80.37	80.38	75.14	72.29	68.64	592.50

Table-5.13(b): Relative Electric Potential Change (REPC) value of the same Surface Electrode (SE) between Healthy Lung at Expiration and Pulmonary Edema.

$\frac{V_e - V_{pe}}{V_e} \times 100\%$	SE-1 (%)	SE-2 (%)	SE-3 (%)	SE-4 (%)	SE-5 (%)	SE-6 (%)	SE-7 (%)	SE-8 (%)	Average REPC value (%)
	0.92	4.06	5.54	6.39	6.39	5.54	4.06	1.05	4.24

5.3(C). Simulation Study-3: Existing Opposite Current Drive at the vertices of the semi-minor axis of the chest cross section EIT Protocol

5.3(C-1) Case-1: For Healthy Lung at Inspiration and Expiration

Table-5.14(a): Electric Potentials of 8 different Surface Electrode (SE) due to different Electrical Conductivities and Relative Permittivity of Healthy Lung Tissues for inspiration and expiration at Constant Current =1mA and Frequency=50 KHz.

Electrical Conductivity (Sm^{-1}) & Relative Permittivity	SE-1 Potential (mV)	SE-2 Potential (mV)	SE-3 Potential (mV)	SE-4 Potential (mV)	SE-5 Potential (mV)	SE-6 Potential (mV)	SE-7 Potential (mV)	SE-8 Potential (mV)	Sum of SE Potential (1 to 8) (mV)
Inspiration 0.103 & 4272.50	68.88	66.38	66.23	68.95	69.88	72.60	72.45	69.97	555.34
Expiration 0.262 & 8531.40	68.13	66.18	65.87	68.11	68.83	71.07	70.77	68.81	547.77

Table-5.14(b): Relative Electric Potential Change (REPC) value of the same Surface Electrode (SE) between Healthy Lung at Inspiration and Expiration.

$\frac{V_i - V_e}{V_i} \times 100\%$	SE-1 (%)	SE-2 (%)	SE-3 (%)	SE-4 (%)	SE-5 (%)	SE-6 (%)	SE-7 (%)	SE-8 (%)	Average REPC value (%)
	1.09	0.30	0.54	1.22	1.50	2.11	2.32	1.66	1.34

5.3(C-2) Case-2: For Healthy Lung at Inspiration and Pneumothorax (Collapsed Lung)

Table-5.15(a): Electric Potentials of 8 different Surface Electrode (SE) due to different Electrical Conductivities and Relative Permittivity of Healthy Lung Tissue for Inspiration and Pneumothorax (Collapsed Lung) at Constant Current =1mA and Frequency=50 KHz.

Electrical Conductivity (Sm^{-1}) & Relative Permittivity	BP-1 Potential (mV)	BP-2 Potential (mV)	BP-3 Potential (mV)	BP-4 Potential (mV)	BP-5 Potential (mV)	BP-6 Potential (mV)	BP-7 Potential (mV)	BP-8 Potential (mV)	Sum of BP Potential (1 to 8) (mV)
Inspiration 0.103 & 4272.50	68.88	66.38	66.23	68.95	69.88	72.60	72.45	69.97	555.34
Pneumotho-rax (Collapsed Lung) 0.60 & 1000	67.51	65.98	65.61	67.44	67.99	69.82	69.46	67.92	541.73

Table-5.15(b): Relative Electric Potential Change (REPC) value of the same Surface Electrode (SE) between Healthy Lung at Inspiration and Pneumothorax (Collapsed Lung).

$\frac{V_i - V_{pn}}{V_i} \times 100\%$	SE-1 (%)	SE-2 (%)	SE-3 (%)	SE-4 (%)	SE-5 (%)	SE-6 (%)	SE-7 (%)	SE-8 (%)	Average REPC value (%)
	1.99	0.60	0.94	2.19	2.70	3.83	4.13	2.93	2.41

5.3(C-3) Case-3: For Healthy Lung at Expiration and Pneumothorax (Collapsed Lung)

Table-5.16(a): Electric Potentials of 8 different Boundary Probe (BP) due to different Electrical Conductivities and Relative Permittivity of Lung Tissues Lung Tissues for Expiration and Pneumothorax (Collapsed Lung) at Constant Current =1mA and Frequency=50 KHz.

Electrical Conductivity (Sm^{-1}) & Relative Permittivity	SE-1 Potential (mV)	SE-2 Potential (mV)	SE-3 Potential (mV)	SE-4 Potential (mV)	SE-5 Potential (mV)	SE-6 Potential (mV)	SE-7 Potential (mV)	SE-8 Potential (mV)	Sum of SE Potential (1 to 8) (mV)
Expiration 0.262 & 8531.40	68.13	66.18	65.87	68.11	68.83	71.07	70.77	68.81	547.77
Pneumothor-ax (Collapsed Lung) 0.60 & 1000	67.51	65.98	65.61	67.44	67.99	69.82	69.46	67.92	541.73

Table-5.16(b): Relative Electric Potential Change (REPC) value of the same Surface Electrode (SE) between Healthy Lung at Expiration and Pneumothorax (Collapsed Lung).

$\frac{V_e - V_{pn}}{V_e} \times 100\%$	SE-1 (%)	SE-2 (%)	SE-3 (%)	SE-4 (%)	SE-5 (%)	SE-6 (%)	SE-7 (%)	SE-8 (%)	Average REPC value (%)
	0.91	0.30	0.40	0.98	1.22	1.76	1.85	1.29	1.09

5.3(C-4) Case-4: For Healthy Lung at Inspiration and Pulmonary Edema

Table-6.17(a): Electric Potentials of 8 different Surface Electrode (SE) due to different Electrical Conductivities and Relative Permittivity of Healthy Lung Tissue for Inspiration and Pulmonary Edema at Constant Current =1mA and Frequency=50 KHz.

Electrical Conductivity (Sm^{-1}) & Relative Permittivity	SE-1 Potential (mV)	SE-2 Potential (mV)	SE-3 Potential (mV)	SE-4 Potential (mV)	SE-5 Potential (mV)	SE-6 Potential (mV)	SE-7 Potential (mV)	SE-8 Potential (mV)	Sum of SE Potential (1to 8) (mV)
Inspiration 0.103 & 4272.50	68.88	66.38	66.23	68.95	69.88	72.60	72.45	69.97	555.34
Pulmonary Edema 1.50 & 98.56	67.04	65.79	65.43	66.95	67.34	68.88	68.52	67.27	537.22

Table-5.17(b): Relative Electric Potential Change (REPC) value of the same Surface Electrode (SE) between Healthy Lung at Inspiration and Pulmonary Edema

$\frac{V_i - V_{pe}}{V_i} \times 100\%$	SE-1 (%)	SE-2 (%)	SE-3 (%)	SE-4 (%)	SE-5 (%)	SE-6 (%)	SE-7 (%)	SE-8 (%)	Average Change (%)
	2.67	0.89	1.21	2.90	3.64	5.12	5.42	3.86	3.21

6. 3(C-5) Case-5: For Healthy Lung at Expiration and Pulmonary Edema

Table-5.18(a): Electric Potentials of 8 different Surface Electrode (SE) due to different Electrical Conductivities and Relative Permittivity of Healthy Lung Tissue for Expiration and Pulmonary Edema at Constant Current =1mA and Frequency=50 KHz.

Electrical Conductivity (Sm^{-1}) & Relative Permittivity	SE-1 Potential (mV)	SE-2 Potential (mV)	SE-3 Potential (mV)	SE-4 Potential (mV)	SE-5 Potential (mV)	SE-6 Potential (mV)	SE-7 Potential (mV)	SE-8 Potential (mV)	Sum of SE Potential (1to 8) (mV)
Expiration 0.262 & 8531.40	68.13	66.18	65.87	68.11	68.83	71.07	70.77	68.81	547.77
Pulmonary Edema 1.50 & 98.56	67.04	65.79	65.43	66.95	67.34	68.88	68.52	67.27	537.22

Table-5.18(b): Relative Electric Potential Change (REPC) value of the same Surface Electrode (SE) between Healthy Lung at Expiration and Pulmonary Edema.

$\frac{V_e - V_{pe}}{V_e} \times 100\%$	SE-1 (%)	SE-2 (%)	SE-3 (%)	SE-4 (%)	SE-5 (%)	SE-6 (%)	SE-7 (%)	SE-8 (%)	Average REPC value (%)
	1.60	0.59	0.67	1.70	2.17	3.08	3.18	2.24	1.90

5.3(D). Simulation Study-4: Existing Opposite Current Drive (along the right lung) Electrical Impedance Tomography (EIT) Protocol

5.3 (D-1) Case-1: For Healthy Lung at Inspiration and Expiration

Table-5.19(a): Electric Potentials of 8 different Surface Electrode (SE) due to different Electrical Conductivities and Relative Permittivity of Healthy Lung Tissues for inspiration and expiration at Constant Current =1mA and Frequency=50 KHz.

Electrical Conductivity (Sm^{-1}) & Relative Permittivity	SE-1 Potential (mV)	SE-2 Potential (mV)	SE-3 Potential (mV)	SE-4 Potential (mV)	SE-5 Potential (mV)	SE-6 Potential (mV)	SE-7 Potential (mV)	SE-8 Potential (mV)	Sum of SE Potential (1 to 8) (mV)
Inspiration 0.103 & 4272.50	67.07	66.68	68.98	69.59	69.84	70.46	72.75	72.38	557.75
Expiration 0.262 & 8531.40	66.08	65.82	67.65	68.04	68.18	68.57	70.39	70.13	544.86

Table-5.19(b): Relative Electric Potential Change (REPC) value of the same Surface Electrode (SE) between Healthy Lung at Inspiration and Expiration.

$\frac{V_i - V_e}{V_i} \times 100\%$	SE-1 (%)	SE-2 (%)	SE-3 (%)	SE-4 (%)	SE-5 (%)	SE-6 (%)	SE-7 (%)	SE-8 (%)	Average REPC value (%)
	1.47	1.30	1.94	2.24	2.37	2.68	3.23	3.10	2.29

5.3(D-2) Case-2: For Healthy Lung at Inspiration and Pneumothorax (Collapsed Lung)

Table-5.20(a): Electric Potentials of 8 different Surface Electrode (SE) due to different Electrical Conductivities and Relative Permittivity of Healthy Lung Tissue for Inspiration and Collapsed Lung (Pneumothorax) at Constant Current =1mA and Frequency=50 KHz.

Electrical Conductivity (Sm^{-1}) & Relative Permittivity	SE-1 Potential (mV)	SE-2 Potential (mV)	SE-3 Potential (mV)	SE-4 Potential (mV)	SE-5 Potential (mV)	SE-6 Potential (mV)	SE-7 Potential (mV)	SE-8 Potential (mV)	Sum of SE Potential (1 to 8) (mV)
Inspiration 0.103 & 4272.50	67.07	66.68	68.98	69.59	69.84	70.46	72.75	72.38	557.75
Pneumotho-rax (Collapsed Lung) 0.60 & 1000	65.23	64.98	66.44	66.68	66.77	67.01	68.46	68.21	533.78

Table-5.20(b): Relative Electric Potential Change (REPC) value of the same Surface Electrode (SE) between Healthy Lung at Inspiration and Pneumothorax (Collapsed Lung).

$\frac{V_i - V_{pn}}{V_i} \times 100\%$	SE-1 (%)	SE-2 (%)	SE-3 (%)	SE-4 (%)	SE-5 (%)	SE-6 (%)	SE-7 (%)	SE-8 (%)	Average REPC value (%)
	2.74	2.55	3.68	4.18	4.40	4.90	5.90	5.76	4.26

5.3(D-3) Case-3: For Healthy Lung at Expiration and Pneumothorax (Collapsed Lung)

Table-5.21(a): Electric Potentials of 8 different Surface Electrode (SE) due to different Electrical Conductivities and Relative Permittivity of Lung Tissues Lung Tissues for Expiration and Pneumothorax (Collapsed Lung) at Constant Current =1mA and Frequency=50 KHz.

Electrical Conductivity (Sm^{-1}) & Relative Permittivity	SE-1 Potential (mV)	SE-2 Potential (mV)	SE-3 Potential (mV)	SE-4 Potential (mV)	SE-5 Potential (mV)	SE-6 Potential (mV)	SE-7 Potential (mV)	SE-8 Potential (mV)	Sum of SE Potential (1 to 8) (mV)
Expiration 0.262 & 8531.40	66.08	65.82	67.65	68.04	68.18	68.57	70.39	70.13	544.86
Collapsed Lung 0.60 & 1000	65.23	64.98	66.44	66.68	66.77	67.01	68.46	68.21	533.78

Table-5.21(b): Relative Electric Potential Change (REPC) value of the same Surface Electrode (SE) between Healthy Lung at Expiration and Pneumothorax (Collapsed Lung).

$\frac{V_e - V_{pn}}{V_e} \times 100\%$	SE-1 (%)	SE-2 (%)	SE-3 (%)	SE-4 (%)	SE-5 (%)	SE-6 (%)	SE-7 (%)	SE-8 (%)	Average REPC value (%)
	1.29	1.28	1.79	2.00	2.07	2.28	2.74	2.74	2.02

5.3(D-4) Case-4: For Healthy Lung at Inspiration and Pulmonary Edema

Table-5.22(a): Electric Potentials of 8 different Surface Electrode (SE) due to different Electrical Conductivities and Relative Permittivity of Healthy Lung Tissue for Inspiration and Pulmonary Edema at Constant Current =1mA and Frequency=50 KHz.

Electrical Conductivity (Sm^{-1}) & Relative Permittivity	SE-1 Potential (mV)	SE-2 Potential (mV)	SE-3 Potential (mV)	SE-4 Potential (mV)	SE-5 Potential (mV)	SE-6 Potential (mV)	SE-7 Potential (mV)	SE-8 Potential (mV)	Sum of SE Potential (1to 8) (mV)
Inspiration 0.103 & 4272.50	67.07	66.68	68.98	69.59	69.84	70.46	72.75	72.38	557.75
Pulmonary Edema 1.50 & 98.56	64.57	64.28	65.47	65.62	65.67	65.82	67.02	66.72	525.17

Table-5.22(b): Relative Electric Potential Change (REPC) value of the same Surface Electrode (SE) between Healthy Lung at Inspiration and Pulmonary Edema.

$\frac{V_i - V_{pe}}{V_i} \times 100\%$	SE-1 (%)	SE-2 (%)	SE-3 (%)	SE-4 (%)	SE-5 (%)	SE-6 (%)	SE-7 (%)	SE-8 (%)	Average REPC value (%)
	3.73	3.60	5.09	5.70	5.97	6.59	7.88	7.82	5.80

5.3(D-5) Case-5: For Healthy Lung at Expiration and Pulmonary Edema

Table-5.23(a): Electric Potentials of 8 different Surface Electrode (SE) due to different Electrical Conductivities and Relative Permittivity of Healthy Lung Tissue for Expiration and Pulmonary Edema at Constant Current =1mA and Frequency=50 KHz.

Electrical Conductivity (Sm^{-1}) & Relative Permittivity	SE-1 Potential (mV)	SE-2 Potential (mV)	SE-3 Potential (mV)	SE-4 Potential (mV)	SE-5 Potential (mV)	SE-6 Potential (mV)	SE-7 Potential (mV)	SE-8 Potential (mV)	Sum of SE Potential (1to 8) (mV)
Expiration 0.262 & 8531.40	66.08	65.82	67.65	68.04	68.18	68.57	70.39	70.13	544.86
Pulmonary Edema 1.50 & 98.56	64.57	64.28	65.47	65.62	65.67	65.82	67.02	66.72	525.17

Table-5.23(b): Relative Electric Potential Change (REPC) value of the same Surface Electrode (SE) between Healthy Lung at Expiration and Pulmonary Edema.

$\frac{V_e - V_{pe}}{V_e} \times 100\%$	SE-1 (%)	SE-2 (%)	SE-3 (%)	SE-4 (%)	SE-5 (%)	SE-6 (%)	SE-7 (%)	SE-8 (%)	Average REPC Change (%)
	2.29	2.34	3.22	3.56	3.68	4.01	4.79	4.86	3.59

5.4. Simulation Study-5: Proposed Anterior-Posterior Electrical Impedance Technique (APEIT) Protocol through Right Lung.

5.4.1 Case-1: For Healthy Lung at Inspiration and Expiration

Table-5.24(a): Electric Potentials of 8 different Surface Electrode (SE) due to different Electrical Conductivities and Relative Permittivity of Healthy Lung Tissues for inspiration and expiration at Constant Current =1mA and Frequency=50 KHz.

Electrical Conductivity (Sm^{-1}) & Relative Permittivity	SE-1 Potential (mV)	SE-2 Potential (mV)	SE-3 Potential (mV)	SE-4 Potential (mV)	SE-5 Potential (mV)	SE-6 Potential (mV)	SE-7 Potential (mV)	SE-8 Potential (mV)	Sum of SE Potential (1 to 8) (mV)
Inspiration 0.103 & 4272.50	71.14	73.25	75.47	73.36	71.28	73.12	75.60	73.16	586.38
Expiration 0.262 & 8531.40	69.12	70.85	72.85	70.99	69.25	70.71	72.85	70.73	567.35

Table-5.24(b): Relative Electric Potential Change (REPC) value of the same Surface Electrode (SE) between Healthy Lung at Inspiration and Expiration.

$\frac{V_i - V_e}{V_i} \times 100\%$	SE-1 (%)	SE-2 (%)	SE-3 (%)	SE-4 (%)	SE-5 (%)	SE-6 (%)	SE-7 (%)	SE-8 (%)	Average REPC value (%)
	2.84	3.28	3.47	3.23	2.85	3.30	3.64	3.32	3.24

5.4.2 Case-2: For Healthy Lung at Inspiration and Pneumothorax (Collapsed Lung)

Table-5.25(a): Electric Potentials of 8 different Surface Electrode (SE) due to different Electrical Conductivities and Relative Permittivity of Healthy Lung Tissue for Inspiration and Pneumothorax (Collapsed Lung) at Constant Current =1mA and Frequency=50 KHz.

Electrical Conductivity (Sm^{-1}) & Relative Permittivity	SE-1 Potential (mV)	SE-2 Potential (mV)	SE-3 Potential (mV)	SE-4 Potential (mV)	SE-5 Potential (mV)	SE-6 Potential (mV)	SE-7 Potential (mV)	SE-8 Potential (mV)	Sum of SE Potential (1to 8) (mV)
Inspiration 0.103 & 4272.50	71.14	73.25	75.47	73.36	71.28	73.12	75.60	73.16	586.38
Pneumotho-rax (Collapsed Lung) 0.60 & 1000	67.43	68.86	70.67	69.00	67.54	68.66	70.50	68.68	551.34

Table-5.25(b): Relative Electric Potential Change (REPC) value of the same Surface Electrode (SE) between Healthy Lung at Inspiration and Pneumothorax (Collapsed Lung).

$\frac{V_i - V_{pn}}{V_i} \times 100\%$	SE-1 (%)	SE-2 (%)	SE-3 (%)	SE-4 (%)	SE-5 (%)	SE-6 (%)	SE-7 (%)	SE-8 (%)	Average REPC value (%)
	5.22	5.99	6.36	5.94	5.25	6.10	6.75	6.12	5.97

5.4.3 Case-3: For Healthy Lung at Expiration and Pneumothorax (Collapsed Lung)

Table-6.26(a): Electric Potentials of 8 different Surface Electrode (SE) due to different Electrical Conductivities and Relative Permittivity of Lung Tissues Lung Tissues for Expiration and Pneumothorax (Collapsed Lung) at Constant Current =1mA and Frequency=50 KHz.

Electrical Conductivity (Sm^{-1}) & Relative Permittivity	SE-1 Potential (mV)	SE-2 Potential (mV)	SE-3 Potential (mV)	SE-4 Potential (mV)	SE-5 Potential (mV)	SE-6 Potential (mV)	SE-7 Potential (mV)	SE-8 Potential (mV)	Sum of SE Potential (1 to 8) (mV)
Expiration 0.262 & 8531.40	69.12	70.85	72.85	70.99	69.25	70.71	72.85	70.73	567.35
Pneumotho-rax(Collapsed Lung) 0.60 & 1000	67.43	68.86	70.67	69.00	67.54	68.66	70.50	68.68	551.34

Table-5.26(b): Relative Electric Potential Change (REPC) value of the same Surface Electrode (SE) between Healthy Lung at Expiration and Pneumothorax (Collapsed Lung).

$\frac{V_e - V_{pn}}{V_e} \times 100\%$	SE-1 (%)	SE-2 (%)	SE-3 (%)	SE-4 (%)	SE-5 (%)	SE-6 (%)	SE-7 (%)	SE-8 (%)	Average REPC value (%)
	2.45	2.81	2.99	2.80	2.47	2.90	3.23	2.90	2.82

5.4.4 Case-4: For Healthy Lung at Inspiration and Pulmonary Edema

Table-5.27(a): Electric Potentials of 8 different Surface Electrode (SE) due to different Electrical Conductivities and Relative Permittivity of Healthy Lung Tissue for Inspiration and Pulmonary Edema at Constant Current =1mA and Frequency=50 KHz.

Electrical Conductivity (Sm^{-1}) & Relative Permittivity	SE-1 Potential (mV)	SE-2 Potential (mV)	SE-3 Potential (mV)	SE-4 Potential (mV)	SE-5 Potential (mV)	SE-6 Potential (mV)	SE-7 Potential (mV)	SE-8 Potential (mV)	Sum of SE Potential (1 to 8) (mV)
Inspiration 0.103 & 4272.50	71.14	73.25	75.47	73.36	71.28	73.12	75.60	73.16	586.38
Pulmonary Edema 1.50 & 98.56	66.14	67.35	69.01	67.47	66.23	67.07	68.66	67.08	539.01

Table-5.27(b): Relative Electric Potential Change (REPC) value of the same Surface Electrode (SE) between Healthy Lung at Inspiration and Pulmonary Edema.

$\frac{V_i - V_{pe}}{V_i} \times 100\%$	SE-1 (%)	SE-2 (%)	SE-3 (%)	SE-4 (%)	SE-5 (%)	SE-6 (%)	SE-7 (%)	SE-8 (%)	Average REPC value (%)
	7.03	8.06	8.56	8.03	7.09	8.27	9.18	8.31	8.07

5.4.5 Case-5: For Healthy Lung at Expiration and Pulmonary Edema

Table-5.28(a): Electric Potentials of 8 different Surface Electrode (SE) due to different Electrical Conductivities and Relative Permittivity of Healthy Lung Tissue for Expiration and Pulmonary Edema at Constant Current =1mA and Frequency=50 KHz.

Electrical Conductivity (Sm^{-1}) & Relative Permittivity	SE-1 Potential (mV)	SE-2 Potential (mV)	SE-3 Potential (mV)	SE-4 Potential (mV)	SE-5 Potential (mV)	SE-6 Potential (mV)	SE-7 Potential (mV)	SE-8 Potential (mV)	Sum of SE Potential (1 to 8) (mV)
Inspiration 0.103 & 4272.50	69.12	70.85	72.85	70.99	69.25	70.71	72.85	70.73	567.35
Pulmonary Edema 1.50 & 98.56	66.14	67.35	69.01	67.47	66.23	67.07	68.66	67.08	539.01

Table-5.28(b): Relative Electric Potential Change (REPC) value of the same Surface Electrode (SE) between Healthy lung at Expiration and Pulmonary Edema.

$\frac{V_e - V_{pe}}{V_e} \times 100\%$	SE-1 (%)	SE-2 (%)	SE-3 (%)	SE-4 (%)	SE-5 (%)	SE-6 (%)	SE-7 (%)	SE-8 (%)	Average REPC value (%)
	4.31	4.96	5.27	4.96	4.36	5.15	5.75	5.16	4.99

5.5. Comparison of REPC values between four Existing EIT Protocols and Proposed Anterior -Posterior EIT Protocol

Table-6.29: For Healthy Lung at Inspiration and Expiration

Surface Electrode Protocol Type	**SE-1 (%)**	**SE-2 (%)**	**SE-3 (%)**	**SE-4 (%)**	**BP-5 (%)**	**SE-6 (%)**	**SE-7 (%)**	**SE-8 (%)**	**Average REPC value (%)**
Existing Adjacent Current Drive EIT Protocol	2.13	1.84	1.75	1.68	1.57	1.40	0.74	0.18	1.41
Existing Opposite Current Drive at the vertices of the semi-major axis of the chest cross section EIT Protocol	0.46	1.85	2.32	2.71	2.71	2.32	1.85	0.52	1.84
Existing Opposite Current Drive at the vertices of the semi-minor axis of the chest cross section EIT Protocol	1.09	0.30	0.54	1.22	1.50	2.11	2.32	1.66	1.34
Existing Opposite Current Drive along the right lung EIT Protocol	1.47	1.30	1.94	2.24	2.37	2.68	3.23	3.10	2.29
Proposed Anterior-Posterior EIT Protocol	**2.84**	**3.28**	**3.47**	**3.23**	**2.85**	**3.30**	**3.64**	**3.32**	**3.24**

Table-5.30: For Healthy Lung at Inspiration and Pneumothorax (Collapsed Lung)

Surface Electrode Protocol Type	**SE-1 (%)**	**SE-2 (%)**	**SE-3 (%)**	**SE-4 (%)**	**BP-5 (%)**	**SE-6 (%)**	**SE-7 (%)**	**SE-8 (%)**	**Average REPC value (%)**
Existing Adjacent Current Drive EIT Protocol	4.35	3.87	3.70	3.59	3.37	2.98	1.55	0.36	2.97
Existing Opposite Current Drive at the vertices of the semi-major axis of the chest cross section EIT Protocol	0.94	3.87	4.95	5.75	5.76	4.95	3.87	1.06	3.89
Existing Opposite Current Drive at the vertices of the semi-minor axis of the chest cross section EIT Protocol	1.99	0.60	0.94	2.19	2.70	3.83	4.13	2.93	2.41
Existing Opposite Current Drive along the right lung EIT Protocol	2.74	2.55	3.68	4.18	4.40	4.90	5.90	5.76	4.26
Proposed Anterior -Posterior EIT Protocol	**5.22**	**5.99**	**6.36**	**5.94**	**5.25**	**6.10**	**6.75**	**6.12**	**5.97**

Table-5.31: For Healthy Lung at Expiration and Pneumothorax (Collapsed Lung)

Surface Electrode Protocol Type	**SE-1 (%)**	**SE-2 (%)**	**SE-3 (%)**	**SE-4 (%)**	**BP-5 (%)**	**SE-6 (%)**	**SE-7 (%)**	**SE-8 (%)**	**Average REPC value (%)**
Existing Adjacent Current Drive EIT Protocol	2.27	2.07	1.98	1.94	1.83	1.60	0.81	0.18	1.59
Existing Opposite Current Drive at the vertices of the semi-major axis of the chest cross section EIT Protocol	0.48	2.06	2.69	3.12	3.13	2.69	2.06	0.55	2.10
Existing Opposite Current Drive at the vertices of the semi-minor axis of the chest cross section EIT Protocol	0.91	0.30	0.40	0.98	1.22	1.76	1.85	1.29	1.09
Existing Opposite Current Drive along the right lung EIT Protocol	1.29	1.28	1.79	2.00	2.07	2.28	2.74	2.74	2.02
Proposed Anterior-Posterior EIT Protocol	**2.45**	**2.81**	**2.99**	**2.80**	**2.47**	**2.90**	**3.23**	**2.90**	**2.82**

Table-5.32: For Healthy Lung at Inspiration and Pulmonary Edema

Surface Electrode Protocol Type	**SE-1 (%)**	**SE-2 (%)**	**SE-3 (%)**	**SE-4 (%)**	**BP-5 (%)**	**SE-6 (%)**	**SE-7 (%)**	**SE-8 (%)**	**Average REPC value (%)**
Existing Adjacent Current Drive EIT Protocol	6.45	5.85	5.63	5.48	5.20	4.55	2.31	0.56	4.50
Existing Opposite Current Drive at the vertices of the semi-major axis of the chest cross section EIT Protocol	1.37	5.84	7.74	8.93	8.93	7.74	5.84	1.56	5.99
Existing Opposite Current Drive at the vertices of the semi-minor axis of the chest cross section EIT Protocol	2.67	0.89	1.21	2.90	3.64	5.12	5.42	3.86	3.21
Existing Opposite Current Drive along the right lung EIT Protocol	3.73	3.60	5.09	5.70	5.97	6.59	7.88	7.82	5.80
Proposed Anterior-Posterior EIT Protocol	**7.03**	**8.06**	**8.56**	**8.03**	**7.09**	**8.27**	**9.18**	**8.31**	**8.07**

Table-5.33: For Healthy Lung at Expiration and Pulmonary Edema

Surface Electrode Protocol Type	**SE-1 (%)**	**SE-2 (%)**	**SE-3 (%)**	**SE-4 (%)**	**BP-5 (%)**	**SE-6 (%)**	**SE-7 (%)**	**SE-8 (%)**	**Average REPC value (%)**
Existing Adjacent Current Drive EIT Protocol	4.42	4.09	3.95	3.87	3.69	3.19	1.58	0.38	3.15
Existing Opposite Current Drive at the vertices of the semi-major axis of the chest cross section EIT Protocol	0.92	4.06	5.54	6.39	6.39	5.54	4.06	1.05	4.24
Existing Opposite Current Drive at the vertices of the semi-minor axis of the chest cross section EIT Protocol	1.60	0.59	0.67	1.70	2.17	3.08	3.18	2.24	1.90
Existing Opposite Current Drive along the right lung EIT Protocol	2.29	2.34	3.22	3.56	3.68	4.01	4.79	4.86	3.59
Proposed Anterior-Posterior EIT Protocol	**4.31**	**4.96**	**5.27**	**4.96**	**4.36**	**5.15**	**5.75**	**5.16**	**4.99**

Table-5.34: For Average Relative Electrode Potential Change (REPC) value for the Surface Electrode (SE)

Surface Electrode (SE) Protocol Type	**Average REPC of the surface electrode (Between Healthy Lung at Inspiration and Expiration) (%)**	**Average REPC of the surface electrode (Between Healthy Lung at Inspiration and Pneumothorax (Collapsed Lung)) (%)**	**Average REPC of the surface electrode (Between Healthy lung at Expiration and Pneumothorax (Collapsed Lung)) (%)**	**Average REPC of the surface electrode (Between Healthy Lung at Inspiration and Pulmonary Edema) (%)**	**Average REPC of the surface electrode (Between Healthy Lung at Expiration and Pulmonary Edema) (%)**
Existing Adjacent Current Drive EIT Protocol	1.41	2.97	1.59	4.50	3.15
Existing Opposite Current Drive at the vertices of the semi-major axis of the chest cross section EIT Protocol	1.84	3.89	2.10	5.99	4.24
Existing Opposite Current Drive at the vertices of the semi-minor axis of the chest cross section EIT Protocol	1.34	2.41	1.09	3.21	1.90
Existing Opposite Current Drive along the right lung EIT Protocol	2.29	4.26	2.02	5.80	3.59
Proposed Anterior -Posterior EIT Protocol	**3.24**	**5.97**	**2.82**	**8.07**	**4.99**

5.4. Simulation Study-5(b): Proposed Anterior-Posterior Electrical Impedance Technique (APEIT) Protocol through Left Lung with presence of Heart.

5.4.1 Case-1: For Healthy Lung at Inspiration and Expiration

Table-5.24(a): Electric Potentials of 8 different Surface Electrode (SE) due to different Electrical Conductivities and Relative Permittivity of Healthy Lung Tissues for inspiration and expiration at Constant Current =1mA and Frequency=50 KHz.

Electrical Conductivity (Sm^{-1}) & Relative Permittivity	SE-1 Potential (mV)	SE-2 Potential (mV)	SE-3 Potential (mV)	SE-4 Potential (mV)	SE-5 Potential (mV)	SE-6 Potential (mV)	SE-7 Potential (mV)	SE-8 Potential (mV)	Sum of SE Potential (1 to 8) (mV)
Inspiration 0.103 & 4272.50(for lung) 0.195 &16982 (for heart)	70.95	72.25	73.27	72.04	71.03	72.53	74.14	72.61	578.82
Expiration 0.262 & 8531.40(for lung) 0.195 &16982 (for heart)	69.66	70.85	71.81	70.69	69.77	71.04	72.42	71.04	567.28

Table-5.24(b): Relative Electric Potential Change (REPC) value of the same Surface Electrode (SE) between Healthy Lung at Inspiration and Expiration.

$\frac{V_i - V_e}{V_i} \times 100\%$	SE-1 (%)	SE-2 (%)	SE-3 (%)	SE-4 (%)	SE-5 (%)	SE-6 (%)	SE-7 (%)	SE-8 (%)	Average REPC value (%)
	1.82	1.94	1.99	1.87	1.77	2.05	2.32	2.16	1.99

5.6. Simulation study-6: For Single Frequency: Tumor added Right Lung for different sizes (5%, 10%, 20% volume of the right lung) Tumors

5.6(A) at Inspiration condition

5.6.1(a) Table-5.55: Surface Potentials at 8 different Electrodes due to Tumor (5% volume of Right Lung) with Inspiration. (Current =1mA, Frequency=50 KHz, Inspiration: Electrical Conductivity= 0.1030 (Sm^{-1}) and Relative Permittivity=4272.50, Tumor: Electrical Conductivity= 1.50 (Sm^{-1}) and Relative Permittivity= 98.56).

Tumor Position & Size(Sphere Shape-Radius) cm	SE-1 Potential (mV)	SE-2 Potential (mV)	SE-3 Potential (mV)	SE-4 Potential (mV)	SE-5 Potential (mV)	SE-6 Potential (mV)	SE-7 Potential (mV)	SE-8 Potential (mV)	Sum of SE Potential (1 to8) (mV)
(0,-8,23) & 2.79	70.69	72.72	74.88	72.83	70.83	72.57	74.93	72.62	582.06

5.6.1(b) Table-5.56: Electric Potentials of 8 different Surface Electrode (SE) due to Electrical Conductivity 0.103 (Sm^{-1}) and Relative Permittivity 4272.50 of Lung Tissues at Current = 1mA and Frequency 50 KHz.

Right Lung Position (cm)	SE-1 Potential (mV)	SE-2 Potential (mV)	SE-3 Potential (mV)	SE-4 Potential (mV)	SE-5 Potential (mV)	SE-6 Potential (mV)	SE-7 Potential (mV)	SE-8 Potential (mV)	Sum of SE Potential (1 to8) (mV)
(0,-8,23)	71.14	73.25	75.47	73.36	71.28	73.12	75.60	73.16	586.38

5.6.1(c) Table-6.57: Relative Electric Potential Change (REPC) value of the same surface electrode (Between Healthy lung (Inspiration) and 5% Tumor with Inspiration).

$\frac{V_i - V_t}{V_i} \times 100\%$	SE-1 (%)	SE-2 (%)	SE-3 (%)	SE-4 (%)	SE-5 (%)	SE-6 (%)	SE-7 (%)	SE-8 (%)	Average REPC value (%)
	0.64	0.73	0.77	0.72	0.63	0.76	0.88	0.74	0.73

5.6.2(a)Table-5.58: Surface Potentials at 8 different Surface Electrodes due to Tumor (10% volume of Right Lung) with Inspiration. (Current =1mA, Frequency=50 KHz, Inspiration: Electrical Conductivity= 0.1030 (Sm^{-1}) and Relative Permittivity=4272.50, Tumor: Electrical Conductivity= 1.50 (Sm^{-1}) and Relative Permittivity= 98.56).

Tumor Position & Size(Sphere Shape-Radius) (cm)	SE-1 Potential (mV)	SE-2 Potential (mV)	SE-3 Potential (mV)	SE-4 Potential (mV)	SE-5 Potential (mV)	SE-6 Potential (mV)	SE-7 Potential (mV)	SE-8 Potential (mV)	Sum of SE Potential (1to8) (mV)
(0,-8,23) & 3.51	70.19	72.13	74.23	72.24	70.32	71.96	74.19	72.00	577.26

5.6.2(b)Table- 5.59: Electric Potentials of 8 different Surface Electrode (SE) due to Electrical Conductivity 0.103 (Sm^{-1}) and Relative Permittivity 4272.50 of Lung Tissues at Current = 1mA and Frequency 50 kHz.

Right Lung Position (cm)	SE-1 Potential (mV)	SE-2 Potential (mV)	SE-3 Potential (mV)	SE-4 Potential (mV)	SE-5 Potential (mV)	SE-6 Potential (mV)	SE-7 Potential (mV)	SE-8 Potential (mV)	Sum of SE Potential (1 to8) (mV)
(0,-8,23)	71.14	73.25	75.47	73.36	71.28	73.12	75.60	73.16	586.38

5.6.2 (c) Table-5.60: Relative Electric Potential Change (REPC) value of the same surface electrode **(**Between Healthy lung (Inspiration) and 10% Tumor with Inspiration).

$\frac{V_i - V_t}{V_i} \times 100\%$	SE-1 (%)	SE-2 (%)	SE-3 (%)	SE-4 (%)	SE-5 (%)	SE-6 (%)	SE-7 (%)	SE-8 (%)	Average REPC value (%)
	1.34	1.52	1.64	1.52	1.35	1.58	1.86	1.58	1.55

5.6.3 (a) Table-5.61: Surface Potentials at 8 different Surface Electrodes due to Tumor (20% volume of Right Lung) with Inspiration (Current =1mA, Frequency=50 KHz, Inspiration: Electrical Conductivity= 0.1030 (Sm^{-1}) and Relative Permittivity=4272.50, Tumor: Electrical Conductivity= 1.50 (Sm^{-1}) and Relative Permittivity= 98.56).

Tumor Position & Size(Sphere Shape-Radius) cm	SE-1 Potential (mV)	SE-2 Potential (mV)	SE-3 Potential (mV)	SE-4 Potential (mV)	SE-5 Potential (mV)	SE-6 Potential (mV)	SE-7 Potential (mV)	SE-8 Potential (mV)	Sum of SE Potential (1to8) (mV)
(0,-8,23) & 4.42	68.74	70.45	72.37	70.55	68.86	70.24	72.11	70.27	563.59

5.6.3 (b) Table-5.62: Electric Potentials of 8 different Surface Electrode (SE) due to Electrical Conductivity 0.103 (Sm^{-1}) and Relative Permittivity 4272.50 of Lung Tissues at Current = 1mA and Frequency 50 KHz.

Right Lung Position (cm)	SE-1 Potential (mV)	SE-2 Potential (mV)	SE-3 Potential (mV)	SE-4 Potential (mV)	SE-5 Potential (mV)	SE-6 Potential (mV)	SE-7 Potential (mV)	SE-8 Potential (mV)	Sum of SE Potential (1 to8) (mV)
(0,-8,23)	71.14	73.25	75.47	73.36	71.28	73.12	75.60	73.16	586.38

5.6.3 (c) Table-5.63: Relative Electric Potential Change (REPC) value of the same surface electrode (Between Healthy lung (Inspiration) 20% Tumor with Inspiration).

$\frac{V_i - V_t}{V_i} \times 100\%$	SE-1 (%)	SE-2 (%)	SE-3 (%)	SE-4 (%)	SE-5 (%)	SE-6 (%)	SE-7 (%)	SE-8 (%)	Average REPC value (%)
	3.38	3.82	4.10	3.82	3.40	3.93	4.61	3.94	3.88

5.6 (B) At Expiration Condition

5.6.4(a) Table-5.64: Surface Potentials at 8 different Surface Electrodes due to Tumor (5% volume of Right Lung) with Expiration (Current =1mA, Frequency=50 KHz, Expiration: Electrical Conductivity= 0.262 (Sm^{-1}) and Relative Permittivity=8531.40, Tumor: Electrical Conductivity= 1.50 (Sm^{-1}) and Relative Permittivity= 98.56)

Tumor Position & Size (Sphere Shape-Radius) (cm)	SE-1 Potential (mV)	SE-2 Potential (mV)	SE-3 Potential (mV)	SE-4 Potential (mV)	SE-5 Potential (mV)	SE-6 Potential (mV)	SE-7 Potential (mV)	SE-8 Potential (mV)	Sum of SE Potential (1 to8) (mV)
(0,-8,23) & 2.79	68.74	70.40	72.36	70.53	68.87	70.24	72.29	70.26	563.70

5.6.4(b) Table-**5.65:** Electric Potentials of 8 different Surface Electrodes (SE) due to Electrical Conductivity 0.262 (Sm^{-1}) and Relative Permittivity 8531.40 of Lung Tissues at Current = 1mA and Frequency 50 kHz

Right Lung Position (cm)	SE-1 Potential (mV)	SE-2 Potential (mV)	SE-3 Potential (mV)	SE-4 Potential (mV)	SE-5 Potential (mV)	SE-6 Potential (mV)	SE-7 Potential (mV)	SE-8 Potential (mV)	Sum of SE Potential (1 to8) (mV)
(0,-8,23)	69.12	70.85	72.85	70.99	69.25	70.71	72.85	70.73	567.35

5.6.4(c) Table- 5.66: Relative Electric Potential Change (REPC) value of the same surface electrode **(**Between Healthy lung (Expiration) and 5% Tumor with Expiration).

$\frac{V_e - V_t}{V_e} \times 100\%$	SE-1 (%)	SE-2 (%)	SE-3 (%)	SE-4 (%)	SE-5 (%)	SE-6 (%)	SE-7 (%)	SE-8 (%)	Average REPC value (%)
	0.55	0.62	0.68	0.64	0.55	0.66	0.77	0.65	0.64

5.6.5(a) Table-5.67: Surface Potentials at 8 different Surface Electrodes due to Tumor (10% volume of Right Lung) with Expiration (Current =1mA, Frequency=50 KHz, Expiration: Electrical Conductivity= 0.262 (Sm^{-1}) and Relative Permittivity=8531.40, Tumor: Electrical Conductivity= 1.50 (Sm^{-1}) and Relative Permittivity= 98.56).

Tumor Position & Size(Sphere Shape-Radius) (cm)	SE-1 Potential (mV)	SE-2 Potential (mV)	SE-3 Potential (mV)	SE-4 Potential (mV)	SE-5 Potential (mV)	SE-6 Potential (mV)	SE-7 Potential (mV)	SE-8 Potential (mV)	Sum of SE Potential (1 to8) (mV)
(0,-8,23) & 3.51	68.38	69.97	71.88	70.10	68.49	69.79	71.73	69.81	560.15

5.6.5(b) Table-5.68: Electric Potentials of 8 different Surface Electrode (SE) due to Electrical Conductivity 0.262 (Sm^{-1}) and Relative Permittivity 8531.40 of Lung Tissues at Current = 1mA and Frequency 50 KHz

Right Lung Position (cm)	SE-1 Potential (mV)	SE-2 Potential (mV)	SE-3 Potential (mV)	SE-4 Potential (mV)	SE-5 Potential (mV)	SE-6 Potential (mV)	SE-7 Potential (mV)	SE-8 Potential (mV)	Sum of SE Potential (1 to8) (mV)
(0,-8,23)	69.12	70.85	72.85	70.99	69.25	70.71	72.85	70.73	567.35

5.6.5 (c) Table- 5.69: Relative Electric Potential Change (REPC) value of the same surface electrode (Between Healthy lung (Expiration) and 10% Tumor with Expiration).

$\frac{V_e - V_t}{V_e} \times 100\%$	SE-1 (%)	SE-2 (%)	SE-3 (%)	SE-4 (%)	SE-5 (%)	SE-6 (%)	SE-7 (%)	SE-8 (%)	Average REPC value (%)
	1.08	1.24	1.34	1.25	1.10	1.30	1.55	1.29	1.27

5.6.6(a)Table-5.70: Surface Potentials at 8 different Surface Electrodes due to Tumor (20% volume of Right Lung) with Expiration (Current =1mA, Frequency=50 KHz, Expiration: Electrical Conductivity= 0.262 (Sm^{-1}) and Relative Permittivity=8531.40, Tumor: Electrical Conductivity= 1.50 (Sm^{-1}) and Relative Permittivity= 98.56).

Tumor Position & Size(Sphere Shape) (cm)	SE-1 Potential (mV)	SE-2 Potential (mV)	SE-3 Potential (mV)	SE-4 Potential (mV)	SE-5 Potential (mV)	SE-6 Potential (mV)	SE-7 Potential (mV)	SE-8 Potential (mV)	Sum of SE Potential (1 to8) (mV)
(0,-8,23) & 4.42	67.55	69.03	70.82	69.14	67.66	68.81	70.53	68.83	552.37

5.6.6(b)Table-5.71: Electric Potentials of 8 different Surface Electrode (SE) due to Electrical Conductivity 0.262 (Sm^{-1}) and Relative Permittivity 8531.40 of Lung Tissues at Current = 1mA and Frequency 50 KHz

Right Lung Position (cm)	SE-1 Potential (mV)	SE-2 Potential (mV)	SE-3 Potential (mV)	SE-4 Potential (mV)	SE-5 Potential (mV)	SE-6 Potential (mV)	SE-7 Potential (mV)	SE-8 Potential (mV)	Sum of SE Potential (1 to8) (mV)
(0,-8,23)	69.12	70.85	72.85	70.99	69.25	70.71	72.85	70.73	567.35

5.6.6 (c) Table- 5.72: Relative Electric Potential Change (REPC) value of the same surface electrode (Between Healthy lung (Expiration) and 20% Tumor with Expiration).

$\frac{V_e - V_t}{V_e} \times 100\%$	SE-1 (%)	SE-2 (%)	SE-3 (%)	SE-4 (%)	SE-5 (%)	SE-6 (%)	SE-7 (%)	SE-8 (%)	Average REPC value (%)
	2.27	2.56	2.79	2.60	2.30	2.68	3.19	2.68	2.63

5.7. Simulation Study-7: for Multi Frequency EIT (MF-EIT) or Electrical Impedance Spectroscopy (EIS)

5.7 (A) At Inspiration Condition

5.7.1 Table-5.45: Electric Potentials of 8 different Surface Electrode (SE) due to different Frequencies of Lung Tissues at Constant Current =1mA, Electrical Conductivity =0.0824 (Sm^{-1}) and Relative Permittivity=4272.50

Frequency (kHz)	SE-1 Potential (mV)	SE-2 Potential (mV)	SE-3 Potential (mV)	SE-4 Potential (mV)	SE-5 Potential (mV)	SE-6 Potential (mV)	SE-7 Potential (mV)	SE-8 Potential (mV)	Sum of SE Potential (1 to8) (mV)
20	71.76	73.96	76.23	74.06	71.91	73.82	76.37	73.87	591.98
50	71.56	73.74	76.01	73.85	71.71	73.60	76.15	73.66	590.30
100	70.85	73.01	75.27	73.13	71.00	72.88	75.40	72.93	584.47
150	69.73	71.85	74.06	71.95	69.87	71.72	74.19	71.77	575.14
200	68.25	70.31	72.46	70.41	68.39	70.18	72.59	70.23	562.82

5.7.2 Table-5.46: Electric Potentials of 8 different Surface Electrode (SE) due to different Frequencies of Lung Tissues at Constant Current =1mA, Electrical Conductivity = 0.0927 (Sm^{-1}) and Relative Permittivity=4272.50

Frequency (kHz)	SE-1 Potential (mV)	SE-2 Potential (mV)	SE-3 Potential (mV)	SE-4 Potential (mV)	SE-5 Potential (mV)	SE-6 Potential (mV)	SE-7 Potential (mV)	SE-8 Potential (mV)	Sum of SE Potential (1 to8) (mV)
20	71.54	73.69	75.94	73.80	71.69	73.56	76.08	73.61	589.90
50	71.33	73.49	75.73	73.60	71.48	73.35	75.86	73.40	588.25
100	70.65	72.77	74.99	72.88	70.79	72.64	75.13	72.68	582.54
150	69.54	71.63	73.80	71.73	69.68	71.49	73.94	71.53	573.34
200	67.59	69.54	71.63	69.66	67.74	69.42	71.72	69.45	561.20

5.7.3 Table-5.47: Electric Potentials of 8 different Surface Electrode (SE) due to different Frequencies of Lung Tissues at Constant Current =1mA, Electrical Conductivity =0.1030 (Sm^{-1}) and Relative Permittivity=4272.50

Frequency (kHz)	SE-1 Potential (mV)	SE-2 Potential (mV)	SE-3 Potential (mV)	SE-4 Potential (mV)	SE-5 Potential (mV)	SE-6 Potential (mV)	SE-7 Potential (mV)	SE-8 Potential (mV)	Sum of SE Potential (1 to8) (mV)
20	71.33	73.45	75.68	73.56	71.48	73.32	75.80	73.36	587.97
50	71.14	73.25	75.47	73.36	71.28	73.12	75.60	73.16	586.37
100	70.45	72.54	74.74	72.65	70.60	72.41	74.86	72.45	580.71
150	69.36	71.40	73.57	71.52	69.50	71.28	73.69	71.32	571.65
200	67.91	69.90	72.02	70.02	68.04	69.78	72.14	69.82	559.63

5.7.4 Table-5.48: Electric Potentials of 8 different Surface Electrode (SE) due to different Frequencies of Lung Tissues at Constant Current =1mA, Electrical Conductivity =0.1133 (Sm^{-1}) and Relative Permittivity=4272.50

Frequency (kHz)	SE-1 Potential (mV)	SE-2 Potential (mV)	SE-3 Potential (mV)	SE-4 Potential (mV)	SE-5 Potential (mV)	SE-6 Potential (mV)	SE-7 Potential (mV)	SE-8 Potential (mV)	Sum of SE Potential (1 to8) (mV)
20	71.14	73.22	75.43	73.34	71.29	73.09	75.55	73.13	586.17
50	70.95	73.03	75.22	73.14	71.10	72.89	75.34	72.94	584.60
100	70.27	72.32	74.50	72.44	70.41	72.19	74.62	72.23	579.00
150	69.18	71.20	73.35	71.32	69.33	71.07	73.46	71.11	570.02
200	67.75	69.72	71.82	69.84	67.89	69.60	71.93	69.64	558.17

5.7.5 Table-5.49: Electric Potentials of 8 different Surface Electrode (SE) due to different Frequencies of Lung Tissues at Constant Current =1mA, Electrical Conductivity =0.1236 (Sm^{-1}) and Relative Permittivity=4272.50

Frequency (kHz)	SE-1 Potential (mV)	SE-2 Potential (mV)	SE-3 Potential (mV)	SE-4 Potential (mV)	SE-5 Potential (mV)	SE-6 Potential (mV)	SE-7 Potential (mV)	SE-8 Potential (mV)	Sum of SE Potential (1to8) (mV)
20	70.97	73.01	75.19	73.13	71.11	72.88	75.31	72.92	584.50
50	70.77	72.81	74.99	72.93	70.92	72.67	75.10	72.72	582.92
100	70.09	72.12	74.28	72.23	70.25	71.99	74.39	72.03	577.40
150	69.03	71.00	73.14	71.13	69.17	70.88	73.24	70.92	568.51
200	67.59	69.54	71.63	69.66	67.74	69.42	71.72	69.45	556.75

5.7 (B) At Expiration Condition

5.7.6 Table-5.50: Electric Potentials of 8 different Surface Electrode (SE) due to different Frequencies of Lung Tissues at Constant Current=1mA, Electrical Conductivity =0.2096 (Sm^{-1}) and Relative Permittivity=8531.40

Frequency (kHz)	SE-1 Potential (mV)	SE-2 Potential (mV)	SE-3 Potential (mV)	SE-4 Potential (mV)	SE-5 Potential (mV)	SE-6 Potential (mV)	SE-7 Potential (mV)	SE-8 Potential (mV)	Sum of SE Potential (1 to8) (mV)
20	69.81	71.63	73.69	71.77	69.95	71.50	73.74	71.53	573.60
50	69.62	71.43	73.49	71.56	69.75	71.29	73.53	71.32	572.00
100	68.94	70.74	72.78	70.87	69.08	70.61	72.82	70.63	566.47
150	67.87	69.63	71.63	69.76	68.00	69.50	71.67	69.53	557.59
200	66.44	68.17	70.12	68.29	66.58	68.03	70.15	68.06	545.84

5.7.7 Table-5.51: Electric Potentials of 8 different Surface Electrode (SE) due to different Frequencies of Lung Tissues at Constant Current=1mA, Electrical Conductivity =0.2358 (Sm^{-1}) and Relative Permittivity=8531.40

Frequency (kHz)	SE-1 Potential (mV)	SE-2 Potential (mV)	SE-3 Potential (mV)	SE-4 Potential (mV)	SE-5 Potential (mV)	SE-6 Potential (mV)	SE-7 Potential (mV)	SE-8 Potential (mV)	Sum of SE Potential (1 to8) (mV)
20	69.55	71.32	73.35	71.46	69.68	71.18	73.38	71.21	571.11
50	69.35	71.13	73.15	71.26	69.48	70.98	73.18	71.01	569.54
100	68.89	70.45	72.45	70.58	68.82	70.30	72.47	70.34	564.11
150	67.64	69.36	71.33	69.48	67.76	69.22	71.35	69.24	555.37
200	66.23	67.91	69.84	68.05	66.36	67.77	69.86	67.80	543.81

5.7.8 Table-5.52: Electric Potentials of 8 different Surface Electrode (SE) due to different Frequencies of Lung Tissues at Constant Current=1mA, Electrical Conductivity =0.2620 (Sm^{-1}) and Relative Permittivity=8531.40

Frequency (kHz)	SE-1 Potential (mV)	SE-2 Potential (mV)	SE-3 Potential (mV)	SE-4 Potential (mV)	SE-5 Potential (mV)	SE-6 Potential (mV)	SE-7 Potential (mV)	SE-8 Potential (mV)	Sum of SE Potential (1 to8) (mV)
20	69.31	71.04	73.05	71.18	69.44	70.90	73.06	70.92	568.87
50	69.12	70.85	72.85	70.99	69.25	70.71	72.85	70.73	567.34
100	68.47	70.18	72.16	70.32	68.60	70.03	72.17	70.06	562.01
150	67.43	69.11	71.05	69.24	67.55	68.96	71.06	68.98	553.38
200	66.04	67.68	69.58	67.81	66.16	67.53	69.60	67.57	541.97

5.7.9 Table-5.53: Electric Potentials of 8 different Surface Electrode (SE) due to different Frequencies of Lung Tissues at Constant Current=1mA, Electrical Conductivity =0.2882 (Sm^{-1}) and Relative Permittivity=8531.40

Frequency (KHz)	SE-1 Potential (mV)	SE-2 Potential (mV)	SE-3 Potential (mV)	SE-4 Potential (mV)	SE-5 Potential (mV)	SE-6 Potential (mV)	SE-7 Potential (mV)	SE-8 Potential (mV)	Sum of SE Potential (1to8) (mV)
20	69.10	70.79	72.78	70.93	69.23	70.64	72.76	70.67	566.87
50	68.92	70.60	72.58	70.73	69.04	70.45	72.57	70.47	565.38
100	68.26	69.94	71.90	70.08	68.40	69.79	71.89	69.81	560.07
150	67.23	68.88	70.81	69.01	67.35	68.73	70.80	68.75	551.56
200	65.85	67.47	69.36	67.60	65.98	67.32	69.35	67.34	540.27

5.7.10 Table-5.54: Electric Potentials of 8 different Surface Electrode (SE) due to different Frequencies of Lung Tissues at Constant Current=1mA, Electrical Conductivity =0.3144 (Sm^{-1}) and Relative Permittivity=8531.40

Frequency (KHz)	SE-1 Potential (mV)	SE-2 Potential (mV)	SE-3 Potential (mV)	SE-4 Potential (mV)	SE-5 Potential (mV)	SE-6 Potential (mV)	SE-7 Potential (mV)	SE-8 Potential (mV)	Sum of SE Potential (1 to8) (mV)
20	68.90	70.57	72.53	70.71	69.04	70.41	72.50	70.43	565.07
50	68.73	70.38	72.34	70.51	68.85	70.22	72.31	70.24	563.58
100	68.09	69.73	71.66	69.86	68.21	69.57	71.63	69.59	558.33
150	67.06	68.67	70.58	68.80	67.18	68.52	70.55	68.53	549.88
200	65.69	67.27	69.14	67.41	65.81	67.13	69.12	67.14	538.71

5.8. Simulation Study-8: For Single Frequency Electrical Impedance Tomography

5.8 (A) At Inspiration Condition

5.8.1 Table-6.35: Electric Potentials of 8 different Surface Electrode (SE) due to different Electrical Conductivities of Lung Tissues at Constant Current =1mA, Frequency=20 KHz and Relative Permittivity=4272.50

Electrical Conductivity (Sm^{-1})	SE-1 Potential (mV)	SE-2 Potential (mV)	SE-3 Potential (mV)	SE-4 Potential (mV)	SE-5 Potential (mV)	SE-6 Potential (mV)	SE-7 Potential (mV)	SE-8 Potential (mV)	Sum of SE Potential (1 to8) (mV)
0.0824	71.76	73.96	76.23	74.06	71.91	73.82	76.37	73.87	591.98
0.0927	71.54	73.69	75.94	73.80	71.69	73.56	76.08	73.61	589.90
0.1030	71.33	73.45	75.68	73.56	71.48	73.32	75.80	73.36	587.97
0.1133	71.14	73.22	75.43	73.34	71.29	73.09	75.55	73.13	586.17
0.1236	70.97	73.01	75.19	73.13	71.11	72.88	75.31	72.92	584.50

5.8.2 Table-5.36: Electric Potentials of 8 different Surface Electrode (SE) due to different Electrical Conductivities of Lung Tissues at Constant Current =1mA, Frequency=50 KHz and Relative Permittivity=4272.50

Electrical Conductivity (Sm^{-1})	SE-1 Potential (mV)	SE-2 Potential (mV)	SE-3 Potential (mV)	SE-4 Potential (mV)	SE-5 Potential (mV)	SE-6 Potential (mV)	SE-7 Potential (mV)	SE-8 Potential (mV)	Sum of SE Potential (1 to 8) (mV)
0.0824	71.56	73.74	76.01	73.85	71.71	73.60	76.15	73.66	590.30
0.0927	71.33	73.49	75.73	73.60	71.48	73.35	75.86	73.40	588.25
0.1030	71.14	73.25	75.47	73.36	71.28	73.12	75.60	73.16	586.37
0.1133	70.95	73.03	75.22	73.14	71.10	72.89	75.34	72.94	584.60
0.1236	70.77	72.81	74.99	72.93	70.92	72.67	75.10	72.72	582.92

5.8.3 Table-5.37: Electric Potentials of 8 different Surface Electrode (SE) due to different Electrical Conductivities of Lung Tissues at Constant Current =1mA, Frequency=100 KHz and Relative Permittivity=4272.50

Electrical Conductivity (Sm^{-1})	SE-1 Potential (mV)	SE-2 Potential (mV)	SE-3 Potential (mV)	SE-4 Potential (mV)	SE-5 Potential (mV)	SE-6 Potential (mV)	SE-7 Potential (mV)	SE-8 Potential (mV)	Sum of SE Potential (1 to8) (mV)
0.0824	70.85	73.01	75.27	73.13	71.00	72.88	75.40	72.93	584.47
0.0927	70.65	72.77	74.99	72.88	70.79	72.64	75.13	72.68	582.54
0.1030	70.45	72.54	74.74	72.65	70.60	72.41	74.86	72.45	580.71
0.1133	70.27	72.32	74.50	72.44	70.41	72.19	74.62	72.23	579.00
0.1236	70.09	72.12	74.28	72.23	70.25	71.99	74.39	72.03	577.40

5.8.4 Table-5.38: Electric Potentials of 8 different Surface Electrode (SE) due to different Electrical Conductivities of Lung Tissues at Constant Current =1mA, Frequency=150 KHz and Relative Permittivity=4272.50

Electrical Conductivity (Sm^{-1})	SE-1 Potential (mV)	SE-2 Potential (mV)	SE-3 Potential (mV)	SE-4 Potential (mV)	SE-5 Potential (mV)	SE-6 Potential (mV)	SE-7 Potential (mV)	SE-8 Potential (mV)	Sum of SE Potential (1 to 8) (mV)
0.0824	69.73	71.85	74.06	71.95	69.87	71.72	74.19	71.77	575.14
0.0927	69.54	71.63	73.80	71.73	69.68	71.49	73.94	71.53	573.34
0.1030	69.36	71.40	73.57	71.52	69.50	71.28	73.69	71.32	571.65
0.1133	69.18	71.20	73.35	71.32	69.33	71.07	73.46	71.11	570.02
0.1236	69.03	71.00	73.14	71.13	69.17	70.88	73.24	70.92	568.51

5.8.5 Table-5.39: Electric Potentials of 8 different Surface Electrode (SE) due to different Electrical Conductivities of Lung Tissues Constant Current =1mA, Frequency=200 KHz and Relative Permittivity=4272.50

Electrical Conductivity (Sm^{-1})	SE-1 Potential (mV)	SE-2 Potential (mV)	SE-3 Potential (mV)	SE-4 Potential (mV)	SE-5 Potential (mV)	SE-6 Potential (mV)	SE-7 Potential (mV)	SE-8 Potential (mV)	Sum of SE Potential (1 to8) (mV)
0.0824	68.25	70.31	72.46	70.41	68.39	70.18	72.59	70.23	562.82
0.0927	68.07	70.10	72.24	70.21	68.21	69.97	72.36	70.03	561.20
0.1030	67.91	69.90	72.02	70.02	68.04	69.78	72.14	69.82	559.63
0.1133	67.75	69.72	71.82	69.84	67.89	69.60	71.93	69.64	558.17
0.1236	67.59	69.54	71.63	69.66	67.74	69.42	71.72	69.45	556.75

5.8 (B) At Expiration Condition

5.8.6 Table-5.40: Electric Potentials of 8 different Surface Electrode (SE) due to different Electrical Conductivities of Lung Tissues at Constant Current =1mA, Frequency=20 KHz & Relative Permittivity=8531.40

Electrical Conductivity (Sm^{-1})	SE-1 Potential (mV)	SE-2 Potential (mV)	SE-3 Potential (mV)	SE-4 Potential (mV)	SE-5 Potential (mV)	SE-6 Potential (mV)	SE-7 Potential (mV)	SE-8 Potential (mV)	Sum of SE Potential (1 to8) (mV)
0.2096	69.81	71.63	73.69	71.77	69.95	71.50	73.74	71.53	573.60
0.2358	69.55	71.32	73.35	71.46	69.68	71.18	73.38	71.21	571.11
0.2620	69.31	71.04	73.05	71.18	69.44	70.90	73.06	70.92	568.87
0.2882	69.10	70.79	72.78	70.93	69.23	70.64	72.76	70.67	566.87
0.3144	68.90	70.57	72.53	70.71	69.04	70.41	72.50	70.43	565.07

5.8.7 Table-5.41: Electric Potentials of 8 different Surface Electrode (SE) due to different Electrical Conductivities of Lung Tissues at Constant Current =1mA, Frequency=50 KHz & Relative Permittivity=8531.40

Electrical Conductivity (Sm^{-1})	SE-1 Potential (mV)	SE-2 Potential (mV)	SE-3 Potential (mV)	SE-4 Potential (mV)	SE-5 Potential (mV)	SE-6 Potential (mV)	SE-7 Potential (mV)	SE-8 Potential (mV)	Sum of SE Potential (1 to8) (mV)
0.2096	69.62	71.43	73.49	71.56	69.75	71.29	73.53	71.32	572.00
0.2358	69.35	71.13	73.15	71.26	69.48	70.98	73.18	71.01	569.54
0.2620	69.12	70.85	72.85	70.99	69.25	70.71	72.85	70.73	567.34
0.2882	68.92	70.60	72.58	70.73	69.04	70.45	72.57	70.47	565.38
0.3144	68.73	70.38	72.34	70.51	68.85	70.22	72.31	70.24	563.58

5.8.8 Table-5.42: Electric Potentials of 8 different Surface Electrode (SE) due to different Electrical Conductivities of Lung Tissues at Constant Current =1mA, Frequency=100 KHz & Relative Permittivity=8531.40.

Electrical Conductivity (Sm^{-1})	SE-1 Potential (mV)	SE-2 Potential (mV)	SE-3 Potential (mV)	SE-4 Potential (mV)	SE-5 Potential (mV)	SE-6 Potential (mV)	SE-7 Potential (mV)	SE-8 Potential (mV)	Sum of SE Potential (1 to8) (mV)
0.2096	68.94	70.74	72.78	70.87	69.08	70.61	72.82	70.63	566.47
0.2358	68.89	70.45	72.45	70.58	68.82	70.30	72.47	70.34	564.11
0.2620	68.47	70.18	72.16	70.32	68.60	70.03	72.17	70.06	562.01
0.2882	68.26	69.94	71.90	70.08	68.40	69.79	71.89	69.81	560.07
0.3144	68.09	69.73	71.66	69.86	68.21	69.57	71.63	69.59	558.33

5.8.9 Table-5.43: Electric Potentials of 8 different Surface Electrode (SE) due to different Electrical Conductivities of Lung Tissues at Constant Current =1mA, Frequency=150 KHz and Relative Permittivity=8531.40

Electrical Conductivity (Sm^{-1})	SE-1 Potential (mV)	SE-2 Potential (mV)	SE-3 Potential (mV)	SE-4 Potential (mV)	SE-5 Potential (mV)	SE-6 Potential (mV)	BP-7 Potential (mV)	SE-8 Potential (mV)	Sum of SE Potential (1to8) (mV)
0.2096	67.87	69.63	71.63	69.76	68.00	69.50	71.67	69.53	557.59
0.2358	67.64	69.36	71.33	69.48	67.76	69.22	71.35	69.24	555.37
0.2620	67.43	69.11	71.05	69.24	67.55	68.96	71.06	68.98	553.38
0.2882	67.23	68.88	70.81	69.01	67.35	68.73	70.80	68.75	551.56
0.3144	67.06	68.67	70.58	68.80	67.18	68.52	70.55	68.53	549.88

5.8.10 Table-5.44: Electric Potentials of 8 different Surface Electrode (SE) due to different Electrical Conductivities of Lung Tissues at Constant Current =1mA, Frequency=200 KHz and Relative Permittivity=8531.40

Electrical Conductivity (Sm^{-1})	SE-1 Potential (mV)	SE-2 Potential (mV)	SE-3 Potential (mV)	SE-4 Potential (mV)	SE-5 Potential (mV)	SE-6 Potential (mV)	SE-7 Potential (mV)	SE-8 Potential (mV)	Sum of SE Potential (1 to8) (mV)
0.2096	66.44	68.17	70.12	68.29	66.58	68.03	70.15	68.06	545.84
0.2358	66.23	67.91	69.84	68.05	66.36	67.77	69.86	67.80	543.81
0.2620	66.04	67.68	69.58	67.81	66.16	67.53	69.60	67.57	541.97
0.2882	65.85	67.47	69.36	67.60	65.98	67.32	69.35	67.34	540.27
0.3144	65.69	67.27	69.14	67.41	65.81	67.13	69.12	67.14	538.71

5.9. Human Thorax Phantom Study using Maltron Bio Scan 920-11 Analyser

Table-6.76: Tabulated values for different concentration of NaCl (%) in solution and corresponding electrical conductivity.

No. of Observations	Concentration of NaCl (%) in solution	Corresponding Electrical Conductivity (Sm^{-1})
1	0.54	0.952
2	0.72	1.210
3	0.90	1.520
4	1.08	1.858
5	1.26	2.162

Table- 5.77: Electric Potentials of 8 different Surface Electrodes due to different Electrical Conductivities of NaCl (%) in Phantom Solutions at Constant Current =0.8 mA, Frequency=50 KHz and Relative Permittivity=15 (for NaCl)

Electrical Conductivity (Sm^{-1})	SE-1 Potential (mV)	SE-2 Potential (mV)	SE-3 Potential (mV)	SE-4 Potential (mV)	SE-5 Potential (mV)	SE-6 Potential (mV)	SE-7 Potential (mV)	SE-8 Potential (mV)	Sum of SE Potential (1 to 8) (mV)
0.952	14.72	14.88	15.68	14.80	14.40	14.80	16.08	15.04	120.40
1.210	11.20	11.36	12.00	11.28	10.96	11.36	12.24	11.44	91.84
1.520	9.04	9.20	9.68	9.04	8.96	9.12	9.84	9.12	74.00
1.858	7.76	7.84	8.24	7.76	7.60	7.84	8.40	7.92	63.36
2.162	6.72	6.80	7.12	6.80	6.56	6.80	7.28	6.88	54.96

Table-5.78: Sum of Eight Surface Electrodes Potential (mV) due to different Concentrations of NaCl (%) in Phantom solution.

No. of Observations	Concentration of NaCl (%) in solution	Corresponding Electrical Conductivity (Sm^{-1})	Sum of SE Potential (1 to 8) (mV)
1	0.54	0.952	120.40
2	0.72	1.210	91.84
3	0.90	1.520	74.00
4	1.08	1.858	63.36
5	1.26	2.162	54.96